Structural and Functional Magnetic Resonance Imaging (MRI) in the prediction and characterization of Mild Cognitive Impairment (MCI) and Alzheimer's Disease (AD)

Giovanna Zamboni

Green Templeton College, University of Oxford
Trinity Term 2012

Structural and Functional Magnetic Resonance Imaging (MRI) in the prediction and characterization of Mild Cognitive Impairment (MCI) and Alzheimer's Disease (AD)

General Abstract

The aim of the research presented in this thesis was to improve the characterisation of the changes in brain structure and function that occur at different stages of Alzheimer's disease (AD) progression, from pre-symptomatic AD, to mild cognitive impairment (MCI), to clinically evident dementia, using magnetic resonance imaging (MRI) techniques.

Baseline structural MRI data from a cohort of healthy older adults who were followed prospectively for ten years, during which time some developed MCI and some AD, were analysed. It was found that *structural* MRI could detect volume loss in medial-temporal lobes up to 7-10 years before clinical symptoms of AD appear. In addition, volumetric variability of medial-temporal regions detected by *structural* MRI across cognitively healthy older adults correlated with their performance on a task of visuospatial associative memory, and functional activation of the same regions occurred during successful performance of the same task on *functional* MRI (fMRI).

Three groups of participants - cognitively healthy controls, people with MCI, and patients with probable AD - were then recruited and underwent a multimodal MRI protocol, which included *functional* sequences acquired at rest and during the execution of two different cognitive tasks (visuospatial associative memory and self-appraisal). Cross-sectional comparisons showed: (i) that successful visuospatial associative memory performance was associated with increased functional activity (measured with task fMRI) in lateral prefrontal regions in AD patients relative to controls and (ii) that increased functional activity overlapped with frontal brain networks showing increased functional connectivity (measured with resting fMRI) in the same AD patients. Further, by demonstrating group- and condition-specific decreased frontal activity in AD patients relative to controls during a self-appraisal fMRI task, it was shown the specific utility of fMRI to unravel cognitive mechanisms underlying specific neuropsychological symptoms such as unawareness of cognitive impairment (*anosognosia*) in MCI and AD.

In conclusion, *structural* MRI can detect morphological changes in the preclinical stage of AD, possibly earlier than previously described, and these reliably match cognitive functioning in older adults. In the MCI and AD stages, once symptoms of cognitive impairment are clinically evident and measurable, task-related and resting *functional* MRI can inform on residual brain function detectable over and above the known changes in brain morphology and cognitive performance that have already occurred at these stages, emerging as a sensitive marker of residual ability that could potentially be used to measure the effect of new treatments.

A thesis submitted in partial fulfilment of the requirements for the degree of Doctor of Philosophy in the University of Oxford
This thesis contains approximately 43000 words

Table of Contents

Acknowledgments

Firstly, I would like to acknowledge all the participants and their families, without whose passionate commitment this research could not have occurred, and the Oxford NIHR Biomedical Research Centre and Sir Stewart Halley Trust, who provided funding.

I am extremely grateful to many colleagues who have helped with several aspects of the research presented in this thesis:

- Research Nurse Ellen McCulloch had a critical role in the preparation of documents related to ethical approval, organised and supervised recruitment of participants, and helped greatly with consent procedures and participants' neuropsychological assessment;
- Research Assistant Erin Drazich assisted in all the steps related to data collection and analysis presented in this thesis. Ellen, Erin and myself have been a team, which I felt privileged to lead. Thank you both deeply, without your commitment and enthusiasm this research would have not been possible;
- OPTIMA Clinical Manager Sharon Christie assisted with recruitment and provided critical support and help throughout all the phases of the research;
- Dr Celeste de Jager and all research nurses of OPTIMA contributed to data collection and neuropsychological assessment presented in *Chapters 3-4*;
- Prof A. David Smith, founder and former director of OPTIMA, organized the longitudinal study presented in *Chapters 3* and *4*, and kindly agreed to share the data;
- Dr Manuela Tondelli contributed to the analysis of imaging data and interpretation of findings presented in *Chapter 3*; she also gave insightful comments on the findings presented in the other experimental Chapters;
- Ian Wilson helped in preparing the presentation of fMRI experimental stimuli;
- Prof Wilcock, Dr Stewart, and my other colleagues of the OXMAC memory clinic of the John Radcliffe Hospital, together with the research support staff from Thames Valley DeNDRoN, critically helped with recruitment and referral of patients for the study presented in *Chapters 5-7*;
- Steve Knight, research assistant at OCMR, operated the MRI scans of the study presented in *Chapters 5-7*, demonstrating invaluable kindness and patience to all the participants;

- Dr Mark Jenkinson critically contributed to all the steps of imaging analysis, from the setting up of the fMRI paradigms to the preparation of publications;
- Dr Nicola Filippini generously taught resting-state and other FSL analysis techniques;
- The fMRIB' analysis group and IT personnel assisted in dealing with all analysis and computing problems;
- Dr Clare Mackay and Dr Gwenelle Douaud gave critical suggestions on the interpretation of data presented in *Chapters 5-7*;
- Dr Jonathan Brooks and Dr Yazhuo Kong helped with the monitoring and analysis of physiological noise;
- Grzegorz Agacinski helped in retrieving information regarding OPTIMA participants;
- Donald Warden performed APOE genotyping;
- Dr Rita Marasco performed white matter hyperintensity ratings;
- Dr Anne-Marie Haigh and Dr Natalie Voets carried out detailed proof reading and gave insightful feedback on this thesis.

Special thanks go to my supervisors, Prof Gordon Wilcock and Prof Irene Tracey, who have provided invaluable guidance and support throughout my time in Oxford.
Finally, to my husband Davide, for his loving and strong support.

This thesis is dedicated to my mother Genoeffa,
who sadly died shortly before its completion. Grazie di tutto mamma.

Publications

Papers presented in this thesis

- **Zamboni** & Wilcock *"Lack of awareness of symptoms in people with dementia: the structural and functional basis"* International Journal of Geriatric Psychiatry, 2010 Oct 28
- Tondelli, Wilcock, de Jager, Nichelli, Jenkinson, **Zamboni**. *"Structural MRI changes detectable up to ten years before cognitive impairment due to Alzheimer's Disease".* Neurobiology of aging, 2011 July 20
- **Zamboni**, Drazich, McCulloch, Filippini, Mackay, Jenkinson, Tracey, Wilcock. *"Functional neuroanatomy of impaired self-appraisal in Alzheimer's disease and Mild cognitive impairment"*, Cortex, published online 2012 May 8, DOI: 10.1016/j.cortex.2012.04.011
- **Zamboni,** De Jager, Drazich, Doudau, Jenkinson, Smith, Tracey, Wilcock. "Structural and functional bases of visuospatial associative memory in older adults". Neurobiology of aging, published online 2012 Aug 7, DOI: 10.1016/j.neurobiolaging.2012.07.011
- **Zamboni**, Wilcock, Doudau, Drazich, Filippini, Brooks, Jenkinson, Smith, Tracey, Mackay "Resting functional connectivity is sensitive to residual activity in Alzheimer's disease", *submitted*
- Kong, **Zamboni**, Drazich, Wilcock, Tracey, Brooks "Physiological noise modelling for resting fMRI in older adults", *in preparation*

Abstracts presented at scientific conferences:

- Self-appraisal in Alzheimer's disease, mild cognitive impairment and normal aging: An fMRI study. **Zamboni G.**, Drazich E., McCulloch E., Tracey I., Wilcock G. Alzheimer's Association International Conference on Alzheimer's Disease 2010 (ICAD), 10-15th July, Honolulu, Hawaii (USA)
- The structural and functional neuroanatomy of successful visuospatial learning in normal aging. **Zamboni G.**, Drazich E., Jenkinson M., De Jager C., Smith A.D., Tracey I., Wilcock G. Alzheimer's Association International Conference on Alzheimer's Disease 2010 (ICAD), 10-15th July, Honolulu, Hawaii (USA)
- Early brain correlates of later cognitive impairment in healthy elderly: a voxel-based morphometry MRI study. M. Tondelli, G. Wilcock, P. Nichelli, A.D. Smith, **G. Zamboni**.

XXX Congresso della Società Italiana di Neurologia, Catania (Italy), 23-27th October 2010.

- Resting and task-related fMRI in Mild Cognitive Impairment and Alzheimer's disease. **Zamboni G.**, Drazich E., Filippini N., McCulloch E., Tracey I., Wilcock G. Alzheimer's Association International Conference on Alzheimer's Disease 2011 (ICAD), 15-20th July, Paris (France).

Oral presentations and invited talks:

- Early brain correlates of later cognitive impairment in healthy elderly: a structural MRI study. **Zamboni G.**, Tondelli M., de Jager C., Smith A.D., Wilcock G. *Platform presentation, British Geriatric Society Autumn Meeting 2010, Brighton, 4th November 2010*
- Brain MRI procedures: how can they add to our knowledge about the symptoms and progression of Alzheimer's disease? **Zamboni G.** *Alzheimer's Research UK Public Meeting, Oxford, 19th March 2011*
- Impaired self-awareness in Alzheimer's dementia and Mild Cognitive Impairment. **Zamboni G.**, Drazich E., McCulloch E., Tracey I., Wilcock G. *British Neuropsychology Society Spring Meeting, London, 31st March 2011*
- Improved MRI characterization of structural and functional changes from preclinical to clinical Alzheimer's disease. **G. Zamboni.** *Invited talk, The Computational, Cognitive and Clinical Neuroimaging Laboratory (C3NL)-Brain Meeting, Imperial College, London, 20th March 2012*

Projects and grants awarded:

Sir Halley Stewart Trust (UK): "Imaging in dementia – the establishment of functional magnetic resonance imaging procedures for Alzheimer's disease"- £70000

Abbreviations

Aβ, amyloid beta

AD, Alzheimer's disease

ADLs, activities of daily living

AQ-D, Anosognosia Questionnaire-Dementia

ATL, anterior temporal lobe

BADLS, Bristol activities of daily living scale

BET, Brain Extraction Tool

BBR, Boundary-Based Registration

CDR, clinical dementia rating scale

CSF, cerebrospinal fluid

CT, computed tomography

DMN, default mode network

EPI, echoplanar imaging

FDG, fluorodeoxyglucose

FEAT, FMRI Expert Analysis Tool

FDG-PET, 18-fluorodeoxyglucose positron emission tomography

FIRST, FMRIB's Integrated Registration & Segmentation Tool

FLAIR, fluid attenuated inversion recovery

FMRI, functional magnetic resonance imaging

FMRIB, Oxford centre for Functional MRI of Brain

FNIRT, FMRIB's Non-linear Image Registration Tool

FSL, FMRIB's Software Library

FWHM, full width at half maximum

GDS, geriatric depression scale

GM, grey matter

GLM, general linear model

HC, healthy control

HVLT-R, Hopkins verbal learning test-revised

ICA, Independent Component Analysis

MCI, mild cognitive impairment

MELODIC, Multivariate Exploratory Linear Optimized Decomposition into Independent Components

MMSE, Mini-Mental State Examination

MNI, Montreal Neurological Institute

MoCA, Montreal Cognitive Assessment

MPFC, medial prefrontal cortex

MRI, magnetic resonance imaging

MTL, medial temporal lobes

NFTs, neurofibrillary tangles

NPI, neuropsychiatric inventory

LPFC, lateral prefrontal cortex

OCMR, Oxford Centre for Magnetic Resonance imaging

OPTIMA, Oxford Project to Investigate Memory and Ageing

OXMAC, Oxford Memory Assessment Clinic

PET, positron emission tomography

PiB, Pittsburgh compound-B

PCC, posterior cingulate cortex

PNM, physiological noise modelling

PPC, precuneus and posterior cingulate cortex

ROI, region-of-interest

RSNs, resting state networks

SIENA, Structural Image Evaluation (with Normalisation) of Atrophy

TFCE, Threshold-Free Cluster Enhancement

VBM, voxel-based morphometry

List of figures

Chapter 7

16. Summary of imaging studies on anosognosia in dementia
17. Self and other-appraisal fMRI paradigm
18. Within-group results of self- and other-appraisal fMRI
19. FMRI results: conditions comparison in AD and interaction group-by-condition
20. FMRI results of event-related follow-up analysis

List of Tables

Preface

As treatment of Alzheimer's disease (AD) moves toward the identification of therapies targeting abnormalities occurring in the pre-dementia phase, the importance of early and accurate diagnosis is increasing, as is the need for sensitive measures for tracking disease progression and response to treatments.

The aim of the work reported in this thesis was to improve the characterisation of the changes in brain *structure* and *function* that occur at different stages of the continuum that goes from pre-symptomatic AD to mild cognitive impairment (MCI) to clinically evident dementia, using advanced MRI techniques.

Previous research has shown that *structural* MRI can detect changes in brain structure in the AD phase (once clinical diagnostic criteria for dementia are fulfilled) and possibly also in the MCI phase (once the earliest cognitive symptoms become measurable). However, less is known about whether structural changes are detectable earlier, in the preclinical, asymptomatic phase preceding MCI. Indeed, grey matter atrophy is still considered a late or downstream event in the pathology of AD. Thus, the aim of the first part of the research presented in this thesis was to further explore whether changes in morphology are detectable even in the preclinical phase of the disease, and whether they match inter-subject variability in cognitive functioning in older adults. The potential sensitivity of structural MRI to early changes in cognitive abilities was explored using data from cognitively healthy older adults, some of whom developed MCI or dementia, followed prospectively for ten years.

As for *functional* MRI (fMRI), previous studies have shown decreased task-related functional activity in patients with AD compared to healthy controls, variable results in MCI patients, and even less consistent results in comparisons between the three groups with respect to resting functional connectivity. Therefore, the aim of the second part of the research presented in this thesis was to improve the characterization of the functional changes in both MCI and AD

patients with respect to cognitive performance and underlying structural changes (which in these phases are already significant). To achieve this, another group of healthy controls and patients with MCI and AD were recruited and underwent a multimodal MRI protocol, which included *structural* MRI sequences and *functional* MRI sequences acquired during resting wakefulness and during the execution of two different cognitive tasks (visuospatial associative memory and self-appraisal). Cross-sectional analyses tested whether task-related functional activity shown by patients with MCI and AD during visuospatial associative memory reflected efficient residual function and whether it overlapped with brain networks/circuits showing altered functional connectivity. Finally, the functional activity elicited by a self-appraisal task, which does not directly test memory and is relatively easy for patients to perform, was examined for its ability to inform about the cognitive mechanisms of unawareness of cognitive impairment (anosognosia) in MCI and AD patients, a symptom with significant implications for diagnosis, especially in the pre-dementia phases.

The structure of the thesis is as follows:

- *Chapter 1* contains an overview of AD, including a brief description of different pathogenic hypotheses and a critical discussion of the recently proposed revisions of diagnostic criteria that emphasise the current view that dementia is the final stage of a process that begins much earlier, but remains "sub-clinical" for years. A brief discussion of the currently available non-MRI *biomarkers* will be presented in this chapter.
- *Chapter 2* focuses on the role of MRI imaging in the diagnosis and characterization of different phases of AD. Status of knowledge, advantages and limitation of structural MRI, task-related fMRI, and resting fMRI will be discussed separately, highlighting which unsolved issues and research questions this thesis was aimed to address. At the end of this chapter the specific aims and research questions of this thesis are described in detail.

- *Chapter 3* describes experimental findings from T1-weighted structural MRI in a group of cognitively healthy older adults followed longitudinally for ten years with clinical and neuropsychological assessments. Differences between those who remained cognitively healthy for 10 years and those who developed MCI and AD were explored using a whole-brain statistical methodology.
- *Chapter 4* describes experimental findings from structural MRI in the same group of healthy older adults (although at a slightly different time point) in relation to their performance on cognitive testing of visuospatial associative memory. It also introduces the novel paradigm for fMRI that was set up on the basis of these results and performed by another group of newly recruited healthy older adults. It then describes the overlapping findings of this multimodal (structural and functional) approach.
- *Chapter 5* introduces the second part of the thesis and describes the imaging protocol and experimental procedures employed to investigate cross-sectional differences between patients with probable AD, patients with amnestic MCI, and age-matched healthy controls. A thorough description of participant recruitment strategy, study design, and imaging analysis methods is provided.
- *Chapters 6 and 7* report the experimental findings of the multi-modality MRI protocol described in *Chapter 5*. More precisely, *Chapter 6* describes results of task-related fMRI of visuospatial associative memory in association with results of resting fMRI; *Chapter 7* presents results of task-related fMRI of self-appraisal, following a brief review on imaging of unawareness of disease. Functional results will be characterized with respect to cognitive performance as well as structural changes.
- Finally *Chapter 8* contains a summary of the main findings reported, the conclusions of the research presented in the thesis, the directions for future studies and potential applications.

Chapter 1

Alzheimer's disease in the era of biomarkers

1.1 Alzheimer's Disease (AD)

Alzheimer's disease (AD) is a progressive neurodegenerative disorder characterized by the gradual onset of cognitive impairment and loss of functioning. In 1906, a German psychiatrist and neuropathologist named Alois Alzheimer presented for the first time the clinical symptoms of the disease that were later renamed in his honour (Alzheimer, 1907; Alzheimer, 1911). More than a century later, AD is the most common form of dementia, one of the most frequent diseases in the aging population, the main cause of disability in later life, and the fourth most common cause of death (in high-income countries). According to the World Alzheimer report, in 2010 there were an estimated 36.5 million people worldwide living with dementia, and that number is estimated to almost double every 20 years, to 65.7 million in 2030, and 115.4 million in 2050 (http://www.alz.co.uk/research/world-report). The increase is mainly due to the fact that incidence of AD increases exponentially with age after 60 years and life expectancy is expected to increase, but also because of the current absence of disease-modifying therapies. These factors make AD a significant public health problem with enormous cost for both the individual and society (i.e., estimated world cost was 600 billion US dollar in 2010). In addition, poor recognition, "under-diagnosis" and stigma cause significant problems for people with AD and their families and this has an enormous impact on societies. Thus, the last World Alzheimer report advocated that the World Health Organization (WHO) should declare dementia a world health priority.

1.1.1 Neuropathology and pathophysiology

Brains of patients with AD demonstrate neuronal loss and shrinkage of large cortical neurons with synaptic degeneration, which are thought to ultimately mediate the cognitive and behavioural manifestations of the disorder because of their high correlation with dementia severity (Bobinski et al., 2000). At macroscopic level, this is reflected in widespread atrophy, which predominantly involves the medial aspect of the temporal lobe then spreads throughout the brain in late stages of the disease.

Histological hallmarks of AD include those initially described by Alzheimer and are now referred to as senile or neuritic plaques and neurofibrillary tangles (NFTs).

Neuritic plaques are extracellular structures composed of an amyloid core surrounded by a layer of degenerating neurites and reactive glia. The amyloid core contain β-amyloid protein (Aβ), a 40-42 amino acid peptide that is derived from the proteolytic cleavage of the large transmembrane amyloid precursor protein (APP) (Masters et al., 1985). Aβ is produced during normal cell metabolism and forms soluble oligomers, which aggregate into insoluble fibrils. Fibrils accumulate into an insoluble extracellular β-pleated sheet that forms the neuritic plaque. Longer forms, especially the 42 amino acid variant ($A\beta_{1-42}$), are more insoluble and particularly prone to fibril formation. Neuritic plaque burden was previously thought to correlate with AD severity, but more recent evidence suggests that the oligomeric forms of Aβ may be responsible for symptomatic synaptic dysfunction (Lacor et al., 2004). Some investigators have suggested that sequestration of Aβ into fibrillar forms may even serve as a protective mechanism against oligomeric forms of Aβ that are toxic for synapses (Lee et al., 2004).

Neurofibrillary tangles (NFTs) are intraneuronal cytoplasmic inclusions composed of hyper-phosphorylated tau (Grundke-Iqbal et al., 1986). Normal tau is an axonal protein associated with microtubule binding and stabilization. Its abnormal phosphorylation, which occurs in several neurodegenerative disorders, causes disruption of microtubules and alters the

neuron's transport system, ultimately causing neuronal death (Iqbal et al., 2005). Deposition of NFTs begins in the entorhinal cortex then spreads to the hippocampus and amygdala then accumulate in association cortex (Braak and Braak, 1997, 1991). The evolution of NFT pathology correlates with measurements of cognitive impairment (Arriagada et al., 1992; Braak and Braak, 1991), as well as with the degree of brain atrophy detected by structural MRI (Whitwell et al., 2008a). In addition to neuritic plaques and NFTs, many other histopathological lesions have been described in AD, including the granulovacuolar degeneration and neuropil threads (Braak and Braak, 1991).

Amyloid versus tau hypotheses

A central but controversial issue in the pathogenesis of AD is the relationship between amyloid deposition and NFT formation and their role in disease onset and progression. According to one of the most prominent views known as "amyloid cascade hypothesis", AD pathophysiology begins with the abnormal processing of the transmembrane APP and aggregation of the more insoluble resulting peptides, mostly $A\beta_{1-42}$, into fibrils that form the neuritic plaques. Subsequently, it is thought that the microtubule-associated tau protein in neurons becomes abnormally hyper-phosphorylated and forms NFTs that disrupt neurons. Oxidative and inflammatory stresses contribute to loss of synaptic and neuronal integrity, and eventually, neuron loss results in brain atrophy (Hardy and Higgins, 1992; Hardy and Selkoe, 2002). According to this aetiopathogenetic hypothesis, secretase inhibition, inhibition of β-sheet formation, or immunomodulation of serum β-amyloid concentrations are potential targets for therapies to prevent or slow AD pathology. However, these strategies have not proved effective in human clinical trials to date. In addition, although animal models suggest that isoforms of Aβ may cause synaptic changes, it remains unknown whether they are sufficient to trigger the neurodegenerative process in sporadic AD. Thus, according to a different aetiopathogenetic hypothesis, AD is instead triggered by a variety of factors affecting tau

phosphorylation (Iqbal et al., 2005). Abnormal hyper-phosphorylation of tau directly leads to neurodegeneration. According to this hypothesis, inhibition of tau protein kinases, activation of the tau phosphatases, and promotion of the clearance of the abnormally hyper-phosphorylated tau are potential targets for therapies to prevent or slow AD pathology (Gong et al., 2010).

Other factors

Several other processes have been implied in the AD pathogenesis. They include oxidative stress, Ca2+ dysregulation, inflammation, and cerebrovascular disease, which can all potentially lead or contribute to synaptic dysfunction and neurodegeneration (Pimplikar et al., 2010).

Studies have demonstrated that an increase in oxidative damage selectively occurs within the brain regions involved in regulating cognitive performance and that indexes of oxidative damage are significantly increased in AD brain tissue compared with age-matched controls (Ding et al., 2007). Increased intracellular calcium has also been shown to damage various cellular components such as proteins, DNA, and lipids and may result in apoptotic cellular death. As for inflammatory processes, it has been shown that reactive microglia are embedded in neuritic plaques, and that cytokines and complement fragments are increased in the serum, cortical plaques, and neurons of patients with AD. However, whether markers of immune and inflammatory processes actively participate in the neurodegenerative process or instead represent an epiphenomenon remains unclear. In addition to the effects of inflammatory processes taking place in the brain, it should also be mentioned that systemic, peripheral inflammatory processes might also have a role in AD (Holmes and Butchart, 2011). This may occur through a direct effect of pro-inflammatory cytokines on the blood-brain barrier, or through their indirect effect on cerebral vasculature.

Finally, the role of cerebrovascular disease in AD is increasingly been considered. Epidemiologic studies have shown that, in particular in the elderly subjects, vascular risks factors and indicators of vascular pathology are associated with cognitive impairment and AD (Snowdon et al., 1997; Hofman et al., 1997). Related to this, it has been demonstrated that the relationship between the neuropathological hallmarks of AD (NFTs and neuritic plaques) and the presence of clinical dementia decreases with advancing age, further suggesting that clinical dementia in the elderly is a multifactorial and heterogeneous disorder (Savva et al., 2009). On histopathology, very rarely the histological hallmarks of AD occur in isolation: indeed, most elderly subjects have some degree of cerebrovascular disease as well as some AD type pathology (Esiri et al., 1999). Although the effects of the two types of pathology may "summate independently", recent evidence is showing that cerebrovascular disease in isolation needs to be relatively severe to be associated with dementia (Smallwood et al., 2012; Pantoni et al., 2005; Lee et al., 2011).

1.1.2 From pathophysiology to biomarkers

According to the Biomarkers Definitions Working Group, a "biomarker" is defined as "a characteristic that is objectively measured and evaluated as an indicator of normal biological processes, pathogenic processes, or pharmacologic responses to a therapeutic intervention" (2001). As such, biomarkers have many applications in several phases of disease detection and monitoring, including the following:

(i) early diagnosis

(ii) staging of disease or classification of the extent of disease

(iii) prognosis

(iv) prediction and monitoring of clinical response to interventions.

Among the several biomarkers proposed for AD up to now (Hampel et al., 2008; Blennow et al., 2010; Johnson et al.), the most validated are the following:

- CSF $A\beta_{1-42}$ levels decrease in AD and correlate with neuritic plaque load in the brain (Strozyk et al., 2003). The most widely accepted explanation for the reduction in CSF $A\beta_{1-42}$ in AD is that aggregation of Aβ into plaques (and, hence, retention of the peptide in the brain parenchyma) results in reduced availability of Aβ to diffuse into the CSF (Blennow et al., 2010).
- CSF total tau (t-tau) levels increase in AD but also in other conditions in which neuronal and axonal damage occurs, including tissue damage (stroke or brain trauma) or rapid neuronal degeneration (Creutzfeldt–Jakob disease). Increased CSF t-tau has also been associated with faster progression from MCI to AD and with rapid cognitive decline in AD (Samgard et al., 2010).
- CSF phosphorylated tau (p-tau) levels increase in AD and reflect both the phosphorylation state of tau and the formation of NFT in the brain. Instead, it is normal in Creutzfeldt–Jakob disease or acute stroke. Thus, increased p-tau is considered specific for AD and differentiates AD from other dementias, including frontotemporal dementia and dementia with Lewy bodies (Hampel et al., 2004). In addition, it has been associated with increased risk of progression from MCI to AD and with rapid cognitive decline in AD.
- Positron emission tomography (PET) with ^{18}fluorodeoxyglucose (^{18}FDG) in patients with AD shows a typical pattern of reduced cortical uptake in posterior and lateral temporal regions, medial parietal regions, particularly in the posterior cingulate gyrus and precuneus, and medial temporal lobes including hippocampus; with progression of the disease, metabolic deficit spreads to prefrontal association areas as well (Foster et al., 1983; Chase et al., 1984). FDG hypo-metabolism parallels cognitive function and

histopathological diagnosis of AD at autopsy (Furst et al., 2012; Hoffman et al., 2000), and can predict conversion to MCI in the elderly (de Leon et al., 2001).

- PET with tracers targeting insoluble fibrillar Aβ [including the most studied Pittsburgh Compound-B (PiB), but also the newly developed fluorine-18-labelled tracers (florbetaben, florbetapir, flutemetamol)] in patients with AD shows abnormal uptake in regions of the cortical midline (medial prefrontal cortex, posterior cingulate and precuneus) and lateral temporal-parietal associative cortex. Several studies have shown that increased uptake occurs in about 95% of patients with a clinical diagnosis of AD, 60% of patients with a clinical diagnosis of MCI, 93% of patients with MCI who then progressed to AD within 3 years, and 24% of cognitively normal controls who may be in the preclinical phase of AD [percentages taken from a review study (Johnson et al.)]. Indeed, it is thought that, by being a direct surrogate for Aβ pathology, amyloid PET has the potential to detect the very beginnings of AD pathophysiology in the asymptomatic stage.
- Structural MRI in patients with AD shows atrophy especially prominent in the medial temporal lobes and medial regions of parietal lobes. *Chapter 2* of the present thesis describes in detail current knowledge about structural MRI.

Based on the amyloid cascade hypothesis, a hypothetical model on the temporal order in which biomarkers of AD become abnormal during the natural history of AD has been recently proposed (Jack et al., 2011a; Jack et al., 2010). It assumes that, in accordance with the amyloid cascade hypothesis, the first biomarkers to become abnormal "pre-clinically", i.e. before the earliest symptoms manifest, are CSF $A\beta_{1-42}$ and amyloid PET, which are classified as "biomarkers of amyloid". Secondly and in proximity of the clinical presentation of cognitive problems, other biomarkers that reflect neuronal damage and synaptic dysfunction become abnormal. These include increased CSF tau, abnormal FDG-PET, and, ultimately, atrophy on

structural MRI, which are classified as “biomarkers of neurodegeneration” and correlate closely with cognitive symptoms.

This model has been criticised for its bias towards the amyloid cascade hypothesis when this has not been conclusively proven. In addition, the correspondence between pathophysiology and biomarkers of amyloid deposition and neurodegeneration may be too simplistic, as it may be that a certain biomarker does not fit perfectly on the causal pathway between pathogenesis and resulting clinical symptoms. As an example, it is still unclear whether Aβ deposition is a causal factor for developing the clinical syndrome of AD or whether its accumulation represents an epiphenomenon of early AD (Lee et al., 2004).

In addition, recent imaging studies (including the research study reported in *Chapter 3* of the present thesis) have shown that structural MRI can become abnormal early in the preclinical phase of AD and up to ten years before clinical symptoms, challenging the view that changes in brain structure are a relatively late event in the progression to AD (Dickerson et al., 2011; Tondelli et al., 2011).

1.1.3 Diagnostic criteria

For almost 30 years clinical diagnosis of AD has been based on a two-step process: (i) identification of a *dementia* syndrome and (ii) identification of clinical features suggestive of *AD*. The Diagnostic and Statistical Manual of Mental Disorders, Fourth Edition (DSM-IV) criteria characterised *dementia* as gradual and progressive decline in cognitive function with impairments in recent memory and one additional cognitive domain (i.e., aphasia, apraxia, or disturbed executive functions) that is not due to other medical or psychiatric illness, and results in impairment in social or occupational functioning (American Psychiatric Association, 1994). The National Institute of Neurological and Communicative Disorders and Stroke and the Alzheimer's Disease and Related Disorders Association (NINCDS-ARDA) characterised ''probable AD'' on the presence of deficits in two or more areas of cognition, including memory, that are progressively worsening, confirmed by clinical and neuropsychological testing, not associated with delirium or other brain/systemic illnesses that could be the cause of the dementia (McKhann et al., 1984). The diagnosis is further supported by impaired function in activities of daily living (ADLs) and the presence of a family history. ''Definite AD'' required clinical features for probable AD and autopsy confirmation. The main limitations of these criteria are that they exclude recent advances in the fields of imaging and CSF biomarkers, and lack of specificity in distinguishing non-AD dementias. However they were used in the research presented in this thesis because we included data collected before new criteria were proposed (see below) and for consistency with existing literature.

In 2007, new criteria were proposed with the aim of diagnosing AD at the earliest stage and to improve specificity in detecting clinical presentation typical for AD (Dubois et al., 2007). They emphasise the role of significantly impaired episodic memory on testing and also introduce the role abnormal biomarkers, namely (1) structural MRI, (2) CSF Aβ or tau, or (3) FDG- or amyloid-

PET. “Probable AD” is defined by the fulfilment of clinical core criteria plus at least one of supportive biomarker criteria.

In 2010, the National Institute on Aging (NIA) and Alzheimer’s Association convened expert panels to revise and update diagnostic criteria for AD, which were published in April 2011 (McKhann et al., 2011). The authors emphasised the distinction between *AD dementia* as a clinical syndrome and *AD pathophysiology* as the set of pathophysiological changes due to AD that are found along the entire disease course, from the preclinical phase to the phase of symptomatic dementia. These criteria are broad enough to include non-amnestic and atypical presentations (i.e., posterior cortical atrophy and logopenic aphasia). Biomarkers are only included for use in research settings, but not among the core criteria, as the authors acknowledge that they may not be always available in clinical settings and are still not necessary for the clinical diagnosis of AD dementia. However, biomarkers enhance the likelihood that *AD dementia* is specifically associated with *AD pathophysiology.*
Criteria for *all-cause dementia* are similar to the DSM-IV criteria except that memory impairment is not considered the *sine qua non* condition anymore, but can be one of at least two impairments of cognitive domains or behaviour necessary to give a clinical diagnosis of dementia. *Core clinical criteria for AD* include criteria for all-cause dementia criteria plus insidious onset, clear-cut history of worsening of cognition by report or observation, either amnestic or non-amnestic presentations, and the absence of elements suggestive of cerebrovascular disease, other neurodegenerative dementias, or other active neurological or non-neurological medical conditions.

1.2 Mild Cognitive Impairment (MCI)

1.2.1 Diagnostic criteria

The transition from normal ageing to dementia is a continuous process that progressively involves, to a variable extent and in different stages, episodic memory, executive functions, language, and visuospatial skills (Backman et al., 2004). This transitional state is often characterized as mild cognitive impairment (MCI) (Albert et al., 2011; Petersen et al., 1999; Winblad et al., 2004), but has also been indicated as pre-dementia or prodromal dementia (Dubois and Albert, 2004).

MCI

The term "mild cognitive impairment" was first used in 1999 (Petersen et al., 1999). Petersen and colleagues emphasized memory impairment, either reported subjectively or measured with cognitive testing, as the central diagnostic criterion. Broader conceptualizations were later undertaken to also include impairment of different cognitive domains that would possibly capture transitional stages leading to other, non-AD dementias. In addition, distinctions between amnestic MCI and non-amnestic MCI, as well as between single- or multiple-domain were introduced (Winblad et al., 2004). Updated criteria for MCI include the following:

1. Cognitive and functional status judged not normal, but also not consistent with a diagnosis of dementia (as defined by DSM IV);
2. Presence of cognitive decline established by the presence of memory complaints reported by participant or informant and/or by the evidence of decline over time on objective neuropsychological testing;
3. Intact functional status, with preserved basic activities of daily living or only minimal impairment in complex instrumental functions.

These criteria are currently used in several longitudinal databases and cohorts, such as the Alzheimer's disease Neuroimaging Initiative (ADNI, http://adni.loni.ucla.edu) and the Oxford Project to Investigate Memory and Ageing (OPTIMA, http://www.medsci.ox.ac.uk/optima) and have been used in numerous clinical trials on MCI (Feldman et al., 2007; Petersen et al., 2005). They were also used in the research presented in this thesis.

Prodromal AD

The concept of MCI raised controversy in relation to its clinical heterogeneity and lack of specificity in predicting AD (Dubois, 2000). As an alternative, criteria for "prodromal AD" were proposed in 2004. They focus on the pattern of deficits on neuropsychological examination and introduce the use of imaging and CSF biomarkers to exclude non-AD causes (Dubois and Albert, 2004). Although these criteria have been recently used in some studies to assess clinical efficacy and safety of novel drugs (Dubois et al., 2012), they have not yet replaced the use of the MCI criteria.

"MCI due to AD"

In 2011 the NIA and Alzheimer's Association also called for a revision of the criteria for the symptomatic pre-dementia phase of AD, which they termed "MCI due to AD" (Albert et al., 2011). They distinguished "core clinical criteria", which should be used in clinical settings, from "research criteria", which should be primarily used in research settings, but may also be used clinically in some circumstances and difficult cases. These newly proposed criteria are similar in principle to those for MCI described above, but do not mention distinction between amnestic or non-amnestic MCI and suggest considering additional information. More precisely, the *clinical* evaluation of "*MCI due to AD"* requires two steps: (i) to establish the presence of "clinical and cognitive criteria for MCI", (ii) to examine if the aetiology is consistent with the AD

pathophysiological process, for example considering genetic results or excluding alternative aetiologies.

The *research* criteria for "*MCI due to AD"* include the use of biomarkers, which are classified according to whether they reflect beta-amyloid pathology (decreased levels of $A\beta_{42}$ in the CSF, evidence of $A\beta$ deposition in PET scan) or neuronal injury (elevated levels of tau in the CSF, temporoparietal/precuneus hypo-metabolism or hypo-perfusion in PET or SPECT scans, atrophy of hippocampus or medial temporal lobes on structural MRI). These biomarkers are used to provide increasing levels of certainty that AD pathology is the cause of an individual's cognitive decline.

1.2.2 Predictors of conversion to AD

Between 4 and 6 % of all people over age 65 are diagnosed with amnestic MCI (Manly et al., 2005) and convert to AD at a variable rate of 12 - 19 % a year (Ravaglia et al., 2006; Fischer et al., 2007; Petersen et al., 2005). A major question in the field of MCI research concerns the ability to predict which MCI subjects are more likely to progress to dementia or AD more rapidly than others. All the biomarkers presented in chapter 1.1.2 and recently included among the research criteria for the diagnosis of MCI due to AD have been evaluated in longitudinal studies to test their predictive value:

- CSF biomarkers: studies have shown that the best predictors of conversion are scores that take into account both CSF $A\beta_{1-42}$ and either t-tau (Vemuri et al., 2009) or p-tau (Desikan et al., 2012), but not CSF $A\beta_{1-42}$ alone.
- PET imaging: studies indicate that AD patterns of FDG-PET at the MCI stage are predictive for progression to AD and that they may outperform other measures such as cognitive scores, and CSF biomarkers (Anchisi et al., 2005; Caroli et al., 2012; Drzezga et al., 2003; Drzezga et al., 2005). Several longitudinal studies have also

shown that amyloid imaging predicts conversion, with PIB-positive MCI subjects significantly more likely to convert to AD than PIB-negative patients at a rate above 80% over 12-to-36 months follow-up and faster converters having higher PIB retention levels at baseline than slower converters (Forsberg et al., 2008; Koivunen et al., 2011; Okello et al., 2009).

- Structural MRI: retrospective comparisons between MCI patients who remained cognitively stable and those who progressed to a clinical diagnosis of AD have highlighted the importance of atrophy in medial temporal structures (hippocampus and entorhinal cortex) but also other brain areas in predicting conversion to AD (Apostolova et al., 2006; Devanand et al., 2007; Vemuri et al., 2009; McEvoy et al., 2009; Whitwell et al., 2008b). Several groups have shown that information derived from quantitative structural MRI can provide information not only for discriminating groups of subjects, but also for predicting individual patient prognosis (Davatzikos et al., 2008; McEvoy et al., 2009). See chapter 2.2.2 for further discussion on the value of structural MRI in MCI.

Additional predictors of conversion to AD are clinical severity and apolipoprotein E (APOE) status. Patients who have more severe memory impairment are more likely to progress to AD than those with less severe memory impairment. Whether the patient with MCI is a carrier of the allele $\varepsilon 4$ of APOE gene, which is a well-known risk factor for the development of AD in general (Corder et al., 1993), also has a predictive value of progression from MCI to AD (Petersen et al., 1995).

1.3 Preclinical AD

1.3.1 Diagnostic criteria

Increasing evidence is showing that the earliest neuropathological changes associated with AD occur years before a diagnosis of dementia can be given clinically (Ohm et al., 1995; Smith, 2002a; Bateman et al., 2012). It has been suggested that the course of AD pathology is likely to be 20 to 30 years (Weiner et al., 2012). Several studies in preclinical populations have provided preliminary evidence that imaging and CSF biomarker abnormalities consistent with AD pathophysiology are detectable years before the emergence of overt clinical symptoms (Dickerson et al., 2011; Jack et al., 2009; Vemuri et al., 2009). In April 2011, the NIA and the Alzheimer's Association gave diagnostic guidelines aimed to define "preclinical AD", to be used only in research settings (Sperling et al., 2011). It was thought that defining a preclinical phase of AD would provide an opportunity for potential intervention with disease-modifying therapies in this phase. The authors based the guidelines on the current prevailing hypothesis about the pathophysiological mechanisms of AD (Hardy and Selkoe, 2002; Hardy and Higgins, 1992) and on the interpretative framework that suggests that biomarkers of brain Aβ amyloid deposition become abnormal first, then are subsequently followed by changes in biomarkers of neuronal injury or neurodegeneration (Jack et al., 2010) (see paragraphs 1.1.1 and 1.1.2). The guidelines for preclinical AD define three stages according to presence/absence of these biomarkers, each associated with increasing likelihood to progress to AD: 1) Asymptomatic cerebral amyloid deposition; 2) Amyloid positivity plus evidence of synaptic dysfunction and/or early neurodegeneration; and 3) Amyloid positivity plus evidence of neurodegeneration plus subtle cognitive decline (not typical for MCI).

The use of these biomarkers in the clinical setting is not recommended, as many individuals who satisfy the proposed research criteria may not develop the clinical features of AD in their lifetime.

Chapter 2

Brain MRI findings associated with MCI and AD

2.1 Brain MRI techniques and derived measurements

MRI is a powerful and flexible imaging modality, which does not use ionizing radiations, is non-invasive and relatively inexpensive in comparison with other imaging modalities such as PET and SPECT. Individuals can be imaged longitudinally without concerns about carcinogenicity. The advent and widespread use of MRI has revolutionised the clinical management of neurodegenerative diseases over the past two decades, and MRI scanners (1.5 or 3 Tesla) are available in the majority of hospitals of high-income countries. In many countries MRI is now considered part of the standard evaluation of patients assessed for dementia/cognitive impairment (Hort et al., 2010; Knopman et al., 2001; Sorbi et al., 2012). It provides not only clinical information (i.e., differential diagnosis between dementias and exclusion of treatable causes of such as tumours and hematoma) but also several research measures potentially useful (i) to investigate the natural history of neurodegenerative diseases and (ii) to evaluate the effects of novel treatments. At the time of the writing of this chapter, a literature search revealed a total of 14840 publications with key words of “AD” and “MRI” published since 1981.

Information obtained with brain MRI can be classified in two categories: structural and functional.

Structural MRI provides *static* anatomical information about brain macroscopic tissue morphology including atrophy or focal damage, for both Grey Matter (GM) and White Matter (WM) structures. It is acquired using high-resolution T1-, T2-weighted or diffusion tensor imaging (DTI) sequences. T1-weighted MRI is the preferred modality to examine GM as it provides particularly good contrast between GM and WM. The contrast used to obtain this

type of image is given by different T1 relaxation times, which are specific between different types of tissue. T1 relaxation time refers to the time hydrogen atoms require to revert back to the resting state on the longitudinal axis after having been tilted away from the direction of the magnetic field by the application of a radio-frequency pulse during the MRI scan. A number of tools of varying technological complexity, ranging from simple subjective rating scales to sophisticated computerized algorithms, have been developed to interpret T1-weighted images, either to study the volumes of *a priori* defined regions of interest (ROIs) or GM across the whole brain. ROI analyses have progressed from manual tracing of individual GM regions to fully automated segmentation methods. However these methods require *a priori* decisions concerning which structures are affected. In addition, important differences occurring outside of or overlapping the ROI may go unobserved (Ferreira et al., 2011). Instead, computational MRI data analysis methods based on voxel-based morphometry (VBM) or analysis of local cortical deformations can capture subtle changes/differences in the localisation of regional GM structure and provide maps of estimated atrophy without *a priori* focus on specific regions (Thompson et al., 2001; Ashburner and Friston, 2000, 2001; Busatto et al., 2008; MacDonald et al., 2000). Neuroanatomical features can be compared within and between groups of individuals, taking into account age, sex, and other variables, to assess the structural basis of normality and disease. Although there is potential to use these methods in single-case analysis, they need to be studied in much greater depth before being transferred to clinical practice (Ashburner et al., 2003).

Functional MRI provides *dynamic* physiological information about the brain. It relies on the Blood Oxygen Level Dependent (BOLD) contrast to measure haemodynamic signal changes related to neural activity. The majority of fMRI studies use ultra-fast MR imaging techniques such as echo planar (EPI), which are sensitive to the alterations in local tissue magnetic susceptibility effects due to the presence of an endogenous contrast (i.e., changes in the

concentration of deoxyhaemoglobin in the capillaries). The BOLD contrast is dependent upon local changes in the cerebral blood flow, cerebral blood volume, deoxyhaemoglobin concentration, local haematocrit, and changes in oxygen consumption. When a brain area is more active it consumes more oxygen and this increased demand causes the increase of blood flow to the active area (Ogawa et al., 1993; Ogawa et al., 1992). BOLD dependent fMRI can be used to produce activation maps showing which parts of the brain are involved in a particular mental process engaged when performing a task (task-related fMRI). *Task-related* fMRI imaging compares the levels of brain activity during task performance and a control condition ("baseline or "rest"), providing an indirect measurement of brain activity related to cognitive processing engaged in response to the specific task. BOLD signal changes following stimulation are generally small, in the order of 2-5%, and strongly dependent on the magnetic field strength used. The major drawback of using the BOLD signal to detect neuronal activity evoked by a certain task is that it requires a significant period of time of few seconds before it reaches its peak in a targeted brain region, whereas neuronal activation following stimulation happens in a range of few milliseconds. This delay affects the temporal resolution of fMRI. In addition, there is criticism about the use of the BOLD signal in mapping neuronal activity. For example, some authors believe that BOLD signal changes are generated more by synaptic than neuronal body activity thus activations may be located significantly far from the true site of neuronal activation (Arthurs and Boniface, 2002). Moreover, as synaptic activity can be either excitatory or inhibitory, the interpretation of fMRI results may be less straightforward than is currently believed (Logothetis, 2008).

Spontaneous fluctuations of BOLD signal can also be studied in the absence of tasks, while participants are at rest (resting fMRI). *Resting* fMRI measures low-frequency spontaneous fluctuations (0.01-0.1 Hz) that are temporally correlated and correspond to resting-state networks (RSNs). Commonly identified networks include: visual, auditory, sensory-motor,

default-mode, executive control and fronto-parietal RSNs (Beckmann et al., 2005). Mapping these spontaneous fluctuations at rest can indirectly inform on functional networks utilized by the brain in action (Smith et al., 2009). The amplitude of these fluctuations of the BOLD signal is comparable with that displayed in task-related experiments (Damoiseaux et al., 2006). Resting fMRI has only relatively recently been shown to be abnormal in clinical populations. It has a great potential, as it can be acquired in relatively short time and does not require a cognitive task to be performed within the MRI scanner.

2.2 Structural T1-weighted MRI

It is currently well established that GM volume as measured by structural MRI decreases along the continuum that goes from preclinical to clinically evident AD, paralleling the loss of cognitive function. The GM volume loss (also indicated as cerebral atrophy) reflects a decrease in synaptic density, neuronal loss and cell shrinkage. In addition, it may also reflect alterations in glial cell's density and volume (Rodriguez and Verkhratsky, 2011), and fluid shifts from brain parenchyma to CSF spaces (Fox et al., 2005).

Imaging-autopsy studies have shown that regional volumes of critical structures (i.e. hippocampus) measured with manual or automated techniques on *ante* mortem structural MRI are closely related to *post* mortem neuronal counts (Bobinski et al., 2000) and NFTs deposition measured with Braak stages (Gosche et al., 2002; Jack et al., 2002). Similarly, computer-based imaging techniques assessing distribution of atrophy in the whole brain showed that the topographical pattern of atrophy parallels the distribution of NFTs in later disease stages (Whitwell et al., 2008a) and Braak stages (Vemuri et al., 2008). In addition, several studies have shown that the amount, distribution, and rate of volume loss are all closely correlated with cognitive deficits as tested by neuropsychological assessment, both cross-sectionally and longitudinally (Vemuri et al., 2008; Ridha et al., 2008).

The fact that cerebral atrophy starts early and continues in the advanced phases and correlates well with clinical decline has led to atrophy on MRI being suggested as a marker of disease progression and a potential outcome measure in trials (Ridha et al., 2008; Fox et al., 2000). Thus, whereas markers of amyloid and tau pathology indicate the presence of AD pathology, clinical state is better captured by the extent of neurodegeneration, for which atrophy may be considered an in vivo measure.

2.2.1 Structural MRI in AD

Several studies conducted over the past 20 years have shown that in patients with a clinical diagnosis of AD (i.e., fulfilling diagnostic criteria for dementia) structural MRI shows significant and extended atrophy compared with age-matched controls (Jack et al., 1992; Busatto et al., 2008).

Early MRI studies only focused on regional volumes of single structures, especially the memory-related structures of the medial temporal lobes (MTL), which are among the earliest sites of pathologic involvement (Braak et al., 1998). They repeatedly showed that volumes of the hippocampus and entorhinal cortex in patients with AD are significantly decreased compared with age-matched controls (Kesslak et al., 1991; Jack et al., 1992; Jack et al., 1997; Chan et al., 2001), with the degree of atrophy correlating with memory impairment. Several rating scales have been developed to quantify the degree of atrophy and are widely used. They provide 80–85% sensitivity and specificity to distinguish patients with AD from those with no cognitive impairment (Duara et al., 2008; Scheltens et al., 2002). Longitudinal studies using manual or automated techniques to calculate rates of hippocampal atrophy from serial MRIs obtained 6 months or 1 year apart observed that there is a significant difference between the rate of change in patients with AD (3–6% per year) and the rate in control subjects (0.3–2.2% per year). Sensitivity and specificity are approximately 90% for predicting the decline in

dementia, thus superior to medial temporal lobe atrophy extracted from baseline MRI only (Fox et al., 1996a; Jack et al., 2000; Barnes et al., 2007; Barnes et al., 2008a; Barnes et al., 2004; Barnes et al., 2008b).

Computer-based imaging techniques for quantitative MRI have allowed for efficient characterisation of the amount and distribution of atrophy across the whole brain and outside of the MTL (Ashburner et al., 2003; Fischl and Dale, 2000). They revealed that by the time AD is diagnosed clinically atrophy already involves, in addition to the MTL, the parietal and posterior superior temporal regions on the lateral cerebral surfaces, posterior portion of the cingulate gyrus on the medial surface, and cortical association areas including prefrontal cortices (Scahill et al., 2002; Busatto et al., 2008; Fennema-Notestine et al., 2009a).

The sequence of progression of atrophy on MRI from structures of MTL to posterior cingulate/precuneus, to temporal neocortex and other association areas most closely fits histopathological studies that have derived stages for the spread of neurofibrillary tangles (Braak and Braak, 1991). Nonetheless, a significant minority of AD cases have atypical presentations and in these cases the pattern of atrophy accords with clinical phenotype: with language presentations particularly having left temporal atrophy and visual variants having posterior cortical atrophy.

Structural MRI has also been studied to differentiate AD from other types of dementia and specific features have been incorporated into diagnostic criteria of non-AD dementias (McKeith et al., 2005; Neary et al., 1998; Roman et al., 1993). In patients with the behavioural variant of FTD, frontal lobe volumes are reduced compared with those of both AD patients and age-matched controls (Rosen et al., 2002a; Rosen et al., 2002b). Semantic dementia is associated with asymmetrical anterior temporal lobe atrophy, while progressive nonfluent aphasia is associated with left perisylvian atrophy (Gorno-Tempini et al., 2004). Hippocampal atrophy has been reported in patients with dementia with Lewy bodies (DLB), although to a lesser degree than in AD when matched for clinical severity (Burton et al., 2009).

It should be noted that the typical distribution of atrophy associated with AD is different from the distribution of volumetric chances occurring with normal ageing. Although it has been shown that a certain, minimal degree of hippocampal shrinkage also occurs in normal ageing (Scahill et al., 2003), both cross-sectional and longitudinal studies have shown that, in healthy older adults, age-related volume reduction is more pronounced in prefrontal medial regions, whereas shrinkage of sensory and mediotemporal cortices is minimal (Raz et al., 2007).

2.2.2 Structural MRI in MCI

Several studies have shown substantial differences in brain atrophy between patients with MCI and healthy controls especially prominent in the medial temporal lobe (hippocampus and entorhinal cortex) [for review see (Ries et al., 2008; Fennema-Notestine et al., 2009b)], but also in regions outside MTL, namely in the lateral temporal lobes, medial parietal lobes (retrosplenial, posterior cingulate and precuneus cortices), and lateral associative parietal areas (Hamalainen et al., 2007b; Karas et al., 2004).

However, the most important challenge of MRI studies in MCI has been to differentiate MCI subjects who will progress to AD in the near future (converters) from those who will remain stable (non-converters). Numerous studies have investigated early signs of future conversion in MCI patients based on various structural MRI measurements. Those constraining analysis to structures of MTL (using either manual tracing methods or automated segmentation techniques) have found that lower baseline hippocampal volume is related to progression to AD, with variable sensitivity and specificity ranging between 50 and 80% (Jack et al., 1999; Apostolova et al., 2006; Costafreda et al., 2011). A recent meta-analysis estimated that baseline medial temporal atrophy has 73% sensitivity and 81% specificity for predicting whether patients with amnestic MCI will convert to AD dementia (Yuan et al., 2009). Likewise, longitudinal studies measuring rates of change in regional volume have found that the

hippocampus has greater rates of change in converters than non-converters (Jack et al., 2000; Jack et al., 2005; Chetelat et al., 2008), and that these rates increase close to the time of conversion, but start to change (at 0.3% per year) in the 2-4 years before clinical diagnosis of AD (Jack et al., 2008). Instead, other studies have reported the entorhinal cortex to be a more-sensitive predictor of progression than the hippocampus (Dickerson et al., 2001; Killiany et al., 2002). Studies using VBM for whole-brain analysis have also found the involvement of the hippocampus in regions of greater atrophy in converters relative to non-converters (Chetelat et al., 2005; Whitwell et al., 2008b; Hamalainen et al., 2007b; Karas et al., 2008). Areas outside the MTL, including the fusiform gyrus and lateral temporal lobes (Hamalainen et al., 2008; Karas et al., 2008; Risacher et al., 2009), the posterior cingulate and precuneus (Chetelat et al., 2005), and associative parietal areas (Chetelat et al., 2005; Bozzali et al., 2006) have been variably identified. However, significant findings in extra-MTL regions have not been consistently replicated, and a recent meta-analysis carried out on VBM analyses has shown that amongst the 6 longitudinal studies contrasting stable and converting MCI at baseline, only 2 studies found one common cluster located in the left hippocampus and parahippocampal gyrus (Ferreira et al., 2011). After having shown significant group differences between converters and stable MCI, several studies have focused in finding measures or scores derived from quantitative structural MRI that can provide information that can be given to individual subjects to predict their prognosis (Davatzikos et al., 2008; McEvoy et al., 2009).

2.2.3 Structural MRI in preclinical AD and people at risk

Longitudinal studies on individuals who subsequently develop sporadic AD have mainly studied subjects in the MCI phase, i.e. who already have some cognitive symptoms, and have followed them longitudinally to test for conversion to AD for variable periods of 18-36 months (Ferreira et al., 2011). Relatively little is still known about the preclinical phase of sporadic AD. Only a

few studies focused on healthy subjects who later converted to MCI or AD thus following them for periods of up to 6 years to study if baseline brain structure was already different in the preclinical phase (Kaye et al., 1997; den Heijer et al., 2006; Hall et al., 2008; Rusinek et al., 2003; Smith et al., 2007; Martin et al., 2010). Among these, the studies that used VBM to differentiate subjects who would have developed AD from controls, showed heterogeneous results highlighting the role of atrophy in the MTL in combination with that in anterior-lateral temporal regions as long as 5.4 years before development of clinical symptoms suggestive of MCI (Smith et al., 2007), or in the basal forebrain as long as 4.5 years before the development of clinical symptoms suggestive of AD (Hall et al., 2008). A study by den Heijer and colleagues on a large cohort of more than 500 cognitively healthy people found that that ROI-based measurements of hippocampus and amygdala volumes were strongly associated with the risk of dementia, and that they were already decreased by 5% in baseline structural MRIs of cognitively healthy adults who would develop dementia in 6 years (den Heijer et al., 2006). A longitudinal study by Rusinek and colleagues found that in a group of 45 healthy elderly followed longitudinally for 6 years with serial MRIs, the rate of atrophy in MTL, through its interactions with sex and age, was the most significant predictor of cognitive decline (Rusinek et al., 2003).

One of the aims of the research presented in this thesis was to establish whether changes in brain structure occur even earlier, up to 10 years before clinical diagnosis of sporadic AD (see paragraph 2.5 and *Chapter 3*).

Very recently Dickerson and colleagues also looked at baseline structural MRIs of healthy subjects who developed clinical AD within a timeframe of 10 years (Dickerson et al., 2011). They employed a hypothesis-driven approach using regions of interest (ROIs) based a previous cross-sectional study comparing patients with mild AD to controls on cortical thickness (Dickerson et al., 2009). They found that subtle neuroanatomical abnormalities were

detectable in asymptomatic individuals nearly a decade before they were diagnosed with AD. They used a score derived by measures of cortical thickness of several regions of temporal, medial-parietal and frontal cortices and demonstrated that it is useful not only for assessing risk of AD dementia but also for predicting time to onset (Dickerson et al., 2011). In *Chapter 3* of this thesis another study that explored baseline structural MRIs of healthy subjects who developed clinical AD within a timeframe of 10 years will be presented (Tondelli et al., 2011).

To study changes occurring in the preclinical phase, researchers have also studied cognitively healthy subjects with autosomal dominant familial AD (Fox et al., 1996b; Fox et al., 2001; Ridha et al., 2006) or people with an increased genetic risk of developing AD (i.e., young carriers of the APOE ε4 allele or family members of patients with AD).

Ridha and colleagues found that carriers of autosomal dominant mutations in APP and PS1 followed longitudinally showed significantly decreased hippocampal volumes relative to controls 3 years before clinical diagnosis of dementia and that measures of hippocampal atrophy rates were different from controls more than 5 years before clinical diagnosis of dementia (Ridha et al., 2006). Very recently, a study on a bigger group of 128 carriers of autosomal dominant mutations used their age at baseline assessment and their parents' age at onset of symptoms of AD to calculate the estimated years from expected symptom onset. The authors found that decreased atrophy of bilateral hippocampi in mutation carriers relative to non-carriers could be detected 15 years before expected symptom onset (Bateman et al., 2012).

In people at risk because of their APOE genotype, hippocampal volume reduction has been widely reported in ε4-carriers compared to non-carriers (den Heijer et al., 2006; Lemaitre et al., 2005). However, other studies did not detect significant hippocampal volumetric differences between the two groups (Moffat et al., 2000; Filippini et al., 2011; Filippini et al., 2009).

2.2.4 Advantages and limitations of structural MRI in AD

Cross-sectional and longitudinal studies described in previous paragraphs convincingly demonstrate that quantitative MRI measures of grey matter volume loss are sensitive to the neurodegeneration that occurs in established AD, and suggest that atrophy can be detected prior to cognitive decline, providing support for the notion that structural MRI can be used to detect AD prior to the onset of dementia. An obvious strength of MRI is its availability. In most European and US centres it is regarded as an essential investigation for dementia (Hort et al., 2010; Sorbi et al., 2012), not only because it is part of proposed diagnostic criteria for MCI and AD (Albert et al., 2011; Dubois et al., 2007) but also for differential diagnosis of other dementias (McKeith et al., 2005; Neary et al., 1998). Compared with other imaging markers, cerebral atrophy has better correlation with cognitive decline and does not have floor or ceiling effects (Johnson et al., 2012). Accordingly, significant effort is currently being made worldwide to standardise and validate hippocampal volumetry so that it can be adopted for diagnosis and in clinical trials (Jack et al., 2011b). However, structural MRI obviously does not detect directly the histopathology of AD and lacks specificity, as atrophy patterns typical of AD may overlap with other diseases. Most importantly, changes detectable by structural MRI take a relatively long time (at least months) to occur and do not provide information about function, limiting their use in short-term studies aimed to measure dynamic changes in response to potential treatments. Thus, other types of MRI measures, which provide information about the function of the brain, may be important methods to include in proof-of-concept studies on new therapies (Dickerson and Sperling, 2005; Johnson et al., 2012).

2.3 Functional MRI during memory tasks

As one of the earliest and most dominant symptoms of AD is the impairment of episodic memory, a number of imaging studies have assessed the functional changes in neuronal activity in the brain during performance of episodic memory tasks, with the hypothesis of a prominent involvement of medial-temporal lobes. Most frequently, fMRI tasks used to study episodic memory are based on the "subsequent memory" paradigm, consisting of an *encoding phase*, in which a series of novel items is presented during the MRI scan, followed by a *testing phase*, in which recognition of previously presented items is tested, either during or soon after the MRI scan. While some studies have used presentation of single items (Golby et al., 2005; Rombouts et al., 2000), most studies have used paired-associated items, i.e. face–name associations (Sperling, 2007; Sperling et al., 2003) or object-location associations (Gould et al., 2005), to specifically study associative memory processes, given the established role of the hippocampal formation in forming new associations between previously unrelated items of information (Eichenbaum et al., 1989; Squire and Zola-Morgan, 1991).

2.3.1 Memory-related functional MRI in AD

Several studies have demonstrated that fMRI performed during the encoding phase of memory tasks (Johnson et al., 2005; Machulda et al., 2003; Sperling et al., 2003) can detect differences – at a group level – between healthy elderly volunteers and patients with AD. Quite consistently, it has been shown that these differences consist of reduced activation of the medial temporal regions during episodic memory tasks in patients with AD relative to controls (Rombouts et al., 2000; Johnson et al., 2005; Machulda et al., 2003; Sperling et al., 2003; Pariente et al., 2005; Golby et al., 2005; Remy et al., 2005). Increased prefrontal cortical activity in AD patients relative to controls has also been reported (Remy et al., 2005; Sole-Padulles et al., 2009; Sperling, 2007; Pariente et al., 2005) but less consistently. This has led to

the suggestion that such changes may represent an attempted compensatory mechanism during hippocampal failure. Indeed, Remy and colleagues found a direct relationship between prefrontal increased activation and task performance (Remy et al., 2005), Pariente and colleagues demonstrated that activity in regions of increased activation correlated with MMSE scores (Pariente et al., 2005), and Solé-Padullés and colleagues showed that this increased activation correlated positively with proxies of cognitive reserve, suggesting that active compensatory mechanisms are still at work in patients with higher cognitive reserve (Sole-Padulles et al., 2009). However, such findings have not been confirmed by other studies. As an example, Gould and colleagues found that when subjective difficulty was equated in a paired-associate learning task, AD patients showed a similar activation pattern to controls, suggesting that apparent compensatory increases may be largely accounted for by the greater difficulty patients have completing such tasks (Gould et al., 2006a).

It is important to note that all the above-mentioned fMRI studies recruited small numbers of participants (i.e., less than 15 per groups). In addition, most of them [all except (Pariente et al., 2005) and (Gould et al., 2006a)] used block-designs, in which encoding of a series of novel items ("Novel" blocks) is followed by the presentation of repeated items ("Repeated" blocks), focusing on the Novel versus Repeated contrast, which provides information about encoding of novel stimuli but does not allow a separation of trials *a posteriori* on the basis of whether their encoding and recognition were successful or not. Only a few studies used event-related paradigms, which allow classifying the encoding of each single item (or association) on the basis of whether it was subsequently recognised or not. These studies showed no or little significant differences between controls and AD patients in activation of MTL in response to successful encoding/recognition (Gould et al., 2005; Pariente et al., 2005).

Several memory-related fMRI studies have also provided evidence that successful memory formation necessitates not only activation of MTL, but also coordinated deactivation of other brain structures. Regions that typically demonstrate deactivation during active tasks of

encoding and recognition are now considered part of the "default-mode network'' (DMN), which includes precuneus and posterior cingulate, medial prefrontal cortex and lateral-parietal bilateral regions. The "deactivation" of these regions is altered in older adults (Miller et al., 2008a) and in patients with AD (Celone et al., 2006; Pihlajamaki and Sperling, 2009). However, the concept of "deactivation" is always relative to what is chosen as baseline (i.e. fixation cross or control task) and although studies of "activation" and "deactivation" from the same dataset have been published separately [see for example (Gould et al., 2006b) and (Gould et al., 2005) or (Sperling et al., 2001) and (Pihlajamaki et al., 2008)], it is difficult to interpret their results in a coherent and unequivocal way. Related to this is the fact that the default mode network is being increasingly studied using independent component analysis methods on fMRI during rest or low demanding tasks (Greicius et al., 2004) rather than with task-related deactivations (see paragraph 2.4).

2.3.2 Memory-related functional MRI in MCI

With respect to MCI, several studies have demonstrated increased medial temporal activation during memory tasks (Celone et al., 2006; Dickerson et al., 2005; Hamalainen et al., 2007a), even when considering only successful memory trials (Kircher et al., 2007), suggesting that there may be a phase of paradoxically increased activation early in the course of prodromal AD (Dickerson et al., 2005; Kircher et al., 2007). However, these results have been contradicted by other studies showing opposite directionality of changes in medial temporal regions in MCI patients relative to healthy older controls (Machulda et al., 2003; Johnson et al., 2006; Petrella et al., 2007). The variability of fMRI data from MCI subjects (e.g., Is MCI associated with hypo- or hyper-activation of the MTL during memory encoding?) relates to several factors:
(i) the different fMRI paradigm tasks used, each addressing a slightly different aspect of memory (i.e., *encoding* or *recognition*, *associative* or *non-associative* memory) in different

modalities (i.e. *verbal* rather than *visual*); (ii) the heterogeneity of patients included in the MCI groups; (iii) the complex relationships between their degree of impairment and their ability to perform the memory task used as an fMRI paradigm.

Cross-sectional studies suggested that the hyperactivity may be present only at early stages of MCI, when a patient's cognitive performance is still relatively preserved, whereas it may decline in more advanced stages of MCI and become similar to the pattern seen in AD patients (Celone et al., 2006). Related to this, prospective studies on cognitively healthy older participants or on patients with a diagnosis of MCI followed longitudinally have shown that baseline hyper-activation of MTL is a predictor of future cognitive decline (Miller et al., 2008b). In addition, the few fMRI studies that used event-related paradigms found that the MCI hyper-activation of MTL was observed during successful memory trials, suggesting that it might represent an early compensatory mechanism when AD pathology starts (Sperling et al., 2009). However, none of these studies explicitly compared activation during successful trials with activations during unsuccessful trials. Thus, it remains unclear whether the MTL hyperactivity efficiently compensates in terms of cognitive performance or whether it is simply a "functionally inefficient" marker of impending neuronal failure.

2.3.3 Memory-related functional MRI in preclinical AD and people at risk

A few task-related fMRI studies using memory paradigms have been published in subjects at risk for AD, including subjects with a family history of AD or carriers of the ε4 allele of APOE. Similar to studies on MCI, some studies have reported decreased medial temporal lobe activation in subjects with genetic risk (Trivedi et al., 2006; Filippini et al., 2011), whereas others have reported evidence of increased MTL activity in cognitively intact individuals with genetic risk (Bookheimer et al., 2000; Filippini et al., 2009). With the increasing consideration of indicators of amyloid deposition as markers of preclinical AD, a few recent studies have

started to look at differences between subjects grouped according to presence or absence of such markers. Sperling and colleagues found that task-related deactivations occurring during encoding of novel items (relative to baseline) or during repetition of familiar items (relative to novel) in the posterior cingulate are decreased in PIB positive older adults (i.e., potentially in the preclinical phase of disease) (Sperling et al., 2009; Vannini et al., 2011a). However, caution is required when interpreting results from task-related deactivations and especially when the neurobiological validity of grouping criteria has not been clearly established (i.e., whether amyloid PET positive subjects have indeed preclinical AD).

2.3.4 Advantages and limitations of memory task-fMRI in AD

There are several limitations and challenges in performing task-fMRI studies in patients with MCI and AD.

First of all, BOLD fMRI is known to be variable across subjects, and, to date, only very few studies have examined the reproducibility of fMRI activation in healthy or cognitively impaired older subjects (Putcha et al., 2011; Clement and Belleville, 2009).

Secondly (and more specific to neurodegenerative diseases), the fact that patients need to be able to perform the cognitive task in the scan makes task-related fMRI not suitable for those most severely impaired. Even when patients are able to perform the task in the scan, their performance is usually significantly different from the performance of healthy controls. Up to now, only few studies have taken into account the fact that patients and controls invariably perform differently during the execution of memory-related fMRI tasks adopting event-related paradigms (Gould et al., 2005; Peters et al., 2009). This not only allows studying functional changes in relation to actual performance, but also allows identifying and excluding those who randomly pressed response buttons.

Another important issue that limits the interpretability of memory-related fMRI studies concerns the relationship between structural and functional changes. Among the published studies using memory paradigms in AD and MCI patients, only a few have tried to account for the presence of tissue atrophy (Dickerson et al., 2004; Petrella et al., 2007).

Therefore, one of the aims of the research presented in this thesis was to overcome limitations of previous task-related fMRI studies, by using fMRI paradigms and fMRI data analyses that allow characterisation of functional activity with respect to between-subject and/or between-group variability in cognitive performance and GM atrophy (see paragraph 2.5 and *Chapter 5*).

Lastly, the majority of fMRI cross-sectional studies on AD have recruited and grouped together patients irrespective of whether they were taking cholinesterase inhibitors (the approved

treatment for mild and moderate AD) or not (Diamond et al., 2007; Golby et al., 2005; Gould et al., 2006a; Gould et al., 2005; Peters et al., 2009). However, several studies have suggested that cholinergic stimulation with cholinesterase inhibitors influences regional cerebral blood flow (Ebmeier et al., 1992) and BOLD signal in patients with MCI and AD (Petrella et al., 2008; Saykin et al., 2004; Shanks et al., 2007). Therefore, in the research presented in this thesis (see *Chapter 5*), great effort was made to recruit patients with AD who were not taking cholinesterase inhibitors and, in general, to only include participants who were not taking psychotropic treatments.

2.4 Functional MRI at rest (resting fMRI)

It has been shown that fMRI signal (BOLD signal) not only changes as a consequence of cognitive, "task-related" demand, but also shows low frequency spontaneous fluctuations which are organized within specific spatial patterns in the brain (Gusnard and Raichle, 2001; Fox and Raichle, 2007). The networks of brain regions whose spontaneous activity rise and fall coherently have been named "*resting state networks"*. Several networks have been identified and associated with specific cognitive functions (De Luca et al., 2006; Smith et al., 2009). Among them, the default mode network (DMN), which includes the posterior cingulate cortex (PCC) and precuneus, the hippocampus, the medial prefrontal cortex (MPFC), and lateral-parietal regions, is thought to be specifically engaged during self-reflection or when subjects are at rest, and has received the most attention in AD and MCI (Raichle et al., 2001). As mentioned in paragraph 2.3.1, the DMN was the first identified and studied with standardized methods for analysis of task-related fMRI, by looking at task-induced deactivations (i.e., decreases in BOLD signal during experimental conditions compared to baseline or resting conditions). More recently, it has been explored using a variety of functional connectivity methods, which continue to be increasingly explored and optimised (Cole et al., 2010). Most of these methods are *model-driven* and require *a priori* hypotheses regarding the functional connectivity between a brain region of interest (ROI, or "seed") and the rest of the brain (seed-based correlation analysis). Others instead use *data-driven* approaches such as independent component analysis (ICA) and allow analysis of functional connectivity within large-scale networks. These ICA-based analytical techniques have shown great potential in distinguishing/isolating networks of coherent and unconstrained brain activity, thus allowing identification of separate spatial maps in healthy young and old adults as well as in clinical populations (De Luca et al., 2006; Damoiseaux et al., 2008; Damoiseaux et al., 2011).

2.4.1 Resting fMRI in AD

The DMN is a particularly relevant network in AD research, since DMN structures are vulnerable to atrophy, amyloid deposition, and show a reduced metabolism in AD (Buckner et al., 2005). Thus most of the early resting-state studies focused on the DMN. Grecius and colleagues were among the first showing that DMN activity is reduced in patients with AD compared to healthy controls (Greicius et al., 2004). By using ICA, they showed that whereas the DMN in healthy elderly included PCC and hippocampus bilaterally, in AD patients it only involved to a less extent the PCC and right hippocampus. ROI-based studies focusing on the hippocampus showed decreased functional connectivity between this region and MPFC, PCC and precuneus, but also increased functional connectivity with frontal regions (Wang et al., 2006; Allen et al., 2007). Other ROI-based studies focusing on the PCC showed decreased connectivity between this region and ventral MPFC and hippocampus in patients with AD, but increase connectivity with frontoparietal regions (Zhang et al., 2009; Zhang et al., 2010). An intensified decrease of functional connectivity was observed with greater disease severity (Zhang et al., 2010; Wu et al., 2011).

More recent studies that used ICA improved methods (the majority also including patients with mild MCI) confirmed that patients with AD had significant decreased functional integrity and connectivity in regions of the DMN, mainly in the PCC rather than hippocampus (Gili et al., 2011; Agosta et al., 2011; Damoiseaux et al., 2011; Binnewijzend et al., 2011). Among them, the few studies that also explored other resting state networks emerged by ICA, found that that functional connectivity within frontal and frontoparietal networks (variably indicated as “executive” and “frontal-parietal” networks or “anterior DMN” and “ventral DMN”) was increased in patients with AD relative to controls, and thus had the opposite connectivity effect than the DMN (Agosta et al., 2011; Damoiseaux et al., 2011; Jones et al., 2011).

To summarise, most of resting-state studies showed AD-related decreases in functional connectivity in the DMN, with evidence for increased functional connectivity as well in more

anterior, frontal regions. Importantly, whereas it was not clear to what extent changes shown by early studies could be explained by atrophy, most recent studies that included inter-subjects differences in distribution of grey matter atrophy as a confounding variable (i.e., variable of no interest) showed that group differences cannot be explained only by atrophy (Wang et al., 2011; Agosta et al., 2011; Damoiseaux et al., 2011; Jones et al., 2011).

2.4.2 Resting fMRI in MCI

Task-induced deactivations have been extensively studied in patients with MCI. Decreased task-related deactivation in patients with MCI relative to control was found in the PCC and precuneus (Rombouts et al., 2005; Celone et al., 2006; Petrella et al., 2007), and in the anterior frontal lobes (Rombouts et al., 2005). More recent resting state fMRI studies using model-free approaches (i.e., ICA) have given somehow confusing results, probably related to the heterogeneity of patients included in the MCI groups. While most of these studies showed reduced functional connectivity within the DMN in MCI patients (especially in PCC and precuneus) relative to controls (Sorg et al., 2007; Qi et al., 2010; Agosta et al., 2011; Gili et al., 2011), others failed to find significant differences between MCI and controls (Binnewijzend et al., 2011; Rombouts et al., 2009). Even more conflicting results were found when exploring networks involving frontal and parietal regions: as an example, Sorg and colleagues found decreased functional connectivity in MCI patients in the “executive attention network” (Sorg et al., 2007), Qi and colleagues found increased functional connectivity in MCI patients in lateral frontoparietal regions of DMN (Qi et al., 2010); and Agosta and colleagues did not find significant differences between MCI and controls in networks different from DMN (Agosta et al., 2011). Importantly, most of the more recent studies corrected for regional grey matter atrophy differences (Binnewijzend et al., 2011; Agosta et al., 2011).

Recently, longitudinal deactivation and resting-state studies also tried to distinguish patients with MCI who have declined and converted to AD from those who remain stable over a 2 to 3 year follow-up period (Binnewijzend et al., 2011; Petrella et al., 2011). MCI converters showed decreased functional connectivity compared to non-converters within the DMN, although in one of these studies the differences between converters and non-converters did not reach statistical significance (Binnewijzend et al., 2011).

2.4.3 Resting fMRI in preclinical AD and people at risk

Studies conducted in healthy subjects at risk of developing AD because carriers of the ε4 allele of APOE gene showed alterations in resting state functional connectivity compared to non-carriers. Both increases (Filippini et al., 2009) and decreases (Sheline et al., 2010) of DMN functional connectivity have been reported. Differences have been interpreted in relation to the different ages of the groups studied and with possible different effects of the genetic risk on the ageing brain (Filippini et al., 2011).

A number of resting-state fMRI studies have also been published on cognitively healthy subjects grouped on the basis of presence or absence of amyloid intake on PET scans. Decreased functional connectivity and task-deactivation were observed in PCC and precuneus of cognitively normal elderly with high amyloid burden compared to elderly with low amyloid burden (Hedden et al., 2009; Sperling et al., 2009; Mormino et al., 2011). In addition to the decreased DMN functional connectivity, a study also showed increased connectivity in frontal regions of cognitively normal subjects with higher amyloid depositions (Mormino et al., 2011).

2.4.4 Advantages and limitations of resting fMRI in AD

The two main advantages of resting fMRI that makes it particularly suitable for clinical populations, even for very impaired and fragile patients, are that (i) there is no task involved

and (ii) the time of acquisition is shorter than other functional sequences. In addition, newly available software programmes are increasingly making the analysis automatic and faster, without the several problems related to the experimental designs of task-related fMRI.

However, there are also important limitations to the use of resting fMRI in clinical populations. First, because ICA methods to interrogate resting fMRI studies have been recently developed, there is still quite a significant variability and uncertainty about how to best perform ICA on data from healthy as well as diseased participants (Cole et al., 2010). As an example, there is open discussion on whether studies including different clinical groups (i.e., patients and controls) should run ICA across all groups or in the control group only, since both approaches have been used in the existing literature (Damoiseaux et al., 2011; Voets et al., 2012).

Similarly, the optimal number of components to be identified with ICA has not been clearly established and varies from 20 to 70 across different studies (Damoiseaux et al., 2008; Smith et al., 2009). Indeed, if the number of independent components is set lower than the total number of functionally and biologically valid RSNs of the brain, multiple RSNs might be fused together. Instead, if the number of independent components is set higher, the valid RSNs may be split. These methodological considerations are progressively being solved by a number of on-going methodological studies but it appears that 20-25 independent components may be a reasonable assumption (Vemuri et al., 2012).

Second, analyses of task-free resting fMRI data necessitate several pre-processing steps to avoid signal contamination from non-neuronal sources of fluctuations in the BOLD signal, most prominently from movement and low-frequency oscillations induced from the cardiac and respiratory cycle (Vemuri et al., 2012). Several methods are being proposed to specifically address this issue (Chang and Glover, 2009).

While solving methodological controversies was behind the specific aims of the present thesis, we considered and tried to address these issues in order to give biological validity to the interpretation of our findings (see *Chapter 5*).

Lastly, and probably the most important limitation is the relatively little understanding of how resting state networks identified with resting fMRI relate to dynamic functional activations. Although there is increasing evidence that functional networks of the brain at rest reflect those utilized "actively" during execution of tasks (Smith et al., 2009; Fornito et al., 2012), their relationship/correspondence still need to be better characterised. Thus, more studies combining task and resting fMRI are needed to unravel the ultimate meaning of resting state networks.

Therefore, one of the aims of the research presented in this thesis was to establish whether memory-related fMRI and resting fMRI give overlapping information (see paragraph 2.5 and *Chapter 6*).

2.5 Experimental aims and research questions

Given the increasing prevalence of AD and the international effort to identify new disease modifying drugs, we were interested in further characterising structural and functional changes occurring in different phases of AD progression, from the early "preclinical" to the latest "clinical" phases, using advanced MRI techniques. Such novel markers of cognitively relevant structural-functional organization might have potential utility in measuring the outcome of clinical or prevention trials.

Specific research questions and experimental aims addressed in this thesis are:

1) *To investigate if changes in brain morphology detectable by structural MRI occur in the pre-symptomatic, pre-clinical phase of AD (i.e., up to ten years before clinical diagnosis)*

   In the last decade remarkable advances have been reached in the application of structural MRI techniques to detect and measure changes in brain morphology (i.e., atrophy) associated with AD. Changes in brain morphology detectable by structural MRI have been mainly described in the MCI and AD stages. Relatively little is known about the asymptomatic stage preceding cognitive impairment (preclinical AD). Thus, for structural MRI, I focused on preclinical AD and studied baseline brain structure of healthy subjects who later converted to MCI or AD and addressed the following research questions:

   "Do changes in brain structure measurable with structural MRI occur before clinical onset of MCI and AD? If so, how early are they detectable?"

   To answer these questions, structural MRI techniques sensitive to grey matter density were used on previously collected baseline MRI data of healthy older adults followed clinically for 10 years within OPTIMA.

   Experimental findings are presented in *Chapter 3*.

2) *To explore the relationship between performance on a cognitive task and inter-subject variability - in brain structure and functional activity - in cognitively healthy older adults, while also validating the use of multimodal (structural and functional) MRI for unravelling the correlates of cognitive performance*

Changes in brain structure as detected by structural MRI closely match cognitive symptoms, but this has been especially shown in the MCI and AD phases. However, since impaired performance on specific cognitive tests may be one of the earliest changes predicting development of cognitive impairment, I explored the correlation between structural MRI and performance on a specific cognitive task (visuospatial associative memory) in cognitively healthy older adults, irrespective of whether they would later develop MCI/AD or not. For this purpose, I used structural MRI data previously collected from healthy older adults who had performed the visuospatial associative memory task. In addition, to test if results obtained from the correlation between cognitive performance and structural MRI reliably provide information about brain function, an fMRI study was also set up in which another group of healthy older adults performed a similar cognitive task during fMRI scanning. The following research question was tested: *"Does inter-subject structural variability detectable with T1-weighted structural MRI mirror cognitive performance in older adults and inform about which brain regions are activated during cognitive tasks?"*

Experimental findings are presented in *Chapter 4*.

3) *To develop a multi-modal imaging protocol to sensitive to different stages of disease progression (MCI and AD phases) and differentiating these from normal ageing (cognitively healthy controls)*

By indirectly measuring synaptic activity in response to cognitive demands or during rest, functional MRI (fMRI) provides a measure that may be the best correlate of

cognitive performance and a promising technique for following disease progression and treatment response in symptomatic stages (MCI and AD). However, previous fMRI studies on patients with MCI and AD have shown variable results possibly due to methodological limitations such as the lack of consideration of underlying changes in brain structure. I aimed to address the following question: *"Can task-fMRI overcome limitations of previous studies related to underlying differences in structure and performance and thus better quantify residual functions in the symptomatic brain?"*

I recruited patients with MCI and AD and set up a multi-modal protocol, which included both structural and functional MRI sequences. More precisely, fMRI sequences were acquired during performance of two different tasks (memory and self-appraisal) and at rest. The use of a combined approach may help to better interpret fMRI results with respect to differences in underlying brain physiology and morphology, which are already significant at the stage examined in cross-sectional studies on patients with MCI and AD. Detailed descriptions of the MRI protocol and recruitment strategy are presented in *Chapter 5*.

4) *To improve the characterisation of functional changes occurring in MCI and AD, using both fMRI during unconstrained rest and during a memory task*

Previous studies have demonstrated that fMRI during memory tasks can detect differences – at a group level – between cognitively healthy older adults and patients with AD or patients with MCI. But their results are complex and limited by different abilities of patients in performing the tasks and poor experimental designs. Recent use of unconstrained resting fMRI has shown potential utility for assessing brain function in these patient groups, but more understanding of how resting state networks relate to functional integrity of brain is needed. I aimed to address the research question: *"Do measures of task-independent, unconstrained brain functional connectivity*

(resting-fMRI) correspond to measures of task-evoked brain functional organisation (task-fMRI) in patients with AD? In other words, can resting-fMRI give overlapping information to task fMRI in patients with AD?"

Task- and resting-fMRI were combined (i) to refine the previously observed changes in task-related fMRI during memory task, (ii) to better characterise changes in brain network functional connectivity in MCI and AD measured from resting fMRI, and (iii) to compare results from these two distinct functional modalities. These two fMRI modalities have never been used in combination in the same experiment in MCI and AD previously. Experimental findings are presented in *Chapter 6.*

5) *To explore the use of task-related fMRI to unravel the mechanisms of a specific symptom occurring in some patients with MCI and AD (anosognosia or unawareness of disease)*

Whereas most previous research on fMRI in AD has focused on memory functions, less has been undertaken on other cognitive domains. *Anosognosia* refers to the inability to recognize cognitive, behavioural or functional impairment following a neurological disease. Studying anosognosia in dementia is important from a clinical point of view, since its presence may challenge the early diagnosis and identification of those who are at risk of developing AD, given that the diagnosis of MCI requires the presence of "subjective memory complaint" among other criteria.

To explore fMRI's potential beyond the memory dysfunction and identify neural signatures associated with reduced self-awareness, an additional task testing self-appraisal of personal traits was included in the imaging protocol. Specifically, the final study tested *"Can fMRI elucidate the functional mechanisms of anosognosia in MCI and AD patients?"* Experimental findings are presented in *Chapter 7*.

Chapter 3

Structural MRI changes in the preclinical phase of AD

3.1 Abstract

Structural brain changes occurring at different stages of the progression of AD have been mainly described at the point when cognitive symptoms are present, i.e. MCI and dementia. However, less is known about whether structural changes are detectable earlier, in the preclinical, asymptomatic phase preceding MCI. We investigated structural brain differences with MRI (using VBM) between groups of healthy subjects, stratified by subsequent diagnoses of MCI or AD during a 10 years follow-up. Images taken at baseline, at least 4 years before any cognitive symptoms, showed that subjects with future cognitive impairment (preclinical AD and MCI) had reduced brain volume in medial-temporal lobes, posterior cingulate/precuneus, and orbitofrontal cortex, compared to matched subjects who remained cognitively healthy for 10 years. For only those subjects later diagnosed as AD, significantly greater atrophy at baseline was detected in the right medial-temporal lobe.

In conclusion, our results show that structural MRI changes occur early in the preclinical phase of AD and are localized in regions typically affected by AD neuropathology. In particular, atrophy in the right hippocampus seems to be critical in discriminating between healthy people who will develop AD from those who will remain cognitively normal.

3.2 Introduction and rationale

Converging evidence from neuroimaging (Fennema-Notestine et al., 2009a; Jack et al., 2009; Morris et al., 2009; Ries et al., 2008; Yuan et al., 2009) and biochemical (Hampel et al., 2008; Mattsson et al., 2009) research indicates that the pathological process of AD begins years, if not decades, prior to the diagnosis of clinical dementia. Thus, there is a long preclinical phase of AD in which there are no symptoms of cognitive dysfunction but in which AD neuropathology is already on-going (Jack et al., 2010).

Brain atrophy detected by structural MRI is considered a marker of neurodegeneration (Frisoni et al., 2010) and is thought to become abnormal relatively later than other markers of AD neuropathology such as markers of amyloid deposition (Jack et al., 2010).

In the AD phase, once clinical symptoms of AD are evident and clinical diagnostic criteria for dementia are fulfilled, structural MRI shows diffuse cortical atrophy in the medial temporal lobe, in the posterior association cortex, and in other neocortical association areas. Thus, structural MRI is considered a valid marker of symptomatic AD and its progression in the dementia phase.

There is also strong evidence that changes in brain structure can be detected with structural MRI in elderly subjects in the MCI phase. In fact, several studies have shown that subjects with MCI destined to convert to AD have greater atrophy in medial temporal lobes, posterior cingulate, lateral temporal, and parietal cortex compared to healthy controls or stable MCI, although with heterogeneous results in terms of laterality and atrophy extent (Bozzali et al., 2006; Chetelat et al., 2005; Hamalainen et al., 2007b; Karas et al., 2008; Risacher et al., 2009; Whitwell et al., 2008b).

However, less is known about the asymptomatic stage preceding cognitive impairment and about how early and where in the brain the first structural changes occur. To our knowledge, only a few studies have used structural MRI to study the localization of brain atrophy in

healthy subjects who later converted to MCI or AD (den Heijer et al., 2006; Hall et al., 2008; Rusinek et al., 2003; Smith et al., 2007).

The purpose of our study was to identify structural MRI changes of preclinical AD occurring early in the asymptomatic stage, years before any symptoms are measurable. We analysed MRI data in elderly healthy subjects who were followed-up for ten years and remained cognitively healthy for at least four years. Using a whole-brain voxel-based approach, we examined the distribution of brain atrophy suggestive of later progression to cognitive impairment. We hypothesized that early brain atrophy would be detectable several years before the clinical onset of MCI and AD, with a greater emphasis on the medial-temporal lobes (MTL).

3.3 Methods

3.3.1 Participants

A group of 148 healthy, cognitively normal, community-dwelling volunteers were recruited from a longitudinal study (called "the Challenge cohort") carried on within the Oxford Project to investigate Memory and Ageing (OPTIMA) (de Jager et al., 2005; de Jager et al., 2002). They were recruited through talks and radio advertising for those who thought that their memory and thinking were good as compared with their peers. At baseline, all subjects underwent MRI scan, physical examination, and neuropsychological assessment. Cognitive impairment was excluded at baseline based on MMSE (Folstein et al., 1975), CAMCOG (Roth et al., 1986), and NART-IQ (full scale and verbal-IQ). Subjects were sequentially clinically evaluated during a 10-year-long follow-up to identify those who developed amnestic MCI (either single or multiple domain), AD or other dementias and those who remained cognitively normal. More precisely, for the first 5 years of the follow-up, subjects were evaluated annually, then re-evaluated after 7 and 10 years from baseline. Neuropsychological assessment to detect incipient cognitive impairment included, among others tests, free recall and delayed recall of a 10-word list (CERAD)(Morris et al., 1989), Verbal Paired Associates (VPA) (Warrington et al., 1998), Pattern and spatial recognition from the Cambridge Automated Testing battery (CANTAB), CANTAB Paired Associates learning (Robbins et al., 1994). During the first 5 years of follow up, participants also underwent subsequent MRIs that were not used in the analyses in the present study, for which we only evaluated the baseline MRI data (*Chapter 4* reports experimental results from the MRI performed at year 1, second episode). Subjects with a poor quality MRI scan or evidence of previous stroke were not part of the 148 included in the present study.

At each follow-up, clinical diagnoses of amnestic MCI and probable AD were made according to published criteria (McKhann et al., 1984; Petersen et al., 1999). Post-mortem assessment (Mirra et al., 1991) was performed if a participant died.

From the original group of 148 subjects, only those subjects who remained cognitively normal for the first 4 years of the follow-up were selected (n=120), in order to ensure that healthy subjects at baseline were truly cognitively healthy and did not progress to dementia or MCI shortly after enrolment. None of the subjects included reported a subjective memory complaint as assessed by subjective memory questions from the CAMDEX (Roth et al., 1986). Subjects who remained in the study for the full follow-up and continued to have neither cognitive impairment on neuropsychological assessment nor evidence of neurological disorders were included in the healthy control (HC) group (n=65). Subjects who developed amnestic MCI anytime between the 5th and 10th year of follow-up and who did not convert to AD in the same time window were included in the preclinical MCI group (n=32). Subjects who developed probable AD anytime between 5th and 10th years of follow-up – with or without having been through a diagnosis of MCI- were included in the preclinical AD group (n=8); six of them had autopsy confirmation of the diagnosis (Mirra et al., 1991). Subjects who developed vascular dementia or Parkinson dementia during the follow-up were excluded (n=15). Each subject in the preclinical MCI and AD group was age-, education-, and gender-matched to a control subject, in order to minimize any possible effect of these measures on structural imaging results and to provide results unbiased by sample number. Matching was done using the best available match within the control group. In summary, 32 preclinical MCI, 8 preclinical AD, and 40 age- gender- and education-matched HC were included in the imaging analyses (Figure 1). Ethical approval was granted from the central Oxford Research Ethics Committee and informed consent was obtained from participants.

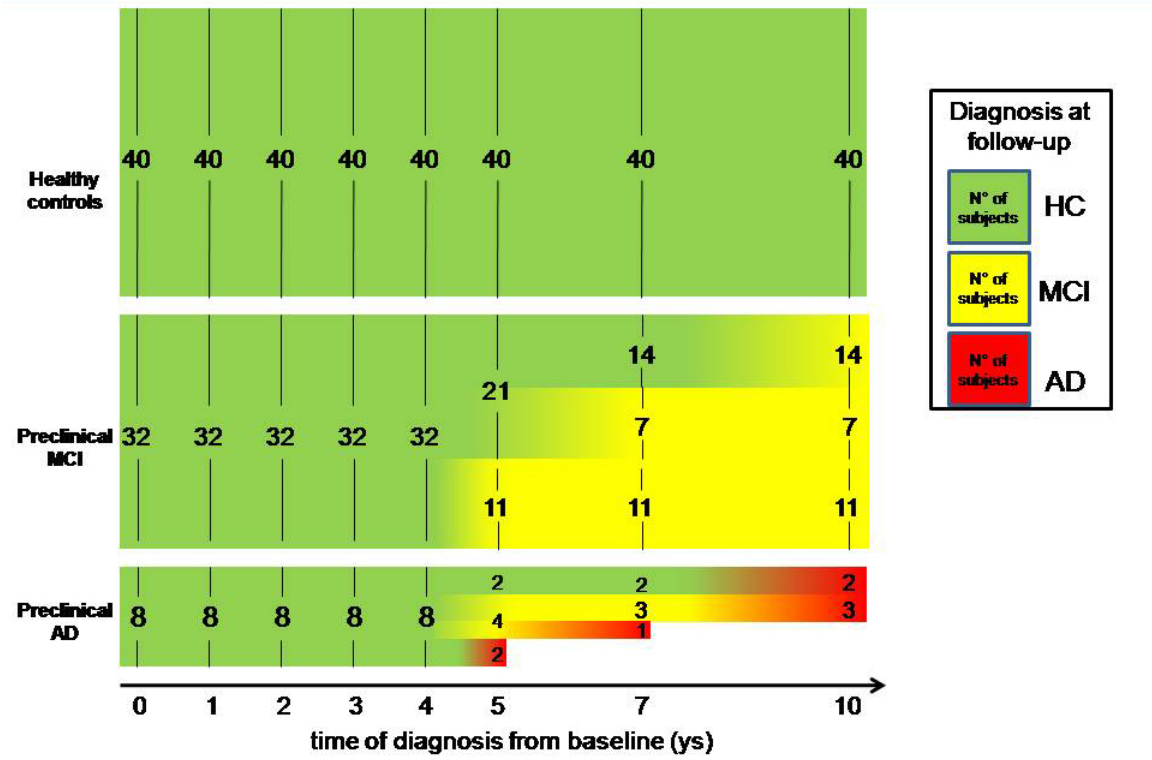

Figure 1. Schematic plot of the natural history for the three groups included in the study
Subjects clinically diagnosed as AD anytime between 5th and 10th years of follow-up – with or without having been through a diagnosis of MCI- were included in the preclinical AD group (n=8). Subjects clinically diagnosed as MCI anytime between the 5th and 10th year of follow-up and who did not convert to AD in the same time window were included in the preclinical MCI group (n=32). Age- gender- and education-matched subjects who remained cognitively healthy for the full 10 year-long follow-up were included in the healthy control group (n=40). Numbers in the x axes indicate when neuropsychological and clinical assessments were performed. The MRIs used in the study were performed at time 0. Colours indicate different cognitive status over the 10 year-long follow-up.

3.3.2 Analysis of demographical and neuropsychological data

Baseline demographic and neuropsychological data were analysed with SPSS 16.0 software using parametric or non-parametric tests, as appropriate. First, we analysed the differences between the preclinical cognitively impaired group (AD and MCI) and healthy controls. Independent t-tests were used to compare the two groups on age, MMSE, CAMCOG, NART full-scale verbal IQ results; the Mann-Witney-U test was used to compare the two groups on years of education; chi-square test was used to compare the two groups on gender and proportion of ApoE ε4 carriers. Secondly, we repeated the statistical analysis to compare the

same data between the preclinical AD, the preclinical MCI and HC groups; for this purpose, ANOVA with post-hoc Bonferroni adjustment or Kruskall-Wallis tests were used as appropriate.

3.3.3 MRI acquisition

Scanning was performed on a Siemens Magnetom Vision 1.5T MRI scanner. T1-weighted brain scan magnetization-prepared rapid gradient echo images were acquired (2-mm axial slices, in-slice resolution 0.86x0.86 mm, TE=7 msecs, TR=15 msecs).

3.3.4 VBM analyses

Structural data were analysed with FSL-VBM, an optimised VBM analysis (www.fmrib.ox.ac.uk/fslvbm) (Douaud et al., 2007) carried out with FSL tools (http://www.fmrib.ox.ac.uk) (Smith et al., 2004). Structural images were brain-extracted and grey matter-segmented before being registered to the MNI 152 standard space using non-linear registration (Andersson et al., 2007). The resulting images were averaged to create a study-specific template by using the same number of subjects from each group (preclinical AD, preclinical MCI and HC) in order to avoid any bias during the registration step that would have favoured one of the groups. Second, all native grey matter images were non-linearly registered to this study-specific template and "modulated" to correct for local expansion (or contraction) due to the non-linear component of the spatial transformation. The modulated segmented images were then smoothed with an isotropic Gaussian kernel with a sigma of 3 mm (FWHM ~7mm). Finally, voxel-wise General Linear Modelling (GLM) was applied using permutation-based non-parametric testing (5000 permutations). Anatomical locations of significant volume loss were determined by reference to the Harvard-Oxford cortical and subcortical structural atlases integrated into FSLview (part of FSL) in addition to careful manual inspection and identification.

First, to identify GM differences between subjects who went on to develop cognitive impairment and those who remained cognitively normal, we performed a t-test comparison between the preclinical cognitively impaired group (AD and MCI) and the HC group. Second, to identify grey matter changes in the preclinical AD and preclinical MCI group separately, we performed an ANOVA test between the three groups. Thirdly, we performed an additional analysis only with subjects diagnosed as AD at the 10th year of follow-up compared to HC, in order to identify earlier volume differences. Finally we repeated all VBM analyses with age, APOE ε4 status (carrier versus non-carrier status), and gender entered as confounder variables in the GLM model so as to control for the potential effect of these variables. For all these analyses, the Threshold-Free Cluster Enhancement (TFCE) correction for multiple comparisons (Smith and Nichols, 2009) was used and the statistical threshold was set at the $p<0.05$.
In addition, we performed a correlation analysis across the whole cohort of subjects (independent from their classification as HC, preclinical MCI, and preclinical AD) to examine the relationship between GM volume at the baseline and global cognitive performance assessed by MMSE score after 5 years and 10 years (or the latest available) from the baseline. MMSE scores were entered as regressors into the model and one-tailed t-tests were performed, assuming that lower follow-up cognitive scores would be associated with decreased tissue density in baseline scans. Given that we had predictions from the results of the previous analyses (group comparisons), for this correlation analysis we accepted the uncorrected statistical threshold of $p<0.001$.

3.3.5 Shape analysis

Complementary to the VBM analysis, we used a different methodology to assess hippocampus and amygdala volume and shape differences between groups. We focused on medial temporal lobe structures because of their accepted role in the early neurodegenerative process in AD

and because we found significant group differences in these regions in the previous VBM analyses. Left and right hippocampus and amygdala were segmented in each subject's baseline structural scan using FMRIB's Integrated Registration and Segmentation Tool (Patenaude et al., 2011) (http://www.fmrib.ox.ac.uk). The FIRST algorithm automatically segments subcortical structures based on the shape and intensity variations, as learnt from a training set. In the process, a surface mesh is created for the subcortical structure of interest using a deformable mesh model. The number of vertices per mesh is also fixed for a certain structure and the correspondence between vertices is enforced during the fitting so that corresponding vertices can be compared across individuals and between groups. A vertex analysis was performed to compare the group of eight preclinical AD subjects and eight gender-, education- and age-matched subjects from the HC group. This vertex analysis compared the vertex locations, after registration to a standard space, between the groups using vertex-wise F-statistics with correction for multiple comparisons by False Discovery Rate (Benjamini et al., 2001). Results with $p<0.05$ (FDR corrected) were considered significant.

Subsequently, we performed a vertex-wise Linear Discriminant Analysis (LDA) using a Leave-One-Out method, to assess how accurately each vertex from the subcortical structure discriminated subjects who converted to AD from subjects that remained healthy over the course of ten years.

3.4 Results

3.4.1 Demographic and neuropsychological data

At baseline, there were no significant differences between the groups in age, years of education, gender, ApoE status, MMSE, CAMCOG, NART-IQ full scale and Verbal IQ (Table1).

	HC (n=40)	Cognitively impaired subjects (n=40)		Group comparison
		Preclinical MCI (n=32)	Preclinical AD (n=8)	
Baseline demographic features				
N of male: female	20:20	18:14	2:6	ns
Age, years (±SD)	76.07 (±5.69)	77.10 (±5.22)	79.39 (±5.01)	ns
N of ApoE ε4 carrier	5	7	2	ns
Years of education	12 (10-19)	12 (10-16)	14 (10-15)	ns
Baseline neuropsychological features				
MMSE	28.62 (±3.72)	28.41 (±1.073)	27.62 (±1.05)	ns
CAMCOG	98.33 (±3.40)	96.13 (±3.19)	95.38 (±4.17)	HC>MCI*
NART Full-scale IQ	119 (±6.92)	115 (±9.01)	122 (±6.3)	ns
NART Verbal IQ	116 (±6.4)	113 (±8.1)	119 (±5.6)	ns

Table 1. Baseline demographic and neuropsychological characteristics of subjects
Reported values for age, MMSE, CAMCOG, NART-IQ and Verbal-IQ scale are means with standard deviation values in parenthesis; reported values for years of education are median with range in parentheses. The last column on the right depicts the results of the comparison between the subgroups. Ns, not significant.* significant at $p<0.05$; this difference was not significant in the assessment repeated 2 years after baseline.

3.4.2 VBM results

3.4.2.1 Group comparison analyses

Compared to the HC group, the preclinical cognitively impaired group (AD and MCI) showed significant grey matter loss in the medial temporal lobe bilaterally, the posterior cingulate and the precuneus. Additional grey matter loss was also identified in orbitofrontal regions bilaterally, in the lateral temporal lobe, and insular cortex bilaterally.

The preclinical AD group compared to the HC group showed a similar pattern of atrophy as previously described, with less extent in all regions but still significant (Figure 2, first row). The direct comparison between preclinical AD and preclinical MCI showed that preclinical AD had greater GM loss in the right medial temporal lobe, and in posterior cingulate and precuneus (p Figure 2, second row). Additional GM loss was found in bilateral orbitofrontal cortex, middle temporal gyrus, insular cortex, and lateral-occipital cortex. At an uncorrected threshold ($p<0.001$), volume reduction was also detected to a lesser extent in left hippocampus.

The comparison between preclinical MCI and HC showed that preclinical MCI had lower GM density in small clusters in the right precentral gyrus, posterior cingulate, and left superior temporal gyrus.

The comparison between those subjects who were diagnosed as AD at the 10th year of follow-up and HC still showed greater atrophy in the right hippocampus, amygdala and bilateral orbitofrontal cortex (Figure 2, third row).

Finally, the same group comparisons repeated by introducing baseline age, APOE ε4-carrier status, and gender as confounder variables in the GLM model showed the same pattern of brain atrophy as previously identified (shown in yellow in Figure 2). Interestingly, the comparison between preclinical AD and HC with the additional confounder variables revealed significant atrophy in the right medial-temporal lobe structures only.

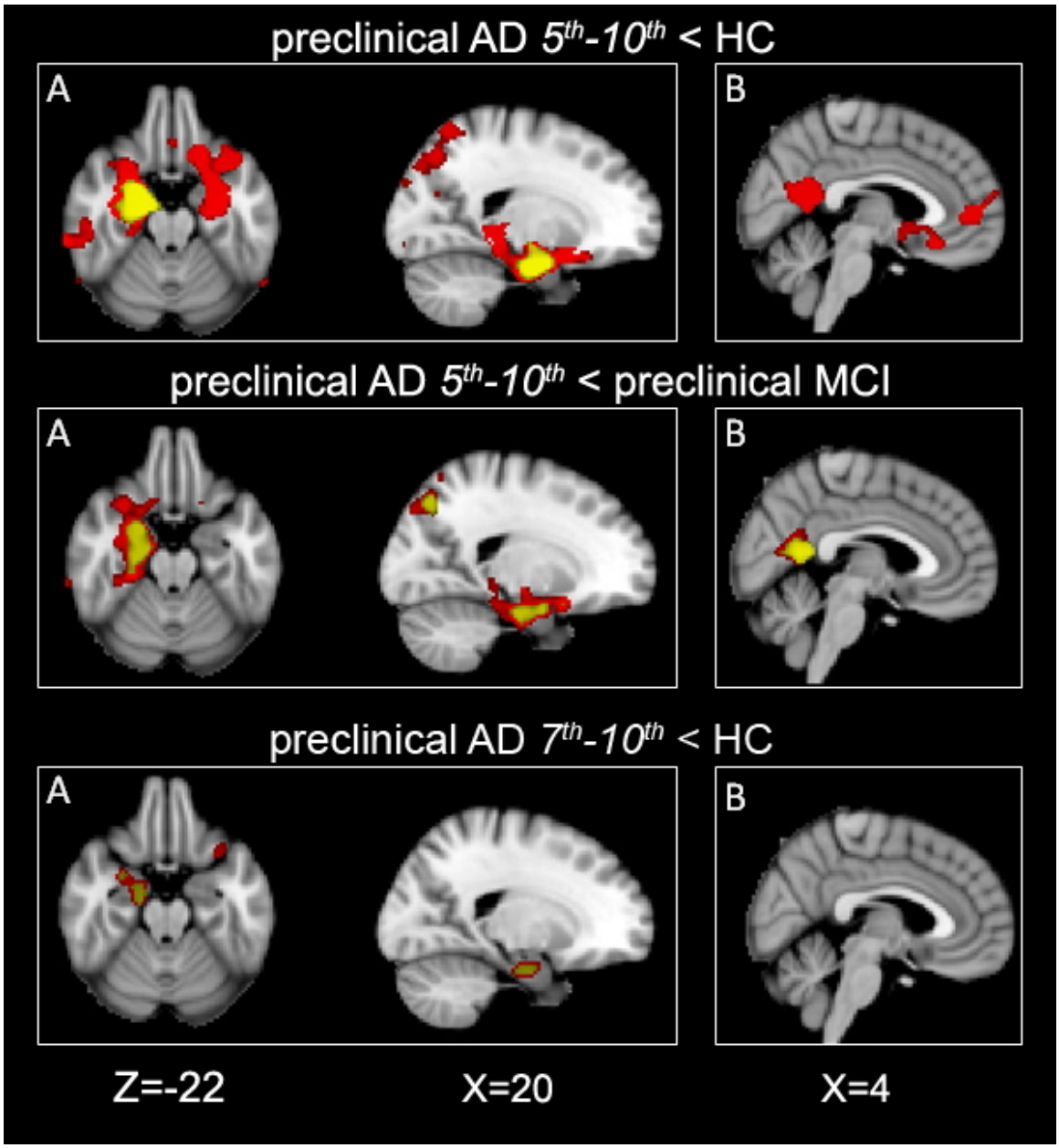

Figure 2 Results of the VBM group comparison analyses
Images are presented to highlight results in medial temporal lobes (A) and medial-posterior cortex (B).
First row: regions of volume loss in the 8 subjects who would develop AD anytime between the 5th to 10th year of follow-up compared to the 40 HC.
Second row: regions of volume loss in the 8 subjects who would develop AD anytime between the 5th to 10th year of follow-up compared to the 32 future MCI.
Third row: regions of volume loss in the 5 subjects who would develop AD anytime between the 7th to 10th year of follow-up compared to the 40 HC.
Results are displayed at p<0.05, TFCE corrected. In red are results of group comparisons with no additional covariates, in yellow the same comparisons performed by adding age, APOE ε4 status, and gender as confounder variables. Images are shown in radiological convention. Coordinates are in MNI.

Region	Side	Anatomical localization	MNI			t-statistic
			x	y	z	
Preclinical AD (5th-10th year) < HC						
Medial-temporal lobe	R	Hippocampus	20	-12	-24	5.53
		Amygdala	24	0	-20	5.00
	L	Hippocampus	-28	-10	-22	3.96
Lateral-temporal lobe	R	Middle Temporal Gyrus	64	-30	-10	5.06
	L	Middle Temporal Gyrus	-56	-60	0	4.24
			-64	-54	-10	3.94
	R/L	Posterior Cingulate/Precuneus	10	54	8	3.68
Medial-posterior cortex			0	-54	18	3.45
Frontal cortex	L	Orbitofrontal cortex	-20	14	-14	4.44
	L	Paracingulate/Cingulate Gyrus	-10	44	10	3.96
	R	Cingulate Gyrus	8	44	2	3.48
	L	Precentral Gyrus	-10	28	56	3.45
Insula	L	Insular cortex	-54	-6	8	4.61
			-38	-8	20	4.48
	R		36	-22	14	4.38
			36	-12	20	4.33
Lateral parietal cortex	L	Inferior parietal lobule	38	-74	26	4.47
	R		32	-74	38	3.73
Preclinical AD (5th-10th year) < MCI						
Medial-temporal lobe	R	Hippocampus	24	-18	-24	4.25
		Amygdala	22	0	-22	4.03
		Parahippocampal Gyrus	26	-28	-26	3.87
Frontal cortex	L	Orbitofrontal cortex	-18	16	-18	4.78
	R	Inferior Frontal Gyrus	44	16	4	3.66
		Middle Frontal Gyrus	48	46	12	3.57
Medial-posterior cortex	R	Posterior Cingulate/Precuneus	0	-56	16	4.64
Lateral-temporal lobe	R	Middle Temporal Gyrus	66	-32	-10	3.71
Lateral parietal cortex	L	Inferior parietal lobule	-46	-72	2	4.45
	R	Superior parietal lobule	20	-74	46	4.11
		Inferior parietal lobule	32	-74	36	4.08
Insula	L	Insular cortex	-36	-12	16	3.85
	R		38	-26	16	3.15
Preclinical AD (7th-10th year) < HC						
Medial temporal lobe	R	Hippocampus/Amygdala	18	-12	-24	4.07
			20	-4	-24	3.46
Medial-prefrontal cortex	L	Orbitofrontal cortex	-32	16	-22	4.10
Lateral parietal cortex	R	Superior parietal lobule	36	-72	36	3.52
Preclinical MCI (5th-10th year) < HC						
Lateral-parietal lobe	R	Precentral Gyrus	56	0	28	4.42
Medial-posterior cortex	R/L	Posterior cingulate	0	-24	38	4.34
Lateral-temporal lobe	L	Superior Temporal Gyrus	-60	4	-2	4.04

Table 2. Regions of GM loss showed by VBM group comparison analyses

R=right; L=left. GM, grey matter; HC, healthy control; L, left; MCI, mild cognitive impairment; MNI, Montreal Neurological Institute.

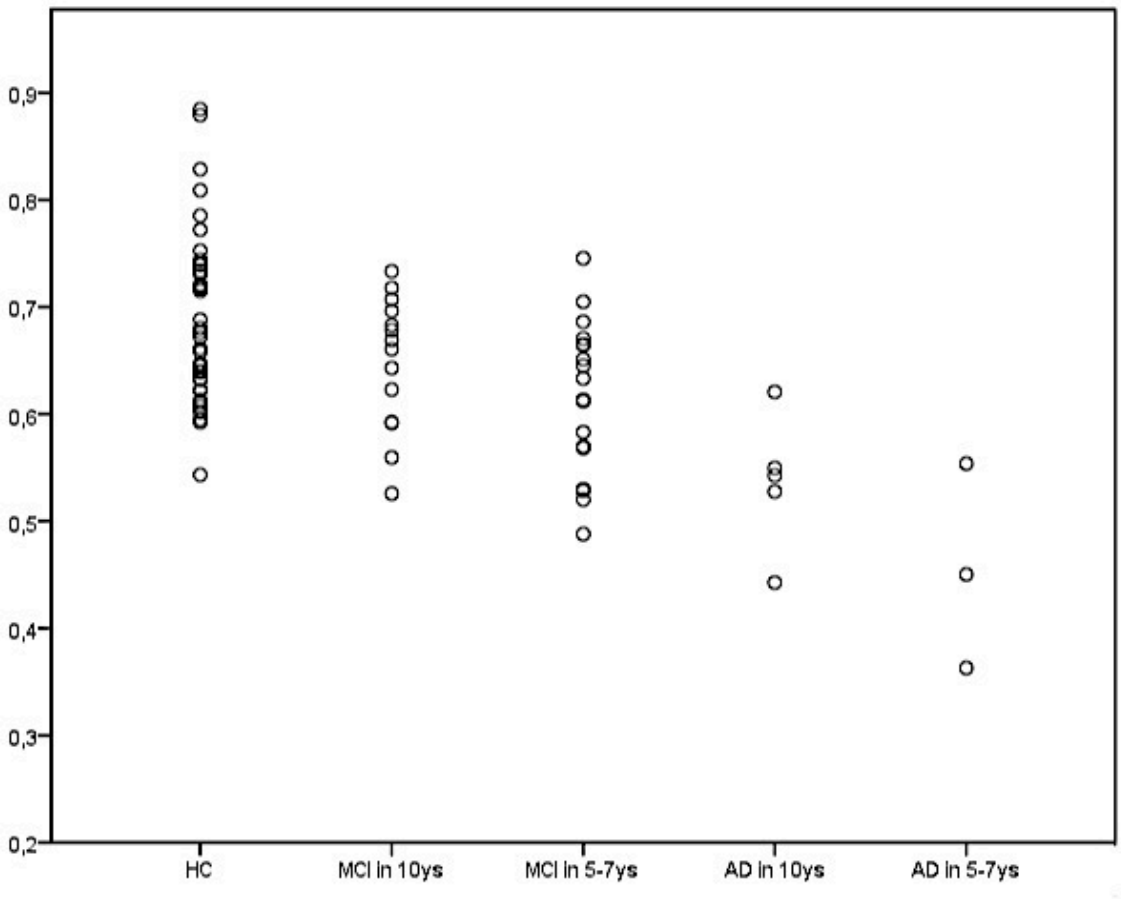

Figure 3. Plot of grey matter volume by time to diagnosis.
Peak values of the right medial temporal lobe cluster resulting from the VBM comparison between preclinical AD and HC (MNI coordinates: 20, -12, -24) are organized by "time to diagnosis" and future diagnosis. In line with the idea that our groups represent different phases of a continuum progressing from normal cognition to AD, preclinical MCI subjects converting later in time are "closer" to HC subjects, whereas preclinical MCI converting sooner are "closer" to preclinical AD subjects.

3.4.2.2 Correlation analysis

The correlation analysis between baseline brain atrophy across all subjects and global cognitive function assessed by MMSE at the end of follow-up showed a significant correlation in the medial temporal lobes bilaterally ($p<0.05$, TFCE-corrected), meaning that the higher the degree of atrophy in this region at baseline, the lower the MMSE score in ten year's time. When performing the same correlation using an earlier MMSE score (at 5 years after the baseline), a significant correlation survived in the right hippocampus and amygdala ($p<0.001$, uncorrected). Left parahippocampus was also involved, but with less extent compared to the atrophy on the right side (Table 3 and Figure 4).

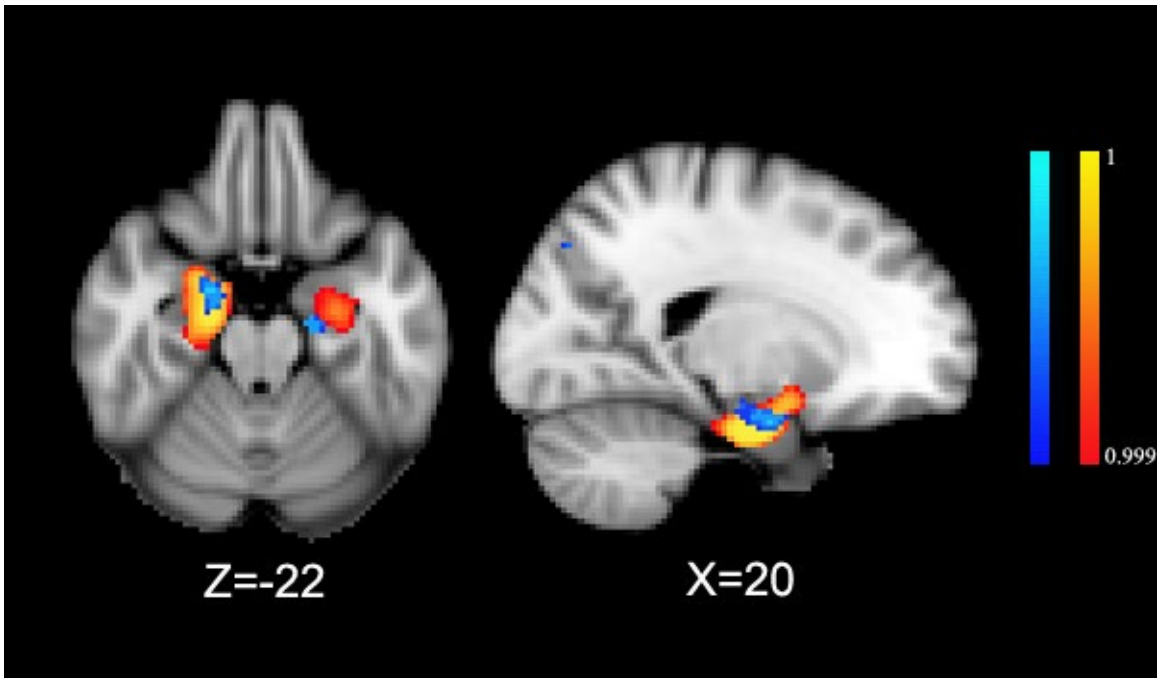

Figure 4. Results of the VBM correlation analysis
Regions of significant correlation between GM volume at baseline and MMSE scores at the 10th year (in yellow-red, $p<0,05$, TFCE corrected) and 5th year (in blue, $p<0.001$, uncorrected) of follow-up. Images are shown in radiological convention. Coordinates are in MNI.

Region	Side	Anatomical localization	MNI			t-statistic
			x	y	z	
MMSE score at the 5th year						
Medial temporal lobe	R	Hippocampus/Amygdala	18	-8	-22	3.96
			20	-4	-22	3.46
	L	Parahippocampal Gyrus	-22	-20	-20	3.27
MMSE score at the 10th year						
Medial temporal lobe	R	Hippocampus/Amygdala	18	-12	-26	5.16
			18	-4	-18	3.27
	L	Hippocampus	-24	-12	-28	4.27

Table 3. Results of VBM correlational analysis
Regions of significant correlation between GM volume at baseline and MMSE scores at the 5th year of follow-up ($p<0.001$, uncorrected) and at the 10th year of follow-up ($p<0.05$, corrected).

3.4.3 Shape analysis using vertex-based statistics and discriminant analysis

From the vertex analysis, only the right hippocampus showed significant local shape difference in the preclinical AD group compared to the HC group (inward movement of vertices from HC to AD subjects) in a ventro-medial region of the head of the right hippocampus. The linear discriminant analysis that was subsequently performed showed that this region could discriminate with high accuracy between the two groups, reaching >93% classification accuracy in 7 vertices within this region (Figure 5). No shape differences were detected in the left hippocampus, or in the right or left amygdala after correction for multiple comparisons.

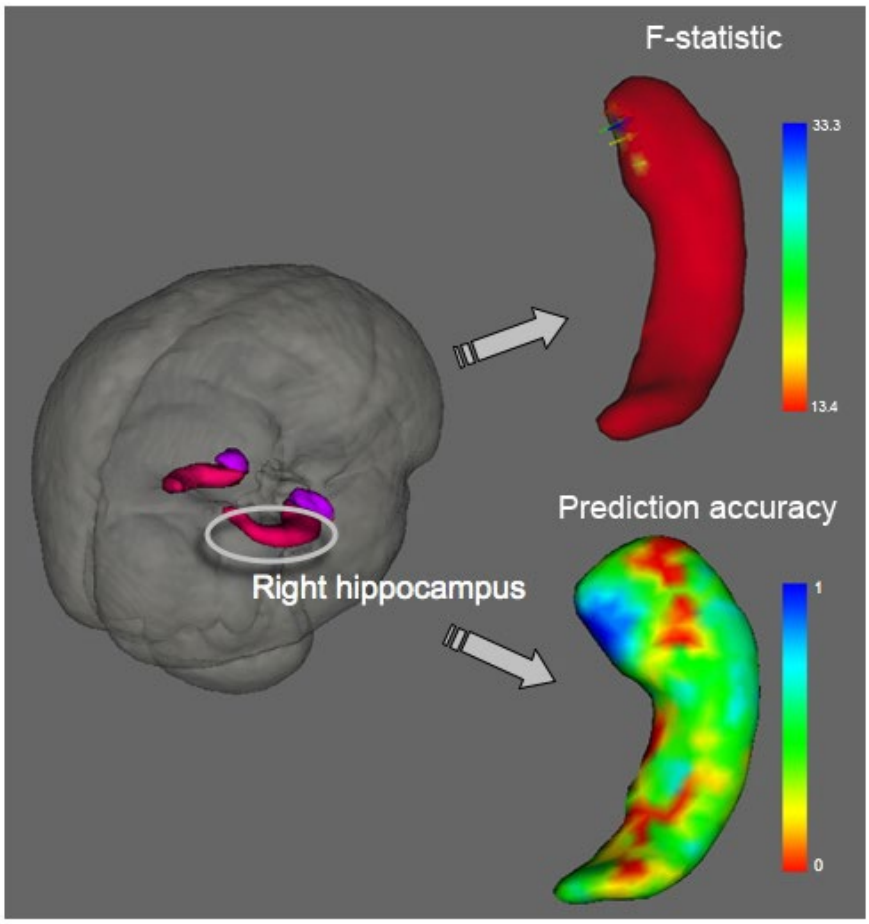

Figure 5. Results of the shape and discriminant analysis for the right hippocampus
Thresholded F statistic (top) and prediction accuracy (bottom) for each vertex in the right hippocampus. Surface colour reflects the F statistic surviving false discovery rate (FDR) correction (with 3 and 12 degrees of freedom, on top) or prediction accuracy (bottom) (see colour bar). Vectors inward direction represents relative atrophy (preclinical AD subjects compared with HC subjects).

3.5 Discussion

3.5.1 Structural MRI changes in the preclinical phase of AD

The VBM analysis showed that healthy subjects with future cognitive impairment (preclinical AD and MCI) had reduced grey matter volume at baseline compared to subjects who remained cognitively normal after 10 years of follow-up. This finding suggests that brain volume differences were already present at an early presymptomatic stage of AD, when subjects had no memory complaint or measurable cognitive impairment that would allow a clinical diagnosis of MCI or dementia according to current criteria. By including only subjects who remained cognitively normal for at least 4 years from baseline, we can reasonably ensure that all subjects were truly healthy at baseline and did not progress to cognitive impairment shortly after enrolment. To our knowledge no previous studies on preclinical MCI and AD have controlled to such an extent that the subjects did not already have some degree of cognitive impairment at baseline and remained cognitively healthy for so many years. The pattern of brain atrophy identified mimicked the typical distribution of brain atrophy that occurs in clinically manifest AD (Busatto et al., 2008; Karas et al., 2004), including atrophy in the bilateral medial and lateral temporal lobes, fronto-orbital cortex, posterior cingulate and precuneus. Medial-temporal lobe atrophy in healthy subjects destined to convert to AD was previously reported in other structural studies, although with different methodology (den Heijer et al., 2006; Hall et al., 2008; Smith et al., 2007). In addition to medial temporal lobe atrophy, group comparisons also revealed brain atrophy in other regions, including fronto-orbital, temporal lateral, insular and posterior associative cortex. The wider distribution of grey matter loss compared to other studies could be explained by our longer follow-up, which allowed us to include healthy controls that were truly free of any cognitive impairment for 10 years: in previous studies follow-up was shorter and it was not possible to rule out that subjects that were considered stable controls did not actually develop some degree of cognitive impairment

soon after the study, and therefore would have already had some degree of atrophy at baseline, as suggested by group differences in neuropsychological characteristics already present at baseline.

When compared to subjects who developed and remained with MCI for the length of follow-up, preclinical AD subjects showed reduced GM density in the right medial temporal lobe, and posterior cingulate/precuneus. This finding is similar to previous structural studies that have demonstrated the same pattern of atrophy when comparing stable MCI subjects to progressive MCI, suggesting that these regions are critical in distinguishing between those who will develop dementia and those who will remain stable (Bozzali et al., 2006; Chetelat et al., 2005; Hamalainen et al., 2007b). In our study this pattern of brain atrophy was already present before the clinical appearance of any cognitive impairment. We cannot be sure that all the subjects that we considered as preclinical stable MCI did not develop dementia after the end of follow-up (this is particularly true for those diagnosed with MCI at the 10^{th} year), but in such case we would expect to have found even less or no volume differences with the preclinical AD.

When the comparison was repeated considering only those subjects who developed AD at the 10th year of follow up, results remained highly significant, but were limited to the right hippocampus and amygdala. Furthermore, across all subjects, the correlation between brain atrophy at baseline and future global cognitive performance assessed by MMSE was significant for the right hippocampus. Finally, a specific involvement of the right but not left hippocampus was also suggested by the results of the shape analysis, which measures the shape of subcortical structures, modelling them as deformable surfaces. This analysis showed that the distribution of grey matter loss in the ventromedial region of the head of the right hippocampus could distinguish between preclinical AD and controls within our group, providing further evidence of the potential key role of the right hippocampus in the earliest preclinical stages of AD.

The finding of greater and earlier atrophy of the right hippocampus compared to the left in preclinical AD was somewhat unexpected. Indeed, despite the large number of studies that have used hippocampal volume as a marker of disease progression in AD and in MCI patients, only few have specifically looked at left-right asymmetries. Barnes et al. showed that in normal controls the right hippocampus has a greater volume than the left and that this asymmetry decreases as AD progresses (Barnes et al., 2005). In a meta-analysis from 14 MRI studies, Shi and colleagues confirmed a consistent asymmetry in volume pattern between left and right hippocampus, with right volume greater than left, both in controls, in MCI, and in AD patients, but with different extents, suggesting that this asymmetry may change dynamically according to disease progression (Shi et al., 2009). This is also supported by studies showing that the functional connectivity of right hippocampus with the rest of the brain decreases in AD patients relative to controls (Wang et al., 2006). Although the small numbers of subjects who developed AD in our cohort suggest caution in the interpretation of this result and needs replication with larger samples, our VBM and shape analyses converge in suggesting a key role of right hippocampal atrophy as an early feature in the AD pathological process.

3.5.2 Methodological considerations

The strength of our study is in the long follow-up, which allowed us to include healthy controls that were truly free of any cognitive impairment for 10 years and preclinical MCI and AD that were cognitively normal for at least 4 years after the baseline MRI. In addition, our subjects had homogeneous clinical and cognitive features at baseline, overcoming a common limitation of previous longitudinal studies in which neuropsychological characteristics were already different between groups at baseline.

The main limitation of our study is the small sample size of the preclinical AD group included in our analyses. However, this reflects the expected incidence of the disease in a UK community-

based cohort. Also the high level of education of our participants has to be mentioned, because higher cognitive reserve, possibly associated with a higher educational level, could have allowed subjects in the preclinical phase of AD to continue performing well in cognitive tasks, therefore delaying the clinical diagnosis with respect to the structural brain changes. Finally, it is possible that by using more detailed neuropsychological tools a closer temporal relationship between brain structural changes and memory decline would have been found. However, priority was given well recognised and broadly used measures of cognition to define onset of clinical symptoms, so that the results could have widespread implications for the ageing population.

3.5.3 Conclusions

In conclusion, the findings presented in this Chapter show that *structural MRI* measurement techniques sensitive to grey matter density can be used to identify the presence of brain atrophy in specific regions known to be associated with AD pathology up to 7-10 years before clinical symptoms of AD occur.

At least two studies recently published have confirmed that structural abnormalities can be detected in the preclinical phase of AD, years before cognitive symptoms (Dickerson et al., 2011); (Bateman et al., 2012), see also discussion in *Chapter 8*, paragraph 8.1.1). Their findings, together with those presented in this Chapter, challenge the view that brain atrophy detectable by structural MRI is a late and "downstream" event in the evolution/progression of AD, suggesting that it possibly occurs earlier than previously thought. Despite the considerable progress in the understanding of the neuropathological basis of AD, there is still much to learn about the sequence, order and timing of events that occur in the brain before AD manifests clinically.

Chapter 4

The structural and functional neuroanatomy of successful visuospatial memory in older adults

Converging evidence from VBM and fMRI

4.1 Abstract

Impaired visuospatial associative memory may be one of the earliest changes predicting cognitive impairment and AD. In this Chapter, the relationship between performance on a visuospatial associative memory task (the Placing Test) and brain structure and function was explored in cognitively healthy older adults.

First, a VBM correlational analysis was performed on structural MRI data from 144 healthy older adults with their scores on the Placing Test. Second, a functional MRI study was carried out on another group of 28 healthy older adults who performed a similar task during functional MRI. Decreased performance on the Placing Test was associated with increased atrophy in medial-temporal regions. Functional activation of the same regions –controlling for the effect of atrophy- occurred during successful performance of the same task. The co-localisation of structural and functional MRI correspondents of visuospatial associative test performance within medial-temporal regions validates multimodal imaging in describing behaviourally-relevant variability in the aging brain and suggests that the Placing Test has the potential for detecting early cognitive changes occurring in preclinical phases of AD.

4.2 Introduction and rationale

Memory impairment, in particular the loss of the ability to form and retain new episodic memories, is the hallmark of early AD (Grady et al., 1988; Elias et al., 2000; Galton et al., 2000; Tierney et al., 1996). As it has been shown that the earliest neuropathological changes associated with AD occur years before a diagnosis of dementia can be given clinically (Ohm et al., 1995; Smith, 2002a), increasing research into the neuropsychology of ageing has focused on identifying cognitive tests that are sensitive to these early pathological changes occurring in the preclinical or 'prodromal' phase of AD (Dubois et al., 2010). The best candidate among such cognitive tests should be specific in detecting the earliest memory dysfunctions but relatively insensitive to the effect of age and other demographic variables. If proven, its specific association with brain structures known to be particularly vulnerable to AD pathology would further corroborate its role in potentially detecting early signs of disease.

Research into the brain correspondents of cognitive dysfunction occurring in AD has been extensive and focused mainly on stages when the cognitive decline is already clinically evident and the degree of brain atrophy advanced (Heun et al., 1997; Jobst et al., 1992; Deweer et al., 1995; Cahn et al., 1998; Kohler et al., 1998; Sarazin et al., 2010; Di Paola et al., 2007). However, given the current importance of focusing on the earliest changes occurring before cognitive decline manifests clinically, it is important to explore whether the association between tests of episodic memory and their potential brain correspondents is also true in populations of healthy older adults and at the time of onset of AD or MCI. In addition, it is important to show if the brain-behaviour association specifically reflects successful cognitive performance and does not depend on non-specific and stage-related effects of the disease.

Among the several possible cognitive tests thought to be sensitive to early changes occurring in preclinical AD, visuospatial paired associate learning task performance has been shown to have very good sensitivity and specificity in discriminating older adults who will develop AD

(Blackwell et al., 2004; Ahmed et al., 2008; Johnson et al., 2009). A visuospatial associative learning test designed in our research centre, namely the Placing Test, can detect early deficits suggestive of cognitive impairment in a population of healthy older adults (Anderson et al., 2006). The test showed high discriminative capacity in distinguishing controls from patients with MCI and AD (de Jager et al., 2003). Importantly, performance on this test was not affected by age, education or gender. The Placing Test measures the ability to remember associations between objects and their locations. It was designed to specifically index the medial-temporal lobe function of forming new memories by binding together the disparate features of experiences as they occur on the basis of widely accepted theories on the role of medial temporal lobe structures in episodic memory (Bunsey and Eichenbaum, 1993; Rajji et al., 2006; Wallenstein et al., 1998). However, the neuroanatomical correlates of the Placing Test have not been directly investigated.

The first aim of the present study was to explore the neuroanatomical correlates of visuospatial associative learning, and more precisely to test the hypothesis that variability in the performance of the Placing Test in a population of healthy older adults specifically correlates with the variability in the morphology of medial temporal lobe structures. For this purpose, we carried out a VBM correlational analysis on a group of 144 healthy older adults who had performed the Placing Test.

The second aim of the present study was to further explore the link between visuospatial associative memory and brain function by establishing if the regions of significant correlation resulting from the VBM analysis were those whose actual activation enables successful visuospatial memory. We therefore used functional MRI (fMRI) on another group of healthy older adults to directly explore neural activity during successful performance of an fMRI-adapted version of the Placing Test.

4.3 Methods

Experiment 1 (VBM study, section 4.3.1) was performed using data collected as a part of a longitudinal cohort study. Experiment 2 (fMRI study, section 4.3.2) was performed with newly collected functional MRI data from another group of healthy elderly. The correspondence between the original paper version of the Placing Test used in Experiment 1 and the computerized, fMRI-adapted version used in Experiment 2 was tested separately and independently in another group of elderly (Pilot, paragraph 4.3.3).

4.3.1 Experiment 1: VBM study

4.3.1.1 Participants

We used data from the second episode of the prospective cohort study (the "Challenge cohort") on cognitively normal older adults recruited in OPTIMA and described in *Chapter 3* (de Jager et al., 2005; de Jager et al., 2002). For the purpose of the present study we present data from the second episode as it had the largest number of participants (n=144, aged 61 to 91 years) who performed both structural MRI and the Placing Test (this test was not part of the neuropsychological battery at the first episode). Cognitive impairment was excluded at this episode based on performance on MMSE and CAMCOG. Exclusions at the second episode were only due to withdrawal from the study, major stroke, or death after episode 1. No participants were excluded on the basis of poor performance on the Placing test, as this was used as experimental variable, thus not used as inclusion/exclusion criterion. Subjects with a poor quality MRI scan or evidence of previous stroke or severe vascular lesions were also excluded.

4.3.1.2 Cognitive assessment: The Placing Test

Neuropsychological assessment included the Placing Test for Objects. Subjects are shown a set of pages divided into four parts (2 rows by 2 columns). Two parts of the page contain a picture of an object and the location of the objects varies randomly across the pages. To control encoding processes, subjects are asked to judge whether the objects are pleasant or unpleasant. After all 10 test objects have been presented, each item is presented individually from a response booklet, in a random order. Subjects are asked in which part of the page in the test booklet the item appeared. To help them, a page divided into four parts is presented, with the quadrants numbered from 1 to 4. Presenting the original object provides a cue to control the retrieval process. The score is the percentage of correctly placed items (de Jager et al., 2003).

4.3.1.3 Image acquisition

Structural MRI scans were performed within 1 month from each subject's neuropsychological assessment. Scanning was performed on a Siemens Magnetom Vision 1.5T MRI scanner as described in Chapter 3.

4.3.1.4 Image analysis

T1-weighted structural images were analysed with FSL-VBM [(Douaud et al., 2007), www.fmrib.ox.ac.uk/fslvbm]. Pre-processing steps were similar to those described in *Chapter 3* and included brain-extraction, grey matter-segmentation, creation of a study-specific grey matter template (from all the 144 images), non-linear registration of the native images to this template, "modulation", and "smoothing" with an isotropic Gaussian kernel with a sigma of 3 mm (FWHM ~7mm). Statistics were performed using permutation-based non-parametric inference within the framework of the general linear model (5000 permutations) (Nichols and Holmes, 2002). To identify regions of significant correlation between grey matter volume and

cognitive performance on the Placing Test, a one-sample t-test was performed, and the contrast of main interest was the one interrogating for correlations between lower test performances and decreased grey matter volume. An additional model including four confounding variables (age, education, global cognitive function as measured by CAMCOG scores, and gender) was also set up, to confirm that the relationship between performance on placing test and grey matter volume was still true after correction for these confounding variables. Results were considered significant at $P < 0.05$, fully corrected for multiple comparisons across space (after initial cluster-forming thresholding at $t>2$). In addition, TFCE correction at $p<0.05$ was also applied (Smith and Nichols, 2009) to see if results were confirmed also when using unbiased cluster-forming threshold.

4.3.2 Experiment 2: fMRI study

4.3.2.1 Participants

A group of 28 cognitively healthy volunteers aged 64 to 91 years was newly recruited for the fMRI study from the controls subjects in the OPTIMA on-going study (LEAD cohort, see http://www.medsci.ox.ac.uk/optima/our-research/current-research). At study entry and in each of the periodic assessments subjects undergo medical assessment, extended neuropsychological assessment, structural MRI imaging. They are classified by an experienced team of physicians, nurses and neuropsychologists as cognitively healthy controls if they do not fulfil criteria for diagnosis of mild cognitive impairment, AD or other dementias, and do not show cognitive impairment on extended medical and neuropsychological examination, which includes CAMCOG (Roth et al., 1986), Clinical Dementia Rating (CDR) Scale (Morris, 1993), NART-IQ, MMSE (Folstein et al., 1975), Montreal Cognitive Assessment (MoCA) (Nasreddine et al., 2005). Depression and other neurological and psychiatric diseases are also excluded, as well as functional impairment. The 28 controls included in Experiment 2 were recruited as part of the cross-sectional study that will be described in *Chapter 5,* which included structural and functional MRI sequences, and –in the same day as the scan- clinical re-examination and neuropsychological assessment.

4.3.2.2 fMRI paradigm

During the fMRI scan, subjects were asked to perform an fMRI-adapted computerised version of the Placing Test, using images of animals from a coloured and shaded revision of the "Snodgrass and Vanderwart" original set, for which normative data are available (Rossion and Pourtois, 2004). Programming of this computerised version was carried out using Presentation version 12.0 (Neurobehavioural System, http://www.neurobs.com). During the scanning session, images were displayed in one of 4 white squares appearing on a computer screen that subjects saw via a system attached to the head coil (Figure 6). Subjects were given a 2-button

response key in their right hand to answer the experimental questions. During the fMRI experiment, they first had to judge if 5 images randomly placed in one of 4 white squares, per item, were pleasant or unpleasant by pressing the 2-button response key (Encoding block). To help them, the question “Pleasant or unpleasant?” was presented above the squares. After a short interval in which they observed a fixation cross in the centre of the screen, subjects were re-presented with each of the 5 images placed in one of the 4 white squares and were asked whether it was in the same square in which it was previously presented or in a different one. To help them, the question ”Was it here?” was presented above the squares. Subjects were instructed to give a Yes/No answer by pressing the same 2-button response key (Recognition block). In each block, 5 image-location associates were presented, each displayed for 6 seconds. The inter-stimulus interval between one associate and another was jittered (mean of 2.8 secs, jittered from 2.5 to 3.5 secs) to allow for event-related analysis within each block. There were 8 different encoding blocks, each followed by its correspondent recognition block, corresponding to a total of 40 paired associates. During the recognition blocks, 50% of images were presented in the same location and 50% were displaced. The image-location associates were created randomly and differently for each subject. Their order of presentation was also random. Performance on the task was measured as rate of correct “hits” minus rate of “false recognitions”. Before the MRI, subjects were given extended, supervised training to familiarize themselves with the encoding and recognition tasks and with button pressing. Different images were used for this purpose to avoid any learning effects.

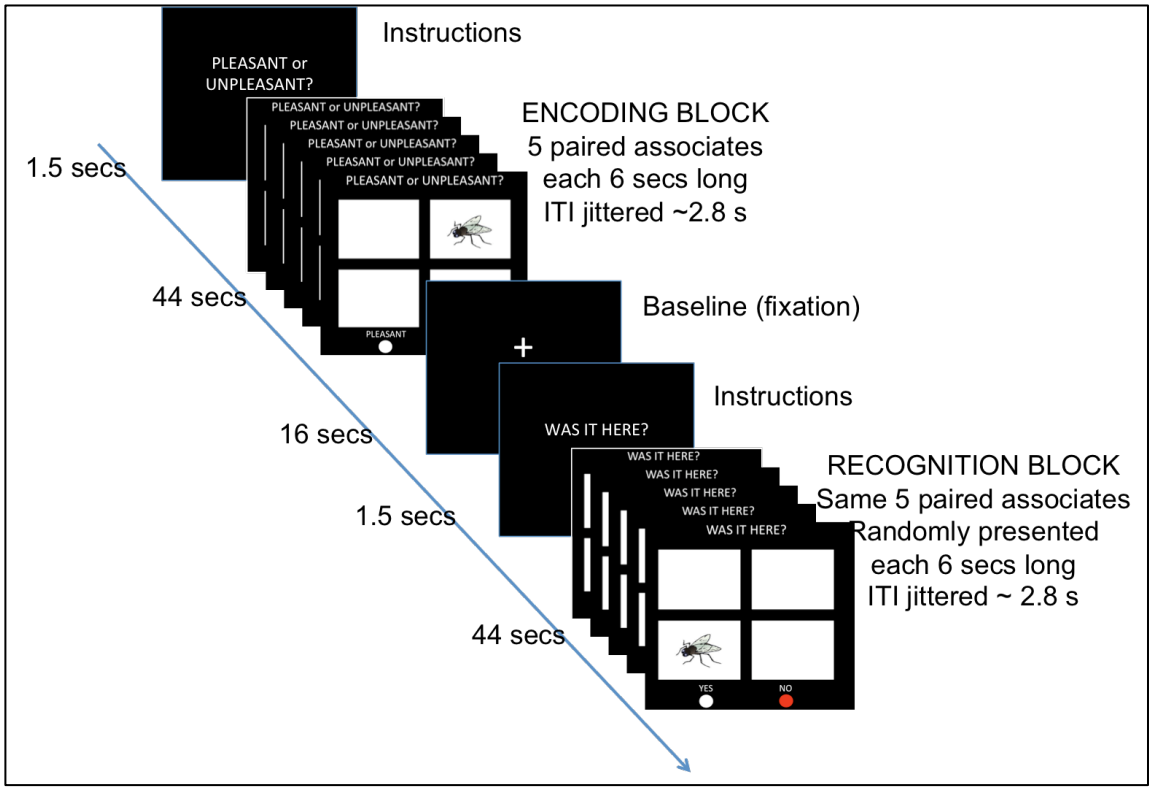

Figure 6. FMRI paradigm
In Experiment 2 (fMRI study) participants were asked to judge the pleasantness of coloured images of animals ("Pleasant or unpleasant?") during the encoding block, and then were asked if the image was in the same square in which it was previously presented ("Was it here?") in the recognition block. They were reminded of the answer codes (Pleasant/Unpleasant and Yes/No) by circles representing the buttons on the bottom of screen, which turned red at the pressing of the corresponding button.

4.3.2.3 Image acquisition

Scanning was performed at the 3-T Trio Siemens MRI scanner at the University of Oxford OCMR Centre. Extended description of the MRI protocol will be reported in *Chapter 5*.

4.3.2.4 Image analysis

FMRI analysis was carried out using FEAT, part of FSL. Pre-statistical processing steps will be described in Chapter 5. Events within both Encoding and Recognition blocks were categorized as successful or unsuccessful, based on whether the subject's forced-choice responses during cued recognition in the Recognition block had been correct (hits and correct rejections) or incorrect (misses and false-recognitions), similar to previous fMRI studies (Gould et al., 2006a;

Gould et al., 2006b). Thus, by using a "subsequent memory paradigm", we inferred if encoding had been successful on the basis of the subsequent performance on recognition (Dickerson and Sperling, 2009; Vannini et al., 2011b). Therefore 4 regressors (successful Encoding, unsuccessful Encoding, successful Recognition, unsuccessful Recognition) were entered separately at the single-subject-level analysis. All the resulting images were entered in a higher-level analysis. Importantly, the general linear model also included an additional four-dimensional nuisance variable representing voxel-specific grey matter density for each subject (Oakes et al., 2007). This was created from the segmented, registered and smoothed T1-weighted images and was included in the fMRI model to help disentangle the effects of inter-subject structural and fMRI signal variations.

Given that our goal was to investigate successful visuospatial learning, and that it has been shown that associative encoding and recognition processes share overlapping anatomical distribution (Alvarez and Squire, 1994; Moscovitch et al., 2005), the most interesting contrast was the one comparing successful encoding and recognition contrasted against unsuccessful encoding and recognition. However, contrasts directly comparing encoding and recognition were explored too. Whole-brain results were explored at the uncorrected voxel significance threshold of $P < 0.001$. In addition, small-volume corrections at $p<0.05$ (cluster and TFCE corrections) were applied in regions of interest for which we had an a priori hypothesis: left and right medial temporal lobes (created using the masks of hippocampus and amygdala of the Oxford-Harvard Atlas of Subcortical Structures integrated in FSL) and the regions resulting from the VBM analysis. After observing significant results, percentage signal changes were extracted to facilitate interpretation and correlation with cognitive/behavioural scores.

4.3.3 Pilot

The correspondence between the original Placing Test and the computer adapted version used in the fMRI paradigm was tested in a pilot study, in which another 11 healthy controls (mean age 74±10 years, mean education 13±5 years, 5 women; mean MMSE 29.6±0.7), 8 subjects with MCI (mean age 78±6 years, mean education 13±4 years, 4 women; mean MMSE 28.2±1.9), and 9 subjects with AD (mean age 78±9 years, mean education 10±4 years, 4 women; mean MMSE 20.2±5.1) were recruited. They performed both the original version of the Placing Test for Objects and the fMRI-adapted computer version (outside of the scanner). Performance on the original version of the Placing Test correlated with overall performance on the computer fMRI-adapted version of the Placing Test significantly across the whole group (r_{28}=0.68, P<0.001) and at the trend level across controls only (r_{11}=0.52, P=0.10).

4.4 Results

4.4.1 Participants characteristics

Participants in Experiment 1 and Experiment 2 did not differ significantly in terms of gender, age, and CAMCOG scores. There was a significant difference between the two groups in years of education. Therefore, number of years of education, among other demographic variables, was included as covariate of no interest in the analyses. There were no significant correlations between performance of Placing Test and age (r_{144}=-0.11, P=0.18; r_{28}=-0.06, P=0.75), CAMCOG scores (r_{144}=0.10, P=0.22; r_{28}=0.20, P=0.39), and years of education (r_{144}=-0.04, P=0.63; r_{28}=-0.08, P=0.68).

	Experiment 1	**Experiment 2**	**Groups comparison §**
group size	144	28	--
gender (M:F)	74:70	12:16	p=0.41
age	74.5 ± 6.2	74.4 ± 6.8	p=0.95
years of education	13.8 ± 3.7	15.3 ± 3.2	p=0.05
CAMCOG	98.2 ± 4.2	99.9 ± 2.9	p=0.06
original Placing Test *	9.1 ± 1.3	--	--
fMRI-adapted Placing Test &	--	0.74 ± 0.2	--

Table 4: Participant demographic and cognitive characteristics
Values for continuous variables are averages followed by standard deviation.
§ P values from comparisons between groups performed with independent t-test (two-tailed) for continuous variables and chi-square tests for dichotomous variables.
* measured as number of correctly placed objects out of 10.
& measured as rate of "hits" minus rate of "false recognitions".

4.4.2 Experiment 1: VBM study

Among the group of 144 healthy older adults, lower performance on the Placing Test correlated with greater atrophy in the anterior medial-temporal lobe (hippocampus and amygdala bilaterally, parahippocampus, mainly on the left), and regions of the superior temporal gyrus and superior temporal sulcus (Figure 7a and Table 5). These results did not change but only decreased in statistical significance when controlling for differences in age, education, global cognitive performance, and gender as demonstrated by the similar correlational analysis in which we added these variables as additional regressors of no-interest.

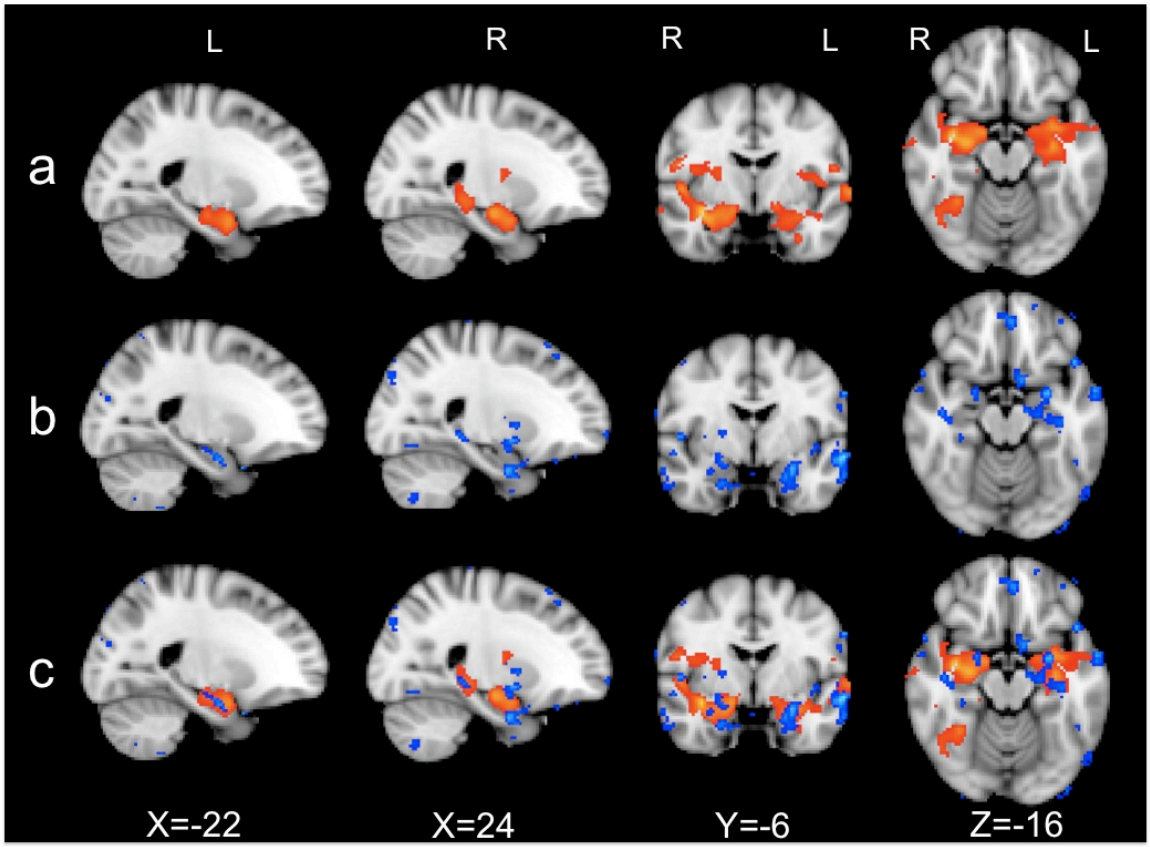

Figure 7. VBM and fMRI correlates of the Placing Test
a) Experiment 1: In red-yellow, regions of significant VBM correlation between grey matter volume and performance on the original Placing Test (P<0.05, cluster-corrected).
b) Experiment 2: In blue, regions of significant fMRI activation during successful relative to unsuccessful encoding and retrieval in the computerised-adapted Placing Test (displayed at P<0.005, uncorrected for visualisation purposes).
c) Overlap: VBM (bottom) and fMRI (top) results (same colours as above).
Coordinates are in MNI. R, right. L, left.

Anatomical localization	side	cluster size	x	y	z	t-Statistic	t-Statistic with covariates
Hippocampus	L *	903	-32	-14	-16	3.24	3.02
Hippocampus			-28	-20	-22	2.74	2.55
Amygdala, Parahippocampus			-30	2	-22	3.72	3.28
Temporal fusiform gyrus			-42	-38	-28	3.76	3.86
Middle temporal gyrus			-68	-48	4	3.59	3.19
Amygdala, Hippocampus	R *	1578	36	-4	-14	3.99	3.57
Hippocampus			28	-12	-14	3.60	3.24
Hippocampus			32	-18	-10	2.68	2.38
Parietal operculum/Inferior parietal lobule			62	-26	18	3.44	3.08
Angular/Supramarginal Gyri			66	-46	18	3.	3.02
Superior temporal gyrus			50	-22	8	3.40	3.07
Hippocampus (posterior part)	R	120	20	-36	-2	2.92	2.55
Parietal operculum	L *	3314	-44	-18	16	4.43	4.01
Supramarginal gyrus			-42	-26	24	4.25	3.83
Superior Temporal gyrus			-68	-36	6	4.12	3.93
Parietal operculum/ Heschl's gyrus			-38	-28	14	3.89	3.51
Temporal fusiform gyrus	R	663	40	-42	-26	4.00	3.70
Middle temporal gyrus	R	17	68	-12	-12	2.56	2.14
Temporal pole	L	168	-56	8	-36	3.28	3.24
Parahippocampus	L	12	-30	-8	-34	2.58	2.46
Parietal operculum	R	59	54	-6	18	2.90	2.37
Cerebellum	R/L	53	6	-74	-46	2.99	2.73
Parahippocampus	R	11	30	-28	-22	2.57	2.38

Table 5. Regions of significant correlation between grey matter volume and the Placing Test (VBM study, Experiment1)
Location in MNI coordinates and max t value for peak values in each cluster (cluster-corrected at $P < 0.05$). Clusters also surviving TFCE correction of $P < 0.05$ are marked with *. Values resulting from the main model including the Placing test only are reported in the column "t-statistic". Values resulting form the additional model with four covariates of no interest (age, years of education, CAMCOG scores, and gender) are reported in the last column ("t-statistic with covariates").

4.4.3 Experiment 2: fMRI study

Among the 28 subjects who performed the fMRI-adapted Placing Test in the MRI scan, successful relative to unsuccessful visuospatial associative learning (encoding and recognition) was associated with significant activation of regions in the hippocampus and amygdala bilaterally, and in the left superior temporal sulcus. Of note, the activation in the head of the hippocampus and amygdala also survived P<0.05 correction in regions of interest (Figure 7b and Table 6). Thus, medial temporal structures were specifically activated when subjects performed the visuospatial associative memory task correctly, relative to when they performed it incorrectly. The fMRI statistical results were independent of the between-subject variability in degree and distribution of grey matter atrophy, as this information was included as additional covariate in the model and used to account for shared variation. Results where this covariate was not included were similar with slightly weaker effects and are also shown for comparison (Table 6).

To test whether functional activity during successful encoding and recognition in the medial temporal lobes reflected the overall performance on the visuospatial associative learning task, we extracted the average signal from the clusters surviving small volume correction (see Table 6) and tested if it correlated with overall score of performance on the fMRI-adapted Placing Test (measured as rate of “hits” minus rate of “false recognitions”). As expected, there was a significant correlation between the fMRI signal and score (r_{28}=0.40, P<0.05). This correlation was not circular because the estimated mean fMRI signal change (measured as % signal change during the successful events relative to the unsuccessful events) is independent of the number of successful and unsuccessful events that are involved in that estimation.

Anatomical localization	side	cluster size	x	y	z	t-Statistic with GM	t-Statistic without GM
Amygdala/ Hippocampus head	L*§	33	-26	-4	-18	4.09	3.95
	R§	24	24	-2	-30	3.98	3.96
Hippocampus body	L	17	-38	-22	-14	4.18	4.04
Middle Temporal Gyrus	L	57	-62	-4	-10	4.72	4.36
Superior Temporal Sulcus	L	52	-66	-22	0	4.02	3.88
Accumbens/caudate head	L	15	-6	16	-2	3.68	3.68
Central gyrus	L	11	-62	-14	40	3.55	3.30
Medial orbitofrontal cortex	L/R	14	-4	46	-18	4.12	3.95
Occipital cortex	L	15	-10	-96	14	3.98	3.50
	R	10	8	-88	16	4.13	3.95
Cerebellum	L	20	-34	-42	-28	3.70	3.41

Table 6: Regions of significant activation for successful relative to unsuccessful performance on the adapted-Placing Test (fMRI study, Experiment 2)
Location in MNI coordinates and max t value for each cluster (uncorrected P < 0.001, cluster size > 10 voxels). *also survived P=0.05 correction in region of interest corresponding to VBM results; § also survived P=0.05 correction in region of interest corresponding to medial temporal lobes.

Figure 7c shows the anatomical overlap of results from VBM and fMRI. It is important to note that the two experiments carried out in two separate samples and with different methodologies could not be directly entered into the same analysis. In the VBM study we tested for significant correlation between differences in brain structure and level of cognitive performance, assuming that the latter is an indirect measurement of level of brain function. Instead, in the fMRI study, we directly tested this assumption by measuring brain functional activity during correct (relative to incorrect) cognitive performance that occurs over and above inter-subjects variability in brain structure.

4.5 Discussion

We aimed to explore the neuroanatomical correlates of visuospatial associative learning in cognitively healthy older adults, as it has been previously demonstrated that impaired performance on tasks measuring this function (i.e., the Placing Test) may predict future development of mild cognitive impairment and dementia.

4.5.1 Structural correlates of successful visuospatial memory

Among a group of 144 healthy older adults aged 61 to 91, lower performance on the Placing Test correlated with decreased grey matter volume in anterior medial temporal-lobes bilaterally including hippocampus, parahippocampus and amygdala.

Medial temporal lobe structures have long been known to play a critical role in episodic memory processes, through their interaction with distributed cortical regions (Scoville and Milner, 1957; Tulving, 2002; Schacter and Wagner, 1999). Correlations between performance on tests of episodic memory and MRI measures of the volumes of the hippocampi and other medial temporal lobe structures have been largely explored in patients with neurodegenerative dementias. Such correlations were first demonstrated in patients with AD using region-of-interest (ROI) approaches (i.e., directly measuring the volume of brain structures for which there is an a priori hypothesis) (Deweer et al., 1995; Cahn et al., 1998; Kohler et al., 1998; de Toledo-Morrell et al., 2000; Heun et al., 1997) and more recently using VBM, which allows the measurement of the degree and the distribution of regional grey matter loss throughout the whole brain and without an a priori hypothesis (Sarazin et al., 2010; Di Paola et al., 2007). In this study it was found that a correlation between brain anatomy and performance on a test of visuospatial memory could also be demonstrated in a population of cognitively healthy older adult, who, by simply being in their age-range, are at risk of developing neurodegenerative diseases such as AD, and –potentially- may already be in preclinical phases of disease.

4.5.2 Functional correlates of successful visuospatial memory

The relationship between successful visuospatial associative memory and brain functional activity was then further explored with fMRI. It was found that successful (relative to unsuccessful) performance of an fMRI-adapted version of the Placing Test was reflected by increased neural response in bilateral medial temporal regions including the hippocampus and amygdala. Of note, these activations resulted from whole brain analysis and not only from interrogation of a priori regions of interest.

These fMRI results further confirm evidence from numerous previous functional imaging studies conducted in young healthy controls showing medial temporal lobe activation during episodic encoding or retrieval (Nyberg et al., 1996; Schacter and Wagner, 1999). More precisely, given the nature of the task used, the results of this Chapter support the notion that the hippocampus is specifically activated by associative memory processes (Henke et al., 1997; Sperling et al., 2001; Zeineh et al., 2003) and by processing of visuospatial material (Maguire et al., 1998; Aguirre et al., 1998). The fMRI results were not affected by differences in brain volume, as subject-specific voxel-wise measures of grey matter volume were explicitly included in the analysis of fMRI data as a covariate of no interest. This shows that the functional activation of medial-temporal regions required by on-going successful memory occurs independently of individual variability in brain morphology of the same regions. In addition, as we intended to compare the fMRI results with VBM results derived from a correlational analysis between performance and grey matter volume, it was important to disentangle the effect of inter-subject structural variations on the fMRI signal.

By comparing activation evoked by successful versus unsuccessful performance on the fMRI task, we showed that regions in the hippocampus and parahippocampus are specifically involved in the formation of associations that can later be correctly retrieved, in line with recent studies of encoding and retrieval that also used event-related designs to disentangle the effect of successful relative to unsuccessful performance (Jackson and Schacter, 2004;

Vannini et al., 2011b). We believe that this further strengthens the brain-behaviour association that we previously identified with the VBM correlational analysis, suggesting that activation of medial temporal structures is specifically required to perform a visuospatial associative memory task correctly, and is not a consequence of non-specific factors such as attention-related processes, overall cognitive performance, or other potential confounders due to senescence.

4.5.3 Converging evidence from structural and functional imaging in older adults

By combining evidence from VBM and fMRI, it was shown that the hypothesis on which the Placing Test was designed, i.e. that it would have directly indexed the medial temporal lobe binding function, was indeed correct. This further supports the view that this test is potentially useful for detecting early cognitive changes occurring in the preclinical phases of AD (de Jager et al., 2003), as it measures the function of the brain structures known to be vulnerable to the earliest changes distinctive of AD pathology.

The co-localization of functional activation during successful visuospatial associative learning and significant correlation between visuospatial memory scores and grey matter volume within the medial temporal lobes (although proven in two separate samples of subjects), demonstrates the potential for multimodal imaging to describe the behaviourally-relevant variability of brain regions in the healthy, as well as in the diseased, brain. This convergence of structural (VBM) and functional (fMRI) imaging results suggests that significant correlations between MRI measures of brain structure/morphology and scores on a certain cognitive task reveal the regions where neuronal activation enables correct performance of that specific task. This further validates the use of VBM correlational approaches in studying brain correlates of complex cognitive/behavioural symptoms in elderly controls and in patients with neurodegenerative dementias, especially for those symptoms that would otherwise be difficult

to “isolate” from other cognitive functions (Rosen et al., 2005). Thus, our findings provide evidence for the assumption that correlational VBM analyses reveal similar anatomical underpinnings to those of functional MRI tasks. They are also in line with previous studies providing evidence that individual brain structural and functional properties explored separately can be united to explain individual differences in behaviour (Tomassini et al., 2011).

4.5.4 Methodological considerations

Several limitations of the study presented in this Chapter should be noted. First of all, although both based on visuospatial paired associates memory, the two versions of the placing test used for the VBM and fMRI study did not correspond perfectly, as adjustments needed to be made to fit the medium of fMRI. The original task tested cued recall, whereas the fMRI task, using a 2-button response, necessarily had to test cued recognition. A brief pilot study showed that the two versions of the task corresponded well, allowing us to make comparisons between the two media. Another limitation was that the two studies were conducted with two different subject groups scanned at different times and with different protocols. However, this may actually be a strength point, as it implies a convergence of evidence even across different groups.

4.5.5 Conclusions

The results emerging from the study presented in this Chapter further demonstrate the potential for multimodal imaging to define brain regions showing behaviourally relevant variability in healthy, as well as in diseased brains. They further validate the use of the Placing Test in detecting changes associated with medial-temporal lobe dysfunction and therefore suggest that it is a potentially useful memory test for detecting the earliest cognitive changes occurring in preclinical phases of AD.

Chapter 5

Protocol development to study cross-sectional differences between controls and patients with MCI and AD

5.1 Abstract

Functional MRI measures functional activity at rest or in response to cognitive demands, which is thought to be a promising measure of dynamic and short-term responses to potential interventions/treatments. Previous fMRI studies on patients with MCI and AD have shown variable results possibly due to methodological limitations. To better characterise the use of fMRI in these stages and overcome some of the limitations of previous cross-sectional studies, a novel multimodal protocol that included both structural and functional MRI sequences was set up. Patients with MCI and AD were recruited for this purpose. A full description of recruiting strategy, MRI sequences and imaging data analyses used in this study is provided in this Chapter. Corresponding experimental results of cross-sectional comparisons between healthy controls, patients with MCI and patients with AD will be presented in *Chapters 6* and *7*.

5.2 Experimental procedures and study design

The present research project was focused on studying cross-sectional differences between patients with a diagnosis of mild probable AD (who were not taking any treatments with cholinesterase inhibitors), patients with a diagnosis of possible pre-dementia including amnestic MCI, and age-matched healthy volunteers. Participants underwent physical examination, neuropsychological evaluation, and MRI scanning. They were asked to participate with a study partner who knew them well enough to give information about their activity of daily living and cognitive performance and who could act as personal consultee and agree to give agreement on their behalf in case they were considered to be lacking mental capacity. Study partners of patients were usually their carers (spouse, family member, partner or friend) and had an up-to-date knowledge of the patient's day-to-day needs and abilities.

5.2.1 Recruitment of study participants

Participants were recruited from the OPTIMA Project and from the Oxford Memory Assessment Clinic (OXMAC) at the John Radcliffe Hospital.

Healthy volunteers were recruited as such if they did not have a subjective or reported memory complaint and performed within the normal range in global cognitive scales (i.e., MMSE>26 and CDR=0). A diagnosis of MCI was given when Peterson's criteria revisions proposed by Winblad et al. (Winblad et al., 2004) were fulfilled. These criteria include: (i) presence of memory complaints by participant or informant; (ii) cognitive and functional status not consistent with a diagnosis of dementia (as defined by DSM IV); (iii) cognitive deficits on memory testing together with report of decline over time by participant or informant; (iv) intact functional status as judged clinically and established by the BADSL+. The diagnosis of AD was given when both the DSM-IV criteria (American Psychiatric Association, 1994) and the NINCDS-ADRDA criteria (McKhann et al., 1984) were fulfilled.

In addition, inclusion criteria for all participants included the presence of an informant or "study partner" (carer, relative or close friend) who knew them well and was willing to take part in the study with them. In the case of patients lacking capacity, the study partner acted as a personal consultee and was asked to sign an agreement form on behalf of the participant. Exclusion criteria included evidence or history of stroke, epilepsy, focal brain lesions, Parkinson's disease, frontotemporal, vascular or atypical dementia, or any major psychiatric disorder including major depression. They also included history of alcohol or substance abuse, contraindication to MRI, presence of behavioural symptoms that would preclude the gathering of data for the study, and active participation in a clinical drug trial. Participants suffering from hypercholesterolemia, diabetes, hypertension, were included in the study if their medical conditions were under stable pharmacological control. Numbers of co-morbidities were matched across the three groups.

A total of 108 older adults were enrolled and consented to take part in the study. Of these, 90 could be clearly classified among the experimental groups: 26 were included as healthy controls, 29 as amnestic MCI, and 35 as probable AD. The remaining participants were excluded because they did not clearly meet the criteria for either control or MCI (n=5), were diagnosed as non-amnestic MCI on neuropsychological assessment (n=2), could not tolerate the MRI for claustrophobia (n=3), or received a different neurological diagnosis during the study (2 were diagnosed as having depression, 1 as having Parkinson's disease, 1 as having semantic dementia, 1 as having Lewy Body dementia, 1 was found to have a vascular malformation at MRI, and 2 were found to have focal brain lesions secondary to previous traumatic brain injury or haemorrhage (which had not been reported at the time of recruitment).

Out of the 90 participants, 1 control, 4 patients with MCI and 5 patients with AD were further excluded because of bad MRI data quality for significant movement artefacts or because of the

presence of severe vascular lesions or WM hyperintensities on FLAIR sequence. Therefore, in *Chapter 6* data from a sample of 80 participants (25 controls, 25 MCI and 30 AD) will be presented.

5.2.2 Study procedures

All participants' assessment took place at the John Radcliffe Hospital site in Oxford. Each assessment included the following:

1. Collection of consent and demographic data,
2. Medical history and physical examination
3. Blood sample
4. Neuropsychological testing
5. Study partner interview
6. Brain MRI scanning

The whole assessment lasted about 6 hours including breaks. Participants were given the choice of performing the assessment in one day or in two days within a week. Neuropsychological testing was performed to study participants' cognitive performance and to look for any correlation between cognitive performance and MRI changes. The following tests and questionnaires were administered: Mini Mental State Examination (MMSE) (Folstein et al., 1975), Montreal Cognitive Assessment (MoCA) (Nasreddine et al., 2005), Clinical Dementia Rating (CDR) Scale (Morris, 1993), Hopkins Verbal Learning Test-Revised (HVLT-R), Backwards digits, Category and Letter fluency (de Jager et al., 2003), Geriatric Depression Scale (GDS). The study partner interview was carried out to gain additional information on the participant's cognitive, functional, and behavioural status and included the following questionnaires: CDR (informant part), Bristol Activities of Daily Living Scale Plus (BADLS+), Neuropsychiatric

Inventory with Caregiver Distress Scale (NPI) (Cummings, 1997). In addition, both the participant and the study partner were asked to complete the Anosognosia Questionnaire-Dementia (AD-Q) (Migliorelli et al., 1995). This aimed to measure the degree of participant awareness of cognitive impairment, by giving the discrepancy between judgments of participant and informant.

Blood samples were collected for genetic testing of APOE, which is known to have a role in the genetics of Alzheimer's disease and may affect the pattern of brain activation measured by fMRI (Filippini et al., 2009). DNA was extracted from blood according to standard procedures to allow polymerase chain reaction (PCR) for the characterisation of APOE genotype. The genotypisation process was performed by the OPTIMA biobank manager within OPTIMA facilities.

5.2.3 Ethics and Safety

This study was carried out in accordance with the principles of the World Medical Association Declaration of Helsinki (last amended October 2008) and in accordance with the principles of the International Conference on Harmonization (ICH) guidelines for good clinical practice (GCP) (GPMP/ICH/135/95). Ethical approval was received from the Bristol Frenchay Research Ethics Committee (Ethics Ref: 09/H0107/8) in April 2009 prior to commencement of study specific procedures. The study followed the guidance and requirements of the Mental Capacity Act 2005 (UK), which establishes a framework for the protection of the rights of people who lack capacity to ensure that their interests and safety are protected when they participate in research and ensure that their wishes and feelings are respected. Participants were assumed to be competent unless otherwise demonstrated. The Act requires that before a person who lacks capacity is enrolled into an approved study, a suitable person is identified who can act as a 'consultee' and advise the researcher on whether the person who lacks capacity would want

to be involved in the project. In this study, 4 patients were assessed as lacking capacity. Their study partners acted as personal consultees and were requested to sign an agreement form on behalf of the patients.

MRI carries no known adverse risk unless participants have metal foreign bodies that are not declared during the standard pre-scan questionnaire. Extra care over this issue was taken during the recruitment screening process and the scan was not done if doubts about metal remained. Every effort was made to minimise the discomfort of lying in the scan to participants. During the scanning, three researchers (a radiographer, a research assistant and myself) directly assisted participants and communicated with them frequently, either personally entering the scanning room or via the intercom system, to assure that they were comfortable. In addition, heart rate and respiratory waveform were monitored during the scan and were used as further indirect information on the wellbeing of participants.

5.3 MRI protocol development

A multi-methodological MRI protocol was assembled to investigate changes occurring in brain function in symptomatic stages (MCI and AD) with respect to differences in underlying brain morphology, which are known to be already detectable at these symptomatic stages. Both *structural* and *functional* MRI sequences were included in this protocol.

5.3.1 Structural MRI

Structural sequences included a 3D MPRAGE (magnetization-prepared rapid acquisition gradient echo: TR 2040 ms, TE 4.7 ms, flip angle 8°, FOV 192 mm, voxel dimension 1 mm isotropic) and an axial FLAIR (Fluid Attenuated Inversion Recovery: TR 9000 ms, TE 89 ms, flip angle 150°, FOV 220 mm, voxel dimension 1.1 mm x 0.9 mm x 3 mm). The MPRAGE is the T1-weighted series that was subsequently used to study GM structure with region of interest (ROI) and voxel-based morphometry (VBM) analyses (see paragraph 5.4.1). It was also used to include information regarding GM in the analyses of functional data as covariate (see paragraph 5.4.3). In T1-weighted images the CSF looks black, the GM dark grey and the WM light grey (Figure 8A).

The FLAIR was included for pathology detection and rating of WM hyper-intensities (i.e., leukoaraiosis) and/or vascular lesions. FLAIR sequence is commonly used as a complement of, or a replacement for, the conventional T2-weighted sequence. In FLAIR images the CSF is suppressed and set to black and this allows a better definition of periventricular lesions and WM hyper-intensities adjacent to the sulci (Figure 8B). The severity of cerebrovascular lesions and leukoaraiosis on MRI was rated by a visiting neuroradiologist blinded to clinical, neuropsychological, and fMRI findings according a modified version of the Fazekas scale (Fazekas et al., 1987; Inzitari et al., 2009). Participants with moderate to severe lesions (grades 2 and 3) were excluded, as it has been recently shown that leukoaraiosis affects BOLD signal

and should be considered a confounding variable in functional MR imaging studies of elderly individuals (Welker et al., 2012).

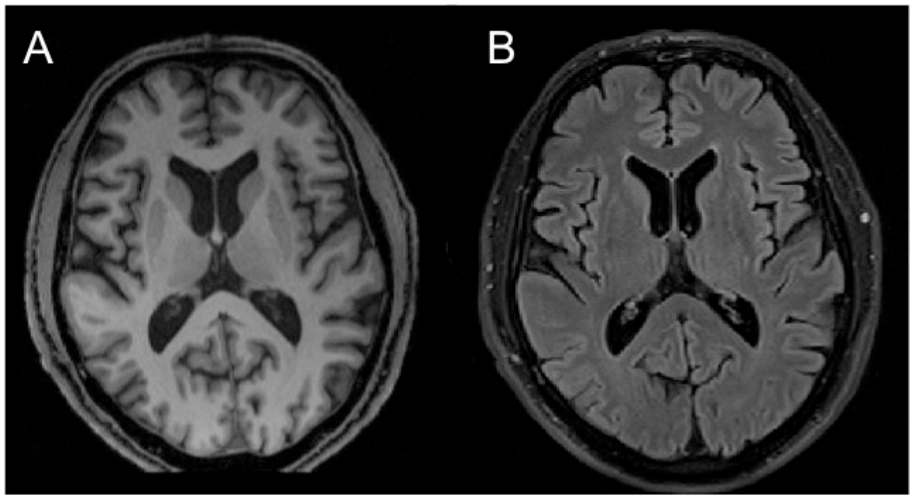

Figure 8 Example images acquired with T1-weighted (A) and FLAIR (B) sequences (from a control subject)

5.3.2 Functional MRI

Functional sequences included 3 separate fMRI BOLD sequences: the first acquired while participants were at rest, in order to measure "resting state activity" or "resting functional connectivity", the second involving a memory task (visuospatial associative memory), and the last one involving a self-appraisal task (which is easy to perform even for participants with memory impairment). Participants were told that the scan time was divided in parts and that they could chose whether carrying on or not after each part.

As discussed in *Chapter 2* (paragraph 2.1), functional MRI (fMRI) provides an *indirect* measure of neural activity by measuring the haemodynamic response to neuronal activity. Increased neuronal activity is associated with an increase in blood flow that exceeds the increase in oxygen consumption, resulting in an increase in the ratio of oxy- to deoxy-haemoglobin. As haemoglobin is diamagnetic when oxygenated, but paramagnetic when deoxygenated, neuronal activity leads to a decrease in magnetic susceptibility and an increase in the blood oxygen level dependent (BOLD) signal (Matthews and Jezzard, 2004).

Single-shot gradient echoplanar imaging (EPI) T2*-weighted images were acquired along the anterior-posterior commissural plane with a slice thickness 3 mm without gap and a matrix size 64 x 64 for all the functional sequences. Details are reported in Table 6.

Resting fMRI scan was performed as the first functional sequence, to exclude potential indirect effects of task (i.e., cognitive rehearsal) on resting. During acquisition of resting fMRI, participants were instructed to lie in dimmed light with their eyes open, to think of nothing in particular, and not to fall asleep.

For *memory-related* fMRI, the experimental paradigm was adapted from the Placing Test, the associative memory test developed in OPTIMA and described in *Chapter 4*, paragraph 4.3.1.2. The Placing test was chosen among other possible memory tests for the following reasons: (i) It was designed to index the function of medial temporal lobe regions (Anderson et al., 2006) and indeed we had found that performance on the Placing test correlated with the degree of atrophy in these regions in a population of older adults (see results reported in *Chapter 4*); (ii) it is sensitive in detecting changes associated with cognitive impairment but not with normal ageing and can be done by all the groups of patients included in the present study (de Jager et al., 2003); (iii) similar fMRI paradigms have been previously used in patients with MCI and AD (de Rover et al., 2011; Gould et al., 2005; Gould et al., 2006a); and (iv) it could easily be adapted to a fMRI task. A full description of this fMRI paradigm is provided in *Chapter 4* (paragraph 4.3.2.2). Before the MRI, subjects were given an extended supervised training with different images and the same response box to familiarize themselves with the tasks. Subjects judged unable to perform the task during training underwent a shorter MRI protocol, which only included structural MRI, resting fMRI, and fMRI of self-appraisal.

For *memory-unrelated* fMRI, a task exploring self- and other-appraisal was used in the assumption that it would have allowed elucidation of the mechanisms underlying *impaired self-awareness* or *anosognosia*, a symptom common in MCI and AD patients that has been little investigated through imaging techniques (Prigatano, 2009). We used an fMRI paradigm similar to those used in previous fMRI studies of self-awareness conducted on healthy adults (Northoff et al., 2006; Schmitz and Johnson, 2007) but adapted to the needs of patients with cognitive impairment. A full description of this fMRI paradigm will be provided in *Chapter 7* (paragraph 7.3.2). Before the MRI, subjects were also given a supervised training on this task, which they all found easy and enjoyable. No participants were excluded because they were unable to perform the task, but several preferred a shorter scan session, and therefore priority was given to resting and memory task-fMRI.

5.3.3 Physiological monitoring

During the acquisition of both *task-* and *resting-fMRI*, physiological fluctuations due to respiratory and cardiac activity were also monitored to account for their effect on functional data. Physiological noise may account for significant portions of spontaneous BOLD fluctuations in human data (Fox and Raichle, 2007; Birn et al., 2006) and its effect may be particularly confounding in groups of older adults and in clinical populations, who are more susceptible to physiological noise due to the presence of brain atrophy and the several confounding factors affecting neurovascular coupling and haemodynamics (Samanez-Larkin and D'Esposito, 2008). Thus, by performing physiological denoising for each subject MRI functional dataset, we made sure that the fMRI results were not contaminated by non-neuronal signal variations due to cardiac and respiratory pulsations and that statistical results were improved by reduction of false positive detection rates. This further increases our

confidence that the signal we measured and used for comparisons across groups truly represented neural activity.

To monitor cardiac and respiratory processes, subjects wore a pulse oximeter and respiratory bellows for all the length of the scan, although physiological data were recorded only during acquisition of resting and task fMRI sequences. Data were logged by the scanner's physiological monitoring unit. The volume trigger from the scanner host computer was also recorded, and all data logged on Acq*Knowledge* version 4.2 (BIOPAC Systems, Inc) at a sampling rate of 100 Hz.

5.3.4 Summary of sequence parameters

MRI scanning sessions were carried out at the 3 Tesla scanner of the University of Oxford Centre for Clinical Magnetic Resonance Research (OCMR) using a 3.0 Tesla Trio Siemens scanner with a 12-channel head-coil. Summary of the parameters we have used for the multi-modality protocol is reported in Table 6.

	Structural		**Functional**		
Sequence	MPRAGE	FLAIR	Epi	Epi	Epi
Condition	----------	----------	Resting State	Memory	Self-appraisal
TR	2040 ms	9000 ms	2000 ms	3000 ms	2000 ms
TE	4.7 ms	89 ms	28 ms	28 ms	28 ms
Flip Angle	8°	150°	89°	89°	89°
Voxel dimension	1x1x1 mm	1.1x0.9x3 mm	3x3x3.5 mm	3x3x3 mm	3x3x3 mm
FoV read	192 mm	220 mm	192 mm	192 mm	224 mm
FoV phase	90.6 %	100%	100%	100%	100%
Base resolution	192	256	64	64	64
Phase resolution	100%	75%	100%	100%	100%
TI	900 ms	2500 ms	----------	---------	----------
Bandwidth	130 Hz/Px	201 Hz/Px	2368 Hz/Px	2368 Hz/Px	2368 Hz/Px
Orientation	Transversal	Transversal	Transversal	Transversal	Transversal

Table 6: sequences and MRI parameters

5.4 Statistical analyses

A general description of the statistical tools used to analyse imaging and non-imaging data will now be provided. However, for each of the experimental Chapters, a section called "Materials and Methods" has been included containing study-specific details or methodological information if different from the following description.

Imaging data analyses were carried out using FMRIB Software Library (FSL) tools (Smith et al., 2004). Processing of imaging data was not blinded to diagnosis as it was based on fully automated techniques. Quality of imaging data (i.e. presence of movements artefacts) was assessed prior to data processing.

5.4.1 T1-weighted structural MRI

ROI analysis:

Because of the known involvement of hippocampus early in the progression of AD, a ROI analysis to compare volumes of the hippocampus among participants was used. ROIs corresponding to the left and right hippocampi were created for each participant from T1-weigheted high-resolution structural images using a newly developed tool for hippocampus-specific alignment and subsequent segmentation with FIRST (FMRIB's Integrated Registration and Segmentation Tool), termed FIRSTv3 (Bishop et al., 2011). Results of this alignment were visually inspected to ensure accuracy. Output volumes were then corrected for total intracranial volume using the covariance method (Buckner et al., 2004; Jack et al., 1989).

VBM analysis:

T1-weighted structural images were analysed with FSL-VBM [(Douaud et al., 2007), www.fmrib.ox.ac.uk/fslvbm], an optimised VBM protocol (Good et al., 2001). Pre-processing was similar to the one described in *Chapters 3* and *4* and included the following steps:

1. Brain extraction: each image was segmented into non-brain and brain tissue (BET- Brain Extraction Tool)
2. Grey matter segmentation: each voxel in the brain was classified as WM, GM or CSF on the basis of its intensity combined with spatial probability of that voxel being WM, GM or CSF (FAST- FMRIB's Automated Segmentation Tool) (Jenkinson, 2003)
3. Registration to a standard template (MNI152) using non-linear registration (FNIRT - FMRIB's Nonlinear Image Registration Tool) (Andersson et al., 2007)
4. Creation of a left-right symmetric, study-specific grey matter template: images resulting from previous steps were averaged and flipped along the x-axis. An equal number (i.e., 25) from each group was randomly selected and used for this purpose to assure that the template was representative of all groups equally
5. Registration to the study-specific template using non-linear registration (FNIRT): this gave a weighted average of tissue density per voxel
6. Modulation: to correct for volume changes due to the registration, the GM volume on the original brain was calculated by multiplying the GM images with the Jacobian determinants (Jacobian warp field) of the deformations used to register the individual brain to the study-specific template
7. Smoothing with an isotropic Gaussian kernel with a sigma of 3 mm (FWHM ~7mm) so that each voxel represents the average of itself and its neighbours
8. Statistical comparisons: permutation-based non-parametric inference within the framework of the general linear model (5000 permutations) (Nichols and Holmes, 2002), which includes full correction for multiple comparisons over space was used to compare GM volume between groups.

5.4.2 Task-related functional fMRI

Analyses of the two task-related fMRI dataset were carried out using FMRIB Expert Analysis Tool (FEAT v 5.98, http://www.fmrib.ox.ac.uk/fsl/feat5/). The analysis consisted of three steps: (i) pre-processing, (ii) single-subject statistical analysis and (iii) multi-subject statistical analysis.

(i) Pre-statistical processing steps:

1) Functional images (EPIs) were checked individually to identify potential scanner artefacts or other acquisition/reconstruction problems
2) Non-brain removal (Smith, 2002b)
3) Head motion correction to assure that through time each voxel remained located at a consistent anatomical point and realign all volumes to a common reference (Jenkinson et al., 2002)
4) Spatial smoothing: images were blurred using a Gaussian kernel of Full Width at Half Maximum (FWHM) of 5 mm. This enabled further removal of random noise and reduced the risk of considering noise-related activation as potential activation of interest. It was also necessary for subsequent statistical analysis using Gaussian random field theory.
5) Temporal filtering: high-pass filtering of 200 secs was used to remove low frequency noise such as drifts related to respiration or to the scanner. The period chosen for the high pass filtering was calculated with 'cut-off calculator' (version 1.1), part of FSL. Low pass temporal filtering was carried using an approach that involves estimating the amount of temporal smoothness in the data and then removing the temporal autocorrelation during the statistical analysis ("prewhitening" process).
6) Unwarping of EPIs to compensate for artefacts due to magnetic field inhomogeneities using fieldmap images (FUGUE- FMRIB's Utility for Geometrically Unwarping EPIs) (Jenkinson, 2003)

7) Registration of EPIs to high-resolution T1-weighted structural images: this was performed using a newly developed implementation of the boundary-based registration (BBR) method (Greve and Fischl, 2009) within the FSL registration tools (Jenkinson et al., 2002), which uses WM boundaries from segmentation of the T1-weighted structural and defines EPIs intensities on samples on either sides of the boundaries. Figure 9 shows how BBR registration improved alignment of images obtained by particularly atrophic brains.
8) Registration of high-resolution T1-weighted structural images to standard space (MNI152) using non-linear registration.

(ii) Single-subject statistical analysis: time series statistical analysis was carried out with local autocorrelation correction. A boxcar convolved with a gamma hemodynamic response function, and its temporal derivative was used to model the data. The most important aspects in canonical HRF modelling are the hemodynamic bolus, the temporal derivative to account for shifts in onset, and dispersion derivatives in order to account for differences in width (Woolrich et al., 2004). We explicitly checked the (temporal) model fit on an individual subject level and found that modelling HRF and the temporal derivative was sufficient for our design. Regressors included in the General Linear Model (GLM) were specific for the task: the model used for memory fMRI has been described in *Chapter 4* (paragraph 4.3.2.4) and the model used for self-appraisal fMRI will be described in *Chapter 7* (paragraph 7.3.3).
Physiological denoising was carried out at this stage: First, cardiac and respiratory phases of each functional volume were derived from their acquisition time relative to a separate physiological recording and modelled via a Fourier basis series with a combination of sine and cosine harmonics by PNM (Physiological noise modelling) (http://www.fmrib.ox.ac.uk/Members/jon/physiological-noise-correction)(Brooks et al., 2008; Harvey et al., 2008), a modification of conventional RETROICOR (Glover et al., 2000). Second,

subject-specific time series obtained with PNM were included as nuisance regressors in the GLM in FEAT single subject analyses. This procedure corrects for the physiological noise in EPI time series and implicitly accounts for loss of degrees of freedom.

(iii) Multi-subject statistical analysis: higher-level (group level) analysis was carried out using FMRIB's Local Analysis of Mixed Effects (FLAME). The GLM included the 3 groups of interest comparison. Each of the contrasts of interest was tested for group averages and difference between groups. Resulting images were corrected for multiple-comparisons using Gaussian Random Field theory with a cluster-forming threshold of $Z>2.3$ and a corrected cluster significance threshold of $P<0.05$. In case there were no significant findings at $p < 0.05$ corrected, an uncorrected $p < 0.005$ value was used to explore data.

After observing significant results, percentage signal changes were extracted to facilitate interpretation and plotting of results. For this purpose, the significant resulting regions were transformed to each subject's functional images space (checking individually that the alignment was accurate) and used as a mask to extract percentage signal change using FSL tools (Featquery, part of FSL).

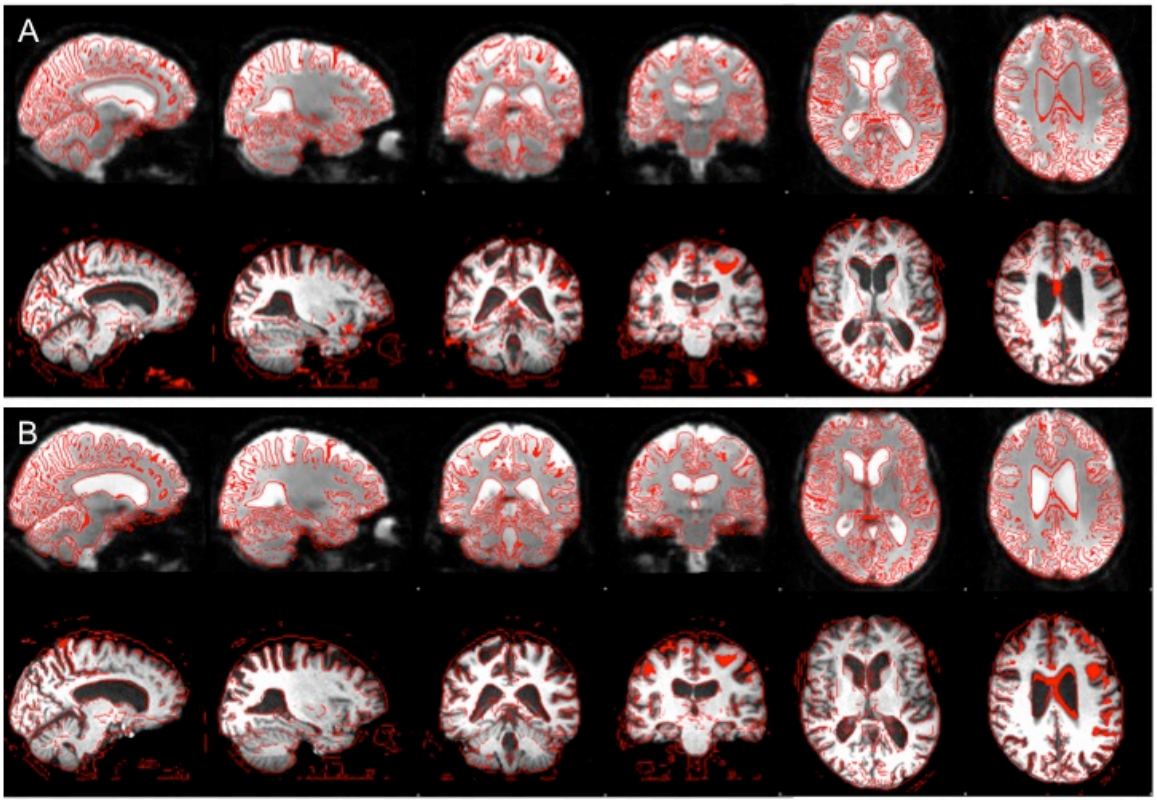

Figure 9 Comparison of registration methods
Alignment of functional image (EPI) to high-resolution T1-weighted structural image of a control subject performed with linear registration (A) and BBR (B). Note how the misalignment of ventricles boundaries obtained with non-linear registration (A) improves with BBR (B).

5.4.3 Resting functional MRI

Analysis of resting fMRI data consisted of four steps: (i) pre-processing, (ii) independent component analysis, (iii) dual regression, and (iv) multi-subject statistical analysis.

(i) Pre-statistical processing

This consisted of motion correction, brain extraction, unwarping using fieldmap and FUGUE, spatial smoothing using FWHM of 6 mm, and high-pass temporal filtering of 150 s (0.007 Hz). Physiological denoising was carried out with PNM: subject-specific time series obtained with PNM were regressed on the pre-processed EPIs so that noise structure could be partially removed from each subject's EPIs.

Images (EPIs) were visually inspected before and after motion correction and before and after physiological denoising: if significant movements were still present the subject was excluded. EPIs volumes were aligned to the individual's T1-weighted structural scan using boundary-based registration (BBR) and to standard space (MNI152) using non-linear registration (FNIRT).

(ii) ICA

Resting-state networks were defined using probabilistic independent component analysis as implemented Multivariate Exploratory Linear Optimized Decomposition into Independent Components FSL tool (MELODIC, http://www.fmrib.ox.ac.uk/fsl/melodic) (Beckmann and Smith, 2004). Pre-processed and denoised functional data containing 180 time points for each subject were temporally concatenated across subjects to create a single 4D data set. Data from an equal number (N=23) of participants in each group were used for this purpose to avoid bias towards the larger group (total number of data sets included was therefore 69). The concatenated 69 fMRI data sets were decomposed using ICA to identify large-scale patterns of functional connectivity in the whole sample. In this analysis data set was decomposed into 25 components in line with previous studies (Damoiseaux et al., 2011).

Biologically valid, nonartifactual RSNs were identified both by visual inspection and by using spatial correlation (i.e., r>0.49) against a set of previously defined maps (Filippini et al., 2009; Smith et al., 2009).

To assure that the chosen dimensionality did not affect results, decomposition into a higher number of components (50) was also explored and resulting maps compared with those resulting from lower dimensionality. Nonartifactual networks found with this higher dimensionality constituted sub-networks of those found with the 25-component decomposition and did not significantly change the results of the group comparisons (data not shown).

(iii) Dual regression

Dual regression was then used to identify individual temporal dynamics and associated

spatial maps of RSNs of interest in all participants, allowing for between-subject voxel-wise statistical comparisons of resting functional connectivity (Filippini et al., 2009). First, spatial regression was performed using ICA spatial maps in a linear model fit against each participant's fMRI data set, resulting in matrices describing temporal dynamics for each component in each participant. Second, temporal regression was performed using each participant's time course matrices in a linear model fit against their fMRI data set, resulting in participant-specific spatial maps. Finally, the different component maps were collected across subjects into single 4D files (1 per original ICA map, with the fourth dimension being subject identification).

(iv) Multi-subject statistical analysis

Voxel-wise statistics were then performed using 'randomise' (Nichols and Holmes, 2002), with voxel-wise grey matter volume included as 4-dimensional confound regressor.

Results were considered significant at $P < 0.05$, fully corrected for multiple comparisons across space (after initial cluster-forming thresholding at $p<0.05$ uncorrected).

To constrain analyses to the cortex, a mean mask created by averaging the grey-matter segmentations obtained from each subject's T1-weighted images was used.

5.4.4 Imaging Covariates

To determine whether BOLD contrast differences between the groups of interest were influenced by structural differences, structural images were used as covariates to interrogate fMRI data. More precisely, an additional four-dimensional nuisance variable representing voxel-specific grey matter density for each subject was included in the general linear models (Oakes et al., 2007). This was created from the segmented, registered and smoothed T1-weighted images and was included in the fMRI model to help disentangle the effects of inter-subject structural and fMRI signal variations.

Chapter 6

Residual functional connectivity and activity in MCI and AD

converging evidence from memory task- and resting-fMRI

6.1 Abstract

Functional MRI has great potential for unravelling the mechanisms of changes in brain function in AD. However, previous task-fMRI studies using memory paradigms have not clearly characterised functional changes with respect to underlying structural differences and were limited by different abilities of patients to perform the cognitive tasks during scanning. Task-unrelated fMRI acquired at rest (resting-fMRI) has even more potential for assessing brain function, but greater understanding of how networks of coherent functional activity at rest relate to the functioning of the brain is needed. As described in *Chapter 5*, task- and resting-fMRI were combined in a multimodal MRI protocol. Results of task-fMRI during execution of visuospatial associative memory task and resting-fMRI are presented in this Chapter. Cross-sectional comparisons between healthy controls, MCI and AD, showed that successful performance of visuospatial associative memory is associated with increased task-fMRI functional activity in lateral prefrontal regions in patients with AD relative to controls, and that such increased functional activity overlaps with increased resting-fMRI functional connectivity of frontal and anterior resting state networks. These findings suggest that task-related and resting *functional* MRI can inform on residual brain function detectable over and above the known changes in brain morphology and cognitive performance, emerging as a sensitive marker of residual ability that could potentially be used to measure the effect of new treatments.

6.2 Introduction and rationale

Structural brain changes occurring in MCI and AD have been well characterised and are especially prominent in the medial temporal lobes (MTL) and in the medial surface of the posterior part of the brain (retrosplenial, posterior cingulate and precuneus cortices) (Bozzali et al., 2006; Chetelat et al., 2005; Hamalainen et al., 2007b; Karas et al., 2008; Risacher et al., 2009; Whitwell et al., 2008b). Atrophy further extends to association areas and frontal regions as AD progresses (Scahill et al., 2002; Busatto et al., 2008; Fennema-Notestine et al., 2009a; Jack et al., 1992). Very recently, it has been shown that atrophy can also be detected in the preclinical, pre-symptomatic stage of AD (Tondelli et al., 2011; Dickerson et al., 2011; Bateman et al., 2012). Thus, there is increasing consensus on both the timecourse and the spatial distribution of changes occurring in brain structure through different stages of AD.

Functional MRI provides an indirect measurement of synaptic activity (Brickman et al., 2009), which allows for the detection of dynamic and short-term changes occurring in brain function that may be the best correlate of cognitive performance. Therefore, it may have the potential to inform on functional adaptive responses occurring over and above the structural changes in different stages of AD and detect the earliest signals of efficacy of interventions and treatments (Dickerson and Sperling, 2005; Sperling, 2011). However, there is no consensus yet about the timecourse and the spatial distribution of changes occurring in brain function through different stages of AD.

Several studies have used fMRI to assess response to episodic memory tasks (task-related fMRI) or to examine spontaneous fluctuations of basal brain function at rest (resting-fMRI) in patients with MCI and AD. However, their results do not show a consistent pattern of changes across different stages of the disease.

In fact, while some task-fMRI studies have shown progressive decrease of MTL functional signal in patients with MCI and AD (Johnson et al., 2006; Petrella et al., 2007; Johnson et al.,

2005; Machulda et al., 2003; Sperling et al., 2003; Pariente et al., 2005), others have shown a relative increase in patients with MCI (Dickerson et al., 2005; Kircher et al., 2007), and have interpreted it as possibly reflecting compensation processes of the MCI phase that counteract the structural damage, but that dissipate in the AD phase when the neuronal loss becomes more widespread than it can accommodate. The variability of results of task-fMRI studies using memory paradigms in patients with MCI and AD probably relates to the relatively small numbers of patients in the earlier studies, to the variable ability of patients to perform the memory task used during the fMRI, and to the fact that they did not account for underlying differences in brain atrophy (Dickerson and Sperling, 2008).

Resting fMRI allows us to assess brain function without the problems related to the use of a cognitive task that patients might find difficult to perform. The default-mode network (DMN) is the most widely studied network in patients with AD and is also commonly found in task-related fMRI experiments when interrogating for deactivations occurring during active task relative to baseline (Greicius et al., 2004; Celone et al., 2006). Several studies have shown that functional connectivity within the DMN is abnormal in patients with MCI and AD. The most consistent finding consists in reduced functional connectivity in patients relative to controls in regions in the precuneus and posterior cingulate cortex (Greicius et al., 2004) and, less consistently, in the hippocampus (Greicius et al., 2004; Wang et al., 2011). However, with the advent of data-driven approaches such as independent component analysis (ICA) non-DMN networks are increasingly being identified and explored (De Luca et al., 2006; Damoiseaux et al., 2008; Damoiseaux et al., 2011). Recent resting-fMRI studies examining these networks have found that that functional connectivity within frontal and frontoparietal networks (variably indicated as “executive” and “frontal-parietal” networks or “anterior DMN” and “ventral DMN”) is increased in patients with AD relative to controls (Agosta et al., 2011; Damoiseaux et al., 2011; Jones et al., 2011). Similar to task-related fMRI, increases in functional connectivity have been interpreted as expression of possible compensatory

mechanisms and have sometimes been correlated with increased scores of cognitive performance (Wang et al., 2011).

However, the relationship between unconstrained brain activity explored with ICA resting-FMRI and changes in brain activity in response to cognitive demand explored with task-related-fMRI has not been directly examined in patients with MCI and AD, although it has been demonstrated in young carriers of the ε4 allele of APOE (Filippini et al., 2009).

In the present Chapter, combined task- and resting-fMRI data from healthy older controls, people with MCI, and patients with AD are presented. Signal changes from both functional modalities were carefully characterized with respect to underlying differences in brain structure and morphology. For task-related fMRI, an event-related fMRI paradigm ("the placing test", see *Chapter 4*) that allowed disentangling successful from unsuccessful performance on encoding and recognition was adopted. For resting-fMRI, different resting state networks identified with group ICA, were separately investigated and compared between groups with the "dual regression" approach. By combining task- and resting-fMRI, improved interpretability of both techniques was achieved by reference to the other.

6.3 Methods

6.3.1 Participants

Recruitment strategies and inclusion and exclusion criteria are described in *Chapter 5*, paragraph 5.2.1. Eighty older adults were included in this part of the study, of whom 30 had a diagnosis of probable AD, 25 had a diagnosis of MCI, and 25 were age- and education-matched cognitively healthy controls.

Physiological monitoring (see paragraph 5.2.3) failed or was not properly recorded for 2 controls during resting-fMRI, for another 3 controls during task-fMRI, for 1 participant with MCI during task-fMRI, and for 2 patients with AD during task-fMRI. In addition, one control did not have unsuccessful performance during task-fMRI therefore was excluded from the task-fMRI group analysis. Finally, 3 patients with AD were unable to perform the task in the scanner.

Thus, we included in the task-fMRI analyses data from 21 controls, 24 MCIs, and 25 ADs, and in the resting-fMRI analyses data from 23 controls, 25 MCIs, and 30 ADs.

Table 8 presents demographic and neuropsychological characteristics of the 70 subjects who where included in the task-fMRI analyses. There were no significant differences in age, years of education, gender, handedness, and family history for dementia, and co-morbidity for other diseases including cardiovascular risks factors between the three groups. The same table also presents behavioural results on the fMRI task (discussed in paragraph 6.4.2.1) and hippocampal volume (discussed in paragraph 6.4.1).

	Controls	MCI	AD	Group Comparisons
Demographic characteristics				
N	21	24	25	---
Gender, F:M	13:8	11:13	10:15	n.s., p=0.32
Age, years	75.8 (7.5)	75.3 (6.7)	75.0 (6.2)	n.s., p=0.91
Education, years	14.9 (3.3)	14.2 (3.1)	13.7(3.5)	n.s., p=0.48
N of cardiovascular risks factors	0.6 (0.6)	0.4 (0.6)	0.6 (0.7)	n.s., p=0.41
Family history of dementia, yes:no[$]	5:11	5:16	10:12	n.s., p=0.31
N of APOE ε4 carriers	7	12	15	n.s., p=0.14
Neuropsychological characteristics				
MMSE total	29.6 (0.6)	26.8 (1.6)	22.5 (3.5)	Controls-MCI** MCI-AD**
MoCA total	27.1 (2.7)	22.2 (2.4)	17.6 (3.7)	Controls-MCI** MCI-AD**
CDR global severity	0	0.5	0.5 (6 patients) 1.0 (17 patients) 2 (2 patients)	---
CDR sum of boxes	0.7 (0.2)	1.7 (0.9)	5.4 (2.6)	Controls-MCI* MCI-AD**
Backward Digit Span	4.5 (1.2)	3.8 (0.8)	3.5 (1.2)	Controls-MCI n.s. MCI-AD n.s.
HVLT total recall	27.1 (5.0)	19.2 (6.1)	12.5 (5.9)	Controls-MCI** MCI-AD*
HVLT delayed recall	6.8 (4.6)	3.6 (3.8)	0.6 (1.7)	Controls-MCI* MCI-AD*
Category Fluency	26.9 (6.6)	19.2 (6.0)	13.5 (5.9)	Controls-MCI** MCI-AD*
Letter Fluency	14.5 (4.9)	12.7 (4.6)	10.0 (4.2)	Controls-MCI n.s. MCI-AD, n.s.
GDS	3.9 (4.3)	7.6 (5.2)	6.2 (3.4)	Controls-MCI* MCI-AD n.s.
NPI	1.3 (2.6)	3.7 (4.9)	10.2 (9.4)	Controls-MCI, n.s. MCI-AD*
BADLS plus	0.4 (0.9)	2.9 (2.7)	18.6 (8.9)	Controls-MCI, n.s. MCI-AD**

Performance on fMRI task (visuospatial associative memory)				
Accuracy	0.73 (0.20)	0.54 (0.25)	0.22 (0.27)	Controls-MCI* MCI-AD**
Anatomical characteristics				
Adjusted left hippocampal volume - mm^3	3779 (395)	3060 (555)	2771 (484)	Controls-MCI** MCI-AD* (p=0.038)
Adjusted right hippocampal volume - mm^3	3910 (450)	3256 (618)	2842 (477)	Controls-MCI** MCI-AD*(p=0.005)
Total intracranial volume – cm^3	1409.17 (119.9)	1426.61 (131.2)	1440.58 (142.5)	n.s., p=0.68

Table 8 Demographical, neuropsychological, behavioural fMRI, and anatomical characteristics of the 70 participants who performed task-fMRI
** Post Hoc Test significant at P<0.001, * Post Hoc Test significant at P<0.05. Comparisons of neuropsychological, fMRI task and anatomical variables between controls and patients with AD were all significant at P<0.001, except for backward digit span (0.08) and GDS (n.s.). Therefore we only specify comparisons with MCI and the other two groups who were significant at variable degrees in different variables.

6.3.2 Image acquisition and analyses

Image parameters are summarised in *Chapter 5*, paragraph 5.3.4.

Statistical analyses of imaging data are also described in *Chapter 5*, paragraph 5.4.

The experimental paradigm and GLM used for task-related fMRI are described in *Chapter 4*, paragraph 4.3.2.

6.4 Results

6.4.1 VBM results

The whole-brain VBM analysis showed that patients with MCI were significantly more atrophic than controls in clusters covering both the body and head of the right and left hippocampus, extending inferiorly to the parahippocampus and – on the left side - also superiorly to the thalamus (Figure 10). Patients with AD were significantly more atrophic than controls in several extended brain regions including medial, anterior and postero-inferior regions of temporal lobes, posterior cingulate/precuneus, lateral temporo-parietal cortices, thalamus, head of caudate, fronto-lateral and insular cortex, and anterior cingulate. AD patients were significantly more atrophic than MCIs in similar regions, but to a lesser extent.

To explore whether the VBM comparison between controls and MCI reflected an earlier involvement of left hippocampus in the progression from normal ageing to MCI, we entered adjusted right and left hippocampal volumes on a mixed ANOVA, with group as between- and hippocampal side (right or left) as within-subject factors. This showed a significant effect of side ($F_{(1,77)}$ =9.5, p<0.005), with the right hippocampus being larger than the left across all the groups, and a significant effect of group ($F_{(2,77)=}$34.9, p<0.001), with controls having bigger hippocampi than both MCI and AD, and MCI bigger hippocampi than AD, as shown by post-hoc tests. The interaction between side and diagnostic group was not significant ($F_{(2,77)}$ <1, n.s.).

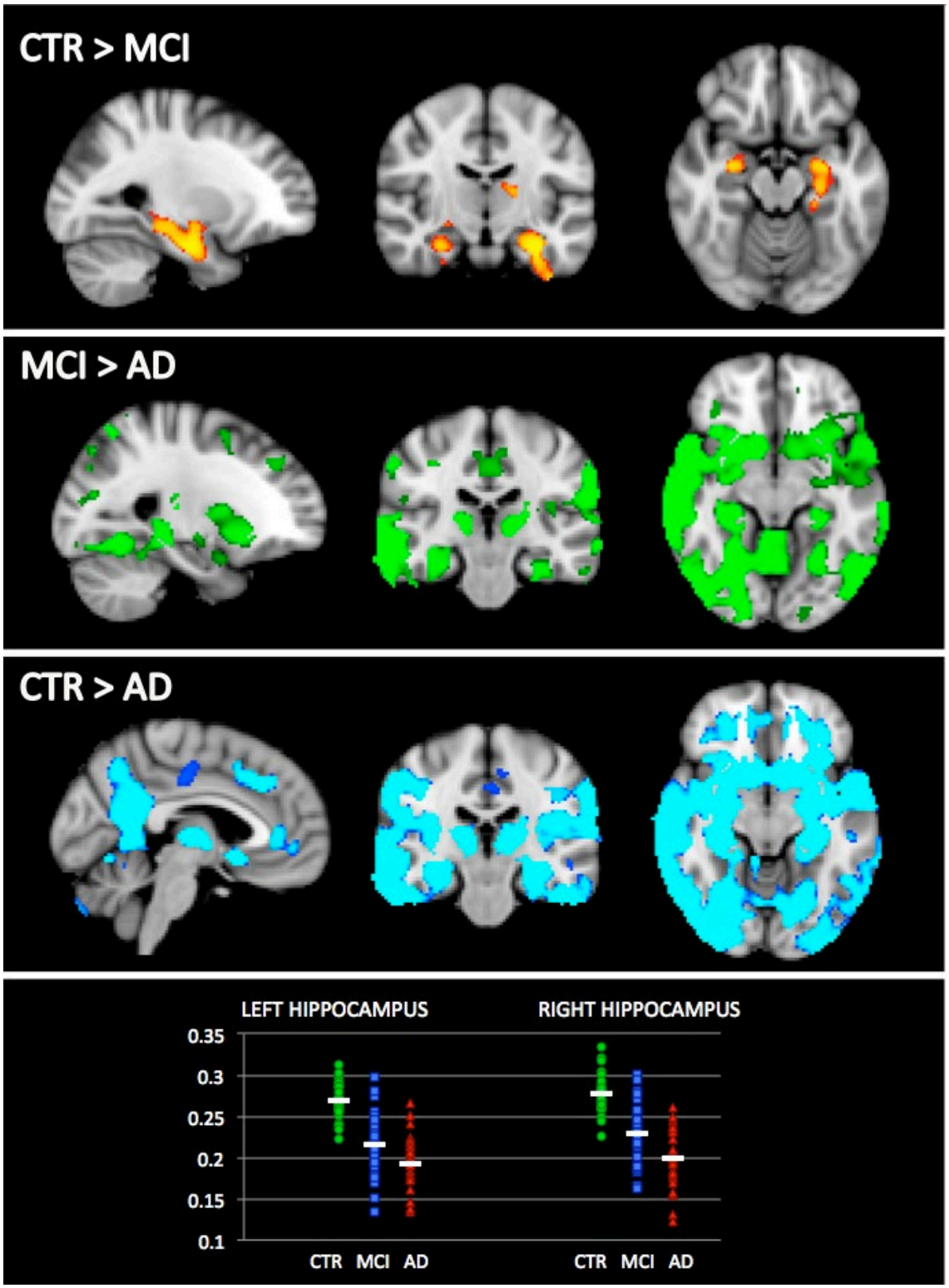

Figure 10 Results of VBM (structural MRI)
VBM analysis results of group comparisons. Age, gender and years of education were included as confounding variables. Images are shown in radiological convention. The plot represents normalised volumes of right and left hippocampus expressed as percentage of total intracranial volume. Controls are represented by green circles, MCI patients by blue squares, and AD patients by red triangles

6.4.2 Memory task-fMRI results

6.4.2.1 Behavioural results of the memory fMRI task

Performance during the fMRI memory task was measured as accuracy (rate of hits minus rate of false recognitions), ranging between -1 and 1 (scores ≤ 0 indicate that a subject was probably guessing). As expected, there were significant differences between groups ($F_{(2,67)}$=25.3, p<0.001), where patients with AD performed significantly worse than patients with MCI, who performed significantly worse than controls (Table 8). One MCI and three AD patients performed below the level of chance: exclusion of these participants from the group fMRI analysis did not change the results.

6.4.2.2 Within-group results

Patterns of activation and deactivation (relative to baseline, i.e. fixation cross) during successful and unsuccessful *encoding* and *recognition* are shown in Figure 11. Controls showed increased activation in the medial temporal lobes for both *encoding* and *recognition* (either successful or unsuccessful), and increased activation in ventral lateral prefrontal regions for *recognition* only. In addition, there were diffuse activations probably related to the visual presentation of stimuli in occipital regions for both tasks. Decreased activations relative to baseline were revealed in medial-parietal regions, including precuneus and posterior cingulate, and in the anterior cingulate for both tasks.

The comparison of *encoding* relative to *recognition* in the control group showed significant differences in medial ventral prefrontal cortex, whereas recognition relative to encoding showed significant differences in the right ventral lateral prefrontal cortex and right lateral parietal cortex and precuneus (see left side of Figure 15).

The comparison of successful relative to unsuccessful *encoding* did not yield significant results in any of the groups. Similarly, we did not find significant differences in hippocampal signal

change between successful and unsuccessful *encoding* when extracting the BOLD signal from subject-specific hippocampal masks (anatomical ROIs).

The comparison of successful relative to unsuccessful *recognition* in the control group revealed several regions, including the left hippocampus, left insula, left putamen, and left supramarginal gyrus (Figure 12). No significant difference was found in the MCI group between successful and unsuccessful *recognition*. Instead, in the AD group, the same comparison revealed significant activations in two clusters covering the lateral prefrontal cortex, anterior insula, putamen and caudate bilaterally, but more extended on the right side. Anatomical ROI analyses confirmed that hippocampal signal change for successful *recognition* was significantly greater than unsuccessful *recognition* in both the right (t_{70}= 2.21, P<0.05) and left hippocampus (t_{70}= 2.30, P<0.05) across the whole sample, but only at the trend level in the left hippocampus and in the control group only (t_{21}= 1.77, P=0.09) when considering groups separately.

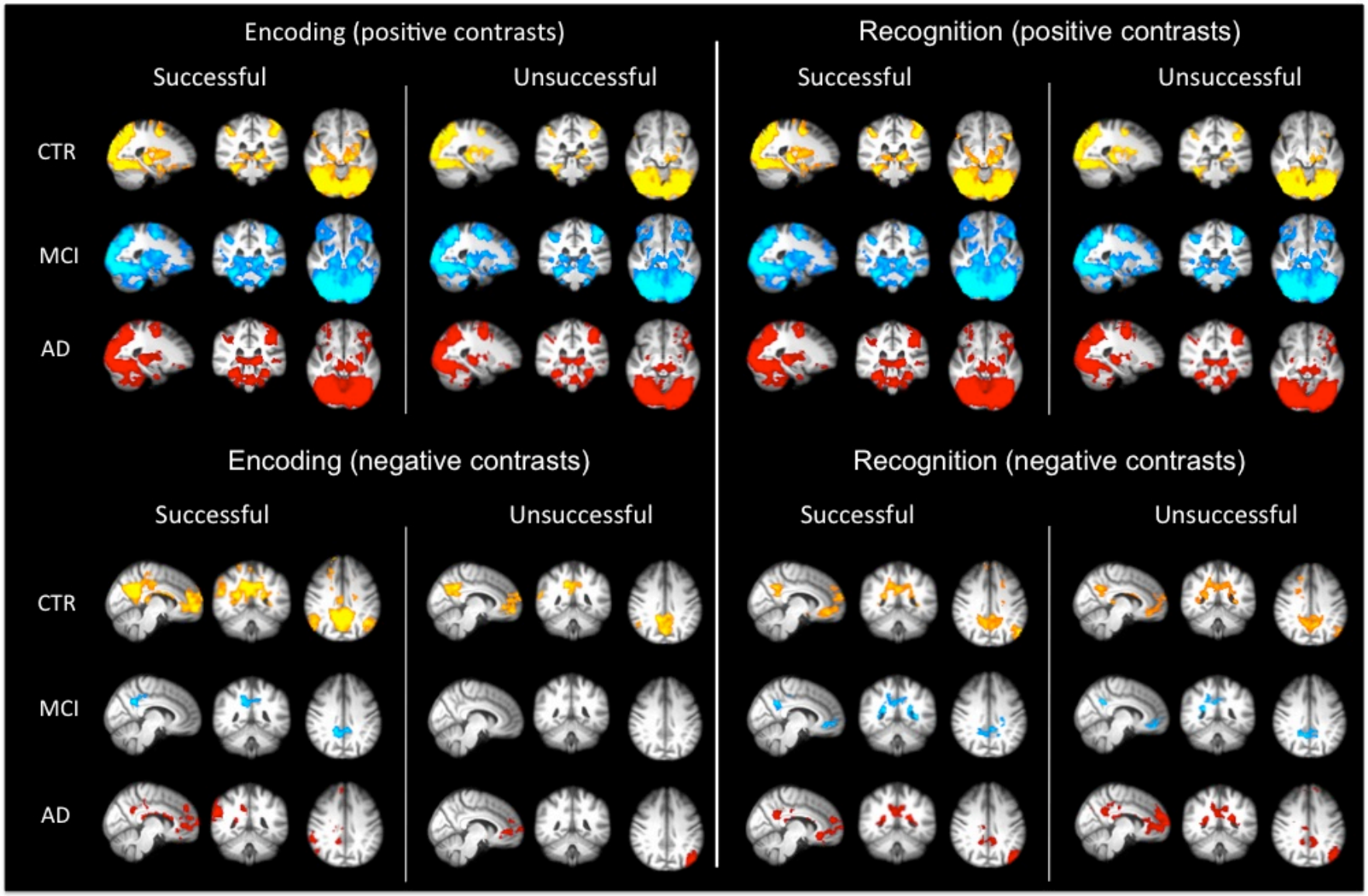

Figure 11 Within-group results of memory task-fMRI

"Positive" contrasts interrogate for increased activation during task relative to baseline, "negative" contrasts for decreased activation (or "deactivation) during task relative to baseline. Analysis was run with the inclusion of voxel-specific grey-matter covariate. Images are shown in radiological convention.

6.4.2.3 Between-group results

Comparisons of successful *encoding* (relative to baseline) between groups showed that controls had greater deactivation than MCI and AD patients in regions of the medial prefrontal cortex including precuneus and posterior cingulate (PPC, see Figure 12). There were no significant group-by condition interactions for *encoding*.

Instead, between-group comparisons of successful relative to unsuccessful *recognition* revealed significant interactions in regions of the lateral prefrontal cortex (LPFC) bilaterally when comparing AD and MCI, and unilateral on the right when comparing AD and controls. These interactions were driven by greater differences between successful and unsuccessful *recognition* in the AD group relative to the other groups (Figure 12).

Analyses on anatomical ROIs showed between-group significant differences in right hippocampal signal change for successful *encoding* relative to baseline ($F_{(2,67)}$=3.4, p<0.05), with the MCI group exhibiting greater activation relative to both the control (P=0.045) and the AD (p=0.019) groups. Similar between-group behaviour showing hyper-activation in the MCI compared to both control and AD groups also occurred for successful *recognition* relative to baseline, although not statistically significant (see bottom-centre plot of Figure 12). However, such "MCI hyper-activation" also occurred for unsuccessful *encoding* and *recognition*. Thus, when comparing successful relative to unsuccessful *encoding* or successful relative unsuccessful *recognition*, the control group was the one with greater hippocampal activation, whereas it appeared decreased in the MCI and in the AD groups, although between-group differences were not significant.

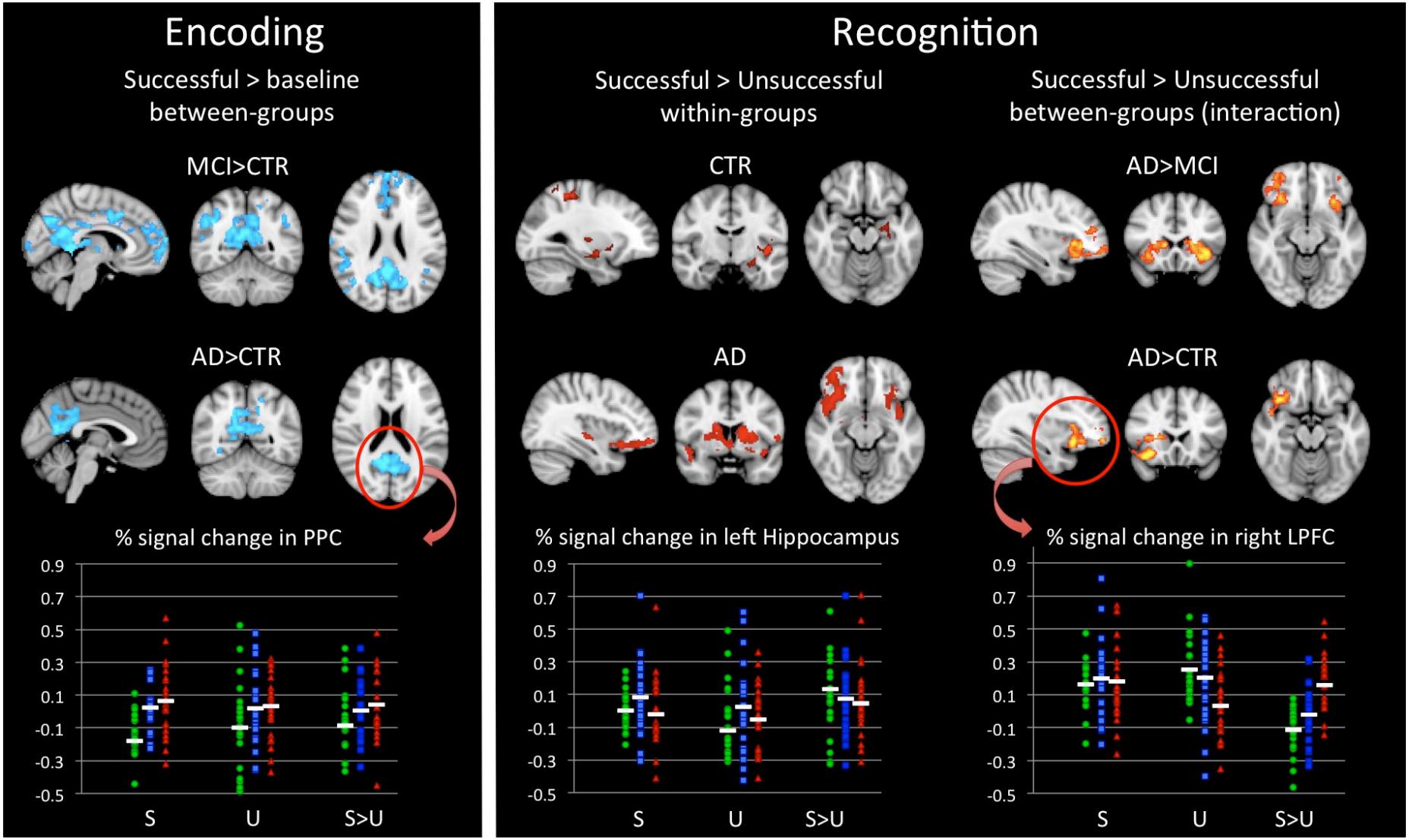

Figure 12 Between-condition and between-group comparisons, and condition by group interaction of memory task-fMRI

Figure 12 Legend (previous page)
Significant results of the analysis of task fMRI carried out at whole-brain (P< 0.05, corrected for multiple comparisons) with voxel-specific grey-matter covariate.
On the left, in blue, regions showing decreased activation for successful *encoding* in controls relative to MCI and AD group respectively.
On the right, in red, regions of significant difference between successful and unsuccessful *recognition* within the controls and AD groups (no significant differences were found in the MCI group); in orange-yellow, regions of significant group-by-condition interaction.
At bottom left, plot of percentage signal change during *encoding* in the PPC functional ROI resulting from the comparison between control and AD. Note that the AD group shows decreased deactivation of this region during both successful and unsuccessful *encoding*.
At bottom-centre, plot of percentage signal change during *recognition* in left hippocampal subject-specific anatomical ROIs. Note that hippocampal hyper-activation in the MCI group compared to both control and AD groups, occurs not only during successful but also during unsuccessful *recognition*.
At bottom right, plot of percentage signal change during Recognition in the right ventral LPFC functional ROI resulting from the group-by-condition interaction.
Controls are represented by green circles, MCI patients by blue squares, and AD patients by red triangles.
PCC, precuneus-posterior cingulate. LPFC, lateral prefrontal cortex. S, successful. U, unsuccessful. Images are shown in radiological convention.

		MNI coordinates			
	Location of peak voxels	**x**	**y**	**z**	**Z value**
Successful > Unsuccessful Recognition in Control					
	L Hippocampus	-26	-10	-16	3.19
	L Putamen	-16	6	-8	3.50
	L Insula	-42	-8	-2	3.97
	L Superior Temporal Sulcus	-52	-38	22	3.22
Successful > Unsuccessful Recognition in MCI					
	---	---	---	---	---
Successful > Unsuccessful Recognition in AD					
	R Frontal Orbital Cortex	32	28	-14	3.76
	R Caudate	14	6	18	3.58
	R frontal Pole	38	48	-12	3.42
	L Insula	-40	0	-14	3.26
	L Putamen	-22	4	10	3.33
	L Caudate	-14	16	10	3.16
Successful > Unsuccessful Recognition in AD > Control					
	R Frontal Orbital Cortex	30	22	-10	4.17
	R Frontal Cortex/Insula	36	20	-14	3.96
Successful > Unsuccessful Recognition in AD > MCI					
	R Frontal Orbital cortex	32	32	-2	3.66
	R Caudate	12	18	6	3.7
	R Frontal Pole	38	40	2	3.30
	L Insula/Frontal Cortex	-36	20	-4	3.96
	L Frontal Orbital Cortex	-30	22	-8	3.95

Table 9 Between-group task fMRI results for Recognition
L, left. R, right.

6.4.3 Resting fMRI results

6.4.3.1 Resting state networks

Seven out of 25 group independent spatial maps could be identified as being functionally and biologically relevant resting state networks (RSNs). They were identified both visually based upon a set of previously defined maps (Beckmann et al., 2005; Damoiseaux et al., 2008) and methodologically using spatial correlation (i.e., r>0.49) with the maps reported in Filippini et al (2009).

A map covering medial parietal (precuneus and posterior cingulate) and ventromedial prefrontal cortex, bilateral lateral temporal and parietal regions, and the hippocampus was identified as the default mode RSN (Figure 13A). As expected from previous task-related deactivations studies (Pihlajamaki and Sperling, 2009), this map overlapped almost perfectly with the map of functional deactivation during encoding (see Figure 15, third column).

Two maps that included primary visual areas, extrastriate regions, and the occipital-temporal junction were respectively identified as the ventromedial and dorsolateral visual RSNs (Figure 13B, C) (Smith et al., 2009; Beckmann et al., 2005). A map covering primary and association auditory cortices including Heschl's gyrus, planum polare and planum temporale, the lateral superior temporal gyrus, and posterior insular cortex corresponded to the auditory RSN (Figure 13D). Two symmetric maps including lateral prefrontal and parietal cortex, dorsal cingulate, and insula were identified as the right and left frontoparietal RSNs (Smith et al., 2009), also known as "working memory" networks (Damoiseaux et al., 2008) or "visual dorsal streams" (Beckmann et al., 2005). They are typically involved in performance of challenging cognitive tasks and have been implicated in attentional and cognitive control functions (Figure 13E, F). The right frontoparietal RSN overlapped with the map of functional activation for recognition relative to encoding (see Figure

15, first column), in line with the recently hypothesised role of this network in supporting strategic searches through memory and monitoring of retrieved information (Fornito et al., 2012).
Lastly, a map including medial prefrontal and fronto-opercular regions was called orbitofrontal RSN and corresponded to the most ventral portions of the "executive control" network (Figure 13G), which is involved in action–inhibition, social cognition, emotion, and empathy (Smith et al., 2009), and has also been indicated as an "anterior" sub-division of the DMN (Damoiseaux et al., 2011; Uddin et al., 2009). This RSN overlapped with the map of functional activation for encoding relative to recognition (see Figure 15, second column), lending support to the role of orbitofrontal cortex in memory processing (Frey and Petrides, 2002).

The default mode RSN and the 3 RSNs involving the prefrontal cortex (the two lateralised frontoparietal RSNs and the orbitofrontal RSN), and a control network in which we did not expect to find any change at baseline (i.e., auditory network) were selected for between-group analyses. The choice of also including frontal RSNs among those of interest was motivated by previous task-related fMRI studies showing increased and possibly compensatory activity in these regions (Schwindt and Black, 2009).

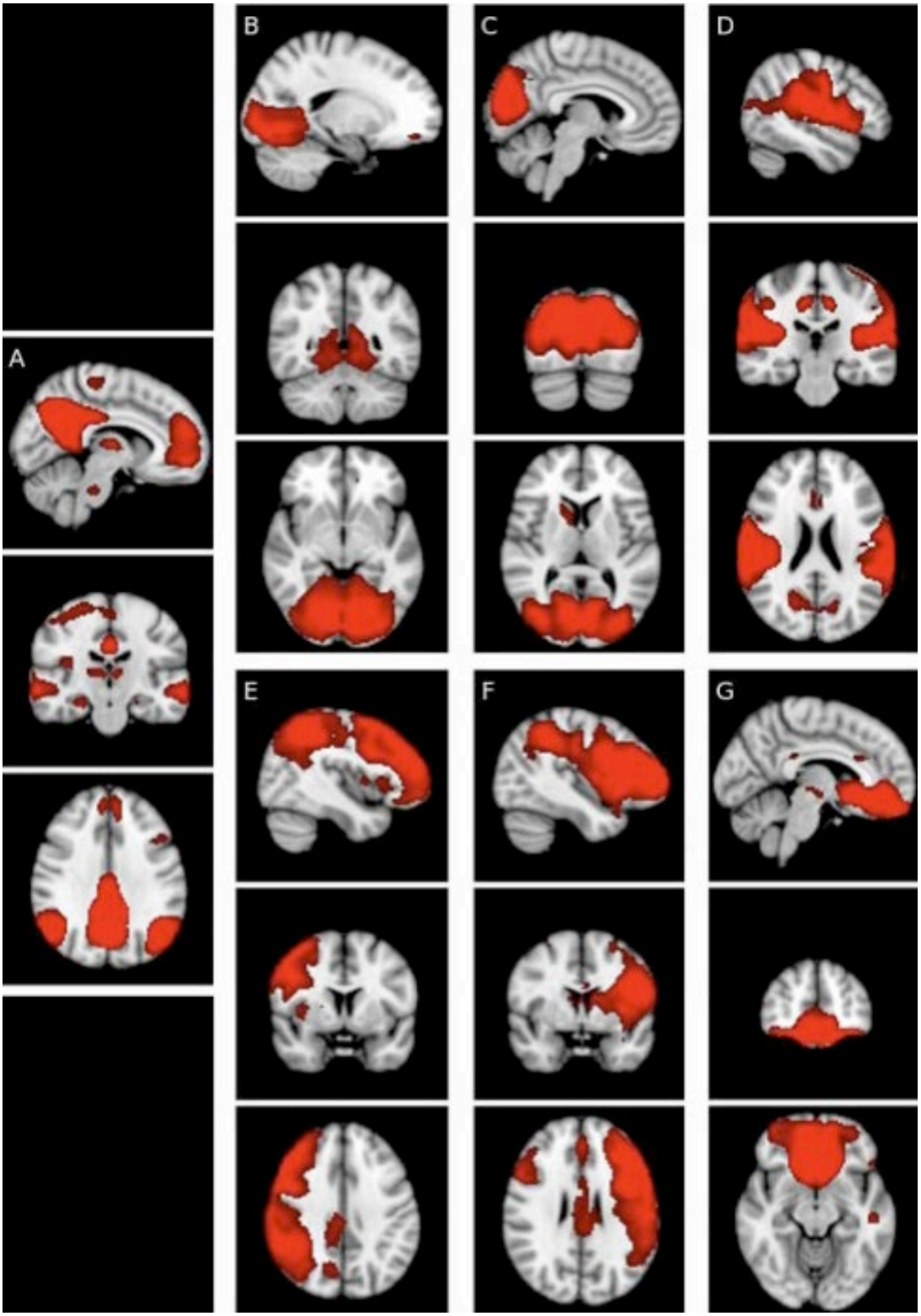

Figure 13 Resting state networks (RSNs)
A) DMN; B) ventromedial visual RSN; C) dorsolateral visual RSN; D) auditory RSN; E) right frontoparietal RSN F); E) left frontoparietal RSN; G) orbitofrontal RSN. Images are shown in radiological convention.

6.4.3.2 Between-group comparisons

Figure 14 shows significant results of the comparisons of coherent unconstrained functional activity within the RSNs of interest between AD and controls.

Within the default mode RSN, controls had greater functional connectivity than AD patients in regions of the medial posterior cortex, including precuneus and posterior cingulated (PPC), extending bilaterally to the posterior part of the hippocampus and to the anterior part of the hippocampus and parahippocampus on the left side only. While removing the variability associated with grey matter volume decreased significant differences in the hippocampi, it did not affect differences in the PPC. Reverse comparisons did not give any significant results. No whole-brain significant differences were found between MCI and any of the other groups, although extraction of parameters estimates showed that MCI had intermediate functional connectivity between controls and AD (Figure 14, top row).

All between-group comparisons within RSNs involving frontal lobes showed significant results in the sense of greater functional connectivity in AD patients relative to controls. More precisely:

- Within the orbitofrontal RSN, AD patients showed greater functional connectivity relative to both controls and MCI groups in orbitofrontal frontal regions, but also in sparse regions of the dorsal medial PFC, caudate, precuneus and insula. Correction for grey matter atrophy did not change the results (Figure 14, second row).

- Within the left frontoparietal RSN, AD patients showed greater functional connectivity than controls in PFC and MTL bilaterally, and in the left parietal cortex; MCI showed greater functional connectivity than controls in left PFC and MTL. Correction for grey matter atrophy only decreased the extent of clusters in MTL (Figure 14, third row).

- Within the right frontoparietal RSN, AD patients showed greater functional connectivity than controls in two clusters of dorsal and ventral lateral PFC. The latter remained after correction for grey matter atrophy but only at the significance level of $P<0.06$ (Figure 14, bottom row).

No significant differences between any of the groups in any direction were found within the control RSN (auditory).

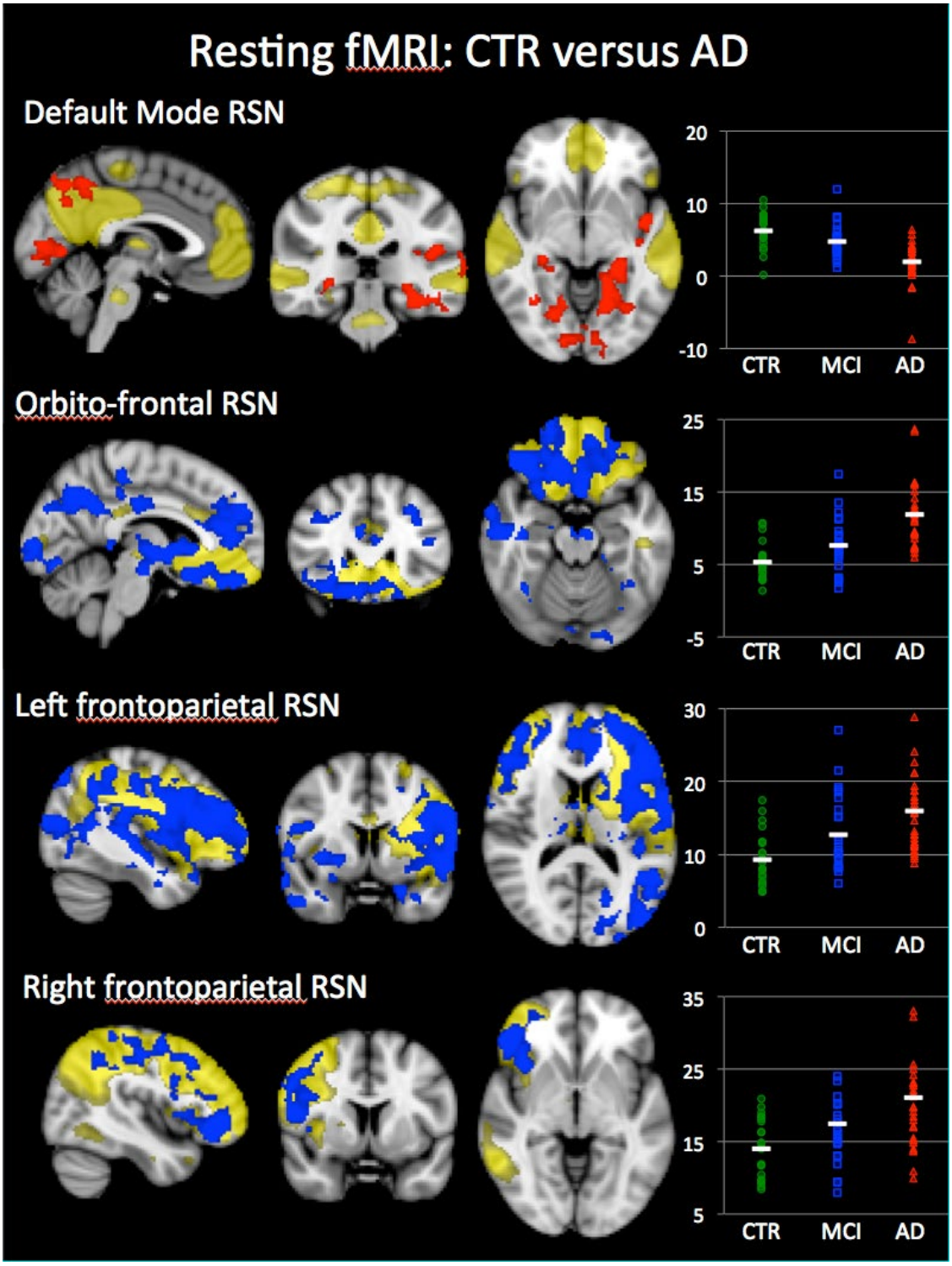

Figure 14 Results of resting-fMRI
Spatial maps of RSNs (transparent yellow) are overlaid with clusters showing significantly reduced (blue) or increased (red) functional connectivity in controls relative to AD. Plots of the connectivity magnitude extracted from each significant cluster for each participant are shown on the right (controls are represented by green circles, MCI patients by blue squares, and AD patients by red triangles). Images are shown in radiological orientation.

6.4.4 Correspondence of task- and resting-fMRI

Figure 15 (right side) shows the anatomical overlap between the significant group-by-condition interaction resulting from task-fMRI and the between-group comparison within the right frontoparietal RSN resulting from resting-fMRI. Comparisons between MCI and AD groups overlapped similarly.

Importantly, there was a significant positive correlation between parameter estimates of task-related functional activation for successful relative to unsuccessful recognition and parameter estimates of resting functional connectivity in the right frontoparietal RSN within the right LPFC region of anatomical overlap between the two (r_{68}=0.32, P<0.05) across the whole sample, which was true at the trend level within the AD group only.

Figure 15 Legend (following page)
Left side of figure: task-fMRI results (orange-yellow) of comparisons between conditions within the control group overlap with resting-fMRI spatial maps (red) of specific RSNs.
- First row: in orange-yellow, task-fMRI results from comparisons between successful encoding and recognition within the control group (cluster corrected at P<0.05).
- Second row: in red, resting-fMRI spatial maps of 3 exemplar resting state networks (thresholded at Z>2, also shown in Figure 13 E, G, and A).
- Third row: anatomical overlap between task- and resting-fMRI (same colours as above).

Right side of figure: task-fMRI group-by-condition interaction overlaps with resting-fMRI results of the between-group comparison within a RSN.
- First row: in orange-yellow, task-fMRI group-by-condition significant interaction revealing regions of greater activation in the AD group relative to controls for successful relative to unsuccessful recognition (also shown in Figure 12, right side).
- Second row: in blue, regions of significantly greater functional connectivity within the right frontoparietal RSN for the AD relative to the control group (also shown in Figure 14, bottom row).
- Third row: plot showing the significant positive correlation (r_{68}=0.32, P<0.05) between parameter estimates of functional activation for successful relative to unsuccessful recognition (on Y-axis) and parameter estimates of functional connectivity within the right frontoparietal RSN (on X-axis), extracted from the region of anatomical overlap between the respective significant clusters. Controls are represented by green circles, MCI blue squares, and AD red triangles.

RSN, resting state network. Coordinates are in MNI. Images are shown in radiological orientation.

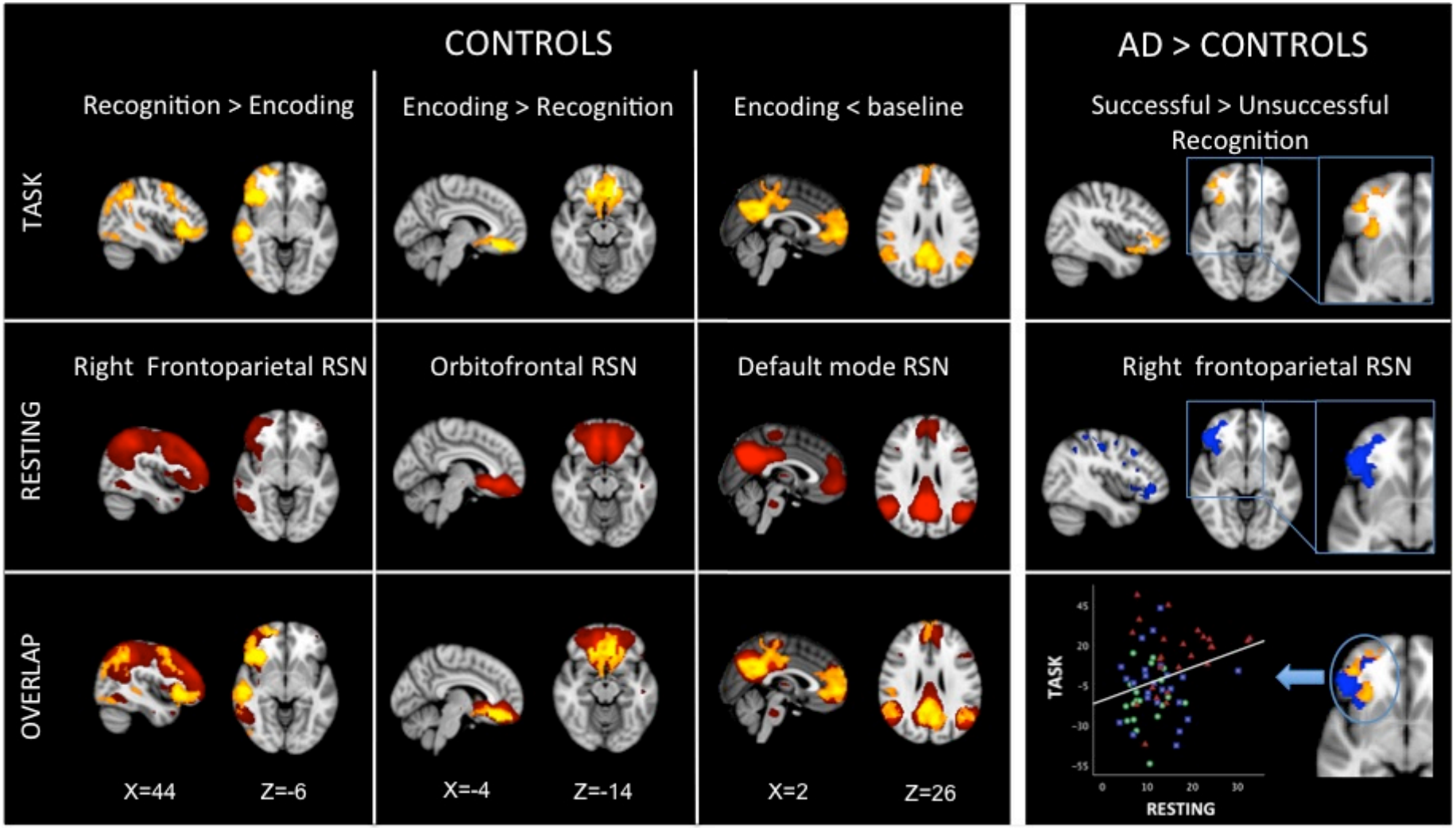

Figure 15 Correspondences between task and resting fMRI

6.5 Discussion

We aimed to test if memory-related fMRI and resting-fMRI give overlapping information on residual functional abilities of patients with MCI and AD. To our knowledge no previous study has combined task- and resting-fMRI in MCI and AD.

We recruited cognitively healthy controls and two patient groups representing different phases of AD progression (MCI and probable AD) and set up a combined MRI protocol, which included functional sequences acquired during the execution of a visuospatial associative memory task (task-fMRI) and during unconstrained rest (resting-fMRI). Findings are discussed according to MRI modality.

6.5.1 Structural MRI

As expected, the VBM results showed significant grey matter loss in AD relative to MCI in several brain regions, and similar but more extended differences in AD relative to the control group, consistent with several previous publications (Scahill et al., 2002; Busatto et al., 2008; Fennema-Notestine et al., 2009a). Volume differences between MCI and controls were confined to the medial temporal lobes, also consistent with several previous publications (Ries et al., 2008; Fennema-Notestine et al., 2009b). Our results from structural MRI are therefore consistent with the well-known pattern of distribution of neuropathological changes typical of AD neurodegeneration, which starts from medial-temporal regions then spreads to medial-parietal cortex and orbitofrontal regions and finally to other neocortical association areas (Braak et al., 1998). They further support our experimental assumption that our groups represent different phases on the AD progression continuum, with the group of amnestic MCI being the intermediate phase.

6.5.2 Memory task-fMRI

6.5.2.1 Within-group results

Patterns of increased and decreased functional activity for *encoding* and *recognition* relative to baseline were similar to what has been shown by previous fMRI studies that have adopted similar experimental paradigms on encoding and recognition (de Rover et al., 2011; Vannini et al., 2011b) or "subsequent memory" experimental paradigms on encoding only (Sperling, 2007; Filippini et al., 2009; Miller et al., 2008a). This correspondence validates our task.

In contrast to the majority of previous studies that used block fMRI paradigms, our event-related design allowed us to classify the visuospatial paired associates as successfully or unsuccessfully encoded and recognised. Increased activation for successful relative to unsuccessful *recognition* was found –among other regions- in the left hippocampus in the control group and in the ventral lateral prefrontal cortex (LPFC) in the AD group. Region-of-interest (ROI) analyses on anatomical hippocampal ROIs confirmed that hippocampal activation for successful *recognition* was significantly greater than unsuccessful recognition in the hippocampus across the whole sample. Hippocampal involvement in successful recognition particularly in the control group is consistent with previous studies that have contrasted successful versus unsuccessful recognition with event-related designs (Pariente et al., 2005; Vannini et al., 2011b). This is in line with the known role of medial temporal structures in episodic retrieval (Nyberg et al., 1996; Schacter and Wagner, 1999) and, more precisely, in the retrieval of previously encoded paired associates (Henke et al., 1997; Zeineh et al., 2003).

The pattern of activation for *recognition* relative to *encoding* in the control group is consistent with the prediction of the HERA (hemispheric encoding retrieval asymmetry) model, which states that the right prefrontal cortex is more involved in episodic retrieval (Tulving et al., 1994a). The

reverse comparison, showing that *encoding* relative to *recognition* engaged ventral medial PFC, is instead consistent with studies that have suggested that this region is involved in various forms of cognition that depend on encoding of spatial and contextual information, through its interactions with the hippocampus (Frey and Petrides, 2002; Kalisch et al., 2006; Kirchhoff et al., 2000). These results validate the functional paradigm we used. In addition, they further suggests that the hyper-activation of right prefrontal cortex found in the AD group represents recruitment of efficient and biologically valid cognitive strategies, not a non-specific effect of the disease on BOLD signal (see following paragraph).

6.5.2.2 Between-group results

Between-group comparisons of functional activation for successful relative to unsuccessful *recognition* revealed hyper-activation of right lateral prefrontal cortex (LPFC) in the AD group relative to both the MCI and control groups. The significant interaction suggests that the mechanisms for residual successful *recognition* in AD patients are fundamentally different from the mechanisms used for successful *recognition* by controls and MCIs. Whereas several previous studies have shown increased prefrontal activation in patients with AD relative to controls (Remy et al., 2005; Sole-Padulles et al., 2009; Sperling, 2007; Pariente et al., 2005) and, among these, at least one showed it using event-related paradigm (Pariente et al., 2005), to our knowledge this has never been tested in a study that included both MCI and AD patients and controlled for both the effect of between-subjects differences in grey matter atrophy and task performance.

The involvement of the right LPFC in episodic retrieval has been known since early PET and fMRI studies of memory (Tulving et al., 1994b; Buckner and Wheeler, 2001). Subsequent studies showed that right LPFC was activated not only when subjects successfully recognised previously presented items (retrieval success) but also when they tried to do so but failed (retrieval mode)

(Tulving, 2002). In line with this, it has been recently showed that right LPFC is involved in post-retrieval processing, i.e. monitoring and evaluating of the outcome of a retrieval attempt (Hayama and Rugg, 2009).

Thus, it is possible that controls exclusively relied on episodic memory abilities (as shown by the hyper-activation of hippocampus) in order to perform the task correctly. Instead AD patients, as a consequence of the advanced dysfunction of MTL were left to rely only on the "retrieval mode" and post-retrieval processing to be able to perform the task correctly. Therefore, the right LPFC hyper-activation in patients with AD may reflect a residual cognitive strategy to maximise task performance.

We did not find significant between-group differences in functional activation for successful relative to unsuccessful *recognition* or *encoding* in the medial temporal lobes (MTL). However, previous fMRI studies found significant decreased activations of hippocampus in AD patients relative to controls (Rombouts et al., 2000; Johnson et al., 2005; Machulda et al., 2003; Sperling et al., 2003; Golby et al., 2005; Remy et al., 2005), even when comparing successful relative to unsuccessful *encoding* and *recognition* (Pariente et al., 2005). We only saw a similar trend with the hippocampal ROI analysis for both *encoding* and *recognition*, but it did not reach statistical significance. It is possible that this inconsistency with previous studies is due to the fact that we removed group differences driven by differences in grey matter atrophy, since we included it as a covariate in both the whole-brain and ROI analyses. Instead, none of the above mentioned studies had accounted for differences in grey matter.

When comparing BOLD signal for *encoding* (relative to baseline) within subject-specific hippocampal anatomical ROIs (but not at the voxel-wise whole brain comparisons) we found increased task-related hippocampal activation in the MCI group compared to controls and patients

with AD. This is consistent with several previous studies that have used block-designs (Celone et al., 2006; Dickerson et al., 2005; Hamalainen et al., 2007a), or even-related designs but only looked at successful memory trials versus baseline (Sperling et al., 2009; Kircher et al., 2007). They suggested that there might be a phase of paradoxically increased activation early in the course of AD when people are at the MCI stage ("inverted U" hypothesis) (Dickerson et al., 2005; Kircher et al., 2007). However, this effect was abolished when we contrasted activation occurring during successful performance of the memory task against activation occurring during unsuccessful performance. Indeed, a trend in the sense of a decrease across the three groups (from controls, to MCI, to AD) was seen. This suggests that the MTL hyper-activation frequently observed in MCI is non-specific for successful encoding and recognition, since it also occurs for unsuccessful memory trials. We speculate that it may therefore represent maladaptive or dysfunctional mechanisms of compensation. This is in agreement with recent evidence that reduction of hippocampal hyper-activation improves memory performance in patients with amnestic MCI (Bakker et al., 2012).

6.5.3 Resting fMRI

Between-group comparisons of resting-fMRI data showed that AD patients had decreased functional connectivity in the default mode network (DMN). Our results on the DMN are consistent with several previous studies that using model-free approaches (i.e., ICA) that have found, in AD patients, significant decreased functional connectivity in the PPC (Gili et al., 2011; Agosta et al., 2011; Damoiseaux et al., 2011; Binnewijzend et al., 2011) and hippocampus (Greicius et al., 2004). Similar to previous studies that also included MCI patients, we did not find significant differences between MCI and controls (Binnewijzend et al., 2011; Agosta et al., 2011; Rombouts et al., 2009). Under statistical threshold of significance, the MCI group showed an intermediate level

of functional connectivity between controls and AD, consistent with those previous studies that had found significant differences (Sorg et al., 2007; Qi et al., 2010; Gili et al., 2011).

In all the 3 RSNs that involved the frontal lobes we found a reverse pattern of between-group differences, with AD patients showing higher functional connectivity than MCI patients, who in turn had higher functional connectivity than controls. These findings are consistent with the few recent studies that also explored other resting state networks revealed by ICA, which found that that functional connectivity within frontal and frontoparietal networks (variably indicated as "executive" and "frontal-parietal" networks or "anterior DMN" and "ventral DMN") was increased in AD patients relative to controls (Agosta et al., 2011; Damoiseaux et al., 2011; Jones et al., 2011). Less consistent results were found when exploring networks involving frontal and parietal regions in MCI patients (Sorg et al., 2007; Qi et al., 2010; Agosta et al., 2011).

Of note, previous studies have compared groups only within masks corresponding to spatial maps of the RSN of interest resulted from the average across groups. However, we explicitly decided not to mask results to allow for comparisons in regions outside the actual spatial map, and this may have decreased statistical power.

6.5.4 Conclusions

One of the most important limitations of resting fMRI is the incomplete understanding of how resting state networks (RSNs) relate to dynamic functional activations engaged during active tasks. To the best of our knowledge, task- and resting-fMRI anatomical correspondence has been shown in one study involving people at risk of developing AD who performed both task- and resting-FMRI (Filippini et al., 2009), but never in MCI or AD patients. Since resting fMRI is increasingly used in AD

and offers several advantages over task-fMRI, one of the aims of our study was to establish whether memory-related fMRI and resting fMRI give mutually consistent information.

We found an almost perfect anatomical correspondence between task-specific spatial maps of functional activity and some of the spatial maps of unconstrained functional connectivity (i.e., RSNs) in the control group (Figure 15). We also found that such correspondence persisted in between-group comparisons: regions of task-specific hyper-activation in the AD group (relative to control and MCI groups) overlapped with regions of increased functional connectivity in the AD group (relative to control and MCI group) in the right LPFC, which has a well established role in monitoring of retrieval processes and in retrieval-related decision-making (Fornito et al., 2012; Hayama and Rugg, 2009). Assuming that task-related frontal hyper-activation for successful recognition in patients with AD reflects residual cognitive ability, we speculate that resting-fMRI too may have the potential for unravelling residual mechanisms put in place by AD patients in order to be able to still perform cognitive tasks correctly.

In conclusion, our results support the idea that networks of coherent functional connectivity of the healthy brain at rest reflect those utilized "actively" during execution of tasks (Smith et al., 2009; Fornito et al., 2012). They further show that this correspondence persists in the diseased brain so that changes in functional connectivity secondary to AD (and potentially to other pathological damages) reflect residual functional abilities of the diseased brain. Ultimately, they suggest that studies aimed to use functional imaging as an outcome measurement of potential treatments and interventions may possibly only need resting-fMRI, rather than having the complication related to the execution of a cognitive task within the MRI scanner.

Chapter 7

Neuroanatomy of impaired self-awareness in MCI and AD

7.1 Abstract

Patients with MCI and AD may be unaware of their cognitive impairment. The neuroanatomical mechanisms underlying this symptom, termed *anosognosia* or *impaired self-awareness*, are still poorly understood. In this Chapter, the functional correlates of self-awareness were explored in healthy older adults, patients with MCI, and patients with probable AD. Participants performed a self- and other-appraisal task during fMRI, in which they were presented with questions regarding themselves (Self condition) or their study partner (Other condition). A study partner accompanied each participant and was asked to complete a paper questionnaire answering the same questions so the responses of participant and study partner could be compared and "discrepancy" scores calculated for each of the 2 conditions (Self and Other).

Behavioural results showed that AD patients had significantly higher "Self discrepancy scores" than controls and MCI patients, whereas there were no significant differences between groups for "Other discrepancy scores". Imaging results showed a significant group-by-condition interaction in brain activation in medial prefrontal and anterior temporal regions, with AD patients showing significantly decreased activation in these regions only for the Self condition.

In conclusion, decreased functional activation of medial prefrontal and anterior temporal cortices is associated with impaired self-awareness in AD patients. This dysfunction, which is specific for Self- but not for Other-appraisal, may be the basis of anosognosia in AD.

7.2 Introduction and rationale

7.2.1 Anosognosia in dementia

Patients with AD or other dementias may be unaware of their cognitive or behavioural disturbances. The inability to recognize cognitive, behavioural, or functional impairment occurring as a consequence of a dementing illness has been variably termed as *anosognosia*, loss of insight, *unawareness of illness*, or *impaired self-awareness* (Prigatano, 2009). It usually indicates a condition in which patients have a preserved capacity to evaluate feedback given by others but nevertheless fail to recognize their medical condition.

Several studies have investigated the neuropsychological correlates of anosognosia in MCI and AD (Kaszniak and Edmonds, 2010; Roberts et al., 2009), showing that anosognosia cannot be explained only on the basis of dementia severity, nor is accounted for by patients' difficulties in grasping and understanding tasks or questionnaires or difficulties in judging and estimating people's features (Kaszniak and Edmonds, 2010). Instead, support has been provided for the hypothesis that anosognosia in MCI and AD reflects, at least in part, a failure to update the enduring self-awareness system based on the set of beliefs of one's own capacities, attitudes, and traits in relation to those of others (also referred to as personal knowledge) (Agnew and Morris, 1998; Kaszniak and Edmonds, 2010).

7.2.2 Imaging correlates of anosognosia in dementia: literature review

Whereas the mechanisms of self-unawareness in terms of neuropsychological and psychological correlates have been extensively reviewed, the number of studies focusing on the anatomical correlates, either structural or functional, is much smaller. However, a clearer understanding of the brain correlates of unawareness of illness in dementia (not only of the neuropsychological

mechanisms) would help to better address several practical/clinical and theoretical issues. At the practical/clinical level, knowing which brain regions are involved in unawareness of disease may help to better characterize patients clinically and, for example, it may help to identify those at risk of developing dangerous behaviour before this occurs.

At a more theoretical level, knowing which brain regions are involved in unawareness of symptoms in dementia could help to choose the best neuropsychological model among those proposed by alternative theories in the metacognitive and anosognosia literature.

We reviewed imaging studies primarily aimed to study the structural or functional (depending on the neuroimaging techniques used) correlates of unawareness of cognitive symptoms in patients with dementia, which have directly measured unawareness in patients and used this measurement as the grouping or dependent variable. Eighteen studies were identified and their findings summarised in Table 10 and Figure 16. They differ in terms of (i) diagnosis of the patient sample included, (ii) method of measurement of unawareness, and (iii) neuroimaging technique, study design and imaging analysis adopted.

The involvement of frontal and/or temporo-parietal cerebral areas was reported in all the studies. Most of the earlier studies showing only frontal involvement had actually adopted regions of interest approaches and only focused on frontal regions, limiting the possible interpretation. However, two studies demonstrated a unique frontal involvement using a whole brain approach (Rosen et al., 2010; Shibata et al., 2008), both showing a medial involvement of the frontal lobes rather than dorso-lateral. Among the other 7 studies adopting a whole-brain voxel-based approach, 3 showed the common involvement of medial frontal and temporo-parietal regions (Hanyu et al., 2008; Mimura and Yano, 2006; Ries et al., 2007). As for the domain, when unawareness was measured with respect to the personality or behavioural changes occurring with

the disease, the unique involvement of lateral temporal-parietal regions emerged (Ruby et al., 2008; Ruby et al., 2007; Zamboni et al., 2010).

In summary, critical areas including medial frontal, medial parietal, and lateral temporal regions emerged. Some of these areas have also been frequently associated with poor awareness in other neurological disorders. This suggests that these regions may be part of an "awareness system", that -if damaged - leads to different types of unawareness. Several task-related functional imaging studies have shown that the same regions are involved in appraisal of self-relevant information in healthy subjects (Amodio and Frith, 2006; Northoff and Bermpohl, 2004). Therefore, it appears that brain regions involved in unawareness of illness in dementia are also involved in self, other, and self-in-relation-to-other processing (Amodio and Frith, 2006; Johnson et al., 2002).

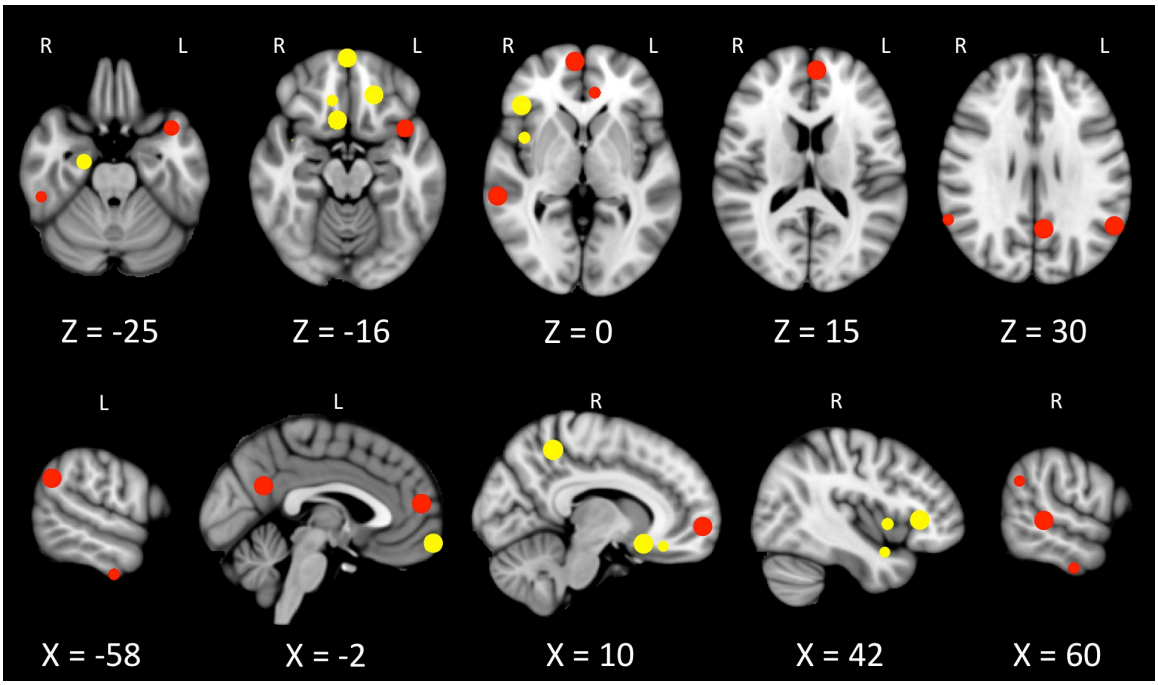

Figure 16 Summary of imaging studies of anosognosia in dementia

The red and yellow spherical markers were centred on the regions resulting from the reviewed studies that adopted voxel-based statistical analyses (see Table 10). Results of studies measuring unawareness as discrepancy between patient and informant are marked in red. Results of studies measuring unawareness as the patient's judgment on self-performance are marked in yellow.

Large spherical markers represent results significant at $p<0.05$ after correction for multiple comparisons, smaller markers represent results significant at $p<0.001$, uncorrected. Coordinates are in the MNI space. L, left; R, right.

Study	Participants	Unawareness measurement	Domain of unawareness	Imaging technique	Study design	Imaging analysis	Results (brain regions involved in unawareness)
Reed *et al.* 1993	20 AD (subset of 57)	Clinical judgment	Memory	Functional: SPECT	Groups comparison: patients divided in 3 groups on unawareness score	Semiquantitative measurement of rCBF from ROIs	Right dorso-lateral frontal cortex
Starkstein *et al.* 1995	24 AD (subset of 46)	Patient-informant discrepancy	Cognitive and behavioural abilities	Functional: SPECT	Groups comparison: patients divided in 2 groups on unawareness score	Semiquantitative measurement of rCBF from ROIs	Right inferior-orbital frontal and right frontal-superior frontal cortex
Ott *et al.* 1996	40 (AD, depression, Parkinson, FTD)	Clinical judgment	Global insight on cognitive and functional abilities	Functional: SPECT	Correlation between unawareness and hypo-perfusion	Semiquantitative measurement of rCBF from ROIs	Right temporo-occipital cortex
Derouesne *et al.* 1999)	78 AD (subset of 88)	Clinical judgment & Patient-informant discrepancy	Several cognitive domains	Functional: SPECT	Groups comparison: patients divided in 2 groups on imaging pattern	Semiquantitative classification of scans on of hypo-perfusion in selected ROIs	Right frontal lobe
Marshall *et al.* 2004	26 AD	Clinical judgment	Global insight	Structural: hysto-pathology	Groups comparison: patients divided in 2 groups on unawareness score	Plaques and neurofibrillary tangles measurement in ROIs	Right hippocampal prosubiculum
Vogel *et al.* 2005	36 AD 30 MCI 33 controls	Patient-informant discrepancy	Memory	Functional: SPECT	Correlation between unawareness and hypo-perfusion	Semiquantitative measurement of rCBF from ROIs	Right inferior frontal gyrus
Harwood *et al.* 2005	41 AD	Clinical judgment	Global insight	Functional: FDG-PET	Correlation between unawareness and hypo-metabolism	Semiquantitative measurement of rCBF from ROIs	Right lateral and dorsolateral frontal cortices
Mendez and Shapira, 2005	29 FTD (frontal variant)	Clinical judgment	Global insight	Functional: SPECT or FDG-PET	Groups comparison: patients divided in 4 groups on imaging pattern	Qualitative classification on pattern of hypo-perfusion	Right frontal lobe
Mimura and Yano, 2006	24 AD 16 controls	Patient's judgment on self-performance	Memory	Functional: SPECT	Correlation between unawareness and hypo-perfusion	Whole brain voxel-based analysis (SPM99)	Medial frontal lobe, right precuneus, right inferior frontal gyrus
Salmon *et al.* 2006	209 AD	Patient's judgment on self-performance Patient-informant discrepancy	Several cognitive domains	Functional: FDG-PET	Correlation between unawareness and hypo-metabolism	Whole brain voxel-based analysis (SPM99)	Self-assessment: right parahippocampus and left orbitofrontal cortex Discrepancy: left temporo-parietal junction

Study	Participants	Unawareness measurement	Domain of unawareness	Imaging technique	Study design	Imaging analysis	Results (brain regions involved in unawareness)
Ries *et al.* 2007	16 MCI 16 controls	Patient-informant discrepancy (IQCODE)	Memory	Functional MRI, task related	Groups comparison on self-awareness task + correlation between unawareness and functional activation	Voxel-based analysis in functional ROIs (SPM2)	Controls > MCI: medial frontal cortex and posterior cingulate Correlation with unawareness in MCI patients: medial frontal cortex and posterior cingulate
Ruby *et al.* 2007	16 FTD 16 controls	Patient-informant discrepancy	Personality changes and social behaviour	Functional: FDG-PET	Correlation between unawareness and hypo-metabolism	Whole brain voxel-based analysis (SPM2)	Left temporal pole (MNI coordinates: -40, 12, -20)
Hanyu *et al.* 2007	43 MCI	Patient-informant discrepancy (Wilson *et al.* , 1989)	Memory	Functional: SPECT	Groups comparison: patients divided in 2 groups on imaging pattern	Qualitative classification of scans in AD pattern and non-AD pattern	Bilateral parietotemporal or posterior cingulated areas
Shibata *et al.* 2008	29 AD	Patient-informant discrepancy (Squire and Zouzounis, 1988)	Memory	Functional: SPECT	Correlation between unawareness and hypo-perfusion	Whole brain voxel-based analysis (SPM2)	Left orbitofrontal cortex (MNI coordinates: -8, 38, 0)
Hanyu *et al.* 2008	38 AD	Patient-informant discrepancy (Wilson *et al.* , 1989)	Memory	Functional: SPECT	Groups comparison: patients divided in 2 groups on unawareness score	Whole brain voxel-based analysis (3D-SSP with Neurostat)	Bilateral lateral and medial frontal lobes, bilateral anterior and posterior cingulate, and left inferior parietal cortex
Ruby *et al.* 2008	14 AD 17 older controls, 17 young controls	Patient-informant discrepancy	Personality changes	Functional MRI, task related	Groups comparison on self-awareness task	Whole brain voxel-based analysis (SPM2)	AD > elderly controls during self-awareness: bilateral intra-parietal sulcus
Rosen *et al.* 2010	39 (2 controls, 2 ASL, 9 AD, 2 MCI, 20 FTD, 4 CBS)	Patient's judgment on self-performance	Several cognitive domains	Structural: MRI	Correlation between unawareness and grey matter atrophy	Whole brain voxel-based analysis (SPM5)	Right orbito-medial frontal cortex
Zamboni *et al.* 2010	64 (38 FTD and 26 CBS)	Patient-informant discrepancy	Behavioural disturbances	Structural: MRI	Correlation between unawareness and grey matter atrophy	Whole brain voxel-based analysis (SPM5)	Right temporo-parietal junction and right superior temporal sulcus

Table 10 Summary of imaging studies on anosognosia in dementia

FTD, frontotemporal degeneration; CBS, corticobasal degeneration syndrome; SPM, statistical parametric mapping.

7.2.3 Study rationale

Previous studies exploring neuroanatomical correlates of anosognosia in dementia have mainly looked at correlations between measurements of anosognosia and variables representing brain function or morphology, without explicitly testing neuropsychological models of anosognosia. Here, we used task-related functional magnetic resonance imaging (fMRI) to directly explore the neural basis of self-awareness in MCI and AD. We adopted an approach that fosters an operational definition of self-awareness in relation/opposition to non-self or others (Lieberman, 2007; Northoff and Bermpohl, 2004), in line with several recent neuroimaging studies showing that the neural activity of certain cortical areas is specific for the evaluation and processing of self-related information relative to non-self-related stimuli. We used an fMRI paradigm adapted to the needs of patients with cognitive impairment similar to paradigms used in previous fMRI studies of self-awareness conducted on healthy adults (Northoff et al., 2006; Schmitz and Johnson, 2007).
We hypothesized that patients with MCI and AD would show a gradient of impaired self-appraisal, which would be reflected in altered neural response to self- relative to other-appraisal in patients with respect to healthy older adults. We anticipated the involvement of anterior regions of the medial prefrontal cortex, which are known to be involved in personal knowledge specifically related to self-representation in healthy adults (Amodio and Frith, 2006; Northoff et al., 2006) and have been shown dysfunctional in patients with autism and other psychiatric diseases (Blair et al., 2010; Lombardo et al., 2010).

7.3 Methods

7.3.1 Participants

Description of study participants and inclusion and exclusion criteria are reported in *Chapter 5*, paragraph 5.2.1. Seventeen patients with AD consented to stay in the MRI scanner long enough to also perform the self-appraisal task in addition to other structural and functional sequences described previously. They were age- education- and gender-matched with an equal number of MCI and control participants. Therefore data from 51 participants (17 patients with AD, 17 patients with MCI, and 17 age- and education-matched healthy controls) are reported in this chapter. There were no significant differences in age, years of education, gender, or handedness between the three groups.

Demographic characteristics [#]				
	Controls	**MCI**	**AD**	**Groups comparison** *
N	17	17	17	---
Gender F:M	8:9	10:7	9:8	n.s., p=0.8
Age (years)	75.5 (4.8)	76.2 (5.9)	76.7 (5.4)	n.s., p=0.9
Years of education	14.9 (2.8)	14.9 (3.3)	14.3 (4.0)	n.s., p=0.8
Neuropsychological characteristics				
	Controls	**MCI**	**AD**	**Groups comparison** *
MMSE	29.85(0.7)	26.8 (1.4)	22.2 (3.0)	p<0.0001[a, b, c]
MoCA	26.4 (2.9)	21.9 (2.4)	16.5 (3.7)	p<0.0001[a, b, c]
Category fluency	26.53 (4.46)	20.53 (5.36)	12.94 (7.39)	p<0.0001[a, b, c]
Backwards Digit Span	4.82 (1.51)	3.71 (0.77)	3.63 (1.15)	P=0.008 [a, b]
Geriatric Depression Scale	3.82 (4.16)	7.88 (5.59)	6.63 (3.28)	p=0.033 [a]
Neuropsychiatric Inventory	1.9(2.9)	3.8 (5.3)	11.0 (8.1)	p<0.0001[b, c]
BADLS plus	0.4 (0.8)	3.0 (2.5)	20.1 (11.2)	p<0.0001[b, c]
AD-Q	-6.9 (5.8)	-9.5 (9.0)	12.2 (11.9)	p<0.0001 [b, c]

Table 11: Demographic and neuropsychological characteristics of participants

[#] Reported values are means with standard deviation values in parenthesis.

*P values from comparisons between groups. [a] post-hoc significant at P<0.05 for comparison controls-MCI, [b] post-hoc significant at P<0.05 for comparison controls-AD, [c] post-hoc significant at P<0.05 for comparison MCI-AD

7.3.2 Self- and Other-appraisal task and fMRI paradigm

In the scanner, participants were presented with questions regarding themselves or their study partner ("Are you [adjective]?" and "Is [study partner's name] [adjective]?", Figure 17). A total of 36 adjectives were selected from an original set of 180 including - but not limited to - the Anderson traits list (Anderson, 1968). They were classified as describing cognitive (n=12), behavioural (n=12), or physical (n=12) traits. Only adjectives judged to be comprehensible to patients with cognitive impairment were included. The selection was undertaken by an experienced team composed of 5 research nurses and 2 neuropsychologists.

In the fMRI experiment, each adjective was presented in each of the 2 experimental conditions: Self and Other. Six Self blocks and 6 Other blocks were presented in pseudorandom order. In each block, 2 cognitive, 2 behavioural and 2 physical traits (total of 6 adjectives per block) were presented randomly and differently for each subject, each displayed on the screen for 5 seconds, and with a jittered inter-stimulus interval of 2-3.5 secs. Adjectives were randomly assembled in blocks. Whether an adjective was first presented in a Self or Other block was also random and different for each subject to rule out any effect of novelty on condition.

Before the MRI scanning, participants were given extended supervised training with different adjectives but with the same response box. They were instructed on pressing one of two response buttons and reassured that that there are no right/wrong answers.

The study partner filled in a paper version of the scan task so the responses of participant and study partner could be compared to obtain "discrepancy" scores (% incongruent responses between partner and participant over total answered questions), regarding both the participant (Self condition) and the study partner (Other condition). In addition, discrepancy scores were further differentiated according whether they referred to cognitive, behavioural, or physical traits. We assumed that the higher the discrepancy score for Self, the higher the degree of anosognosia.

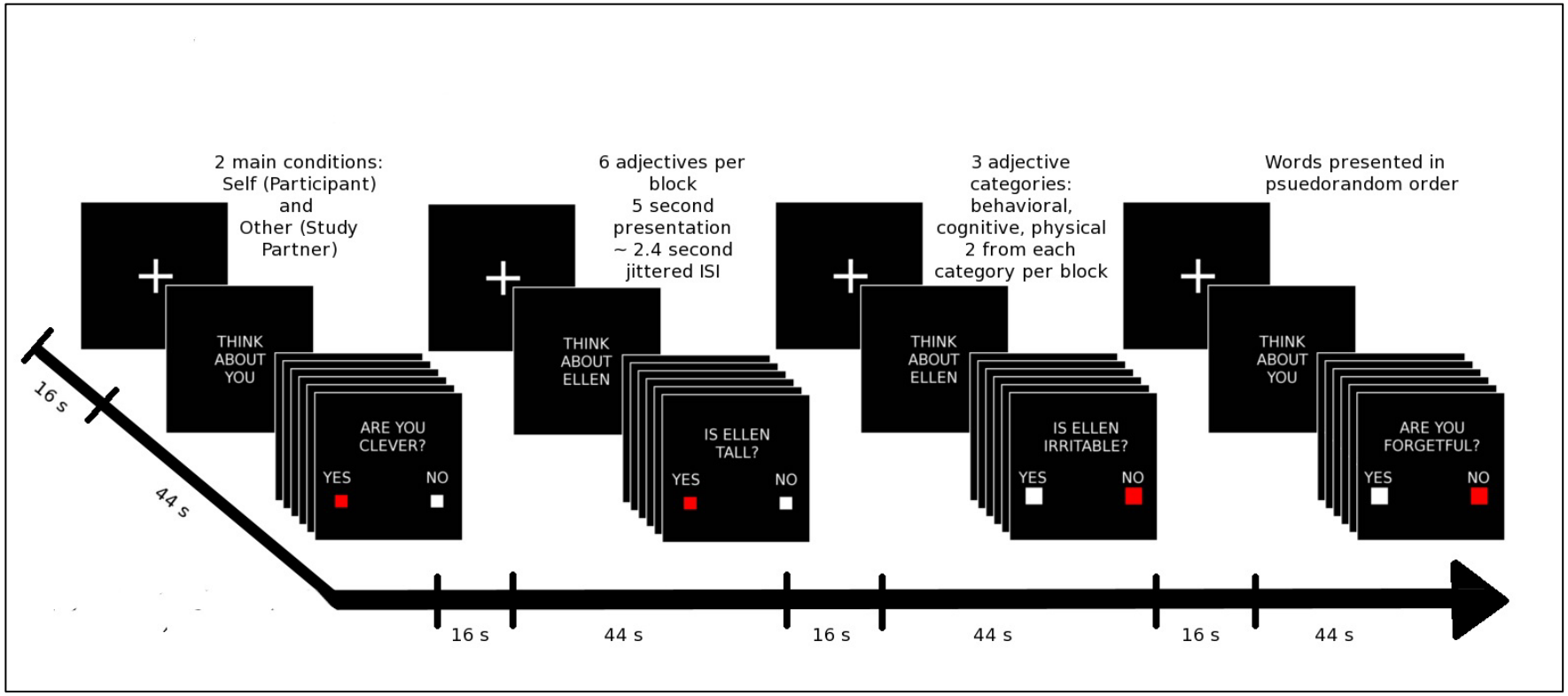

Figure 17 Self and other-appraisal fMRI paradigm.
In the scan participants were asked to give a "yes" or "no" answer to questions regarding themselves (Self condition) or their study partners (Other condition). Small white squares labelled "yes" and "no" representing the two buttons were presented on the bottom part of the screen: when a response button is pressed, the corresponding square changes colour so that the participant is reminded of the task and buttons and can monitor her/his answers

7.3.3 Image acquisition and analysis

A full description of imaging parameters and data pre-processing is provided in Chapter 5, paragraphs 5.2.4 (Summary of sequence parameters) and 5.3.2 (Task-related functional MRI). Data of the self-awareness task were first analysed in a block-design fashion, and regressors for Self and Other blocks were entered in the general linear model at the single-subject level. Higher-level analysis was then carried out using a general linear model that included explanatory variables representing the three groups and an additional four-dimensional nuisance variable representing voxel-specific grey matter density. We tested for group differences and group-by-condition interactions. An additional follow-up analysis was also carried out in an event-related-design fashion, and regressors for each trait's type (cognitive, behavioural, and physical) within each condition (Self and Other) were entered in the general linear model at the single-subject level.

7.4 Results

7.4.1 Behavioural results

7.4.1.1 Discrepancy scores

Discrepancy scores were entered in a mixed 2×3×3 repeated measures ANOVA with condition (Self, Other) and trait type (Cognitive, Behavioural, and Physical) as within-subject factors and group (controls, MCI, and AD) as between-subject factor. There were significant main effects of condition ($F_{1,48}$=4.73, P<0.05), group ($F_{2,48}$=3.99, P<0.05), but no significant main effect of trait's type ($F_{2,48}$=1.37, P=0.26). There was a significant three-way interaction between condition, group and trait type ($F_{4,96}$=3.55, P=0.01), but no significant two-way interaction between condition and group. Subsequent one-way ANOVAs were used to elucidate the significant three-way interaction: There were no significant differences between groups in the Other condition, considering overall Other discrepancy score or trait-specific discrepancy subscores ($F_{2,48}$ tests <1, n.s.), meaning that all the participants had a "similar" extent of disagreement with their respective study-partners when judging them. Instead, there were significant differences between groups in the Self condition ($F_{2,48}$=4.42, P<0.05), with AD patients having overall Self discrepancy scores significantly higher than controls. These differences were driven by subscores concerning cognitive ($F_{2,48}$=3.56, P<0.05) and behavioural ($F_{2,48}$=8.81, P=0.001) traits, but not physical traits ($F_{2,48}$<1, n.s.). Table 12 reports results of paired t-tests performed within each group.

	Controls (N=17)			MCI patients (N=17)			AD patients (N=17)		
Discrepancy scores									
	Other	Self	P*	Other	Self	P*	Other	Self	P*
Overall	19.7	19.6	0.95	18.3	22.1	0.14	21.9	28.1	**0.05**
Cognitive	19.6	18.8	0.84	16.4	22.0	0.25	19.9	31.6	**0.03**
Behavioural	19.9	13.6	0.09	15.7	22.8	0.12	19.4	31.2	**0.02**
Physical	19.4	26.3	0.10	22.5	21.7	0.89	27.5	21.9	0.20

Table 12 Behavioural results of self- and other-appraisal
Discrepancy scores for Other and Self judgments (overall and trait's type specific scores).
* *P* values of the comparison between Other and Self discrepancy scores performed with paired *t*-tests within each group (df=16, two-tailed). Significant results are highlighted in bold.

7.4.1.2 Validity of Self discrepancy score as measurement of anosognosia

The Anosognosia Questionnaire—Dementia (AQ–D), an established measure of anosognosia designed for patients with dementia, with demonstrated reliability and validity (Migliorelli et al., 1995), was used to validate our study discrepancy scores as a measurement of anosognosia. This scale contains questions regarding intellectual functioning in everyday life, which are completed by the patient (and in our case was also completed by the healthy control group) and by an informant or caregiver (in our study, the study partner). As expected, correlation between AQ-D score and Self discrepancy score was positive and significant (r_{51}=0.39, P<0.005, two-tailed), and was driven by the AD patients (r_{17}=0.37, P=0.07, one-tailed). Importantly, in each of the groups and in particular in the AD group, there were no significant correlations between Self discrepancy score and scores on neuropsychological tests assessing dementia severity (MMSE, r_{17}=0.09, n.s., one-tailed), episodic memory (HVLT, r_{17}=0.26, n.s., and MoCA delayed recall, r_{17}= 0.08, n.s., one-tailed), semantic memory (Category Fluency, r_{17}=0.17, n.s., one-tailed), executive functions (Digit Span, Letter Fluency and Executive subscores of MoCA, r_{s17} < 0.08, n.s., one-tailed), behavioural impairment (NPI, r_{17}=0.23, n.s., one-tailed), and depression severity (GDS, r_{17}=0.05, n.s., one-tailed).

7.4.2 fMRI results

7.4.2.1 Within-group results

Within-group results for the Self and Other conditions relative to baseline in the control and MCI groups showed activation of the medial prefrontal cortex (MPFC), medial temporal lobes (MTL), and lateral anterior temporal lobes (ATL) for both conditions (Figure 18). In the AD group, the Other condition relative to baseline led to activations in MPFC and temporal lobes, whereas the Self condition only showed significant activations in motor and visual areas, most probably related to the task.

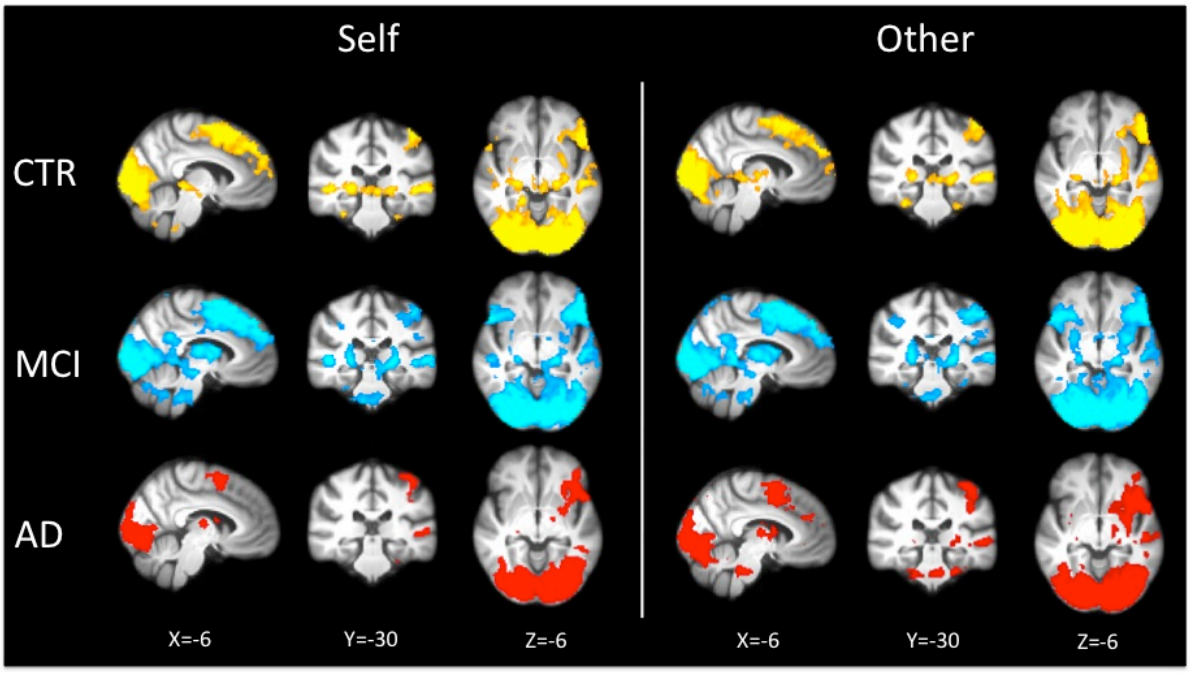

Figure 18 Within-group fMRI results
Group averages for the Self and Other conditions (relative to baseline) for the control, MCI, and AD groups (respectively displayed in yellow, blue and red). Coordinates are in MNI space, images are displayed in radiological convention (left is right).

7.4.2.2 Comparison between conditions and group-by-condition interaction

To establish whether the behavioural results corresponded to significant differences in neural responses, it was important to study the comparison between Self and Other conditions within each group and to explore the presence of significant group-by-condition interactions.

Direct comparison of the two experimental conditions (Other>Self or Self>Other) within either the control and MCI groups did not reveal significant differences. Instead, in the AD group, this direct comparison showed greater activation for Other than Self in the MPFC in the Anterior Cingulate Cortex (ACC), in the posterior cingulate/precuneus, and in the lateral ATL bilaterally (Figure 19A, Table 13). More precisely, in the MPFC there was a more dorsal cluster [rostral-MPFC (Amodio and Frith, 2006) or supragenual-ACC (Northoff et al., 2006)], and a more ventral cluster (orbital-MPFC or pregenual-ACC). The opposite contrast (Self > Other) within the AD group did not yield significant differences.

The dorsal MPFC and left ATL also emerged when interrogating functional data for group-by-condition interaction, tested in the control-AD and MCI-AD group pairs (Figure 19B). These significant interactions were driven by the AD group, who failed to activate these regions specifically in the Self condition (Figure 19C). In fact, whole-brain comparisons between groups showed that controls and MCIs had, in the Self condition, greater activation than AD patients in the same dorsal MPFC. Instead, whole-brain comparisons in the Other condition did not reveal any significant differences, although neural response to the Other condition in the left ATL (measured as % signal change) was significantly greater in AD patients than MCIs and controls (Figure 19C).

7.4.2.3 Correlation between fMRI response and behaviour

To test whether the decreased response to Self-appraisal in the MPFC was specifically related to increasing severity of anosognosia, the relationship between fMRI signal in the regions identified by the group-condition interaction and behavioural measurements of anosognosia (self discrepancy score and AQ–D) was examined. As expected, there were significant inverse correlations between fMRI response in the MPFC during Self condition and the Self Discrepancy score (r_{51}=-0.32, P<0.05, Figure 19E) and the Anosognosia Questionnaire-Dementia (r_{51}=-0.50, P<0.001, Figure 3F). These correlations were driven and still significant within the AD group only (Self Discrepancy r_{17}=-0.52, P<0.05 and AQ-D r_{17}=-0.61, P<0.01, one-tailed), meaning that patients with lower MPFC neural response during-self appraisal were indeed those with a higher degree of anosognosia. Importantly, these correlations remained significant after adjusting for severity of cognitive impairment (MMSE or MoCA) or other neuropsychological measurements including performance on episodic memory (HVLT) and semantic memory (category fluency). This confirmed that the neural response in MPFC during the Self condition was specifically modulated by the task and not driven by cognitive impairment or by a generic effect of the disease on the hemodynamic response.

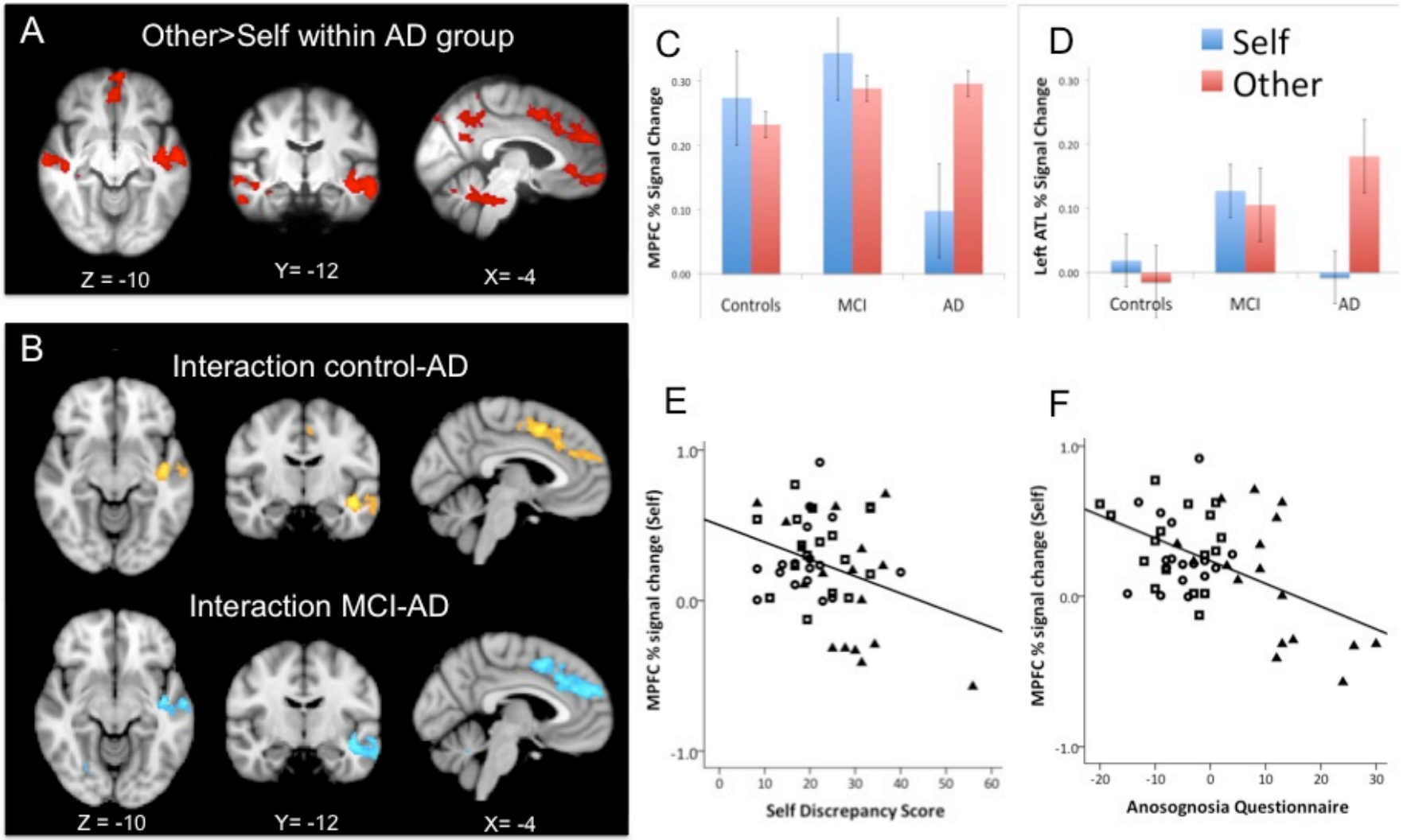

Figure 19 fMRI results: conditions comparison in AD and interaction group-by-condition

Figure 19 Legend (previous page)
A) Regions of greater activation for Other- than Self-appraisal in the AD group
B) The whole-brain analysis revealed interaction effect between group and condition (Self, Other) in dorsal MPFC and left ATL. Images are shown in radiological convention. Coordinates are in MNI space.
C) Measurements of the neural response in the dorsal MPFC (region of overlap between controls-AD and MCI-AD interactions) explains the interaction: all groups had a similar degree of activation during Other condition (in red), whereas the AD group had significantly decreased activation during Self condition (in blue).
D) Measurements of the neural response in the left ATL (region of overlap between controls-AD and MCI-AD significant interactions) reveal that this region was specifically engaged during Other condition by the AD group.
E, F) Scatter plots display the significant inverse correlation between neural response in the MPFC during Self condition and two different behavioural measures of anosognosia: the study specific Self Discrepancy score (r_{51}=-0.32, P<0.05) and the Anosognosia Questionnaire (r_{51}=-0.50, P<0.001). Controls are represented as circles, MCI squares, and AD triangles.

		MNI coordinates			
Group-by-condition interaction	**Location of peak voxels**	**x**	**y**	**z**	**Z value**
Self >Other in Control>AD					
Medial Prefrontal Cortex (MPFC)	L Paracingulate Gyrus	-4	24	36	4.23
(634 voxels)		-4	8	48	3.52
		-19	14	48	3.42
	L Anterior Cingulate Gyrus	-6	38	26	3.59
		-10	-2	48	3.52
	L Superior Frontal Gyrus	-4	24	48	3.5
Anterior Temporal Lobe (ATL)	L Superior Temporal Gyrus	-42	-12	-14	4.66
(545 voxels)		-42	-16	-4	3.37
	L Middle Temporal Gyrus	-62	-14	-20	3.52
		-62	-14	-26	3.02
	L Superior Temporal Sulcus	-62	-12	-12	3.16
		-58	-4	-14	2.97
Self >Other in MCI>AD					
Medial Prefrontal Cortex (MPFC)	L Anterior Cingulate Gyrus	-4	10	48	3.72
(1192 voxels)	L Paracingulate Gyrus	-6	24	36	3.57
		-4	38	26	3.46
		-6	28	32	3.44
	L Superior Frontal Gyrus	-4	48	24	3.59
		-4	52	28	3.56
Anterior Temporal Lobe (ATL)	L Superior Temporal Gyrus	-42	-12	-14	4.43
(658 voxels)	L Superior Temporal Sulcus	-48	-8	-18	3.84
		-60	-12	-10	3.35
	L Middle Temporal Gyrus	-58	-14	-22	3.78
		-62	-14	-20	3.76
		-58	-2	-26	3.34

Table 13 Imaging results of self- and other-appraisal task
Location in MNI coordinates and max Z value for each resulting cluster from the group-by-condition interaction.

7.4.2.4 Follow-up event-related analysis

As there was a three-way significant interaction between condition, group and trait type on behavioural data, an event-related follow-up analysis was done to study the effect of conditions and group separately for each trait type. As expected, the Other>Self comparison within the AD group and the group-by-condition interaction remained significant - although to a less extent - in regions in the MPFC and ATL in all the trait types (Figure 20).

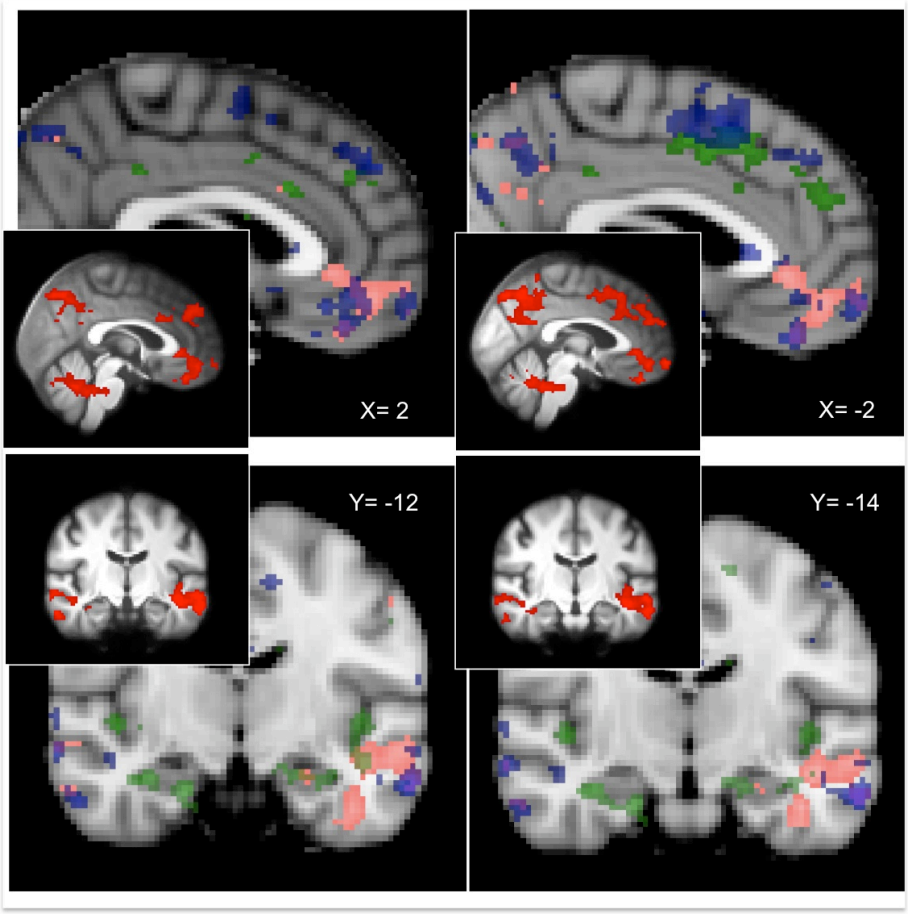

Figure 20 Results of event-related follow-up analysis
Differential contribution of cognitive (pink), behavioural (blue), and physical (green) traits. Note how all the three trait's types contributed to the results of the main analysis in which Self and Other conditions were analysed as blocks (shown for comparison in red smaller images, same contrast than Figure 19A). Results of the event-related analysis are displayed at P<0.01 uncorrected for visualisation purposes.

7.5 Discussion

7.5.1 Self-awareness in AD

By comparing participants' and their study partners' responses about judgments of cognitive, behavioural and physical traits, we found that, in line with predictions, patients with AD had a higher degree of discrepancy with their study partners only when they were asked to judge themselves (Self condition), but not when judging the study partners (Other condition). When examining the underlying neural responses, we found that, in the control and MCI groups, self- and other-appraisal shared similar neuroanatomical substrates, which involved medial prefrontal cortex and medial and lateral temporal lobes. This is consistent with previous studies on healthy subjects showing the involvement of medial prefrontal cortex (MPFC) in processing of information related to oneself but also in processing information related to others perceived as familiar or close, as –for example- in theory of mind tasks (Frith and Frith, 2003; D'Argembeau et al., 2005; Mitchell et al., 2005).

Instead, in the AD group, we found that the two conditions elicited different neural responses, and that the above-mentioned network involving MPFC was only engaged during other-, not self-appraisal. Indeed, there was a significant group-by-condition interaction in the dorsal MPFC and left anterior temporal lobe (ATL). In the MPFC, the interaction was predominantly driven by reduced activation for the Self condition in AD patients relative to controls and MCIs, suggesting that AD patients failed to activate the MPFC specifically during self-appraisal, whereas they were able to engage it during other-appraisal. In the left ATL, the interaction was predominantly driven by increased activation for the Other condition in AD patients relative to controls and MCIs. This suggests that AD patients not only failed to activate the left ATL during self-appraisal, but also hyper-activated it during other-appraisal. Such ATL hyper-activation may represent a compensatory mechanism.

Together with behavioural findings showing impaired self- but not other-appraisal in patients with AD, our results suggest that the dysfunction of a network involving medial prefrontal and anterior temporal cortices is associated with the failure in AD patients of mechanisms necessary for correct and updated self-awareness, which may contribute to anosognosia. The correct functioning of this network may be necessary to maintain an updated and enduring knowledge about ones' cognition and abilities. Importantly, we showed that the dysfunction of this network involving medial prefrontal and anterior temporal cortices did not occur when patients with AD were required to judge others, suggesting further interpretation on its functioning: we speculate that MPFC is necessary for updated self-awareness, and that therefore its activation is directly involved in self-appraisal. As such, its dysfunction leads to impaired self-awareness in AD. However, the MPFC in AD patients is still indirectly activated during other-appraisal as a consequence of a compensatory increase in ATL activation, which provides general (and not necessarily updated) semantic knowledge about people.

The MPFC is known to subserve uniquely human social cognitive functions (Amodio and Frith, 2006). More precisely, the region in the MPFC in which we found the significant interaction is thought to have a special role in self-awareness when a judgmental or evaluative component is required (Johnson et al., 2002; Northoff and Bermpohl, 2004), when the self-judgment occurs within a social context or compared to other persons (Northoff and Bermpohl, 2004), and when it assesses "longer-term" and enduring aspects of the self rather than on-going judgments (Schmitz and Johnson, 2007; Rosen et al., 2010; Buckner and Carroll, 2007).

The anterior regions of temporal lobes are thought to have a critical role in semantic memory and conceptual knowledge (Simmons and Martin, 2009). Recently, it has been argued that rather than serving as a domain-general semantic repository, the ATL appears to support knowledge about people and works in unison with the social cognition system to support learning facts about others (Zahn et al., 2007; Simmons et al.).

7.5.2 Consistency with neuropsychological models of anosognosia

The finding that accurate correct self-appraisal relies on the correct functioning of a network involving regions important for enduring self-awareness (MPFC) and semantic knowledge (ATL) may be partially in line with the model of anosognosia proposed by Morris and Hannesdottir (Morris and Hannesdottir, 2004). This hypothesises the existence of an awareness system providing enduring conscious awareness of abilities that receives inputs from a semantic system storing personal semantic knowledge. Indeed, by exploring explicit self-awareness using a self- versus other-appraisal experimental paradigm, our study may have elucidated the neural correlates of these two systems, in line with some of the predictions of the same model (Hannesdottir and Morris, 2007; Mograbi et al., 2009).

Some of our results are consistent with the hypothesis of an "awareness system" updated by semantic knowledge. These include the fact that the MPFC and ATL showed decreased activation in the AD group specifically for the self-appraisal condition, that their activation was preserved and possibly driven by a compensatory activation of ATL for the other-appraisal condition, and that activation of MPFC was not influenced by impairment of basic cognitive functions. Despite possible similarities, the most important divergence of our results from previous neuropsychological models of anosognosia is that they have highlighted the pivotal role for memory in self awareness (Agnew and Morris, 1998; Conway and Pleydell-Pearce, 2000; Ansell and Bucks, 2006), suggesting that it is the particular pattern of memory impairment in AD responsible for the failure of updating the awareness system, thus leading to an out-dated sense of self (termed "petrified self", see Mograbi et al., 2009). Whereas the involvement of ATL may be consistent with the role of semantic memory, we did not find activation of structures important for episodic memory such as medial temporal lobes. This further confirms that our experimental paradigm did not explore mechanisms of on-going awareness on cognitive performance, but rather a "semanticised" and long-term self-awareness (Mograbi et al., 2009; Piolino et al., 2007). Indeed, by choosing to measure self-

awareness by comparing participants' and study-partners' overt judgments on several traits, we could only derive information concerning the general construct of beliefs a person has of their own capacities, attitudes, and behaviour (explicit self-awareness).

However, impaired explicit self-awareness is only one of several facets of anosognosia in patients with dementia. Other possible aspects of awareness of cognitive abilities have been explored by studying prediction of performance (Cosentino et al., 2007) and online monitoring during execution of cognitive tasks (Moulin et al., 2004; Moulin et al., 2000). Interestingly, a recent fMRI study focused on aspects of error-monitoring found that unaware AD patients had decreased activation compared to aware patients in the same regions we found (anterior cingulate and left temporal gyrus) during the execution of a response inhibition task (Amanzio et al.).

The involvement of MPFC is consistent with a recent correlational imaging study on anosognosia in dementia (Rosen et al., 2010) and with an fMRI study that used a self-appraisal paradigm to study the correlates of anosognosia in patients with MCI (Ries et al., 2007). However, as the authors of that study used a semantic decision task and not other-appraisal as control condition, they could not conclude that the identified regions were specific for self-awareness. In addition, in their study, patients did not differ significantly from controls in behavioural measures of anosognosia, limiting interpretation of their fMRI results.

7.5.3 Self-awareness in MCI

In contrast with our hypotheses, patients with MCI did not show impaired self-awareness in the experimental task. Indeed, although a patient's subjective memory complaint was not a criterion necessary for an MCI diagnosis (as the memory problem could also be reported by the informant to fulfil criteria of inclusion), all our MCI patients explicitly reported difficulties with their memory and tended to overestimate their problem. Accordingly, the neural

responses in the MCI group were not different from the control group suggesting a preserved self-awareness system in this group. Although this may have occurred because of a self-selection bias in the recruitment of the MCI group (with MCI patients aware of their problems more willing to take part in research) and therefore be specific for our study, a tendency to overestimate cognitive deficits has also been found in patients with MCI but not in patients with AD by other researchers (Kalbe et al, 2005). In addition, a recent study suggested that subjective memory complaint in healthy elderly is associated with prospective brain changes suggestive of incipient dementia, but that it tends to disappear close to the clinical onset of dementia (Stewart et al., 2011). This may have more general implications for the use of subjective memory complaint as central diagnostic criterion for MCI, in line with suggestions of other authors (Roberts et al., 2009).

7.5.4 Methodological considerations

A possible limitation of our experimental paradigm is that the underestimation of deficit demonstrated by patients while judging their cognitive and behavioural traits may have been driven by the fact that AD patients most likely have deteriorated in their cognitive and behavioural functioning overtime, while their study partners have not, therefore the two conditions (Self and Other) were not fully balanced. However, we showed that within the AD group, the degree of activation of MPFC was specifically correlated with behavioural measures of anosognosia (AQ-D), that this association was independent from the degree of cognitive impairment and memory dysfunction, and that the behavioural measures of anosognosia themselves were also not correlated with measurements of cognitive and behavioural impairment. In addition, by including physical traits in the experimental paradigm, it was at least introduced the possibility that study partners might have changed physically, although this remains speculative and should be explicitly addressed in future studies.

A common limitation of fMRI studies comparing clinical groups is that the resulting differences between groups may be driven by differences in brain morphology or in haemodynamic response (i.e. neurovascular coupling), rather than reflecting real differences in neural activation (Samanez-Larkin and D'Esposito, 2008). In the present study, we addressed the issue regarding differences in brain structure in several ways, including improved registration (relative to standard methods) and inclusion in the fMRI model of a covariate that represented voxel-specific grey matter density differences between subjects. Most importantly, since there were no significant group differences in activation in the Other condition but only in the Self condition (significant group-by-condition interaction), we can reliably assume that our fMRI results were not driven by between-group differences in neurovascular coupling and haemodynamic response, as these would have affected all conditions equally.

7.5.6 Conclusions

The correspondence between behavioural and functional neuroimaging results reported in this Chapter contributes to a better understanding of the neuro-anatomical basis of anosognosia in patients with MCI and AD, highlighting the involvement of medial prefrontal and anterior temporal cortices in this common symptom. If replicated, our results may be used as a model to better understand the dynamic changes on human self-awareness occurring in different phases of AD, and to test if anosognosia has a predictive value for progression to dementia in the MCI phase.

Chapter 8

Conclusions

8.1 Summary of main findings

Over the past 20 years brain MRI has contributed significantly to the understanding of different aspects of AD, and has been increasingly used not only for clinical characterisation and differential diagnosis, but also to provide insight into the effects of the disease, its natural history, and its spatial and temporal evolution in the brain. Brain MRI is also increasingly used in clinical trials, as part of inclusion criteria and/or as a surrogate outcome measure.
The overall aim of this thesis was to complement the major achievements already made in the field and improve our understanding of the changes in brain *structure* and *function* detectable with MRI techniques that occur in different stages of AD progression, from pre-symptomatic phases, to MCI, to clinically evident dementia.

More precisely, this thesis was aimed to answer the following questions (see paragraph 2.5):

1. Do changes in brain structure measurable with structural MRI occur in the presymptomatic phase of AD, i.e., before clinical onset of MCI and AD?
2. Does inter-subject structural variability detectable with T1-weighted structural MRI mirror cognitive performance in older adults and inform about which brain regions are activated during cognitive tasks?
3. Can task-fMRI overcome limitations of previous studies related to underlying differences in structure and performance and thus better quantify residual functions in the symptomatic brain?
4. Do measures of task-independent, unconstrained brain functional connectivity (resting-fMRI) correspond to measures of task-evoked brain functional organisation (task-fMRI) in patients with AD?

5. Can fMRI inform on mechanisms of specific cognitive symptoms in patients with MCI and AD, and, more precisely, which are the functional mechanisms of anosognosia in these patients?

Each of these five research questions has been addressed separately in *Chapters 3 to 7*. A summary of the main findings is presented in the following sections (paragraphs 8.1.1 to 8.1.5), each entitled according to the "major answer" it gave.

8.1.1 Structural MRI changes are detectable up to 7-10 years before a clinical diagnosis of AD

In *Chapter 3,* I investigated structural brain differences between groups of healthy subjects stratified by later diagnosis of conversion to MCI or AD, using VBM and subcortical shape analyses. At baseline, all subjects presented with homogeneous clinical and cognitive features. In addition, by including only those subjects who remained cognitively normal for at least 4 years from baseline, we improved the probability that all subjects were truly healthy at baseline and would not progress to cognitive impairment soon after baseline assessment. Thus, this was a *structural* MRI study on the preclinical phase of AD. Our results showed that *structural* MRI can detect volume loss in medial temporal lobes up to 10 years before the diagnosis of AD becomes evident.

At the time of data analysis and submission for publication, to the best of my knowledge there were no published papers showing that changes could occur in preclinical AD 7-to-10 years before clinical symptoms. Indeed, a frequently cited review paper published in Lancet Review in 2010 on a hypothetical model of dynamic changes occurring in different biomarkers had suggested that structural MRI becomes abnormal relatively late in the progression of AD (Jack et al., 2010). A study published in 2011 (Dickerson et al., 2011) and the study described in *Chapter 3* of the present thesis instead suggest that these changes occur possibly earlier than

previously thought. Very recently, data from patients with familial forms of AD have also showed that atrophy begins about 10 years before measurable clinical impairment: The prospective study from the Dominantly Inherited Alzheimer Network (DIAN) found that, by analysing baseline data of mutation carriers in relation to estimated years from expected symptom onset (calculated using parental age of onset of symptoms), brain atrophy could be detected 15 years before expected symptom onset and that global cognitive impairment could be detected 5 years before expected symptom onset (possibly due to a "recency bias" in reporting the parental age of disease onset), confirming a time-window of about 10 years between brain atrophy and clinical diagnosis (Bateman et al., 2012).

8.1.2 Structural and functional MRI correlates of a test sensitive to early cognitive dysfunction co-localise in regions vulnerable to AD in healthy older adults

In *Chapter 4* we further explored the potential of T1-weighted structural MRI in healthy older adults and its relationship with cognitive functioning. We tested if it can identify regions vulnerable to cognitive variability in a population of cognitively healthy older adults who, simply due to their age-range, are at risk of developing neurodegenerative diseases such as AD. By using a VBM correlational approach, we found that decreased performance on a test of visuospatial associates learning sensitive to early cognitive impairment (the Placing Test) correlated with atrophy in brain regions known to be vulnerable to early pathological changes of AD, i.e. the medial temporal lobes (MTL). Thus, although we studied cognitively healthy people, our findings suggest that structural MRI has potential to detect regions vulnerable to early AD damage, which is responsible for early cognitive dysfunction in the preclinical phase of AD. We then further explored if, through such correlation with behaviour, structural MRI informs on actual brain function. We found that successful (relative to unsuccessful)

performance of an fMRI-adapted version of the Placing Test was reflected by increased neural response in the same regions of MTL, including the hippocampus and amygdala.

Several factors contribute to individual variability in brain structure and function in older adults. In addition to genetic and developmental factors, they include processes occurring specifically with senescence such as neuronal shrinkage/loss, dendritic and spine degeneration, changes in synaptic function (Fjell and Walhovd, 2010; Barnes, 1994; Morrison and Hof, 1997), and small vessel disease, . In addition, increasing evidence from both neuropathological and amyloid PET imaging studies shows that a substantial proportion of cognitively normal older individuals already have occult AD pathology. It is therefore plausible that these "pathological" changes also contribute to variability in brain structure and function in non-demented older adults, and potentially lead to cognitive changes (Sperling et al., 2009; Vannini et al., 2011a). A mechanistic understanding of how and to what extent each of these factors impact individual differences in brain structure and function in healthy older adults was not the goal of the study presented in *Chapter 4* and could not be addressed with the imaging methods available. However, by using multimodal MRI to explore the effect on cognitive performance of different aspects of brain structure and function, I possibly accounted for the effect of several neurobiological determinants of individual behavioural/cognitive variability in older adults. Since brain regions exhibiting performance-related properties are possibly related to the earliest symptomatic changes occurring with disease, the results presented in *Chapter 4* concerning brain-behaviour relationships can possibly be applied to the diseased brain in both pre- and post-symptomatic phases.

8.1.3 Multimodal MRI imaging is feasible in patients with MCI and AD

In *Chapter 5*, we described details about establishing a multi-modality MRI protocol, which combined structural and functional sequences. Functional sequences were acquired at rest

and during the execution of two different cognitive tasks, one memory-related (visuospatial associative memory) and one memory-unrelated (self-appraisal). Healthy older controls and patients representing different symptomatic phases of AD progression (amnestic MCI and probable AD) were recruited and cross-sectional comparisons between the three groups performed. Methodological issues concerned with controlling for the effect of underlying structural differences and physiological noise on the fMRI signal were explicitly addressed, making the study novel and possibly more informative than previous studies on MCI and AD patients that have used resting only or task-fMRI only. Resting fMRI was successfully performed in almost all participants, although data from a few of them had to be disregarded because of movement artefacts. Task fMRI data were successfully acquired in the majority, but not all, of the patients. Patients who could not learn to do the task or were assessed likely to become distressed during its execution in the MRI scan were identified during the training prior to scan. They were not asked to perform task-fMRI but only resting-fMRI. Strategies about how to undertake fMRI in cognitively impaired patients and older and vulnerable adults were detailed.

8.1.4 Resting functional connectivity is sensitive to residual functional activity in AD

Chapter 6 jointly reported the results of structural MRI, resting-fMRI and memory-related task-fMRI assessments from the research protocol described in *Chapter 5*. It was found that fMRI can detect significant differences in task-related functional activity and resting functional connectivity between control, MCI and AD groups occurring over and above changes in brain structure, and overcoming limitations of previous studies related to differences in performance with an event-related study.

Localization and directionality of between-group differences in memory-related fMRI were specific for contrasts comparing successful relative to unsuccessful performance of the

cognitive task, showing that fMRI is useful to unravel whether functional changes are efficient (i.e., reflect mechanisms responsible of residual abilities in patients with MCI and AD) or whether they are inefficient (i.e., reflect aberrant mechanisms of compensation not behaviourally effective).

First, I found that hyper-activation of medial temporal lobes frequently observed in MCI is non-specific for successful encoding and recognition, since it also occurs for unsuccessful memory trials. I speculated that it may therefore represent maladaptive or aberrant mechanisms of compensation, in line with recent evidence that reducing hippocampal activation in MCI has therapeutic potential (Bakker et al., 2012).

Second, I showed that mechanisms for residual successful relative to unsuccessful recognition in AD patients involve hyper-activation of a region in the right lateral prefrontal cortex, which is known to be involved in successful retrieval, but also in the monitoring and evaluating of retrieval outcome. I speculated that the hyper-activation of this region by patients with AD reflects a residual cognitive strategy to maximise task performance.

Third, I then found that this same right lateral prefrontal region showed significantly higher functional connectivity in AD patients relative to controls when comparing groups on functional connectivity within the right frontoparietal resting state network, which has been shown to have a role in supporting strategic searches through memory and retrieval monitoring (Fornito et al., 2012). I concluded that the co-localisation of performance specific between-group results of task-fMRI and between-group results of resting-fMRI suggests that resting-fMRI can indirectly inform on mechanisms put in place by AD patients in order to be able to still perform a cognitive task correctly. It may therefore have a potential as a marker of residual ability, which could be possibly used to measure the effect of new treatments in patients with AD.

8.1.5 Functional MRI unravels mechanisms of anosognosia in AD

In *Chapter 7*, I presented results from fMRI performed during a self- and other-appraisal task, which did not directly test memory and was relatively easy for patients to undertake in the scanner. This task was chosen because it would indirectly inform on the functional mechanisms underlying unawareness of disease (also called anosognosia), a common symptom in MCI and AD patients for which functional correlates have been little explored. Behavioural results showed that patients with AD presented impaired self-appraisal but normal other-appraisal abilities, whereas MCI and controls had both normal self- and other-appraisal abilities. In fMRI, this was reflected in a significant interaction between group (AD versus either MCI or control) and condition (self- versus other-appraisal) in the dorsal medial prefrontal cortex (MPFC) and left anterior temporal lobe. The interaction was driven by the fact that during self-appraisal controls and MCIs had significantly greater MPFC activation than AD patients, suggesting that AD patients failed to activate this region specifically during self-appraisal, whereas they were able to engage it during other-appraisal. The fact that between-group differences in fMRI signal were condition-specific (i.e., for self- but not for other-appraisal) further support the use of fMRI in AD as a tool useful to unravel the mechanisms underlying specific cognitive symptoms. More precisely, results presented in *Chapter 7* suggest that the dysfunction of a network involving medial prefrontal and anterior temporal cortices is associated with the failure in AD patients of mechanisms necessary for correct and updated self-awareness and may therefore lead to anosognosia.

The study of self-awareness and anosognosia has important consequences in terms of diagnosis and potential prediction of AD in the elderly. In fact, memory complaint is one of the central diagnostic criteria for MCI, and therefore it is possible that older adults with early cognitive impairment and anosognosia may go under-diagnosed. On the other hand, some authors have suggested that early subjective concern about one's own cognition may predict the development of dementia in cognitively healthy elderly even before the MCI phase

(Reisberg and Gauthier, 2008), and others have shown that such concern tends to disappear close to the clinical onset of dementia (Stewart et al., 2011). This suggests that subjective memory complaint may be predictive of MCI development in the pre-clinical AD phase, whereas its opposite (i.e., anosognosia) may be predictive of progression to AD in the MCI phase.

8.2 Future directions

The results presented in this thesis have potentially opened new lines for future research. Here, some suggestions are proposed.

1) There is a need to understand more about which elements of underlying pathology are reflected in MRI measures. More precisely, do functional changes occur before or after the pathological changes due to AD? Are functional changes an adaptive response to pathology or catalysts to AD-related pathological changes? The combined use of fMRI and other imaging techniques, such as spectroscopy or PET using amyloid detection compounds might help to address these further questions. Each imaging modality has its own set of limitations. However, as long as these are appreciated and taken into account, imaging is likely to have an increasing role in detecting efficacy of treatments.

2) Only a few task-fMRI studies using memory paradigms have examined whether signal changes detected in the MCI phase can predict further progression over time. To the best of my knowledge, no studies have tested if baseline resting- or task-fMRI can predict future development of cognitive impairment in healthy controls. An important future direction of the research presented in this thesis would be to establish whether baseline fMRI can predict future progression of cognitive decline in healthy older

adults and patients with MCI, and distinguish those who will remain stable over time from those who will decline cognitively in a certain period of time (i.e., two years).

3) Resting state networks analysis has rapidly increased over the past years and is considered a useful approach to study network-related functional brain changes particularly in clinical population where task-related fMRI acquisition is difficult to perform. In *Chapter 6* I suggested that networks of coherent functional connectivity of the healthy brain at rest reflect those utilized "actively" during execution of tasks. I further speculated that this correspondence persists in the diseased brain and that changes in functional connectivity secondary to AD reflect residual functional abilities of the diseased brain. However, how best to interpret resting state data is not clear yet and additional studies combining task- and resting-fMRI, and possibly conducted in other clinical populations, are necessary to understand more deeply the relationship between resting state networks and behaviour/cognition.

4) Related to the previous point, a possible future direction specific to the findings presented in *Chapter 7* regards the relationship between resting-fMRI and task-fMRI of self-appraisal, since the regions specific for self- and other-appraisal in the MCI and control group presented in *Chapter 7* resembles the map of the default mode network (DMN) presented in *Chapter 6*. Indeed, among several explanations suggested for the DMN, the fact that it may reflect self-reflection processes has been argued by many authors. Thus, it would be important to directly test (i) if DMN functional connectivity specifically relates to self- rather than other-appraisal, and (ii) if resting-fMRI also gives overlapping information to condition-specific task-fMRI in the case of the self-appraisal task, in parallel with the combined resting- and memory-related task-fMRI

presented in *Chapter 6*. I aim to further explore the correlation between anosognosia, self-appraisal and the DMN (and other RSNs) in future studies.

5) Results from task-fMRI presented in *Chapter 6* evoke precise hypotheses about the functional changes that should potentially occur in response to pharmacological or behavioural interventions aimed to improve residual abilities in patients with MCI and AD. For example, potential treatments/interventions should be aimed to enhance prefrontal-efficient rather than hippocampal-inefficient residual functional activity in patients with MCI and AD. Combined results of task- and resting-fMRI presented in the same chapter further suggest that studies aimed to test treatment efficacy using imaging outcomes may possibly only need resting-fMRI, rather than having the complication of a task. To confirm this, studies showing the effect of treatment on both task and resting fMRI data are needed. A study aimed to investigate the effect of one of the treatments currently approved for AD (donepezil) has been planned and is currently on-going. In general, additional work to validate fMRI as a potential outcome measure for use in clinical trials is needed. It is likely that fMRI may have the greatest utility in early "proof of concept" studies, to detect an efficacy signal over a relatively short time frame.

8.3 Conclusions

The aim of the research presented in this thesis was to isolate specific markers of changes in brain *structure* and *function* detectable with MRI techniques that occur in different stages of AD progression, from pre-symptomatic phases, to MCI, to clinically evident dementia.

The first part of the research presented in this thesis focused on the use of *structural* MRI to characterise brain *structural* changes that occur in the pre-symptomatic, preclinical phase of AD. It was found that voxel-based whole-brain structural MRI techniques could detect atrophy in the medial temporal lobes of people in the preclinical stage of AD years before any cognitive decline, and possibly earlier than previously reported. These findings are consistent with those of other recent studies. They challenge the view that grey matter atrophy detected by structural MRI occurs late in the progression of AD and is a "downstream event" in the cascade of pathogenic events that leads to dementia, thus contributing to a better understanding of the natural history and biology of AD. Ultimately, these findings further support the view that hippocampal atrophy detectable with structural MRI should be included among criteria for the clinical diagnosis of AD and MCI, further emphasising the need to standardise and reach consensus on automated methods to obtain hippocampal volumetry.

The second part of the research presented in this thesis focused on the use of *functional* MRI to improve cross-sectional characterisation of brain *functional* changes occurring in the later, symptomatic phases of AD. In fact, since fMRI is a relatively recent, still developing technique among other imaging markers of AD, there is no consensus yet on the distribution and magnitude of abnormalities that it can detect in MCI and AD. This is particularly true for resting fMRI, which explores unconstrained, task-unrelated functional connectivity during rest. It was found that task-fMRI (during a visuospatial associative memory task) and resting-fMRI informed on preserved, residual, and possibly compensatory brain function in patients with

AD. The correspondence between memory-related task-fMRI and resting-fMRI is one of the most novel findings of the research presented in this thesis. It suggests that resting-fMRI has a potential to be a marker of residual and adaptive functional abilities in AD and could possibly be used to measure the effect of treatments.

Finally, it was found that the functional activity elicited by a self-appraisal task informed on the mechanisms underlying anosognosia for cognitive impairment in MCI and AD, emerging as a sensitive marker of this common symptom. Since anosognosia may challenge the presence of a cognitive complaint and its reporting by patients, it has significant implications for early diagnosis, especially in the pre-dementia phases. It is therefore expected to increasingly become the object of attention and consideration and, ultimately, also a possible target of specific interventions.

In conclusion, the findings of the second part of this thesis suggest that fMRI (and possibly the combination of resting- and task-fMRI) may prove increasingly useful to detect AD-related dynamic brain dysfunction as well as adaptive and residual function, and ultimately to monitor response to pharmacological or non-pharmacological interventions.

References

Biomarkers and surrogate endpoints: preferred definitions and conceptual framework. *Clin Pharmacol Ther,* 69(3): 89-95, 2001.

Agnew SK and Morris RG. The heterogeneity of anosognosia for memory impairment in Alzheimer's disease: A review of the literature and a proposed model *Aging & Mental Health,* 2(1): 7-19, 1998.

Agosta F, Pievani M, Geroldi C, Copetti M, Frisoni GB, and Filippi M. Resting state fMRI in Alzheimer's disease: beyond the default mode network. *Neurobiol Aging*, 2011.

Aguirre GK, Zarahn E, and D'Esposito M. Neural components of topographical representation. *Proc Natl Acad Sci U S A,* 95(3): 839-846, 1998.

Ahmed S, Mitchell J, Arnold R, Nestor PJ, and Hodges JR. Predicting rapid clinical progression in amnestic mild cognitive impairment. *Dement Geriatr Cogn Disord,* 25(2): 170-177, 2008.

Albert MS, DeKosky ST, Dickson D, Dubois B, Feldman HH, Fox NC, Gamst A, Holtzman DM, Jagust WJ, Petersen RC, Snyder PJ, Carrillo MC, Thies B, and Phelps CH. The diagnosis of mild cognitive impairment due to Alzheimer's disease: recommendations from the National Institute on Aging-Alzheimer's Association workgroups on diagnostic guidelines for Alzheimer's disease. *Alzheimers Dement,* 7(3): 270-279, 2011.

Allen G, Barnard H, McColl R, Hester AL, Fields JA, Weiner MF, Ringe WK, Lipton AM, Brooker M, McDonald E, Rubin CD, and Cullum CM. Reduced hippocampal functional connectivity in Alzheimer disease. *Arch Neurol,* 64(10): 1482-1487, 2007.

Alvarez P and Squire LR. Memory consolidation and the medial temporal lobe: a simple network model. *Proc Natl Acad Sci U S A,* 91(15): 7041-7045, 1994.

Alzheimer A. Uber eine eigenartige Erkangkung der Hirnrinde. In *Allgemeine Zeitschrift fur Psychiatrie und Psychisch-Gerichtliche Medizin*, 1907: 146-148.

Alzheimer A. Über eigenartige Krankheitsfälle des späteren Alters. *Zbl. ges. Neurol. Psych,* 4: 356–385, 1911.

Amanzio M, Torta DM, Sacco K, Cauda F, D'Agata F, Duca S, Leotta D, Palermo S, and Geminiani GC. Unawareness of deficits in Alzheimer's disease: role of the cingulate cortex. *Brain,* 134(Pt 4): 1061-1076, 2011.

American Psychiatric Association TFoD-I. *Diagnostic and statistical manual of mental disorders : DSM-IV*. Washington, DC: American pyschiatric association, 1994.

Amodio DM and Frith CD. Meeting of minds: the medial frontal cortex and social cognition. *Nat Rev Neurosci,* 7(4): 268-277, 2006.

Anchisi D, Borroni B, Franceschi M, Kerrouche N, Kalbe E, Beuthien-Beumann B, Cappa S, Lenz O, Ludecke S, Marcone A, Mielke R, Ortelli P, Padovani A, Pelati O, Pupi A, Scarpini E, Weisenbach S, Herholz K, Salmon E, Holthoff V, Sorbi S, Fazio F, and Perani D. Heterogeneity of brain glucose metabolism in mild cognitive impairment and clinical progression to Alzheimer disease. *Arch Neurol,* 62(11): 1728-1733, 2005.

Anderson EJ, de Jager CA, and Iversen SD. The Placing Test: preliminary investigations of a quick and simple memory test designed to be sensitive to pre-dementia Alzheimer's disease but not to normal ageing. *J Clin Exp Neuropsychol,* 28(6): 843-858, 2006.

Anderson NH. Likableness ratings of 555 personality-trait words. *J Pers Soc Psychol,* 9(3): 272-279, 1968.

Andersson JLR, Jenkinson M, and Smith S. Non-linear optimisation. *FMRIB technical report TR07JA1 from* http://www.fmrib.ox.ac.uk/analysis/techrep 2007.

Ansell EL and Bucks RS. Mnemonic anosognosia in Alzheimer's disease: a test of Agnew and Morris (1998). *Neuropsychologia,* 44(7): 1095-1102, 2006.

Apostolova LG, Dutton RA, Dinov ID, Hayashi KM, Toga AW, Cummings JL, and Thompson PM. Conversion of mild cognitive impairment to Alzheimer disease predicted by hippocampal atrophy maps. *Arch Neurol,* 63(5): 693-699, 2006.

Arriagada PV, Growdon JH, Hedley-Whyte ET, and Hyman BT. Neurofibrillary tangles but not senile plaques parallel duration and severity of Alzheimer's disease. *Neurology,* 42(3 Pt 1): 631-639, 1992.

Arthurs OJ and Boniface S. How well do we understand the neural origins of the fMRI BOLD signal? *Trends Neurosci,* 25(1): 27-31, 2002.

Ashburner J, Csernansky JG, Davatzikos C, Fox NC, Frisoni GB, and Thompson PM. Computer-assisted imaging to assess brain structure in healthy and diseased brains. *Lancet Neurol,* 2(2): 79-88, 2003.

Ashburner J and Friston KJ. Voxel-based morphometry--the methods. *Neuroimage,* 11(6 Pt 1): 805-821, 2000.

Ashburner J and Friston KJ. Why voxel-based morphometry should be used. *Neuroimage,* 14(6): 1238-1243, 2001.

Backman L, Jones S, Berger AK, Laukka EJ, and Small BJ. Multiple cognitive deficits during the transition to Alzheimer's disease. *J Intern Med,* 256(3): 195-204, 2004.

Bakker A, Krauss GL, Albert MS, Speck CL, Jones LR, Stark CE, Yassa MA, Bassett SS, Shelton AL, and Gallagher M. Reduction of hippocampal hyperactivity improves cognition in amnestic mild cognitive impairment. *Neuron,* 74(3): 467-474, 2012.

Barnes CA. Normal aging: regionally specific changes in hippocampal synaptic transmission. *Trends Neurosci,* 17(1): 13-18, 1994.

Barnes J, Boyes RG, Lewis EB, Schott JM, Frost C, Scahill RI, and Fox NC. Automatic calculation of hippocampal atrophy rates using a hippocampal template and the boundary shift integral. *Neurobiol Aging,* 28(11): 1657-1663, 2007.

Barnes J, Foster J, Boyes RG, Pepple T, Moore EK, Schott JM, Frost C, Scahill RI, and Fox NC. A comparison of methods for the automated calculation of volumes and atrophy rates in the hippocampus. *Neuroimage,* 40(4): 1655-1671, 2008a.

Barnes J, Scahill RI, Boyes RG, Frost C, Lewis EB, Rossor CL, Rossor MN, and Fox NC. Differentiating AD from aging using semiautomated measurement of hippocampal atrophy rates. *Neuroimage,* 23(2): 574-581, 2004.

Barnes J, Scahill RI, Frost C, Schott JM, Rossor MN, and Fox NC. Increased hippocampal atrophy rates in AD over 6 months using serial MR imaging. *Neurobiol Aging,* 29(8): 1199-1203, 2008b.

Barnes J, Scahill RI, Schott JM, Frost C, Rossor MN, and Fox NC. Does Alzheimer's disease affect hippocampal asymmetry? Evidence from a cross-sectional and longitudinal volumetric MRI study. *Dement Geriatr Cogn Disord,* 19(5-6): 338-344, 2005.

Bateman RJ, Xiong C, Benzinger TL, Fagan AM, Goate A, Fox NC, Marcus DS, Cairns NJ, Xie X, Blazey TM, Holtzman DM, Santacruz A, Buckles V, Oliver A, Moulder K, Aisen PS, Ghetti B, Klunk WE, McDade E, Martins RN, Masters CL, Mayeux R, Ringman JM, Rossor MN, Schofield PR, Sperling RA, Salloway S, and Morris JC. Clinical and biomarker changes in dominantly inherited Alzheimer's disease. *N Engl J Med,* 367(9): 795-804, 2012.

Beckmann CF, DeLuca M, Devlin JT, and Smith SM. Investigations into resting-state connectivity using independent component analysis. *Philos Trans R Soc Lond B Biol Sci,* 360(1457): 1001-1013, 2005.

Beckmann CF and Smith SM. Probabilistic independent component analysis for functional magnetic resonance imaging. *IEEE Trans Med Imaging,* 23(2): 137-152, 2004.

Benjamini Y, Drai D, Elmer G, Kafkafi N, and Golani I. Controlling the false discovery rate in behavior genetics research. *Behav Brain Res,* 125(1-2): 279-284, 2001.

Binnewijzend MA, Schoonheim MM, Sanz-Arigita E, Wink AM, van der Flier WM, Tolboom N, Adriaanse SM, Damoiseaux JS, Scheltens P, van Berckel BN, and Barkhof F. Resting-state fMRI changes in Alzheimer's disease and mild cognitive impairment. *Neurobiol Aging,* 33(9): 2018-2028, 2011.

Birn RM, Diamond JB, Smith MA, and Bandettini PA. Separating respiratory-variation-related fluctuations from neuronal-activity-related fluctuations in fMRI. *Neuroimage,* 31(4): 1536-1548, 2006.

Bishop CA, Jenkinson M, Andersson J, Declerck J, and Merhof D. Novel Fast Marching for Automated Segmentation of the Hippocampus (FMASH): method and validation on clinical data. *Neuroimage,* 55(3): 1009-1019, 2011.

Blackwell AD, Sahakian BJ, Vesey R, Semple JM, Robbins TW, and Hodges JR. Detecting dementia: novel neuropsychological markers of preclinical Alzheimer's disease. *Dement Geriatr Cogn Disord,* 17(1-2): 42-48, 2004.

Blair KS, Geraci M, Hollon N, Otero M, DeVido J, Majestic C, Jacobs M, Blair RJ, and Pine DS. Social norm processing in adult social phobia: atypically increased ventromedial frontal cortex responsiveness to unintentional (embarrassing) transgressions. *Am J Psychiatry,* 167(12): 1526-1532, 2010.

Blennow K, Hampel H, Weiner M, and Zetterberg H. Cerebrospinal fluid and plasma biomarkers in Alzheimer disease. *Nat Rev Neurol,* 6(3): 131-144, 2010.

Bobinski M, de Leon MJ, Wegiel J, Desanti S, Convit A, Saint Louis LA, Rusinek H, and Wisniewski HM. The histological validation of post mortem magnetic resonance imaging-determined hippocampal volume in Alzheimer's disease. *Neuroscience,* 95(3): 721-725, 2000.

Bookheimer SY, Strojwas MH, Cohen MS, Saunders AM, Pericak-Vance MA, Mazziotta JC, and Small GW. Patterns of brain activation in people at risk for Alzheimer's disease. *N Engl J Med,* 343(7): 450-456, 2000.

Bozzali M, Filippi M, Magnani G, Cercignani M, Franceschi M, Schiatti E, Castiglioni S, Mossini R, Falautano M, Scotti G, Comi G, and Falini A. The contribution of voxel-based morphometry in staging patients with mild cognitive impairment. *Neurology,* 67(3): 453-460, 2006.

Braak H and Braak E. Neuropathological stageing of Alzheimer-related changes. *Acta Neuropathol,* 82(4): 239-259, 1991.

Braak H and Braak E. Diagnostic criteria for neuropathologic assessment of Alzheimer's disease. *Neurobiol Aging,* 18(4 Suppl): S85-88, 1997.

Braak H, Braak E, Bohl J, and Bratzke H. Evolution of Alzheimer's disease related cortical lesions. *J Neural Transm Suppl,* 54: 97-106, 1998.

Brickman AM, Small SA, and Fleisher A. Pinpointing synaptic loss caused by Alzheimer's disease with fMRI. *Behav Neurol,* 21(1): 93-100, 2009.

Brooks JC, Beckmann CF, Miller KL, Wise RG, Porro CA, Tracey I, and Jenkinson M. Physiological noise modelling for spinal functional magnetic resonance imaging studies. *Neuroimage,* 39(2): 680-692, 2008.

Buckner RL and Carroll DC. Self-projection and the brain. *Trends Cogn Sci,* 11(2): 49-57, 2007.

Buckner RL, Head D, Parker J, Fotenos AF, Marcus D, Morris JC, and Snyder AZ. A unified approach for morphometric and functional data analysis in young, old, and demented adults using automated atlas-based head size normalization: reliability and validation against manual measurement of total intracranial volume. *Neuroimage,* 23(2): 724-738, 2004.

Buckner RL, Snyder AZ, Shannon BJ, LaRossa G, Sachs R, Fotenos AF, Sheline YI, Klunk WE, Mathis CA, Morris JC, and Mintun MA. Molecular, structural, and functional characterization of Alzheimer's disease: evidence for a relationship between default activity, amyloid, and memory. *J Neurosci,* 25(34): 7709-7717, 2005.

Buckner RL and Wheeler ME. The cognitive neuroscience of remembering. *Nat Rev Neurosci,* 2(9): 624-634, 2001.

Bunsey M and Eichenbaum H. Critical role of the parahippocampal region for paired-associate learning in rats. *Behav Neurosci,* 107(5): 740-747, 1993.

Burton EJ, Barber R, Mukaetova-Ladinska EB, Robson J, Perry RH, Jaros E, Kalaria RN, and O'Brien JT. Medial temporal lobe atrophy on MRI differentiates Alzheimer's disease from dementia with Lewy bodies and vascular cognitive impairment: a prospective study with pathological verification of diagnosis. *Brain,* 132(Pt 1): 195-203, 2009.

Busatto GF, Diniz BS, and Zanetti MV. Voxel-based morphometry in Alzheimer's disease. *Expert Rev Neurother,* 8(11): 1691-1702, 2008.

Cahn DA, Sullivan EV, Shear PK, Marsh L, Fama R, Lim KO, Yesavage JA, Tinklenberg JR, and Pfefferbaum A. Structural MRI correlates of recognition memory in Alzheimer's disease. *J Int Neuropsychol Soc,* 4(2): 106-114, 1998.

Caroli A, Prestia A, Chen K, Ayutyanont N, Landau SM, Madison CM, Haense C, Herholz K, Nobili F, Reiman EM, Jagust WJ, and Frisoni GB. Summary Metrics to Assess Alzheimer Disease-Related Hypometabolic Pattern with 18F-FDG PET: Head-to-Head Comparison. *J Nucl Med,* 53(4): 592-600, 2012.

Celone KA, Calhoun VD, Dickerson BC, Atri A, Chua EF, Miller SL, DePeau K, Rentz DM, Selkoe DJ, Blacker D, Albert MS, and Sperling RA. Alterations in memory networks in mild cognitive impairment and Alzheimer's disease: an independent component analysis. *J Neurosci,* 26(40): 10222-10231, 2006.

Chan D, Fox NC, Scahill RI, Crum WR, Whitwell JL, Leschziner G, Rossor AM, Stevens JM, Cipolotti L, and Rossor MN. Patterns of temporal lobe atrophy in semantic dementia and Alzheimer's disease. *Ann Neurol,* 49(4): 433-442, 2001.

Chang C and Glover GH. Effects of model-based physiological noise correction on default mode network anti-correlations and correlations. *Neuroimage,* 47(4): 1448-1459, 2009.

Chase TN, Foster NL, Fedio P, Brooks R, Mansi L, and Di Chiro G. Regional cortical dysfunction in Alzheimer's disease as determined by positron emission tomography. *Ann Neurol,* 15 Suppl: S170-174, 1984.

Chetelat G, Fouquet M, Kalpouzos G, Denghien I, De la Sayette V, Viader F, Mezenge F, Landeau B, Baron JC, Eustache F, and Desgranges B. Three-dimensional surface mapping of hippocampal atrophy progression from MCI to AD and over normal aging as assessed using voxel-based morphometry. *Neuropsychologia,* 46(6): 1721-1731, 2008.

Chetelat G, Landeau B, Eustache F, Mezenge F, Viader F, de la Sayette V, Desgranges B, and Baron JC. Using voxel-based morphometry to map the structural changes associated with rapid conversion in MCI: a longitudinal MRI study. *Neuroimage,* 27(4): 934-946, 2005.

Clement F and Belleville S. Test-retest reliability of fMRI verbal episodic memory paradigms in healthy older adults and in persons with mild cognitive impairment. *Hum Brain Mapp,* 30(12): 4033-4047, 2009.

Cole DM, Smith SM, and Beckmann CF. Advances and pitfalls in the analysis and interpretation of resting-state FMRI data. *Front Syst Neurosci,* 4: 8, 2010.

Conway MA and Pleydell-Pearce CW. The construction of autobiographical memories in the self-memory system. *Psychol Rev,* 107(2): 261-288, 2000.

Corder EH, Saunders AM, Strittmatter WJ, Schmechel DE, Gaskell PC, Small GW, Roses AD, Haines JL, and Pericak-Vance MA. Gene dose of apolipoprotein E type 4 allele and the risk of Alzheimer's disease in late onset families. *Science,* 261(5123): 921-923, 1993.

Cosentino S, Metcalfe J, Butterfield B, and Stern Y. Objective metamemory testing captures awareness of deficit in Alzheimer's disease. *Cortex,* 43(7): 1004-1019, 2007.

Costafreda SG, Dinov ID, Tu Z, Shi Y, Liu CY, Kloszewska I, Mecocci P, Soininen H, Tsolaki M, Vellas B, Wahlund LO, Spenger C, Toga AW, Lovestone S, and Simmons A. Automated hippocampal shape analysis predicts the onset of dementia in mild cognitive impairment. *Neuroimage,* 56(1): 212-219, 2011.

Cummings JL. The Neuropsychiatric Inventory: assessing psychopathology in dementia patients. *Neurology,* 48(5 Suppl 6): S10-16, 1997.

D'Argembeau A, Collette F, Van der Linden M, Laureys S, Del Fiore G, Degueldre C, Luxen A, and Salmon E. Self-referential reflective activity and its relationship with rest: a PET study. *Neuroimage,* 25(2): 616-624, 2005.

Damoiseaux JS, Beckmann CF, Arigita EJ, Barkhof F, Scheltens P, Stam CJ, Smith SM, and Rombouts SA. Reduced resting-state brain activity in the "default network" in normal aging. *Cereb Cortex,* 18(8): 1856-1864, 2008.

Damoiseaux JS, Prater KE, Miller BL, and Greicius MD. Functional connectivity tracks clinical deterioration in Alzheimer's disease. *Neurobiol Aging*, 2011.

Damoiseaux JS, Rombouts SA, Barkhof F, Scheltens P, Stam CJ, Smith SM, and Beckmann CF. Consistent resting-state networks across healthy subjects. *Proc Natl Acad Sci U S A,* 103(37): 13848-13853, 2006.

Davatzikos C, Fan Y, Wu X, Shen D, and Resnick SM. Detection of prodromal Alzheimer's disease via pattern classification of magnetic resonance imaging. *Neurobiol Aging,* 29(4): 514-523, 2008.

de Jager C, Blackwell AD, Budge MM, and Sahakian BJ. Predicting cognitive decline in healthy older adults. *Am J Geriatr Psychiatry,* 13(8): 735-740, 2005.

de Jager CA, Hogervorst E, Combrinck M, and Budge MM. Sensitivity and specificity of neuropsychological tests for mild cognitive impairment, vascular cognitive impairment and Alzheimer's disease. *Psychol Med,* 33(6): 1039-1050, 2003.

de Jager CA, Milwain E, and Budge M. Early detection of isolated memory deficits in the elderly: the need for more sensitive neuropsychological tests. *Psychol Med,* 32(3): 483-491, 2002.

de Leon MJ, Convit A, Wolf OT, Tarshish CY, DeSanti S, Rusinek H, Tsui W, Kandil E, Scherer AJ, Roche A, Imossi A, Thorn E, Bobinski M, Caraos C, Lesbre P, Schlyer D, Poirier J, Reisberg B, and Fowler J. Prediction of cognitive decline in normal elderly subjects with 2-[(18)F]fluoro-2-deoxy-D-glucose/poitron-emission tomography (FDG/PET). *Proc Natl Acad Sci U S A,* 98(19): 10966-10971, 2001.

De Luca M, Beckmann CF, De Stefano N, Matthews PM, and Smith SM. fMRI resting state networks define distinct modes of long-distance interactions in the human brain. *Neuroimage,* 29(4): 1359-1367, 2006.

de Rover M, Pironti VA, McCabe JA, Acosta-Cabronero J, Arana FS, Morein-Zamir S, Hodges JR, Robbins TW, Fletcher PC, Nestor PJ, and Sahakian BJ. Hippocampal dysfunction in patients with mild cognitive impairment: a functional neuroimaging study of a visuospatial paired associates learning task. *Neuropsychologia,* 49(7): 2060-2070, 2011.

de Toledo-Morrell L, Dickerson B, Sullivan MP, Spanovic C, Wilson R, and Bennett DA. Hemispheric differences in hippocampal volume predict verbal and spatial memory performance in patients with Alzheimer's disease. *Hippocampus,* 10(2): 136-142, 2000.

den Heijer T, Geerlings MI, Hoebeek FE, Hofman A, Koudstaal PJ, and Breteler MM. Use of hippocampal and amygdalar volumes on magnetic resonance imaging to predict dementia in cognitively intact elderly people. *Arch Gen Psychiatry,* 63(1): 57-62, 2006.

Desikan RS, McEvoy LK, Thompson WK, Holland D, Brewer JB, Aisen PS, Sperling RA, and Dale AM. Amyloid-beta-Associated Clinical Decline Occurs Only in the Presence of Elevated P-tau. *Arch Neurol*, 2012.

Devanand DP, Pradhaban G, Liu X, Khandji A, De Santi S, Segal S, Rusinek H, Pelton GH, Honig LS, Mayeux R, Stern Y, Tabert MH, and de Leon MJ. Hippocampal and entorhinal atrophy in mild cognitive impairment: prediction of Alzheimer disease. *Neurology,* 68(11): 828-836, 2007.

Deweer B, Lehericy S, Pillon B, Baulac M, Chiras J, Marsault C, Agid Y, and Dubois B. Memory disorders in probable Alzheimer's disease: the role of hippocampal atrophy as shown with MRI. *J Neurol Neurosurg Psychiatry,* 58(5): 590-597, 1995.

Di Paola M, Macaluso E, Carlesimo GA, Tomaiuolo F, Worsley KJ, Fadda L, and Caltagirone C. Episodic memory impairment in patients with Alzheimer's disease is correlated with entorhinal cortex atrophy. A voxel-based morphometry study. *J Neurol,* 254(6): 774-781, 2007.

Diamond EL, Miller S, Dickerson BC, Atri A, DePeau K, Fenstermacher E, Pihlajamaki M, Celone K, Salisbury S, Gregas M, Rentz D, and Sperling RA. Relationship of fMRI activation to clinical trial memory measures in Alzheimer disease. *Neurology,* 69(13): 1331-1341, 2007.

Dickerson BC, Bakkour A, Salat DH, Feczko E, Pacheco J, Greve DN, Grodstein F, Wright CI, Blacker D, Rosas HD, Sperling RA, Atri A, Growdon JH, Hyman BT, Morris JC, Fischl B, and Buckner RL. The cortical signature of Alzheimer's disease: regionally specific cortical thinning relates to symptom severity in very mild to mild AD dementia and is detectable in asymptomatic amyloid-positive individuals. *Cereb Cortex,* 19(3): 497-510, 2009.

Dickerson BC, Goncharova I, Sullivan MP, Forchetti C, Wilson RS, Bennett DA, Beckett LA, and deToledo-Morrell L. MRI-derived entorhinal and hippocampal atrophy in incipient and very mild Alzheimer's disease. *Neurobiol Aging,* 22(5): 747-754, 2001.

Dickerson BC, Salat DH, Bates JF, Atiya M, Killiany RJ, Greve DN, Dale AM, Stern CE, Blacker D, Albert MS, and Sperling RA. Medial temporal lobe function and structure in mild cognitive impairment. *Ann Neurol,* 56(1): 27-35, 2004.

Dickerson BC, Salat DH, Greve DN, Chua EF, Rand-Giovannetti E, Rentz DM, Bertram L, Mullin K, Tanzi RE, Blacker D, Albert MS, and Sperling RA. Increased hippocampal activation in

mild cognitive impairment compared to normal aging and AD. *Neurology,* 65(3): 404-411, 2005.

Dickerson BC and Sperling RA. Neuroimaging biomarkers for clinical trials of disease-modifying therapies in Alzheimer's disease. *NeuroRx,* 2(2): 348-360, 2005.

Dickerson BC and Sperling RA. Functional abnormalities of the medial temporal lobe memory system in mild cognitive impairment and Alzheimer's disease: insights from functional MRI studies. *Neuropsychologia,* 46(6): 1624-1635, 2008.

Dickerson BC and Sperling RA. Large-scale functional brain network abnormalities in Alzheimer's disease: insights from functional neuroimaging. *Behav Neurol,* 21(1): 63-75, 2009.

Dickerson BC, Stoub TR, Shah RC, Sperling RA, Killiany RJ, Albert MS, Hyman BT, Blacker D, and Detoledo-Morrell L. Alzheimer-signature MRI biomarker predicts AD dementia in cognitively normal adults. *Neurology,* 76(16): 1395-1402, 2011.

Ding Q, Dimayuga E, and Keller JN. Oxidative damage, protein synthesis, and protein degradation in Alzheimer's disease. *Curr Alzheimer Res,* 4(1): 73-79, 2007.

Douaud G, Smith S, Jenkinson M, Behrens T, Johansen-Berg H, Vickers J, James S, Voets N, Watkins K, Matthews PM, and James A. Anatomically related grey and white matter abnormalities in adolescent-onset schizophrenia. *Brain,* 130(Pt 9): 2375-2386, 2007.

Drzezga A, Grimmer T, Riemenschneider M, Lautenschlager N, Siebner H, Alexopoulus P, Minoshima S, Schwaiger M, and Kurz A. Prediction of individual clinical outcome in MCI by means of genetic assessment and (18)F-FDG PET. *J Nucl Med,* 46(10): 1625-1632, 2005.

Drzezga A, Lautenschlager N, Siebner H, Riemenschneider M, Willoch F, Minoshima S, Schwaiger M, and Kurz A. Cerebral metabolic changes accompanying conversion of mild cognitive impairment into Alzheimer's disease: a PET follow-up study. *Eur J Nucl Med Mol Imaging,* 30(8): 1104-1113, 2003.

Duara R, Loewenstein DA, Potter E, Appel J, Greig MT, Urs R, Shen Q, Raj A, Small B, Barker W, Schofield E, Wu Y, and Potter H. Medial temporal lobe atrophy on MRI scans and the diagnosis of Alzheimer disease. *Neurology,* 71(24): 1986-1992, 2008.

Dubois B. 'Prodromal Alzheimer's disease': a more useful concept than mild cognitive impairment? *Curr Opin Neurol,* 13(4): 367-369, 2000.

Dubois B and Albert ML. Amnestic MCI or prodromal Alzheimer's disease? *Lancet Neurol,* 3(4): 246-248, 2004.

Dubois B, Feldman HH, Jacova C, Cummings JL, Dekosky ST, Barberger-Gateau P, Delacourte A, Frisoni G, Fox NC, Galasko D, Gauthier S, Hampel H, Jicha GA, Meguro K, O'Brien J,

Pasquier F, Robert P, Rossor M, Salloway S, Sarazin M, de Souza LC, Stern Y, Visser PJ, and Scheltens P. Revising the definition of Alzheimer's disease: a new lexicon. *Lancet Neurol,* 9(11): 1118-1127, 2010.

Dubois B, Feldman HH, Jacova C, Dekosky ST, Barberger-Gateau P, Cummings J, Delacourte A, Galasko D, Gauthier S, Jicha G, Meguro K, O'Brien J, Pasquier F, Robert P, Rossor M, Salloway S, Stern Y, Visser PJ, and Scheltens P. Research criteria for the diagnosis of Alzheimer's disease: revising the NINCDS-ADRDA criteria. *Lancet Neurol,* 6(8): 734-746, 2007.

Dubois B, Zaim M, Touchon J, Vellas B, Robert P, Murphy MF, Pujadas-Navines F, Rainer M, Soininen H, Riordan HJ, and Kanony-Truc C. Effect of six months of treatment with v0191 in patients with suspected prodromal Alzheimer's disease. *J Alzheimers Dis,* 29(3): 527-535, 2012.

Ebmeier KP, Hunter R, Curran SM, Dougal NJ, Murray CL, Wyper DJ, Patterson J, Hanson MT, Siegfried K, and Goodwin GM. Effects of a single dose of the acetylcholinesterase inhibitor velnacrine on recognition memory and regional cerebral blood flow in Alzheimer's disease. *Psychopharmacology (Berl),* 108(1-2): 103-109, 1992.

Eichenbaum H, Wiener SI, Shapiro ML, and Cohen NJ. The organization of spatial coding in the hippocampus: a study of neural ensemble activity. *J Neurosci,* 9(8): 2764-2775, 1989.

Elias MF, Beiser A, Wolf PA, Au R, White RF, and D'Agostino RB. The preclinical phase of alzheimer disease: A 22-year prospective study of the Framingham Cohort. *Arch Neurol,* 57(6): 808-813, 2000.

Esiri MM, Nagy Z, Smith MZ, Barnetson L, and Smith AD. Cerebrovascular disease and threshold for dementia in the early stages of Alzheimer's disease. *Lancet,* 354(9182): 919-920, 1999.

Fazekas F, Chawluk JB, Alavi A, Hurtig HI, and Zimmerman RA. MR signal abnormalities at 1.5 T in Alzheimer's dementia and normal aging. *AJR Am J Roentgenol,* 149(2): 351-356, 1987.

Feldman HH, Ferris S, Winblad B, Sfikas N, Mancione L, He Y, Tekin S, Burns A, Cummings J, del Ser T, Inzitari D, Orgogozo JM, Sauer H, Scheltens P, Scarpini E, Herrmann N, Farlow M, Potkin S, Charles HC, Fox NC, and Lane R. Effect of rivastigmine on delay to diagnosis of Alzheimer's disease from mild cognitive impairment: the InDDEx study. *Lancet Neurol,* 6(6): 501-512, 2007.

Fennema-Notestine C, Hagler DJ, Jr., McEvoy LK, Fleisher AS, Wu EH, Karow DS, and Dale AM. Structural MRI biomarkers for preclinical and mild Alzheimer's disease. *Hum Brain Mapp,* 30(10): 3238-3253, 2009a.

Fennema-Notestine C, McEvoy LK, Hagler DJ, Jr., Jacobson MW, Dale AM, and The Alzheimer's Disease Neuroimaging I. Structural neuroimaging in the detection and prognosis of pre-clinical and early AD. *Behav Neurol,* 21(1): 3-12, 2009b.

Ferreira LK, Diniz BS, Forlenza OV, Busatto GF, and Zanetti MV. Neurostructural predictors of Alzheimer's disease: a meta-analysis of VBM studies. *Neurobiol Aging,* 32(10): 1733-1741, 2011.

Filippini N, Ebmeier KP, MacIntosh BJ, Trachtenberg AJ, Frisoni GB, Wilcock GK, Beckmann CF, Smith SM, Matthews PM, and Mackay CE. Differential effects of the APOE genotype on brain function across the lifespan. *Neuroimage,* 54(1): 602-610, 2011.

Filippini N, MacIntosh BJ, Hough MG, Goodwin GM, Frisoni GB, Smith SM, Matthews PM, Beckmann CF, and Mackay CE. Distinct patterns of brain activity in young carriers of the APOE-epsilon4 allele. *Proc Natl Acad Sci U S A,* 106(17): 7209-7214, 2009.

Fischer P, Jungwirth S, Zehetmayer S, Weissgram S, Hoenigschnabl S, Gelpi E, Krampla W, and Tragl KH. Conversion from subtypes of mild cognitive impairment to Alzheimer dementia. *Neurology,* 68(4): 288-291, 2007.

Fischl B and Dale AM. Measuring the thickness of the human cerebral cortex from magnetic resonance images. *Proc Natl Acad Sci U S A,* 97(20): 11050-11055, 2000.

Fjell AM and Walhovd KB. Structural brain changes in aging: courses, causes and cognitive consequences. *Rev Neurosci,* 21(3): 187-221, 2010.

Folstein MF, Folstein SE, and McHugh PR. "Mini-mental state". A practical method for grading the cognitive state of patients for the clinician. *J Psychiatr Res,* 12(3): 189-198, 1975.

Fornito A, Harrison BJ, Zalesky A, and Simons JS. Competitive and cooperative dynamics of large-scale brain functional networks supporting recollection. *Proc Natl Acad Sci U S A*, 2012.

Forsberg A, Engler H, Almkvist O, Blomquist G, Hagman G, Wall A, Ringheim A, Langstrom B, and Nordberg A. PET imaging of amyloid deposition in patients with mild cognitive impairment. *Neurobiol Aging,* 29(10): 1456-1465, 2008.

Foster NL, Chase TN, Fedio P, Patronas NJ, Brooks RA, and Di Chiro G. Alzheimer's disease: focal cortical changes shown by positron emission tomography. *Neurology,* 33(8): 961-965, 1983.

Fox MD and Raichle ME. Spontaneous fluctuations in brain activity observed with functional magnetic resonance imaging. *Nat Rev Neurosci,* 8(9): 700-711, 2007.

Fox NC, Black RS, Gilman S, Rossor MN, Griffith SG, Jenkins L, and Koller M. Effects of Abeta immunization (AN1792) on MRI measures of cerebral volume in Alzheimer disease. *Neurology,* 64(9): 1563-1572, 2005.

Fox NC, Cousens S, Scahill R, Harvey RJ, and Rossor MN. Using serial registered brain magnetic resonance imaging to measure disease progression in Alzheimer disease: power

calculations and estimates of sample size to detect treatment effects. *Arch Neurol,* 57(3): 339-344, 2000.

Fox NC, Crum WR, Scahill RI, Stevens JM, Janssen JC, and Rossor MN. Imaging of onset and progression of Alzheimer's disease with voxel-compression mapping of serial magnetic resonance images. *Lancet,* 358(9277): 201-205, 2001.

Fox NC, Freeborough PA, and Rossor MN. Visualisation and quantification of rates of atrophy in Alzheimer's disease. *Lancet,* 348(9020): 94-97, 1996a.

Fox NC, Warrington EK, Freeborough PA, Hartikainen P, Kennedy AM, Stevens JM, and Rossor MN. Presymptomatic hippocampal atrophy in Alzheimer's disease. A longitudinal MRI study. *Brain,* 119 (Pt 6): 2001-2007, 1996b.

Frey S and Petrides M. Orbitofrontal cortex and memory formation. *Neuron,* 36(1): 171-176, 2002.

Frisoni GB, Fox NC, Jack CR, Jr., Scheltens P, and Thompson PM. The clinical use of structural MRI in Alzheimer disease. *Nat Rev Neurol,* 6(2): 67-77, 2010.

Frith U and Frith CD. Development and neurophysiology of mentalizing. *Philos Trans R Soc Lond B Biol Sci,* 358(1431): 459-473, 2003.

Furst AJ, Rabinovici GD, Rostomian AH, Steed T, Alkalay A, Racine C, Miller BL, and Jagust WJ. Cognition, glucose metabolism and amyloid burden in Alzheimer's disease. *Neurobiol Aging,* 33(2): 215-225, 2012.

Galton CJ, Patterson K, Xuereb JH, and Hodges JR. Atypical and typical presentations of Alzheimer's disease: a clinical, neuropsychological, neuroimaging and pathological study of 13 cases. *Brain,* 123 Pt 3: 484-498, 2000.

Gili T, Cercignani M, Serra L, Perri R, Giove F, Maraviglia B, Caltagirone C, and Bozzali M. Regional brain atrophy and functional disconnection across Alzheimer's disease evolution. *J Neurol Neurosurg Psychiatry,* 82(1): 58-66, 2011.

Glover GH, Li TQ, and Ress D. Image-based method for retrospective correction of physiological motion effects in fMRI: RETROICOR. *Magn Reson Med,* 44(1): 162-167, 2000.

Golby A, Silverberg G, Race E, Gabrieli S, O'Shea J, Knierim K, Stebbins G, and Gabrieli J. Memory encoding in Alzheimer's disease: an fMRI study of explicit and implicit memory. *Brain,* 128(Pt 4): 773-787, 2005.

Gong CX, Grundke-Iqbal I, and Iqbal K. Targeting tau protein in Alzheimer's disease. *Drugs Aging,* 27(5): 351-365, 2010.

Good CD, Johnsrude IS, Ashburner J, Henson RN, Friston KJ, and Frackowiak RS. A voxel-based morphometric study of ageing in 465 normal adult human brains. *Neuroimage,* 14(1 Pt 1): 21-36, 2001.

Good CD, Scahill RI, Fox NC, Ashburner J, Friston KJ, Chan D, Crum WR, Rossor MN, and Frackowiak RS. Automatic differentiation of anatomical patterns in the human brain: validation with studies of degenerative dementias. *Neuroimage,* 17(1): 29-46, 2002.

Gorno-Tempini ML, Dronkers NF, Rankin KP, Ogar JM, Phengrasamy L, Rosen HJ, Johnson JK, Weiner MW, and Miller BL. Cognition and anatomy in three variants of primary progressive aphasia. *Ann Neurol,* 55(3): 335-346, 2004.

Gosche KM, Mortimer JA, Smith CD, Markesbery WR, and Snowdon DA. Hippocampal volume as an index of Alzheimer neuropathology: findings from the Nun Study. *Neurology,* 58(10): 1476-1482, 2002.

Gould RL, Arroyo B, Brown RG, Owen AM, Bullmore ET, and Howard RJ. Brain mechanisms of successful compensation during learning in Alzheimer disease. *Neurology,* 67(6): 1011-1017, 2006a.

Gould RL, Brown RG, Owen AM, Bullmore ET, and Howard RJ. Task-induced deactivations during successful paired associates learning: an effect of age but not Alzheimer's disease. *Neuroimage,* 31(2): 818-831, 2006b.

Gould RL, Brown RG, Owen AM, Bullmore ET, Williams SC, and Howard RJ. Functional neuroanatomy of successful paired associate learning in Alzheimer's disease. *Am J Psychiatry,* 162(11): 2049-2060, 2005.

Grady CL, Haxby JV, Horwitz B, Sundaram M, Berg G, Schapiro M, Friedland RP, and Rapoport SI. Longitudinal study of the early neuropsychological and cerebral metabolic changes in dementia of the Alzheimer type. *J Clin Exp Neuropsychol,* 10(5): 576-596, 1988.

Greicius MD, Srivastava G, Reiss AL, and Menon V. Default-mode network activity distinguishes Alzheimer's disease from healthy aging: evidence from functional MRI. *Proc Natl Acad Sci U S A,* 101(13): 4637-4642, 2004.

Greve DN and Fischl B. Accurate and robust brain image alignment using boundary-based registration. *Neuroimage,* 48(1): 63-72, 2009.

Grundke-Iqbal I, Iqbal K, Tung YC, Quinlan M, Wisniewski HM, and Binder LI. Abnormal phosphorylation of the microtubule-associated protein tau (tau) in Alzheimer cytoskeletal pathology. *Proc Natl Acad Sci U S A,* 83(13): 4913-4917, 1986.

Gusnard DA and Raichle ME. Searching for a baseline: functional imaging and the resting human brain. *Nat Rev Neurosci,* 2(10): 685-694, 2001.

Hall AM, Moore RY, Lopez OL, Kuller L, and Becker JT. Basal forebrain atrophy is a presymptomatic marker for Alzheimer's disease. *Alzheimers Dement,* 4(4): 271-279, 2008.

Hamalainen A, Grau-Olivares M, Tervo S, Niskanen E, Pennanen C, Huuskonen J, Kivipelto M, Hanninen T, Tapiola M, Vanhanen M, Hallikainen M, Helkala EL, Nissinen A, Vanninen RL, and Soininen H. Apolipoprotein E epsilon 4 allele is associated with increased atrophy in progressive mild cognitive impairment: a voxel-based morphometric study. *Neurodegener Dis,* 5(3-4): 186-189, 2008.

Hamalainen A, Pihlajamaki M, Tanila H, Hanninen T, Niskanen E, Tervo S, Karjalainen PA, Vanninen RL, and Soininen H. Increased fMRI responses during encoding in mild cognitive impairment. *Neurobiol Aging,* 28(12): 1889-1903, 2007a.

Hamalainen A, Tervo S, Grau-Olivares M, Niskanen E, Pennanen C, Huuskonen J, Kivipelto M, Hanninen T, Tapiola M, Vanhanen M, Hallikainen M, Helkala E-L, Nissinen A, Vanninen R, and Soininen H. Voxel-based morphometry to detect brain atrophy in progressive mild cognitive impairment. *Neuroimage,* 37(4): 1122-1131, 2007b.

Hampel H, Buerger K, Zinkowski R, Teipel SJ, Goernitz A, Andreasen N, Sjoegren M, DeBernardis J, Kerkman D, Ishiguro K, Ohno H, Vanmechelen E, Vanderstichele H, McCulloch C, Moller HJ, Davies P, and Blennow K. Measurement of phosphorylated tau epitopes in the differential diagnosis of Alzheimer disease: a comparative cerebrospinal fluid study. *Arch Gen Psychiatry,* 61(1): 95-102, 2004.

Hampel H, Burger K, Teipel SJ, Bokde AL, Zetterberg H, and Blennow K. Core candidate neurochemical and imaging biomarkers of Alzheimer's disease. *Alzheimers Dement,* 4(1): 38-48, 2008.

Hannesdottir K and Morris RG. Primary and secondary anosognosia for memory impairment in patients with Alzheimer's disease. *Cortex,* 43(7): 1020-1030, 2007.

Hanyu H, Sato T, Akai T, Shimizu S, Hirao K, Kanetaka H, Iwamoto T, and Koizumi K. Neuroanatomical correlates of unawareness of memory deficits in early Alzheimer's disease. *Dement Geriatr Cogn Disord,* 25(4): 347-353, 2008.

Hardy J and Selkoe DJ. The amyloid hypothesis of Alzheimer's disease: progress and problems on the road to therapeutics. *Science,* 297(5580): 353-356, 2002.

Hardy JA and Higgins GA. Alzheimer's disease: the amyloid cascade hypothesis. *Science,* 256(5054): 184-185, 1992.

Harvey AK, Pattinson KT, Brooks JC, Mayhew SD, Jenkinson M, and Wise RG. Brainstem functional magnetic resonance imaging: disentangling signal from physiological noise. *J Magn Reson Imaging,* 28(6): 1337-1344, 2008.

Hayama HR and Rugg MD. Right dorsolateral prefrontal cortex is engaged during post-retrieval processing of both episodic and semantic information. *Neuropsychologia,* 47(12): 2409-2416, 2009.

Hedden T, Van Dijk KR, Becker JA, Mehta A, Sperling RA, Johnson KA, and Buckner RL. Disruption of functional connectivity in clinically normal older adults harboring amyloid burden. *J Neurosci,* 29(40): 12686-12694, 2009.

Henke K, Buck A, Weber B, and Wieser HG. Human hippocampus establishes associations in memory. *Hippocampus,* 7(3): 249-256, 1997.

Heun R, Mazanek M, Atzor KR, Tintera J, Gawehn J, Burkart M, Gansicke M, Falkai P, and Stoeter P. Amygdala-hippocampal atrophy and memory performance in dementia of Alzheimer type. *Dement Geriatr Cogn Disord,* 8(6): 329-336, 1997.

Hoffman JM, Welsh-Bohmer KA, Hanson M, Crain B, Hulette C, Earl N, and Coleman RE. FDG PET imaging in patients with pathologically verified dementia. *J Nucl Med,* 41(11): 1920-1928, 2000.

Hofman A, Ott A, Breteler MM, Bots ML, Slooter AJ, van Harskamp F, van Duijn CN, Van Broeckhoven C, and Grobbee DE. Atherosclerosis, apolipoprotein E, and prevalence of dementia and Alzheimer's disease in the Rotterdam Study. *Lancet,* 349(9046): 151-154, 1997.

Holmes C and Butchart J. Systemic inflammation and Alzheimer's disease. *Biochem Soc Trans,* 39(4): 898-901, 2011.

Hort J, O'Brien JT, Gainotti G, Pirttila T, Popescu BO, Rektorova I, Sorbi S, and Scheltens P. EFNS guidelines for the diagnosis and management of Alzheimer's disease. *Eur J Neurol,* 17(10): 1236-1248, 2010.

Inzitari D, Pracucci G, Poggesi A, Carlucci G, Barkhof F, Chabriat H, Erkinjuntti T, Fazekas F, Ferro JM, Hennerici M, Langhorne P, O'Brien J, Scheltens P, Visser MC, Wahlund LO, Waldemar G, Wallin A, and Pantoni L. Changes in white matter as determinant of global functional decline in older independent outpatients: three year follow-up of LADIS (leukoaraiosis and disability) study cohort. *BMJ,* 339: b2477, 2009.

Iqbal K, Alonso Adel C, Chen S, Chohan MO, El-Akkad E, Gong CX, Khatoon S, Li B, Liu F, Rahman A, Tanimukai H, and Grundke-Iqbal I. Tau pathology in Alzheimer disease and other tauopathies. *Biochim Biophys Acta,* 1739(2-3): 198-210, 2005.

Jack CR, Jr., Albert MS, Knopman DS, McKhann GM, Sperling RA, Carrillo MC, Thies B, and Phelps CH. Introduction to the recommendations from the National Institute on Aging-Alzheimer's Association workgroups on diagnostic guidelines for Alzheimer's disease. *Alzheimers Dement,* 7(3): 257-262, 2011a.

Jack CR, Jr., Barkhof F, Bernstein MA, Cantillon M, Cole PE, Decarli C, Dubois B, Duchesne S, Fox NC, Frisoni GB, Hampel H, Hill DL, Johnson K, Mangin JF, Scheltens P, Schwarz AJ, Sperling R, Suhy J, Thompson PM, Weiner M, and Foster NL. Steps to standardization and validation of hippocampal volumetry as a biomarker in clinical trials and diagnostic criterion for Alzheimer's disease. *Alzheimers Dement,* 7(4): 474-485 e474, 2011b.

Jack CR, Jr., Dickson DW, Parisi JE, Xu YC, Cha RH, O'Brien PC, Edland SD, Smith GE, Boeve BF, Tangalos EG, Kokmen E, and Petersen RC. Antemortem MRI findings correlate with hippocampal neuropathology in typical aging and dementia. *Neurology,* 58(5): 750-757, 2002.

Jack CR, Jr., Knopman DS, Jagust WJ, Shaw LM, Aisen PS, Weiner MW, Petersen RC, and Trojanowski JQ. Hypothetical model of dynamic biomarkers of the Alzheimer's pathological cascade. *Lancet Neurol,* 9(1): 119-128, 2010.

Jack CR, Jr., Petersen RC, O'Brien PC, and Tangalos EG. MR-based hippocampal volumetry in the diagnosis of Alzheimer's disease. *Neurology,* 42(1): 183-188, 1992.

Jack CR, Jr., Petersen RC, Xu Y, O'Brien PC, Smith GE, Ivnik RJ, Boeve BF, Tangalos EG, and Kokmen E. Rates of hippocampal atrophy correlate with change in clinical status in aging and AD. *Neurology,* 55(4): 484-489, 2000.

Jack CR, Jr., Petersen RC, Xu YC, O'Brien PC, Smith GE, Ivnik RJ, Boeve BF, Waring SC, Tangalos EG, and Kokmen E. Prediction of AD with MRI-based hippocampal volume in mild cognitive impairment. *Neurology,* 52(7): 1397-1403, 1999.

Jack CR, Jr., Petersen RC, Xu YC, Waring SC, O'Brien PC, Tangalos EG, Smith GE, Ivnik RJ, and Kokmen E. Medial temporal atrophy on MRI in normal aging and very mild Alzheimer's disease. *Neurology,* 49(3): 786-794, 1997.

Jack CR, Jr., Shiung MM, Weigand SD, O'Brien PC, Gunter JL, Boeve BF, Knopman DS, Smith GE, Ivnik RJ, Tangalos EG, and Petersen RC. Brain atrophy rates predict subsequent clinical conversion in normal elderly and amnestic MCI. *Neurology,* 65(8): 1227-1231, 2005.

Jack CR, Jr., Twomey CK, Zinsmeister AR, Sharbrough FW, Petersen RC, and Cascino GD. Anterior temporal lobes and hippocampal formations: normative volumetric measurements from MR images in young adults. *Radiology,* 172(2): 549-554, 1989.

Jack CR, Jr., Weigand SD, Shiung MM, Przybelski SA, O'Brien PC, Gunter JL, Knopman DS, Boeve BF, Smith GE, and Petersen RC. Atrophy rates accelerate in amnestic mild cognitive impairment. *Neurology,* 70(19 Pt 2): 1740-1752, 2008.

Jack CR, Lowe VJ, Weigand SD, Wiste HJ, Senjem ML, Knopman DS, Shiung MM, Gunter JL, Boeve BF, Kemp BJ, Weiner M, and Petersen RC. Serial PIB and MRI in normal, mild cognitive impairment and Alzheimer's disease: implications for sequence of pathological events in Alzheimer's disease. *Brain,* 132(Pt 5): 1355-1365, 2009.

Jackson O, 3rd and Schacter DL. Encoding activity in anterior medial temporal lobe supports subsequent associative recognition. *Neuroimage,* 21(1): 456-462, 2004.

Jenkinson M. Fast, automated, N-dimensional phase-unwrapping algorithm. *Magn Reson Med,* 49(1): 193-197, 2003.

Jenkinson M, Bannister P, Brady M, and Smith S. Improved optimization for the robust and accurate linear registration and motion correction of brain images. *Neuroimage,* 17(2): 825-841, 2002.

Jobst KA, Smith AD, Szatmari M, Molyneux A, Esiri ME, King E, Smith A, Jaskowski A, McDonald B, and Wald N. Detection in life of confirmed Alzheimer's disease using a simple measurement of medial temporal lobe atrophy by computed tomography. *Lancet,* 340(8829): 1179-1183, 1992.

Johnson DK, Storandt M, Morris JC, and Galvin JE. Longitudinal study of the transition from healthy aging to Alzheimer disease. *Arch Neurol,* 66(10): 1254-1259, 2009.

Johnson KA, Fox NC, Sperling RA, and Klunk WE. Brain imaging in Alzheimer disease. *Cold Spring Harb Perspect Med,* 2(4): a006213, 2012.

Johnson NA, Jahng GH, Weiner MW, Miller BL, Chui HC, Jagust WJ, Gorno-Tempini ML, and Schuff N. Pattern of cerebral hypoperfusion in Alzheimer disease and mild cognitive impairment measured with arterial spin-labeling MR imaging: initial experience. *Radiology,* 234(3): 851-859, 2005.

Johnson SC, Baxter LC, Wilder LS, Pipe JG, Heiserman JE, and Prigatano GP. Neural correlates of self-reflection. *Brain,* 125(Pt 8): 1808-1814, 2002.

Johnson SC, Schmitz TW, Moritz CH, Meyerand ME, Rowley HA, Alexander AL, Hansen KW, Gleason CE, Carlsson CM, Ries ML, Asthana S, Chen K, Reiman EM, and Alexander GE. Activation of brain regions vulnerable to Alzheimer's disease: the effect of mild cognitive impairment. *Neurobiol Aging,* 27(11): 1604-1612, 2006.

Jones DT, Machulda MM, Vemuri P, McDade EM, Zeng G, Senjem ML, Gunter JL, Przybelski SA, Avula RT, Knopman DS, Boeve BF, Petersen RC, and Jack CR, Jr. Age-related changes in the default mode network are more advanced in Alzheimer disease. *Neurology,* 77(16): 1524-1531, 2011.

Kalisch R, Korenfeld E, Stephan KE, Weiskopf N, Seymour B, and Dolan RJ. Context-dependent human extinction memory is mediated by a ventromedial prefrontal and hippocampal network. *J Neurosci,* 26(37): 9503-9511, 2006.

Karas G, Sluimer J, Goekoop R, van der Flier W, Rombouts SA, Vrenken H, Scheltens P, Fox N, and Barkhof F. Amnestic mild cognitive impairment: structural MR imaging findings predictive of conversion to Alzheimer disease. *AJNR Am J Neuroradiol,* 29(5): 944-949, 2008.

Karas GB, Scheltens P, Rombouts SARB, Visser PJ, van Schijndel RA, Fox NC, and Barkhof F. Global and local gray matter loss in mild cognitive impairment and Alzheimer's disease. *Neuroimage,* 23(2): 708-716, 2004.

Kaszniak AW and Edmonds EC. Anosognosia and Alzheimer's Disease: Behavioral Studies. In Prigatano G (Ed.) *The Study of Anosognosia*. New York: Oxford University Press, 2010.

Kaye JA, Swihart T, Howieson D, Dame A, Moore MM, Karnos T, Camicioli R, Ball M, Oken B, and Sexton G. Volume loss of the hippocampus and temporal lobe in healthy elderly persons destined to develop dementia. *Neurology,* 48(5): 1297-1304, 1997.

Kesslak JP, Nalcioglu O, and Cotman CW. Quantification of magnetic resonance scans for hippocampal and parahippocampal atrophy in Alzheimer's disease. *Neurology,* 41(1): 51-54, 1991.

Killiany RJ, Hyman BT, Gomez-Isla T, Moss MB, Kikinis R, Jolesz F, Tanzi R, Jones K, and Albert MS. MRI measures of entorhinal cortex vs hippocampus in preclinical AD. *Neurology,* 58(8): 1188-1196, 2002.

Kircher TT, Weis S, Freymann K, Erb M, Jessen F, Grodd W, Heun R, and Leube DT. Hippocampal activation in patients with mild cognitive impairment is necessary for successful memory encoding. *J Neurol Neurosurg Psychiatry,* 78(8): 812-818, 2007.

Kirchhoff BA, Wagner AD, Maril A, and Stern CE. Prefrontal-temporal circuitry for episodic encoding and subsequent memory. *J Neurosci,* 20(16): 6173-6180, 2000.

Knopman DS, DeKosky ST, Cummings JL, Chui H, Corey-Bloom J, Relkin N, Small GW, Miller B, and Stevens JC. Practice parameter: diagnosis of dementia (an evidence-based review). Report of the Quality Standards Subcommittee of the American Academy of Neurology. *Neurology,* 56(9): 1143-1153, 2001.

Kohler S, Black SE, Sinden M, Szekely C, Kidron D, Parker JL, Foster JK, Moscovitch M, Winocour G, Szalai JP, and Bronskill MJ. Memory impairments associated with hippocampal versus parahippocampal-gyrus atrophy: an MR volumetry study in Alzheimer's disease. *Neuropsychologia,* 36(9): 901-914, 1998.

Koivunen J, Scheinin N, Virta JR, Aalto S, Vahlberg T, Nagren K, Helin S, Parkkola R, Viitanen M, and Rinne JO. Amyloid PET imaging in patients with mild cognitive impairment: a 2-year follow-up study. *Neurology,* 76(12): 1085-1090, 2011.

Lacor PN, Buniel MC, Chang L, Fernandez SJ, Gong Y, Viola KL, Lambert MP, Velasco PT, Bigio EH, Finch CE, Krafft GA, and Klein WL. Synaptic targeting by Alzheimer's-related amyloid beta oligomers. *J Neurosci,* 24(45): 10191-10200, 2004.

Lee HG, Casadesus G, Zhu X, Takeda A, Perry G, and Smith MA. Challenging the amyloid cascade hypothesis: senile plaques and amyloid-beta as protective adaptations to Alzheimer disease. *Ann N Y Acad Sci,* 1019: 1-4, 2004.

Lee JH, Kim SH, Kim GH, Seo SW, Park HK, Oh SJ, Kim JS, Cheong HK, and Na DL. Identification of pure subcortical vascular dementia using 11C-Pittsburgh compound B. *Neurology,* 77(1): 18-25, 2011.

Lemaitre H, Crivello F, Dufouil C, Grassiot B, Tzourio C, Alperovitch A, and Mazoyer B. No epsilon4 gene dose effect on hippocampal atrophy in a large MRI database of healthy elderly subjects. *Neuroimage,* 24(4): 1205-1213, 2005.

Lieberman MD. Social cognitive neuroscience: a review of core processes. *Annu Rev Psychol,* 58: 259-289, 2007.

Logothetis NK. What we can do and what we cannot do with fMRI. *Nature,* 453(7197): 869-878, 2008.

Lombardo MV, Chakrabarti B, Bullmore ET, Sadek SA, Pasco G, Wheelwright SJ, Suckling J, and Baron-Cohen S. Atypical neural self-representation in autism. *Brain,* 133(Pt 2): 611-624, 2010.

MacDonald D, Kabani N, Avis D, and Evans AC. Automated 3-D extraction of inner and outer surfaces of cerebral cortex from MRI. *Neuroimage,* 12(3): 340-356, 2000.

Machulda MM, Ward HA, Borowski B, Gunter JL, Cha RH, O'Brien PC, Petersen RC, Boeve BF, Knopman D, Tang-Wai DF, Ivnik RJ, Smith GE, Tangalos EG, and Jack CR, Jr. Comparison of memory fMRI response among normal, MCI, and Alzheimer's patients. *Neurology,* 61(4): 500-506, 2003.

Maguire EA, Frith CD, Burgess N, Donnett JG, and O'Keefe J. Knowing where things are parahippocampal involvement in encoding object locations in virtual large-scale space. *J Cogn Neurosci,* 10(1): 61-76, 1998.

Manly JJ, Bell-McGinty S, Tang MX, Schupf N, Stern Y, and Mayeux R. Implementing diagnostic criteria and estimating frequency of mild cognitive impairment in an urban community. *Arch Neurol,* 62(11): 1739-1746, 2005.

Martin SB, Smith CD, Collins HR, Schmitt FA, and Gold BT. Evidence that volume of anterior medial temporal lobe is reduced in seniors destined for mild cognitive impairment. *Neurobiol Aging,* 31(7): 1099-1106, 2010.

Masters CL, Simms G, Weinman NA, Multhaup G, McDonald BL, and Beyreuther K. Amyloid plaque core protein in Alzheimer disease and Down syndrome. *Proc Natl Acad Sci U S A,* 82(12): 4245-4249, 1985.

Matthews PM and Jezzard P. Functional magnetic resonance imaging. *J Neurol Neurosurg Psychiatry,* 75(1): 6-12, 2004.

Mattsson N, Zetterberg H, Hansson O, Andreasen N, Parnetti L, Jonsson M, Herukka S-K, van der Flier WM, Blankenstein MA, Ewers M, Rich K, Kaiser E, Verbeek M, Tsolaki M,

Mulugeta E, Rosen E, Aarsland D, Visser PJ, Schroder J, Marcusson J, de Leon M, Hampel H, Scheltens P, Pirttila T, Wallin A, Jonhagen ME, Minthon L, Winblad B, and Blennow K. CSF biomarkers and incipient Alzheimer disease in patients with mild cognitive impairment. *JAMA,* 302(4): 385-393, 2009.

McEvoy LK, Fennema-Notestine C, Roddey JC, Hagler DJ, Jr., Holland D, Karow DS, Pung CJ, Brewer JB, and Dale AM. Alzheimer disease: quantitative structural neuroimaging for detection and prediction of clinical and structural changes in mild cognitive impairment. *Radiology,* 251(1): 195-205, 2009.

McKeith IG, Dickson DW, Lowe J, Emre M, O'Brien JT, Feldman H, Cummings J, Duda JE, Lippa C, Perry EK, Aarsland D, Arai H, Ballard CG, Boeve B, Burn DJ, Costa D, Del Ser T, Dubois B, Galasko D, Gauthier S, Goetz CG, Gomez-Tortosa E, Halliday G, Hansen LA, Hardy J, Iwatsubo T, Kalaria RN, Kaufer D, Kenny RA, Korczyn A, Kosaka K, Lee VM, Lees A, Litvan I, Londos E, Lopez OL, Minoshima S, Mizuno Y, Molina JA, Mukaetova-Ladinska EB, Pasquier F, Perry RH, Schulz JB, Trojanowski JQ, and Yamada M. Diagnosis and management of dementia with Lewy bodies: third report of the DLB Consortium. *Neurology,* 65(12): 1863-1872, 2005.

McKhann G, Drachman D, Folstein M, Katzman R, Price D, and Stadlan EM. Clinical diagnosis of Alzheimer's disease: report of the NINCDS-ADRDA Work Group under the auspices of Department of Health and Human Services Task Force on Alzheimer's Disease. *Neurology,* 34(7): 939-944, 1984.

McKhann GM, Knopman DS, Chertkow H, Hyman BT, Jack CR, Jr., Kawas CH, Klunk WE, Koroshetz WJ, Manly JJ, Mayeux R, Mohs RC, Morris JC, Rossor MN, Scheltens P, Carrillo MC, Thies B, Weintraub S, and Phelps CH. The diagnosis of dementia due to Alzheimer's disease: recommendations from the National Institute on Aging-Alzheimer's Association workgroups on diagnostic guidelines for Alzheimer's disease. *Alzheimers Dement,* 7(3): 263-269, 2011.

Migliorelli R, Teson A, Sabe L, Petracca G, Petracchi M, Leiguarda R, and Starkstein SE. Anosognosia in Alzheimer's disease: a study of associated factors. *J Neuropsychiatry Clin Neurosci,* 7(3): 338-344, 1995.

Miller SL, Celone K, DePeau K, Diamond E, Dickerson BC, Rentz D, Pihlajamaki M, and Sperling RA. Age-related memory impairment associated with loss of parietal deactivation but preserved hippocampal activation. *Proc Natl Acad Sci U S A,* 105(6): 2181-2186, 2008a.

Miller SL, Fenstermacher E, Bates J, Blacker D, Sperling RA, and Dickerson BC. Hippocampal activation in adults with mild cognitive impairment predicts subsequent cognitive decline. *J Neurol Neurosurg Psychiatry,* 79(6): 630-635, 2008b.

Mimura M and Yano M. Memory impairment and awareness of memory deficits in early-stage Alzheimer's disease. *Rev Neurosci,* 17(1-2): 253-266, 2006.

Mirra SS, Heyman A, McKeel D, Sumi SM, Crain BJ, Brownlee LM, Vogel FS, Hughes JP, van Belle G, and Berg L. The Consortium to Establish a Registry for Alzheimer's Disease (CERAD).

Part II. Standardization of the neuropathologic assessment of Alzheimer's disease. *Neurology,* 41(4): 479-486, 1991.

Mitchell JP, Banaji MR, and Macrae CN. General and specific contributions of the medial prefrontal cortex to knowledge about mental states. *Neuroimage,* 28(4): 757-762, 2005.

Moffat SD, Szekely CA, Zonderman AB, Kabani NJ, and Resnick SM. Longitudinal change in hippocampal volume as a function of apolipoprotein E genotype. *Neurology,* 55(1): 134-136, 2000.

Mograbi DC, Brown RG, and Morris RG. Anosognosia in Alzheimer's disease--the petrified self. *Conscious Cogn,* 18(4): 989-1003, 2009.

Mormino EC, Smiljic A, Hayenga AO, Onami SH, Greicius MD, Rabinovici GD, Janabi M, Baker SL, Yen IV, Madison CM, Miller BL, and Jagust WJ. Relationships between beta-amyloid and functional connectivity in different components of the default mode network in aging. *Cereb Cortex,* 21(10): 2399-2407, 2011.

Morris JC. The Clinical Dementia Rating (CDR): current version and scoring rules. *Neurology,* 43(11): 2412-2414, 1993.

Morris JC, Heyman A, Mohs RC, Hughes JP, van Belle G, Fillenbaum G, Mellits ED, and Clark C. The Consortium to Establish a Registry for Alzheimer's Disease (CERAD). Part I. Clinical and neuropsychological assessment of Alzheimer's disease. *Neurology,* 39(9): 1159-1165, 1989.

Morris JC, Roe CM, Grant EA, Head D, Storandt M, Goate AM, Fagan AM, Holtzman DM, and Mintun MA. Pittsburgh compound B imaging and prediction of progression from cognitive normality to symptomatic Alzheimer disease. *Arch Neurol,* 66(12): 1469-1475, 2009.

Morris RG and Hannesdottir K. Loss of "awareness" in Alzheimer's disease. In Morris RG and Becker JT (Eds.), *Cognitive Neuropsychology of Alzheimer's Disease*. Oxford: Oxford University Press, 2004.

Morrison JH and Hof PR. Life and death of neurons in the aging brain. *Science,* 278(5337): 412-419, 1997.

Moscovitch M, Rosenbaum RS, Gilboa A, Addis DR, Westmacott R, Grady C, McAndrews MP, Levine B, Black S, Winocur G, and Nadel L. Functional neuroanatomy of remote episodic, semantic and spatial memory: a unified account based on multiple trace theory. *J Anat,* 207(1): 35-66, 2005.

Moulin CJ, James N, Freeman JE, and Jones RW. Deficient acquisition and consolidation: intertrial free recall performance in Alzheimer's disease and mild cognitive impairment. *J Clin Exp Neuropsychol,* 26(1): 1-10, 2004.

Moulin CJ, Perfect TJ, and Jones RW. Evidence for intact memory monitoring in Alzheimer's disease: metamemory sensitivity at encoding. *Neuropsychologia,* 38(9): 1242-1250, 2000.

Nasreddine ZS, Phillips NA, Bedirian V, Charbonneau S, Whitehead V, Collin I, Cummings JL, and Chertkow H. The Montreal Cognitive Assessment, MoCA: a brief screening tool for mild cognitive impairment. *J Am Geriatr Soc,* 53(4): 695-699, 2005.

Neary D, Snowden JS, Gustafson L, Passant U, Stuss D, Black S, Freedman M, Kertesz A, Robert PH, Albert M, Boone K, Miller BL, Cummings J, and Benson DF. Frontotemporal lobar degeneration: a consensus on clinical diagnostic criteria. *Neurology,* 51(6): 1546-1554, 1998.

Nichols TE and Holmes AP. Nonparametric permutation tests for functional neuroimaging: a primer with examples. *Hum Brain Mapp,* 15(1): 1-25, 2002.

Northoff G and Bermpohl F. Cortical midline structures and the self. *Trends Cogn Sci,* 8(3): 102-107, 2004.

Northoff G, Heinzel A, de Greck M, Bermpohl F, Dobrowolny H, and Panksepp J. Self-referential processing in our brain--a meta-analysis of imaging studies on the self. *Neuroimage,* 31(1): 440-457, 2006.

Nyberg L, McIntosh AR, Houle S, Nilsson LG, and Tulving E. Activation of medial temporal structures during episodic memory retrieval. *Nature,* 380(6576): 715-717, 1996.

Oakes TR, Fox AS, Johnstone T, Chung MK, Kalin N, and Davidson RJ. Integrating VBM into the General Linear Model with voxelwise anatomical covariates. *Neuroimage,* 34(2): 500-508, 2007.

Ogawa S, Menon RS, Tank DW, Kim SG, Merkle H, Ellermann JM, and Ugurbil K. Functional brain mapping by blood oxygenation level-dependent contrast magnetic resonance imaging. A comparison of signal characteristics with a biophysical model. *Biophys J,* 64(3): 803-812, 1993.

Ogawa S, Tank DW, Menon R, Ellermann JM, Kim SG, Merkle H, and Ugurbil K. Intrinsic signal changes accompanying sensory stimulation: functional brain mapping with magnetic resonance imaging. *Proc Natl Acad Sci U S A,* 89(13): 5951-5955, 1992.

Ohm TG, Muller H, Braak H, and Bohl J. Close-meshed prevalence rates of different stages as a tool to uncover the rate of Alzheimer's disease-related neurofibrillary changes. *Neuroscience,* 64(1): 209-217, 1995.

Okello A, Koivunen J, Edison P, Archer HA, Turkheimer FE, Nagren K, Bullock R, Walker Z, Kennedy A, Fox NC, Rossor MN, Rinne JO, and Brooks DJ. Conversion of amyloid positive and negative MCI to AD over 3 years: an 11C-PIB PET study. *Neurology,* 73(10): 754-760, 2009.

Pantoni L, Basile AM, Pracucci G, Asplund K, Bogousslavsky J, Chabriat H, Erkinjuntti T, Fazekas F, Ferro JM, Hennerici M, O'Brien J, Scheltens P, Visser MC, Wahlund LO, Waldemar G, Wallin A, and Inzitari D. Impact of age-related cerebral white matter changes on the transition to disability -- the LADIS study: rationale, design and methodology. *Neuroepidemiology,* 24(1-2): 51-62, 2005.

Pariente J, Cole S, Henson R, Clare L, Kennedy A, Rossor M, Cipoloti L, Puel M, Demonet JF, Chollet F, and Frackowiak RS. Alzheimer's patients engage an alternative network during a memory task. *Ann Neurol,* 58(6): 870-879, 2005.

Patenaude B, Smith SM, Kennedy DN, and Jenkinson M. A Bayesian model of shape and appearance for subcortical brain segmentation. *Neuroimage*, 2011.

Peters F, Collette F, Degueldre C, Sterpenich V, Majerus S, and Salmon E. The neural correlates of verbal short-term memory in Alzheimer's disease: an fMRI study. *Brain,* 132(Pt 7): 1833-1846, 2009.

Petersen RC, Smith GE, Ivnik RJ, Tangalos EG, Schaid DJ, Thibodeau SN, Kokmen E, Waring SC, and Kurland LT. Apolipoprotein E status as a predictor of the development of Alzheimer's disease in memory-impaired individuals. *JAMA,* 273(16): 1274-1278, 1995.

Petersen RC, Smith GE, Waring SC, Ivnik RJ, Tangalos EG, and Kokmen E. Mild cognitive impairment: clinical characterization and outcome. *Arch Neurol,* 56(3): 303-308, 1999.

Petersen RC, Thomas RG, Grundman M, Bennett D, Doody R, Ferris S, Galasko D, Jin S, Kaye J, Levey A, Pfeiffer E, Sano M, van Dyck CH, and Thal LJ. Vitamin E and donepezil for the treatment of mild cognitive impairment. *N Engl J Med,* 352(23): 2379-2388, 2005.

Petrella JR, Prince SE, Krishnan S, Husn H, Kelley L, and Doraiswamy PM. Effects of Donepezil on Cortical Activation in Mild Cognitive Impairment: A Pilot Double-Blind Placebo-Controlled Trial Using Functional MR Imaging. *AJNR Am J Neuroradiol*, 2008.

Petrella JR, Sheldon FC, Prince SE, Calhoun VD, and Doraiswamy PM. Default mode network connectivity in stable vs progressive mild cognitive impairment. *Neurology,* 76(6): 511-517, 2011.

Petrella JR, Wang L, Krishnan S, Slavin MJ, Prince SE, Tran TT, and Doraiswamy PM. Cortical deactivation in mild cognitive impairment: high-field-strength functional MR imaging. *Radiology,* 245(1): 224-235, 2007.

Pihlajamaki M, DePeau KM, Blacker D, and Sperling RA. Impaired medial temporal repetition suppression is related to failure of parietal deactivation in Alzheimer disease. *Am J Geriatr Psychiatry,* 16(4): 283-292, 2008.

Pihlajamaki M and Sperling RA. Functional MRI assessment of task-induced deactivation of the default mode network in Alzheimer's disease and at-risk older individuals. *Behav Neurol,* 21(1): 77-91, 2009.

Pimplikar SW, Nixon RA, Robakis NK, Shen J, and Tsai LH. Amyloid-independent mechanisms in Alzheimer's disease pathogenesis. *J Neurosci,* 30(45): 14946-14954, 2010.

Piolino P, Chetelat G, Matuszewski V, Landeau B, Mezenge F, Viader F, de la Sayette V, Eustache F, and Desgranges B. In search of autobiographical memories: A PET study in the frontal variant of frontotemporal dementia. *Neuropsychologia,* 45(12): 2730-2743, 2007.

Prigatano GP. Anosognosia: clinical and ethical considerations. *Curr Opin Neurol,* 22(6): 606-611, 2009.

Putcha D, O'Keefe K, LaViolette P, O'Brien J, Greve D, Rentz DM, Locascio J, Atri A, and Sperling R. Reliability of functional magnetic resonance imaging associative encoding memory paradigms in non-demented elderly adults. *Hum Brain Mapp,* 32(12): 2027-2044, 2011.

Qi Z, Wu X, Wang Z, Zhang N, Dong H, Yao L, and Li K. Impairment and compensation coexist in amnestic MCI default mode network. *Neuroimage,* 50(1): 48-55, 2010.

Raichle ME, MacLeod AM, Snyder AZ, Powers WJ, Gusnard DA, and Shulman GL. A default mode of brain function. *Proc Natl Acad Sci U S A,* 98(2): 676-682, 2001.

Rajji T, Chapman D, Eichenbaum H, and Greene R. The role of CA3 hippocampal NMDA receptors in paired associate learning. *J Neurosci,* 26(3): 908-915, 2006.

Ravaglia G, Forti P, Maioli F, Martelli M, Servadei L, Brunetti N, Pantieri G, and Mariani E. Conversion of mild cognitive impairment to dementia: predictive role of mild cognitive impairment subtypes and vascular risk factors. *Dement Geriatr Cogn Disord,* 21(1): 51-58, 2006.

Raz N, Rodrigue KM, and Haacke EM. Brain aging and its modifiers: insights from in vivo neuromorphometry and susceptibility weighted imaging. *Ann N Y Acad Sci,* 1097: 84-93, 2007.

Reisberg B and Gauthier S. Current evidence for subjective cognitive impairment (SCI) as the pre-mild cognitive impairment (MCI) stage of subsequently manifest Alzheimer's disease. *Int Psychogeriatr,* 20(1): 1-16, 2008.

Remy F, Mirrashed F, Campbell B, and Richter W. Verbal episodic memory impairment in Alzheimer's disease: a combined structural and functional MRI study. *Neuroimage,* 25(1): 253-266, 2005.

Ridha BH, Anderson VM, Barnes J, Boyes RG, Price SL, Rossor MN, Whitwell JL, Jenkins L, Black RS, Grundman M, and Fox NC. Volumetric MRI and cognitive measures in Alzheimer disease : comparison of markers of progression. *J Neurol,* 255(4): 567-574, 2008.

Ridha BH, Barnes J, Bartlett JW, Godbolt A, Pepple T, Rossor MN, and Fox NC. Tracking atrophy progression in familial Alzheimer's disease: a serial MRI study. *Lancet Neurol,* 5(10): 828-834, 2006.

Ries ML, Carlsson CM, Rowley HA, Sager MA, Gleason CE, Asthana S, and Johnson SC. Magnetic resonance imaging characterization of brain structure and function in mild cognitive impairment: a review. *J Am Geriatr Soc,* 56(5): 920-934, 2008.

Ries ML, Jabbar BM, Schmitz TW, Trivedi MA, Gleason CE, Carlsson CM, Rowley HA, Asthana S, and Johnson SC. Anosognosia in mild cognitive impairment: Relationship to activation of cortical midline structures involved in self-appraisal. *J Int Neuropsychol Soc,* 13(3): 450-461, 2007.

Risacher SL, Saykin AJ, West JD, Shen L, Firpi HA, and McDonald BC. Baseline MRI predictors of conversion from MCI to probable AD in the ADNI cohort. *Curr Alzheimer Res,* 6(4): 347-361, 2009.

Robbins TW, James M, Owen AM, Sahakian BJ, McInnes L, and Rabbitt P. Cambridge Neuropsychological Test Automated Battery (CANTAB): a factor analytic study of a large sample of normal elderly volunteers. *Dementia,* 5(5): 266-281, 1994.

Roberts JL, Clare L, and Woods RT. Subjective memory complaints and awareness of memory functioning in mild cognitive impairment: a systematic review. *Dement Geriatr Cogn Disord,* 28(2): 95-109, 2009.

Rodriguez JJ and Verkhratsky A. Neuroglial roots of neurodegenerative diseases? *Mol Neurobiol,* 43(2): 87-96, 2011.

Roman GC, Tatemichi TK, Erkinjuntti T, Cummings JL, Masdeu JC, Garcia JH, Amaducci L, Orgogozo JM, Brun A, Hofman A, and et al. Vascular dementia: diagnostic criteria for research studies. Report of the NINDS-AIREN International Workshop. *Neurology,* 43(2): 250-260, 1993.

Rombouts SA, Barkhof F, Goekoop R, Stam CJ, and Scheltens P. Altered resting state networks in mild cognitive impairment and mild Alzheimer's disease: an fMRI study. *Hum Brain Mapp,* 26(4): 231-239, 2005.

Rombouts SA, Barkhof F, Veltman DJ, Machielsen WC, Witter MP, Bierlaagh MA, Lazeron RH, Valk J, and Scheltens P. Functional MR imaging in Alzheimer's disease during memory encoding. *AJNR Am J Neuroradiol,* 21(10): 1869-1875, 2000.

Rombouts SA, Damoiseaux JS, Goekoop R, Barkhof F, Scheltens P, Smith SM, and Beckmann CF. Model-free group analysis shows altered BOLD FMRI networks in dementia. *Hum Brain Mapp,* 30(1): 256-266, 2009.

Rosen HJ, Alcantar O, Rothlind J, Sturm V, Kramer JH, Weiner M, and Miller BL. Neuroanatomical correlates of cognitive self-appraisal in neurodegenerative disease. *Neuroimage,* 49(4): 3358-3364, 2010.

Rosen HJ, Allison SC, Schauer GF, Gorno-Tempini ML, Weiner MW, and Miller BL. Neuroanatomical correlates of behavioural disorders in dementia. *Brain,* 128(Pt 11): 2612-2625, 2005.

Rosen HJ, Gorno-Tempini ML, Goldman WP, Perry RJ, Schuff N, Weiner M, Feiwell R, Kramer JH, and Miller BL. Patterns of brain atrophy in frontotemporal dementia and semantic dementia. *Neurology,* 58(2): 198-208, 2002a.

Rosen HJ, Kramer JH, Gorno-Tempini ML, Schuff N, Weiner M, and Miller BL. Patterns of cerebral atrophy in primary progressive aphasia. *Am J Geriatr Psychiatry,* 10(1): 89-97, 2002b.

Rossion B and Pourtois G. Revisiting Snodgrass and Vanderwart's object pictorial set: the role of surface detail in basic-level object recognition. *Perception,* 33(2): 217-236, 2004.

Roth M, Tym E, Mountjoy CQ, Huppert FA, Hendrie H, Verma S, and Goddard R. CAMDEX. A standardised instrument for the diagnosis of mental disorder in the elderly with special reference to the early detection of dementia. *Br J Psychiatry,* 149: 698-709, 1986.

Ruby P, Collette F, D'Argembeau A, Peters F, Degueldre C, Balteau E, Luxen A, Maquet P, and Salmon E. Perspective taking to assess self-personality: What's modified in Alzheimer's disease? *Neurobiol Aging,* 30(10): 1637-1651, 2008.

Ruby P, Schmidt C, Hogge M, D'Argembeau A, Collette F, and Salmon E. Social mind representation: where does it fail in frontotemporal dementia? *J Cogn Neurosci,* 19(4): 671-683, 2007.

Rusinek H, De Santi S, Frid D, Tsui W-H, Tarshish CY, Convit A, and de Leon MJ. Regional brain atrophy rate predicts future cognitive decline: 6-year longitudinal MR imaging study of normal aging. *Radiology,* 229(3): 691-696, 2003.

Samanez-Larkin GR and D'Esposito M. Group comparisons: imaging the aging brain. *Soc Cogn Affect Neurosci,* 3(3): 290-297, 2008.

Samgard K, Zetterberg H, Blennow K, Hansson O, Minthon L, and Londos E. Cerebrospinal fluid total tau as a marker of Alzheimer's disease intensity. *Int J Geriatr Psychiatry,* 25(4): 403-410, 2010.

Sarazin M, Chauvire V, Gerardin E, Colliot O, Kinkingnehun S, de Souza LC, Hugonot-Diener L, Garnero L, Lehericy S, Chupin M, and Dubois B. The amnestic syndrome of hippocampal type in Alzheimer's disease: an MRI study. *J Alzheimers Dis,* 22(1): 285-294, 2010.

Savva GM, Wharton SB, Ince PG, Forster G, Matthews FE, and Brayne C. Age, neuropathology, and dementia. *N Engl J Med,* 360(22): 2302-2309, 2009.

Saykin AJ, Wishart HA, Rabin LA, Flashman LA, McHugh TL, Mamourian AC, and Santulli RB. Cholinergic enhancement of frontal lobe activity in mild cognitive impairment. *Brain,* 127(Pt 7): 1574-1583, 2004.

Scahill RI, Frost C, Jenkins R, Whitwell JL, Rossor MN, and Fox NC. A longitudinal study of brain volume changes in normal aging using serial registered magnetic resonance imaging. *Arch Neurol,* 60(7): 989-994, 2003.

Scahill RI, Schott JM, Stevens JM, Rossor MN, and Fox NC. Mapping the evolution of regional atrophy in Alzheimer's disease: unbiased analysis of fluid-registered serial MRI. *Proc Natl Acad Sci U S A,* 99(7): 4703-4707, 2002.

Schacter DL and Wagner AD. Medial temporal lobe activations in fMRI and PET studies of episodic encoding and retrieval. *Hippocampus,* 9(1): 7-24, 1999.

Scheltens P, Fox N, Barkhof F, and De Carli C. Structural magnetic resonance imaging in the practical assessment of dementia: beyond exclusion. *Lancet Neurol,* 1(1): 13-21, 2002.

Schmitz TW and Johnson SC. Relevance to self: A brief review and framework of neural systems underlying appraisal. *Neurosci Biobehav Rev,* 31(4): 585-596, 2007.

Schwindt GC and Black SE. Functional imaging studies of episodic memory in Alzheimer's disease: a quantitative meta-analysis. *Neuroimage,* 45(1): 181-190, 2009.

Scoville WB and Milner B. Loss of recent memory after bilateral hippocampal lesions. *J Neurol Neurosurg Psychiatry,* 20(1): 11-21, 1957.

Shanks MF, McGeown WJ, Forbes-McKay KE, Waiter GD, Ries M, and Venneri A. Regional brain activity after prolonged cholinergic enhancement in early Alzheimer's disease. *Magn Reson Imaging,* 25(6): 848-859, 2007.

Sheline YI, Morris JC, Snyder AZ, Price JL, Yan Z, D'Angelo G, Liu C, Dixit S, Benzinger T, Fagan A, Goate A, and Mintun MA. APOE4 allele disrupts resting state fMRI connectivity in the absence of amyloid plaques or decreased CSF Abeta42. *J Neurosci,* 30(50): 17035-17040, 2010.

Shi F, Liu B, Zhou Y, Yu C, and Jiang T. Hippocampal volume and asymmetry in mild cognitive impairment and Alzheimer's disease: meta-analyses of MRI studies. *Hippocampus,* 19(11): 1055-1064, 2009.

Shibata K, Narumoto J, Kitabayashi Y, Ushijima Y, and Fukui K. Correlation between anosognosia and regional cerebral blood flow in Alzheimer's disease. *Neurosci Lett,* 435(1): 7-10, 2008.

Simmons WK and Martin A. The anterior temporal lobes and the functional architecture of semantic memory. *J Int Neuropsychol Soc,* 15(5): 645-649, 2009.

Simmons WK, Reddish M, Bellgowan PS, and Martin A. The selectivity and functional connectivity of the anterior temporal lobes. *Cereb Cortex,* 20(4): 813-825.

Smallwood A, Oulhaj A, Joachim C, Christie S, Sloan C, Smith AD, and Esiri M. Cerebral subcortical small vessel disease and its relation to cognition in elderly subjects: a pathological study in the Oxford Project to Investigate Memory and Ageing (OPTIMA) cohort. *Neuropathol Appl Neurobiol,* 38(4): 337-343, 2012.

Smith AD. Imaging the progression of Alzheimer pathology through the brain. *Proc Natl Acad Sci U S A,* 99(7): 4135-4137, 2002a.

Smith CD, Chebrolu H, Wekstein DR, Schmitt FA, Jicha GA, Cooper G, and Markesbery WR. Brain structural alterations before mild cognitive impairment. *Neurology,* 68(16): 1268-1273, 2007.

Smith SM. Fast robust automated brain extraction. *Hum Brain Mapp,* 17(3): 143-155, 2002b.

Smith SM, Fox PT, Miller KL, Glahn DC, Fox PM, Mackay CE, Filippini N, Watkins KE, Toro R, Laird AR, and Beckmann CF. Correspondence of the brain's functional architecture during activation and rest. *Proc Natl Acad Sci U S A,* 106(31): 13040-13045, 2009.

Smith SM, Jenkinson M, Woolrich MW, Beckmann CF, Behrens TEJ, Johansen-Berg H, Bannister PR, De Luca M, Drobnjak I, Flitney DE, Niazy RK, Saunders J, Vickers J, Zhang Y, De Stefano N, Brady JM, and Matthews PM. Advances in functional and structural MR image analysis and implementation as FSL. *Neuroimage,* 23 Suppl 1: 208-219, 2004.

Smith SM and Nichols TE. Threshold-free cluster enhancement: addressing problems of smoothing, threshold dependence and localisation in cluster inference. *Neuroimage,* 44(1): 83-98, 2009.

Snowdon DA, Greiner LH, Mortimer JA, Riley KP, Greiner PA, and Markesbery WR. Brain infarction and the clinical expression of Alzheimer disease. The Nun Study. *JAMA,* 277(10): 813-817, 1997.

Sole-Padulles C, Bartres-Faz D, Junque C, Vendrell P, Rami L, Clemente IC, Bosch B, Villar A, Bargallo N, Jurado MA, Barrios M, and Molinuevo JL. Brain structure and function related to cognitive reserve variables in normal aging, mild cognitive impairment and Alzheimer's disease. *Neurobiol Aging,* 30(7): 1114-1124, 2009.

Sorbi S, Hort J, Erkinjuntti T, Fladby T, Gainotti G, Gurvit H, Nacmias B, Pasquier F, Popescu BO, Rektorova I, Religa D, Rusina R, Rossor M, Schmidt R, Stefanova E, Warren JD, and Scheltens P. EFNS-ENS Guidelines on the diagnosis and management of disorders associated with dementia. *Eur J Neurol,* 19(9): 1159-1179, 2012.

Sorg C, Riedl V, Muhlau M, Calhoun VD, Eichele T, Laer L, Drzezga A, Forstl H, Kurz A, Zimmer C, and Wohlschlager AM. Selective changes of resting-state networks in individuals at risk for Alzheimer's disease. *Proc Natl Acad Sci U S A,* 104(47): 18760-18765, 2007.

Sperling R. Functional MRI studies of associative encoding in normal aging, mild cognitive impairment, and Alzheimer's disease. *Ann N Y Acad Sci,* 1097: 146-155, 2007.

Sperling R. Potential of functional MRI as a biomarker in early Alzheimer's disease. *Neurobiol Aging,* 32 Suppl 1: S37-43, 2011.

Sperling RA, Aisen PS, Beckett LA, Bennett DA, Craft S, Fagan AM, Iwatsubo T, Jack CR, Jr., Kaye J, Montine TJ, Park DC, Reiman EM, Rowe CC, Siemers E, Stern Y, Yaffe K, Carrillo MC, Thies B, Morrison-Bogorad M, Wagster MV, and Phelps CH. Toward defining the preclinical stages of Alzheimer's disease: recommendations from the National Institute on Aging-Alzheimer's Association workgroups on diagnostic guidelines for Alzheimer's disease. *Alzheimers Dement,* 7(3): 280-292, 2011.

Sperling RA, Bates JF, Chua EF, Cocchiarella AJ, Rentz DM, Rosen BR, Schacter DL, and Albert MS. fMRI studies of associative encoding in young and elderly controls and mild Alzheimer's disease. *J Neurol Neurosurg Psychiatry,* 74(1): 44-50, 2003.

Sperling RA, Bates JF, Cocchiarella AJ, Schacter DL, Rosen BR, and Albert MS. Encoding novel face-name associations: a functional MRI study. *Hum Brain Mapp,* 14(3): 129-139, 2001.

Sperling RA, Laviolette PS, O'Keefe K, O'Brien J, Rentz DM, Pihlajamaki M, Marshall G, Hyman BT, Selkoe DJ, Hedden T, Buckner RL, Becker JA, and Johnson KA. Amyloid deposition is associated with impaired default network function in older persons without dementia. *Neuron,* 63(2): 178-188, 2009.

Squire LR and Zola-Morgan S. The medial temporal lobe memory system. *Science,* 253(5026): 1380-1386, 1991.

Stewart R, Godin O, Crivello F, Maillard P, Mazoyer B, Tzourio C, and Dufouil C. Longitudinal neuroimaging correlates of subjective memory impairment: 4-year prospective community study. *Br J Psychiatry,* 198(3): 199-205, 2011.

Strozyk D, Blennow K, White LR, and Launer LJ. CSF Abeta 42 levels correlate with amyloid-neuropathology in a population-based autopsy study. *Neurology,* 60(4): 652-656, 2003.

Thompson PM, Mega MS, Woods RP, Zoumalan CI, Lindshield CJ, Blanton RE, Moussai J, Holmes CJ, Cummings JL, and Toga AW. Cortical change in Alzheimer's disease detected with a disease-specific population-based brain atlas. *Cereb Cortex,* 11(1): 1-16, 2001.

Tierney MC, Szalai JP, Snow WG, Fisher RH, Nores A, Nadon G, Dunn E, and St George-Hyslop PH. Prediction of probable Alzheimer's disease in memory-impaired patients: A prospective longitudinal study. *Neurology,* 46(3): 661-665, 1996.

Tomassini V, Jbabdi S, Kincses ZT, Bosnell R, Douaud G, Pozzilli C, Matthews PM, and Johansen-Berg H. Structural and functional bases for individual differences in motor learning. *Hum Brain Mapp,* 32(3): 494-508, 2011.

Tondelli M, Wilcock GK, Nichelli P, De Jager CA, Jenkinson M, and Zamboni G. Structural MRI changes detectable up to ten years before clinical Alzheimer's disease. *Neurobiol Aging*, 2011.

Trivedi MA, Schmitz TW, Ries ML, Torgerson BM, Sager MA, Hermann BP, Asthana S, and Johnson SC. Reduced hippocampal activation during episodic encoding in middle-aged individuals at genetic risk of Alzheimer's disease: a cross-sectional study. *BMC Med,* 4: 1, 2006.

Tulving E. Episodic memory: from mind to brain. *Annu Rev Psychol,* 53: 1-25, 2002.

Tulving E, Kapur S, Craik FI, Moscovitch M, and Houle S. Hemispheric encoding/retrieval asymmetry in episodic memory: positron emission tomography findings. *Proc Natl Acad Sci U S A,* 91(6): 2016-2020, 1994a.

Tulving E, Kapur S, Markowitsch HJ, Craik FI, Habib R, and Houle S. Neuroanatomical correlates of retrieval in episodic memory: auditory sentence recognition. *Proc Natl Acad Sci U S A,* 91(6): 2012-2015, 1994b.

Uddin LQ, Kelly AM, Biswal BB, Xavier Castellanos F, and Milham MP. Functional connectivity of default mode network components: correlation, anticorrelation, and causality. *Hum Brain Mapp,* 30(2): 625-637, 2009.

Vannini P, Hedden T, Becker JA, Sullivan C, Putcha D, Rentz D, Johnson KA, and Sperling RA. Age and amyloid-related alterations in default network habituation to stimulus repetition. *Neurobiol Aging*, 2011a.

Vannini P, O'Brien J, O'Keefe K, Pihlajamaki M, Laviolette P, and Sperling RA. What goes down must come up: role of the posteromedial cortices in encoding and retrieval. *Cereb Cortex,* 21(1): 22-34, 2011b.

Vemuri P, Jones DT, and Jack CR, Jr. Resting state functional MRI in Alzheimer's Disease. *Alzheimers Res Ther,* 4(1): 2, 2012.

Vemuri P, Whitwell JL, Kantarci K, Josephs KA, Parisi JE, Shiung MS, Knopman DS, Boeve BF, Petersen RC, Dickson DW, and Jack CR, Jr. Antemortem MRI based STructural Abnormality iNDex (STAND)-scores correlate with postmortem Braak neurofibrillary tangle stage. *Neuroimage,* 42(2): 559-567, 2008.

Vemuri P, Wiste HJ, Weigand SD, Shaw LM, Trojanowski JQ, Weiner MW, Knopman DS, Petersen RC, and Jack CR. MRI and CSF biomarkers in normal, MCI, and AD subjects: predicting future clinical change. *Neurology,* 73(4): 294-301, 2009.

Voets NL, Beckmann CF, Cole DM, Hong S, Bernasconi A, and Bernasconi N. Structural substrates for resting network disruption in temporal lobe epilepsy. *Brain*, 2012.

Wallenstein GV, Eichenbaum H, and Hasselmo ME. The hippocampus as an associator of discontiguous events. *Trends Neurosci,* 21(8): 317-323, 1998.

Wang L, Zang Y, He Y, Liang M, Zhang X, Tian L, Wu T, Jiang T, and Li K. Changes in hippocampal connectivity in the early stages of Alzheimer's disease: evidence from resting state fMRI. *Neuroimage,* 31(2): 496-504, 2006.

Wang Z, Yan C, Zhao C, Qi Z, Zhou W, Lu J, He Y, and Li K. Spatial patterns of intrinsic brain activity in mild cognitive impairment and Alzheimer's disease: a resting-state functional MRI study. *Hum Brain Mapp,* 32(10): 1720-1740, 2011.

Weiner MW, Veitch DP, Aisen PS, Beckett LA, Cairns NJ, Green RC, Harvey D, Jack CR, Jagust W, Liu E, Morris JC, Petersen RC, Saykin AJ, Schmidt ME, Shaw L, Siuciak JA, Soares H, Toga AW, and Trojanowski JQ. The Alzheimer's Disease Neuroimaging Initiative: a review of papers published since its inception. *Alzheimers Dement,* 8(1 Suppl): S1-68, 2012.

Welker KM, De Jesus RO, Watson RE, Machulda MM, and Jack CR. Altered Functional MR Imaging Language Activation in Elderly Individuals with Cerebral Leukoaraiosis. *Radiology*, 2012.

Whitwell JL, Josephs KA, Murray ME, Kantarci K, Przybelski SA, Weigand SD, Vemuri P, Senjem ML, Parisi JE, Knopman DS, Boeve BF, Petersen RC, Dickson DW, and Jack CR, Jr. MRI correlates of neurofibrillary tangle pathology at autopsy: a voxel-based morphometry study. *Neurology,* 71(10): 743-749, 2008a.

Whitwell JL, Shiung MM, Przybelski SA, Weigand SD, Knopman DS, Boeve BF, Petersen RC, and Jack CR, Jr. MRI patterns of atrophy associated with progression to AD in amnestic mild cognitive impairment. *Neurology,* 70(7): 512-520, 2008b.

Winblad B, Palmer K, Kivipelto M, Jelic V, Fratiglioni L, Wahlund LO, Nordberg A, Backman L, Albert M, Almkvist O, Arai H, Basun H, Blennow K, de Leon M, DeCarli C, Erkinjuntti T, Giacobini E, Graff C, Hardy J, Jack C, Jorm A, Ritchie K, van Duijn C, Visser P, and Petersen RC. Mild cognitive impairment--beyond controversies, towards a consensus: report of the International Working Group on Mild Cognitive Impairment. *J Intern Med,* 256(3): 240-246, 2004.

Woolrich MW, Jenkinson M, Brady JM, and Smith SM. Fully Bayesian spatio-temporal modeling of FMRI data. *IEEE Trans Med Imaging,* 23(2): 213-231, 2004.

Wu X, Li R, Fleisher AS, Reiman EM, Guan X, Zhang Y, Chen K, and Yao L. Altered default mode network connectivity in Alzheimer's disease--a resting functional MRI and Bayesian network study. *Hum Brain Mapp,* 32(11): 1868-1881, 2011.

Yuan Y, Gu ZX, and Wei WS. Fluorodeoxyglucose-positron-emission tomography, single-photon emission tomography, and structural MR imaging for prediction of rapid conversion to Alzheimer disease in patients with mild cognitive impairment: a meta-analysis. *AJNR Am J Neuroradiol,* 30(2): 404-410, 2009.

Zahn R, Moll J, Krueger F, Huey ED, Garrido G, and Grafman J. Social concepts are represented in the superior anterior temporal cortex. *Proc Natl Acad Sci U S A,* 104(15): 6430-6435, 2007.

Zamboni G, Grafman J, Krueger F, Knutson KM, and Huey ED. Anosognosia for Behavioral Disturbances in Frontotemporal Dementia and Corticobasal Syndrome: A Voxel-Based Morphometry Study. *Dement Geriatr Cogn Disord,* 29(1): 88-96, 2010.

Zeineh MM, Engel SA, Thompson PM, and Bookheimer SY. Dynamics of the hippocampus during encoding and retrieval of face-name pairs. *Science,* 299(5606): 577-580, 2003.

Zhang HY, Wang SJ, Liu B, Ma ZL, Yang M, Zhang ZJ, and Teng GJ. Resting brain connectivity: changes during the progress of Alzheimer disease. *Radiology,* 256(2): 598-606, 2010.

Zhang HY, Wang SJ, Xing J, Liu B, Ma ZL, Yang M, Zhang ZJ, and Teng GJ. Detection of PCC functional connectivity characteristics in resting-state fMRI in mild Alzheimer's disease. *Behav Brain Res,* 197(1): 103-108, 2009.